

**Studying Fibroblast growth factor (FGF) mediated
cell migration in *Drosophila* larval air sacs.**

Inauguraldissertation

zur
Erlangung der Würde eines Doktors der Philosophie
vorgelegt der
Philosophisch-Naturwissenschaftlichen Fakultät
der Universität Basel

von

Clemens Cabernard

aus Brigels, GR

Basel, 2005

Genehmigt von der Philosophisch-Naturwissenschaftlichen Fakultät
auf Antrag von:

Prof. Dr. Markus Affolter
(Dissertationsleiter)

Prof. Dr. Silvia Arber
(Koreferentin)

Prof. Dr. Walter J. Gehring
(Vorsitzender)

Basel, den 14.12.04

Prof. Dr. Hans-Jakob Wirz
(Dekan)

Index

Index	1
Acknowledgements	5
Prologue	7
Summary	8
I. Introduction	10
1. GENERAL MECHANISMS OF CELL MIGRATION	11
1.1 The migration cycle.....	11
1.1.1 Formation of protrusions and polarization	12
1.1.2 Stabilization of protrusions	13
1.1.3 Transmitting the migratory force	14
1.1.4 Turn over of adhesion sites	14
2. TYPES OF CELL MIGRATION	17
2.1 Amoeboid migration	17
2.2 Mesenchymal migration.....	18
2.3 Collective migration modes	18
3. RHO GTPASES IN CELL MIGRATION	21
3.1 General aspects.....	21
3.2 Rho GTPases as molecular switches.....	21
3.3 Regulators and effectors of RhoGTPases.....	23
4. CELL MIGRATION <i>IN VIVO</i> : EXAMPLES FROM <i>DROSOPHILA MELANOGASTER</i>	27
4.1 Migration of primordial germ cells (PGC).....	27
4.2 Migration of hemocytes	32
4.3 Border cell migration	35
4.4 Mesodermal cell migration.....	41
4.5 Tracheal cell migration	45
4.6 Comparison of cell migration systems in <i>Drosophila</i>	51
5. FGF SIGNALING PATHWAY	58
5.1 FGF signaling in vertebrates	58
5.2 The PLC γ signaling pathway	59
5.3 Src & Crk	59
5.4 SNT1/FRS2.....	60
5.5 FGF signaling in <i>Drosophila</i>	62
5.6 Negative regulation of FGF signaling; findings from <i>Drosophila</i> and vertebrates.....	64
5.6.1 Abnormal wind disc (Awd).....	64
5.6.2 Cbl mediated protein degradation	65
5.6.3 Similar to FGF (Sef).....	65
5.6.4 Sprouty.....	66

6. DEVELOPMENTAL ROLE OF FGF SIGNALING; EXAMPLES FROM VERTEBRATES	68
6.1 Fibroblast growth factors in the development of the vertebrate limb.....	68
6.2 Fibroblast growth factors and their roles during lung morphogenesis	70
7. DEVELOPMENT OF LARVAL AND ADULT AIR SACS	74
7.1 Remodelling of the embryonic tracheal system	74
7.2 Formation of the thoracic air sac during <i>Drosophila</i> third instar larval development.....	77
8. AIM AND STRUCTURE OF THE THESIS	80
8.1 Aim	80
8.2 Structure.....	81
II Results.....	83
1. TOOLS TO STUDY AIR SAC DEVELOPMENT	84
1.1 Live imaging	84
1.2 Genetic manipulations of air sac tracheoblast.....	85
1.2.1 Positive labeling of mutant tracheal cells using the MARCM system	87
2. DEVELOPMENT OF AIR SACS	91
2.1 Air sac development during third instar larval stage.....	91
2.2 Air sac development during pupal stages.....	94
3. CELL DIVISION IN LARVAL AIR SACS	99
3.1 Entry into mitosis in third instar air sacs; expression of stringLacZ	99
3.2 Patterns of cell division in early/mid stage air sacs.....	101
3.3 Cell division rates in late air sacs	103
4. THIRD INSTAR AIR SAC MORPHOLOGY	107
4.1 Polarity of air sac tracheoblasts.....	107
4.2 Air sac architecture	108
4.3 Air sac lumen formation.....	113
5. GUIDED CELL MIGRATION OF AIR SAC TRACHEOBLASTS	116
5.1 Guided cell extensions and cell migration of air sac tracheoblasts	116
5.2 Cellular extensions in tip- and proximal cells	119
6. CELLULAR INTERACTIONS OF AIR SAC TRACHEOBLASTS WITH THE SURROUNDING TISSUE ..	126
6.1 Expression of <i>ovo/shavenbaby</i> in wing imaginal discs	126
7. GENETIC ANALYSIS OF FGF-MEDIATED CELL MIGRATION USING SITE-SPECIFIC MITOTIC RECOMBINATION	129
7.1 General considerations	129
7.2 Distribution and size of wild-type MARCM clones in third instar air sacs	131
7.3 <i>dof</i> & <i>btl</i> mutant clones	134
7.3.1 <i>dof</i> & <i>btl</i> mutant clones in third instar larval branches.....	138
7.4 <i>drk</i> & <i>shc</i> mutant clones show a migration phenotype similar to <i>dof</i> and <i>btl</i>	139
7.5 <i>ras</i> , <i>sos</i> , <i>cnk</i> , <i>ksr</i> mutant clones	142
7.5.1 <i>sos</i> , <i>ras</i> , <i>cnk</i> & <i>ksr</i> mutant clones in third instar larval branches	146

7.6	<i>rca1</i> & <i>cdc2</i> , two genes implicated in the cell cycle	147
7.7	The <i>son-of-sevenless</i> allele <i>sos</i> ^{<i>XMN1025</i>} shows normal clone size but reduced cell migration	150
7.8	Negative regulators of RTK signaling; <i>gap1</i> & <i>sprouty</i>	153
7.9	<i>PI3K</i> and <i>pten</i> mutant clones show air sac migration phenotypes	155
7.10	Regulators of the actin cytoskeleton; <i>rac</i> , <i>mbc</i> , <i>pak</i> , <i>chic</i>	158
7.11	Role of RhoGEFs in air sac.....	163
7.12	Air sac tracheoblasts mutant for different signaling components	165
7.13	Clones deficient for genes implicated in border cell migration.....	168
7.14	Air sacs deficient for <i>bsk</i> , <i>dock</i> and <i>lgl</i>	172
8. CHARACTERIZATION OF RECEPTOR OF ACTIVATED PROTEIN KINASE C (<i>RACK1</i>) DURING DROSOPHILA DEVELOPMENT.		176
8.1	What the papers say	176
8.2	Isolation and characterization of <i>Drosophila rack1</i> mutants.....	178
8.3	Molecular characterization of the <i>rack1</i> alleles.....	181
8.4	Phenotypic analysis of <i>rack1</i> mutants	184
8.4.1	Embryonic phenotypes and lethal phase	184
8.4.2	Mosaic analysis of <i>rack1</i> in the <i>Drosophila</i> female germline.....	186
8.4.3	Analyzing the <i>rack1</i> dumpless phenotype.....	189
8.4.4	Analysis of clone size, cell size and shape of <i>rack1</i> mutant tissue in the imaginal disc epithelium .	192
8.4.5	Analysis of <i>rack1</i> mutant clones in the third instar air sac.....	194
III Discussion.....		197
1. FGF SIGNALING AND <i>RACK1</i> ; TWO INDEPENDENT TOPICS?.....		198
1.1	Air sac development in <i>Drosophila</i> third instar larva	200
1.2	Establishment of air sac shape	201
1.3	Cell migration during air sac development	202
1.4	Genetic dissection of FGF signaling using site-specific mitotic recombination	205
1.4.1	Clone size versus clone position	205
1.4.2	Several mutations show clone positioning phenotypes independent of clone size.....	208
1.5	Do border cells and air sac tracheoblast require the same cytoskeletal regulators?.....	209
1.6	Air sac development does not require Dpp and/or Hh signaling.....	210
1.7	Rack1 is not required for tracheal cell migration.....	210
1.8	Air sacs as a model to study morphogenesis and cell biological questions.....	211
1.9	Concluding remarks and working model	213
IV Materials & Methods		215
1.0	Fly strains and genetics	216
1.1	Generation of T-MARCM stocks.....	216
1.2	Experimental crosses.....	218
1.3	Alleles used for MARCM clones.....	218
1.4	Gain-of function clones.....	219
1.5	Recombination of mutant alleles on FRT chromosomes.....	219

1.6	Slide preparation & imaging	220
1.7	Immunostainings and whole-mount <i>in situ</i> hybridization	221
1.8	Cloning of Rack1 rescue construct, transformants and rescue experiment.	222
1.9	Generation of <i>rack1</i> clones in the germline, air sacs, imaginal discs and ovaries.....	223
Epilogue		224
V REFERENCES		225
VI PUBLICATIONS		247
VII CURRICULUM VITAE		248
VIII EID		250

Acknowledgements

Performing a thesis is like sailing a boat. In order to reach the designated harbor, odd winds, currents as well as supplies have to be taken into account. The interplay of a skilled crew is crucial for reaching the shore safely.

Thus, I would like to thank the team which accompanied me on my way throughout this thesis. Once on the open water, a boater gets easily lost without an experienced navigator. I was more than lucky to have this in the person of my supervisor Prof. Dr. Markus Affolter. His encouragement, guidance as well as enthusiasm for biology, grabbed me like a wave and was motivating as well as rewarding. Thanks very much for the guidance, patience and mostly for the support.

However, without all the other team members, I would still sail far away from my goal. Thus I would like to thank all the members, present and past, of the Affolter lab which accompanied me on my efforts. Thomas Marty ignited the interest for *Drosophila* genetics. Apart from being patient enough to teach me basic genetics, he also showed me a big deal about molecular biology. I'm also very thankful to Andi Ebner, for all the help with stainings, *in situs* etc. but also for the good swimming and general fun we had. I'm more than thankful for the help Valérie Petit provided at the beginning at the air sac project as well as the big efforts Caroline Dossenbach supplied in performing the screen. One person I'm indebted to as well is Ania Jazwinska. Although sharing the flyroom with Ania had some minor drawbacks, I was more than compensated for this with her advice concerning genetics and experimental biology in general. Also Ute Nussbaumer, Jorgos Pyrowolakis, and Britta Hartmann provided very good advice as well as atmosphere. I would also like to say a big thank you to Marc Neumann and Carlos Ribeiro, for solving computer- as well as confocal problems. In addition, Marc kindly accepted to read and comment my thesis for which I'm more than thankful. I'm deeply indebted to Helene Dechanut, Alain Jung and Li Lin for their ongoing contribution to the air sac project. Their work power not just enabled the initiation of a genetic screen but also contributed a big deal to the progression of my project through critical discussions and comments. Thus, I'm more than happy to have them on board and together we will be able to tackle many problems concerning air sac development. Moreover, many thanks to the comments regarding this thesis.

I would also very much like to thank Samir Merabet for discussions and advice as well as Nicole Grieder for counsel and teaching of the ovary experiments.

As, a sailor who requires a boat and a sail, a Drosophilist needs flies in order to work with. A big deal of material has been provided by other laboratories. Thus, I would like to thank all the people who donated flies, even unpublished stocks, freely. Many thanks to Prof. Walther Gehring for providing the Exelixis piggybac insertion lines, Urs Kloter for lots of useful FRT stocks, Liqun Luo and Bruno Bello for MARCM stocks, Ernst Hafen, Konrad Basler, Jacques Montagne, Peter Gallant, Tom Kornberg, Makato Sato, Thomas Raabe, Ilaria Rebay, Mathew Freeman, Pernille Rorth, Denise Montell, Mark Krasnow, Amin Ghabrial, Mark Therrien, Frank Lehner, Frank Sprenger, Stephan Luschnig, Maria Leptin, Norbert Perrimon, Buzz Baum, Heather Sears, Stephen Hou, François Schweisguth, Celeste Berg, and Jennifer Chapin for mutants and other reagents. I'm also very much indebted to Bruno Bello for his encouragement concerning my project, advice as well as very critical reading of this manuscript.

My crosses would only work half as well if they would not be fed by the excellent and nourishing Polenta prepared by Karin Mauro, Bernadette Bruno and Gina Evora. Thanks for the patience and all the hard work. Many thanks also to Greta Backhaus and Liliane Devaja for their secretarial assistance.

Nevertheless, where would I be without the support from my private environment? Thus, I would like to thank first my family, outstanding of all my beloved father. Also my aunt Melanie and my uncle Peter provided many times shelter and good provisions. Many thanks also go to my brother Felix, for the good skiing and mental support. I would also like to thank Vincenzo Maddalena, who accompanied me throughout my time here in Basel and cheered me up numerous times with his company and excellent cooking. Also other friends should not go unnoticed such as Nektarios Palaskas, Thomas Travnika, Phillip Ehrensberger, Lorenzo Simona, Davide Alampi, Martin Oeggerli, Sarina Meinen, Nisha Rüegger, Renato Truffer, Markus Bärtschi, Marino Bertapelle as well as Ann and Oliver Wieben. Thanks a lot for reading and correcting the manuscript Ann! A hearty thank you also goes to Stefan Welmann, for both scientific and non-scientific discussions in the confocal room as well as for many ming-refreshing Unihockey games.

At last, and most importantly, I would like to express my deep gratitude to Femeke Britschgi. Of all the mentioned persons, she was the one who most of all, saw and had to experience my state of emotion throughout calm seas, odd currents, changing winds and upcoming storms. For her endless patience, love and support I find no matching words. Thanks for everything.

Prologue

Drosophila research has a long tradition. Starting in 1909 in the famous fly room at Columbia University in the laboratory of Thomas Hunt Morgan, the first visible mutants were isolated, of which the most prominent was probably the white mutation. Chromosomal aberrations, such as deletions, duplications or translocations were also identified, mostly by Bridges and Sturtevant. The genetic work done at Columbia mainly aimed at a better understanding of Mendelian heredity and culminated in the published book *The Mechanism of Mendelian Heredity* by Morgan, Sturtevant, Muller and Bridges in 1915.

Although early work largely aimed at the understanding of chromosomal mechanics and heredity, it was soon recognized that the power of *Drosophila* genetics can also be applied to study development. The so far unmatched genetic screen by Christiane Nüsslein-Volhard and Eric Wieschaus (Nüsslein-Volhard and Wieschaus, 1980) identified a wealth of mutations which were subsequently used for studying the development of *Drosophila melanogaster* and for the cloning of the corresponding genes. Cloning of *Drosophila* genes, identification of homologues in other organisms and comparison of conserved regulatory sequences became all easier with the sequencing of the *Drosophila* genome (Adams et al., 2000). However, in order to understand the development of an animal, or even of its organs or tissues, more than just the genes and their products have to be known.

With the advent of Green fluorescent protein and its derivatives, a new area in cell- and developmental biology has started. The behavior of cells in living embryos, invertebrate or vertebrate, can be studied, by combining GFP, with the aid of powerful microscopic tools. It has been shown that the possibility to describe morphogenetic events in four dimensions opened the door to a novel understanding of many aspects of developmental biology (Jacinto et al., 2002a; Jacinto et al., 2002b; Jazwinska et al., 2003; Ribeiro et al., 2002). Imaging becomes therefore more and more important in cell- and developmental biology, and the wealth of available mutants and genetic tools in *Drosophila* make this organism an outstanding choice for studying morphogenetic problems by combining the two areas.

This thesis should further illustrate how the integration of microscopic tools with advanced genetics can either enhance our understanding of an already described process or open novel interesting questions.

Summary

Invertebrates and vertebrates use FGF signaling in many developmental processes. Mesoderm formation, limb outgrowth but also the development of the vascular system and the lung rely on FGF ligands. We have chosen to study the *Drosophila* FGF signaling pathway that has been shown to be required for mesodermal- as well as tracheal cell migration. We aimed at a better understanding of FGF signaling to elucidate how the extracellular information, provided by the FGF/Bnl ligand is interpreted in tracheal cells. Using Downstream of FGFR (Dof), an adaptor protein of the FGF signaling pathway, as an entry point, we have previously identified interacting proteins and focused on one prime candidate as a potential linker of FGFR to the cytoskeleton. This candidate protein Receptor of protein kinase C (Rack1) is conserved throughout evolution. *rack1* is expressed in the early embryonic tracheal system and has been proposed to play important roles in cell migration as well as in the regulation of the actin cytoskeleton. We have identified and characterized *rack1* mutants; these mutants are zygotic lethal but neither show a detectable embryonic- nor any other larval phenotype, due to a very high maternal contribution. Removing the maternal store by generating germline clones results in eggs that fail to develop. This developmental arrest is due to an incomplete transfer of maternal product into the oocyte (nurse cell dumping).

In order to characterize the function of *rack1* in the context of FGF signaling, we started to characterize the development of third instar larval air sacs.

It has been reported that this structure develops via cell migration as well as cell division in response to FGF/Bnl signaling. First we confirm the occurrence of cell division and found that in early air sacs, division is ubiquitous and becomes restricted later to the central part of the air sac. We also documented cell behavior during cell migration using live imaging.

To initiate a genetic analysis of *rack1* and other candidate target genes in tracheal cell migration, strains and methods were established, allowing the generation of mosaic air sacs consisting of marked wild-type or mutant cells in an otherwise heterozygous background based on the MARCM system. This system was also applied to characterize cellular shape and dynamics of individual or small groups of air sac tracheoblasts in different parts of the air sac. We found that air sac tip cells extend long and dynamic actin based protrusions and further demonstrated that cells not directly located at the tip do form similar protrusions.

Finally, we took advantage of the our knowledge of air sac architecture and development to study the cell-autonomous requirement of candidate genes in genetic mosaics. We showed

that marked wild-type clones have a preference to be positioned at the tip. Mutants lacking *btl* or *dof*, two genes required for embryonic tracheal cell migration, never populate regions at the migratory front. We inferred that air sac tracheoblast cells lacking *btl* or *dof* are deficient in migration and take this as a readout for measuring cell migration.

Having established criteria for measuring cell migration in air sacs, we tested *rack1* mutants for their involvement in air sac tracheoblast migration and find that this gene is not required for this process. We also analyzed other candidate genes as well as components of the FGF signaling pathway and found evidence that Ras plays a dual role during third instar air sac formation. It appears to integrate signaling input from the EGFR pathway to trigger cell division as well as input from the FGF pathway to activate a cell migratory response. In contrast to border cells, mutants affecting the transcription factor Slow border cells (*Slbo*), the VEGFR (*PVR*) or DE-Cadherin (*Shg*) do not impede air sac tracheoblast migration. Components shown to regulate the actin cytoskeleton in response to PVR signaling such as Myoblast city (*Mbc*) the *Drosophila* Dock180 homologue or the small Rho family GTPases *Rac1*, *Rac2* and Mig-2-like (*Mtl*) as well as the effector Chickadee, the *Drosophila* homologue of Profilin, are essential for air sac tracheoblast migration. Thus, recruitment of these actin cytoskeleton regulators and effectors is mediated via different ligands/receptors in trachea and border cells.

Our studies demonstrate that the development of the air sac during late larval stages is a good system to study guided cell migration and allows the genetic dissection of the FGF signaling pathway.

The tools we developed allow to assay any candidate gene for which a mutant is available and also laid the foundation for the isolation and characterization of genes in a genome wide EMS screen.

I. Introduction

1. General mechanisms of cell migration

At the beginning there is cell migration. During development of invertebrates as well as vertebrates, cell migration is a recurring theme. Already shortly after conception, cell migration plays a fundamental role in shaping the body plan and it orchestrates morphogenesis throughout embryonic development. During gastrulation, large groups of cells migrate collectively as sheets to form a three layered embryo. Subsequently, cells also migrate from various epithelial layers to target locations, where they then differentiate to make up different tissues and organs. Cell migration is also important in the adult such as for the renewal of skin and intestine. Furthermore, also during tissue repair and immune surveillance, leukocytes from the circulation migrate into the surrounding tissue to destroy invading microorganisms, infected cells and to clear debris. However, migration also contributes to important pathological processes, including vascular disease, osteoporosis, chronic inflammatory diseases such as rheumatoid arthritis and multiple sclerosis, cancer and mental retardation due to defects in neuronal migration (Horwitz and Webb, 2003; Ridley et al., 2003).

1.1 The migration cycle

In general, cell migration can be conceptualized as a cyclic process. The initial response of a cell to a migration promoting agent is to polarize and to extend protrusions in the direction of migration. These protrusions can be large, broad lamellipodia, or spike-like filopodia, usually driven by actin polymerization and stabilized by adhering to the extracellular matrix or adjacent cells via transmembrane receptors linked to the actin cytoskeleton. The cell body then translocates forward and the release of adhesions and the retraction of the rear end completes the migratory cycle (Webb et al., 2002) (Ridley et al., 2003). Although many of these features are shared among different types of migrating cells, details can differ greatly. The described features are mostly observed in slow migrating cells such as in fibroblasts but are not as obvious in fast migrating cells such as neutrophils. Moreover cell migration *in vivo* seems to differ from cell migration *in vitro* (Horwitz and Webb, 2003; Ridley et al., 2003).

1.1.1 Formation of protrusions and polarization

In order to extend protrusions, the cell largely depends on actin filaments. These are intrinsically polarized with fast-growing barbed ends and slow growing pointed ends; this inherent polarity is used to drive membrane protrusions. Whereas in lamellipodia actin filaments form a branching dendritic network, filopodia consist of long parallel actin bundles (Jacinto and Wolpert, 2001).

Actin polymerization in lamellipodia is mediated by the Arp2/3 complex which binds to the sides or tip of a preexisting actin filament and induces the formation of a new daughter filament. Activation of the Arp2/3 complex is mediated by the WASP/WAVE family members which themselves are activated at the plasma membrane. The rate and organization of actin filaments in protrusions is regulated by several actin binding proteins. The pool of available actin monomers and free ends is affected for example by Profilin, which prevents self-nucleation by binding to actin monomers and also serves to selectively target monomers to barbed ends. Filament elongation is terminated by capping proteins, thereby restricting the polymerization to new filaments close to the plasma membrane. In addition, new actin monomers are needed for the polymerization at the front end; therefore the required disassembly of older filaments is assisted by the ADF/cofilin family, which sever filaments and promote actin dissociation from the pointed end (Pollard and Borisy, 2003).

Finally, pushing out of the membrane, the actual protrusive event, is believed to occur not by elongation of the actin filament per se but by an elastic Brownian ratchet mechanism, in which thermal energy bends the nascent short filaments, storing elastic energy (Ridley et al., 2003).

Filopodial protrusion is thought to occur by a treadmilling mechanism, in which actin filaments within a bundle elongate at their barbed ends and release actin monomers at their pointed ends. The long and unbranched filament organization is consistent with assembly occurring by elongation rather than by branched nucleation. Therefore many proteins are enriched at filopodial tips, including Ena/VASP proteins, which bind barbed ends of actin filaments and antagonize both capping and branching thereby allowing continuous elongation of filaments. In order to generate the required stiffness for efficient pushing, bundling proteins such as fascin are also present (Pollard and Borisy, 2003; Ridley et al., 2003).

For an individual cell to migrate, it must be polarized, meaning that the molecular processes at the front and the back of the cell are different. Establishing and maintaining of cell polarity

in response to extracellular stimuli appear to be mediated by Rho family GTPases, phosphoinositides 3-kinases (PI3Ks), integrins, microtubules and vesicular transport.

From yeast to humans *cdc42* is a master regulator of cell polarity. Inhibition and global activation can inhibit the directionality of cell migration. Cdc42 mediates polarity by restricting where lamellipodia form or by localizing the microtubule-organizing center (MTOC) and Golgi apparatus in front of the nucleus, oriented towards the leading edge. This facilitates microtubule growth and hence vesicular transport towards the leading edge. However, reorganization of the MTOC seems to be more important in slow moving cells (Fig.1I) (Ridley et al., 2003).

Many migrating cells respond directionally to external stimuli, a process called chemotaxis. In order to respond to shallow gradients of chemoattractants the small difference has to be amplified into steeper intracellular signaling gradients. This is mainly achieved through the phosphoinositides PIP₃ and PIP₂, which become rapidly and highly localized in cells exposed to a chemoattractant. The amplification process involves localized activation of PI3K which generates PIP₃/PIP₂, and the phosphatase PTEN, which removes them. In *Dictyostelium*, PI3K rapidly accumulates at the leading edge in response to a chemoattractant, whereas PTEN becomes restricted to the sides and the rear. Cells with altered PI3K/PTEN activity can usually migrate but show a significant reduced ability to move directionally (Ridley et al., 2003).

Several Rac exchange factors, RacGEFs, are locally activated at the leading edge by PI3K, thereby activating Rac itself, which can then organize the actin cytoskeleton in order to form protrusions. Furthermore several feedback loops are required to maintain directional protrusion an example is the recruitment of PI3K to the plasma membrane by Rac itself, which act then upstream of Rac by PIP₃- sensitive RacGEFs.

The tail of a polarized cell is equally important for proper cell migration. In several cell types, inhibition of Rho leads to an extended tail probably because actomyosin-based contractility of the cell is reduced. RhoA might also act in the tail by stabilizing microtubules, which then could promote focal adhesion turnover (Ridley et al., 2003).

1.1.2 Stabilization of protrusions

For migration to occur, a protrusion must form and then stabilize by attaching to the surroundings. Integrins, heterodimeric receptors consisting of an α - and β - chain with large ligand-binding extracellular domains and short cytoplasmic domains, are a major family of

migration-promoting receptors. They act as the feet of a migrating cell by supporting adhesion to the ECM or other cells via adaptor proteins linking the receptor to the actin cytoskeleton. Furthermore they activate migration-related signaling molecules. Since integrins themselves do not have any catalytic activity, signals are transmitted through interaction with intracellular adaptor proteins. Activated integrins preferentially localize to the leading edge, where new adhesions form. Affinity of integrins is largely regulated by conformational changes in the extracellular domain which results from interactions at the cytoplasmic tail. The GTPase Rap1 or PKC enhance integrin affinity. However, it is important to note that not all protrusions are stabilized by adhesion complexes. During migration *in vivo*, cells extend and retract protrusions for long periods of time suggesting that the stabilization of a protrusion may depend on ligand or receptor density at the leading edge (Ridley et al., 2003; Webb et al., 2002).

1.1.3 Transmitting the migratory force

By connecting the ECM to the intracellular cytoskeleton, integrins serve as traction sites, over which the cell moves and as mechanosensors, probing the physical state of the ECM and transmitting this information into the cell, which responds by altering the cytoskeleton. Migrating cells must be able to detach yet exert traction on the substratum; speed is therefore dependent on the strength of cell attachment, the density of ligands on the substrate and the density and affinity of receptors on the cell. The force transmitted to sites of adhesion derives from the interaction of myosin II with actin filaments that attach to these sites. Myosin II activity is regulated by myosin light-chain (MLC) phosphorylation. MLC phosphorylation activates myosin, resulting in increased contractility and transmission of tension to sites of adhesion. MLC is positively regulated by MLC kinase (MLCK) or Rho kinase (ROCK) and negatively by MLC phosphatase, which is itself phosphorylated and inhibited by ROCK. Whereas MLCK is regulated by intracellular calcium concentration as well as by phosphorylation by a number of kinases, ROCK is regulated by binding Rho-GTP (Ridley et al., 2003; Riento and Ridley, 2003)

1.1.4 Turn over of adhesion sites

Adhesions disassemble at the base of a cell protrusion as new adhesions are formed at the tip of the protrusion. However some adhesions persist and mature into larger, more stable

structures. Targeting of microtubules has been implicated as one factor that promotes adhesion disassembly but also protein kinases such as FAK or Src, phosphatases, as well as Rac with associated proteins, appear to be central regulators of adhesion turnover and stability.

At the rear of migrating cells, adhesions must disassemble too, which is often obtained through high tension on rear adhesions which results in mechanical detachment. Myosin II but also FAK, Src and other regulators might be involved (Ridley et al., 2003).

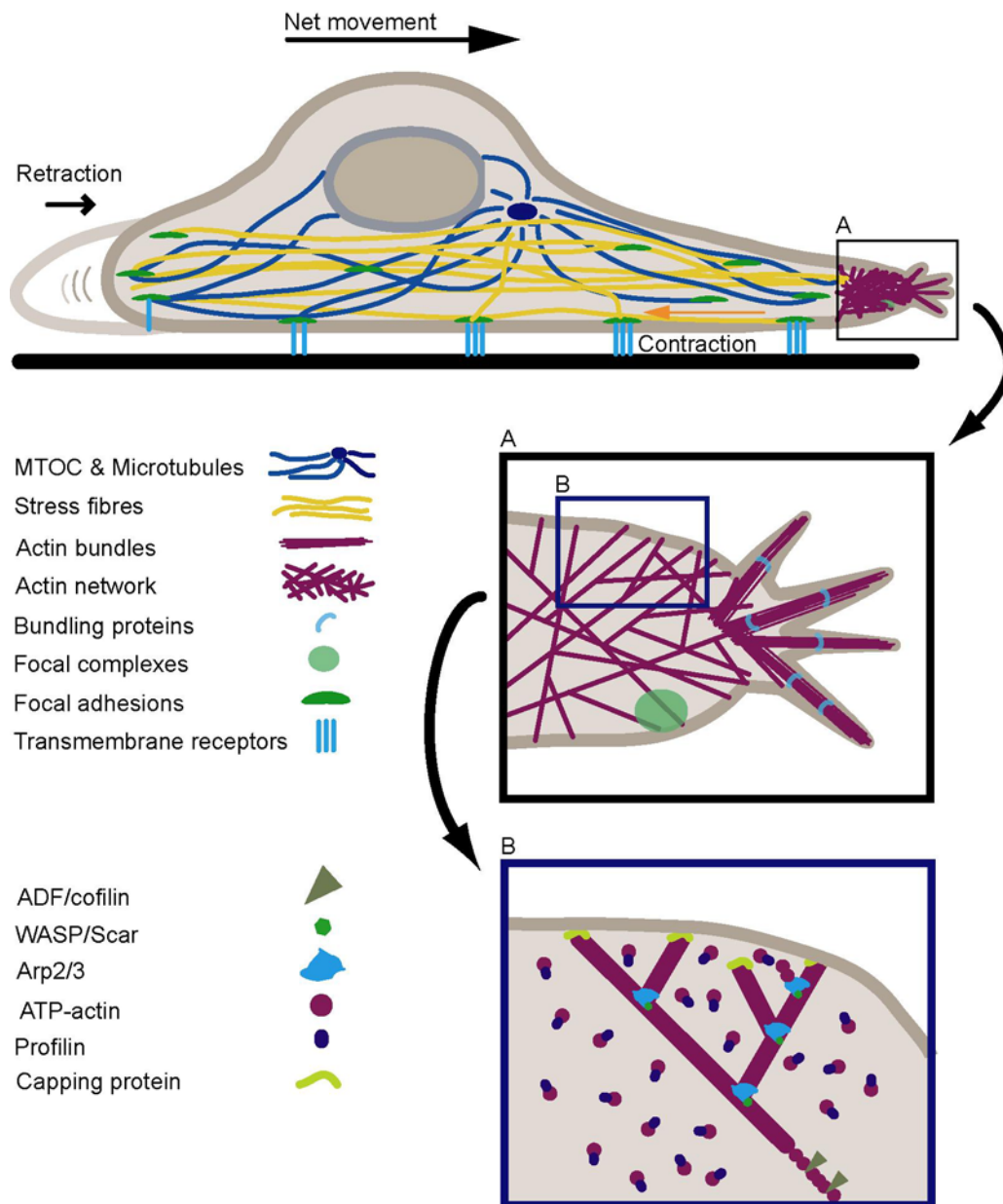


FIGURE 11:

Cell migration is a cyclic process. **A.)** Upon polarization which is also manifested in the localization of the MTOC in front of the nucleus, the cell forms protrusions at the tip in the direction of migration. The branched actin cytoskeleton is focused into filopodia, consisting of parallel actin bundles held together by actin bundling proteins such as fascin or α -actinin. **B.)** Filopodia also originate from actin filaments of the branched network that are prevented from capping and as a result can elongate at the leading edge of lamellipodium. In order to maintain the branched actin network, actin bound to ATP and profilin, which catalyzes the exchange of ADP for ATP, is incorporated into a growing filament by the Arp2/3 complex. This complex is activated by the WASP/Scar proteins. Capping proteins furthermore terminate the elongation of the filament. Since growth at the barbed end is faster than severing at the pointed end, the membrane will be pushed forward, another protrusion forms.

In order for the cell to move, it must be anchored to the substrate, which is achieved through transmembrane receptors. Protrusions are stabilized by the formation of adhesions (focal complexes which mature to focal adhesions) and transmit the generated force of actin-myosin contraction to the substrate via transmembrane receptors. At the cell rear, adhesions are disassembled also by the delivery of components by microtubules, which leads to retraction of the cell rear. This cycle leads to a net cell movement.

Adapted from (Petit et al., 2002; Pollard and Borisy, 2003)

2. Types of cell migration

Two types of cell movements, which can be further subdivided, can be observed during development; mass migration and the migration of individual cells. The former is characterized by the coordinated movement of entire tissues whereby the cells maintain their cohesive contacts while moving. The latter stands out by migration of individual cells, which requires loss of cell-cell contacts (Locascio and Nieto, 2001). These two distinct processes will be further elaborated below and are summarized on figure I2.

2.1 Amoeboid migration

Single cell migration can be further grouped into amoeboid movements (Fig.I2A), migration of single mesenchymal- or chains of mesenchymal cells (Fig.I2B, C).

The most primitive way of migration is amoeboid movement (Fig.I2A), which mimics features of the amoeba *Dictyostelium discoideum*. *Dictyostelium* is an ellipsoid cell with fast deformability and translocates via rapidly alternating cycles of morphological expansion and contraction. Although substrate binding is relatively low and integrins are not expressed, several non-integrin receptors can bind to the ECM. In higher eukaryotes, certain tumor cells, stem cells and most leukocytes show also amoeboid cell movement. Leukocytes are highly deformable, lack stable focal contacts and stress fibers but move at high velocities (2-30 $\mu\text{m}/\text{min}$). These cells are able to enter and move through many different organs, including skin, gut and brain. Stiffness and shape changes are mediated by cortical filamentous actin. T lymphocytes and other leukocytes use protease independent physical mechanisms to overcome matrix barriers, such as adaptation of the cell shape to preformed matrix structures (contact guidance), extension of lateral footholds (elbowing) and squeezing through narrow spaces. To contract and stiffen the cell cortex, actin polymerization along the plasma membrane is required, which is controlled by the small GTPase RhoA and its effector ROCK. Cdc42 and Rac engage adaptor proteins such as WASP that favor localized actin assembly and generate dynamic cell protrusions such as filopodia, lamellipodia and pseudopodia (Friedl, 2004; Haddad et al., 2001).

2.2 Mesenchymal migration

Mesenchymal cells (Fig. I2B, C) adopt in 3D tissues a spindle-shaped, fibroblast-like morphology, as characteristic for fibroblasts, myoblasts or single endothelial cells. The elongated cell shape is dependent on integrin-mediated adhesion dynamics and the presence of high traction forces on both cell poles. Blocking of integrins in spindle shaped fibroblasts causes cell retraction and an impairment in cell migration. Mesenchymal cells also recruit surface proteases to digest and remodel the ECM. Focal contact formation and turnover result in relatively slow migration velocities (0.1-2 μ m/min) in 3D models. If other cells follow along the newly generated matrix defects, a moving cell chain evolves and is guided by matrix strands. Also in mesenchymal cells, Rac and Cdc42 generate pseudopodia and lamellipodia dynamics at outward edges. Depletion of Rac or Cdc42 severely impairs cell migration, through inhibition of cell extension and polarized force generation. Rho stabilized initial integrin-substrate linkages, increases focal size and strength and further thickens actin filaments (Friedl, 2004).

2.3 Collective migration modes

In collective migration, cells maintain their cell-cell contacts and move as multicellular connected strands or chords into tissues (Fig. I2 D-G). Examples include invading epithelial strands or tubes, vascular sprouts and tumor clusters. Keratinocytes migrating across a provisional wound matrix as well as slow border cells in *Drosophila melanogaster* are regarded as specialized forms of collective migration (Friedl, 2004).

The leading edge of a moving cell group in 2D or 3D migration models is formed by one or several cells that utilize actin mediated ruffles and integrin-dependent traction. Junctions within invading collectives are stabilized by cadherins, members of the immunoglobulin superfamily and gap-junctional cell-cell communication. The rear of the leading cell(s) maintain the adhesive interaction with other cells, so neighboring cells are dragged forward by means of cell-cell adhesion. While the leading cells generate actin- and integrin mediated traction, a linear cortical actin network extends along cell-cell junctions into deeper regions of the collective.

Whereas de-differentiated tumor cell groups, which form amorphous cell strands and masses (Fig. 2D,E.) lack an inner lumen and extend within the tissue, non-neoplastic developing

glandular ducts and blood vessels contain polarized cells that form an inner lumen and newly produce a surrounding basement membrane (Fig.2F,G).

A special and more complex example of collective migration is the mass movement in morphogenesis, as seen during convergent extension of the vertebrate embryo or of the dorsal surface in the *Drosophila* embryo. In both cases, movement is carried out by complex multicellular sheets that contain cells linked to each other by cell-cell junctions and other means and move along the underlying or surrounding tissue substrate to form epithelia or organs (Friedl, 2004).

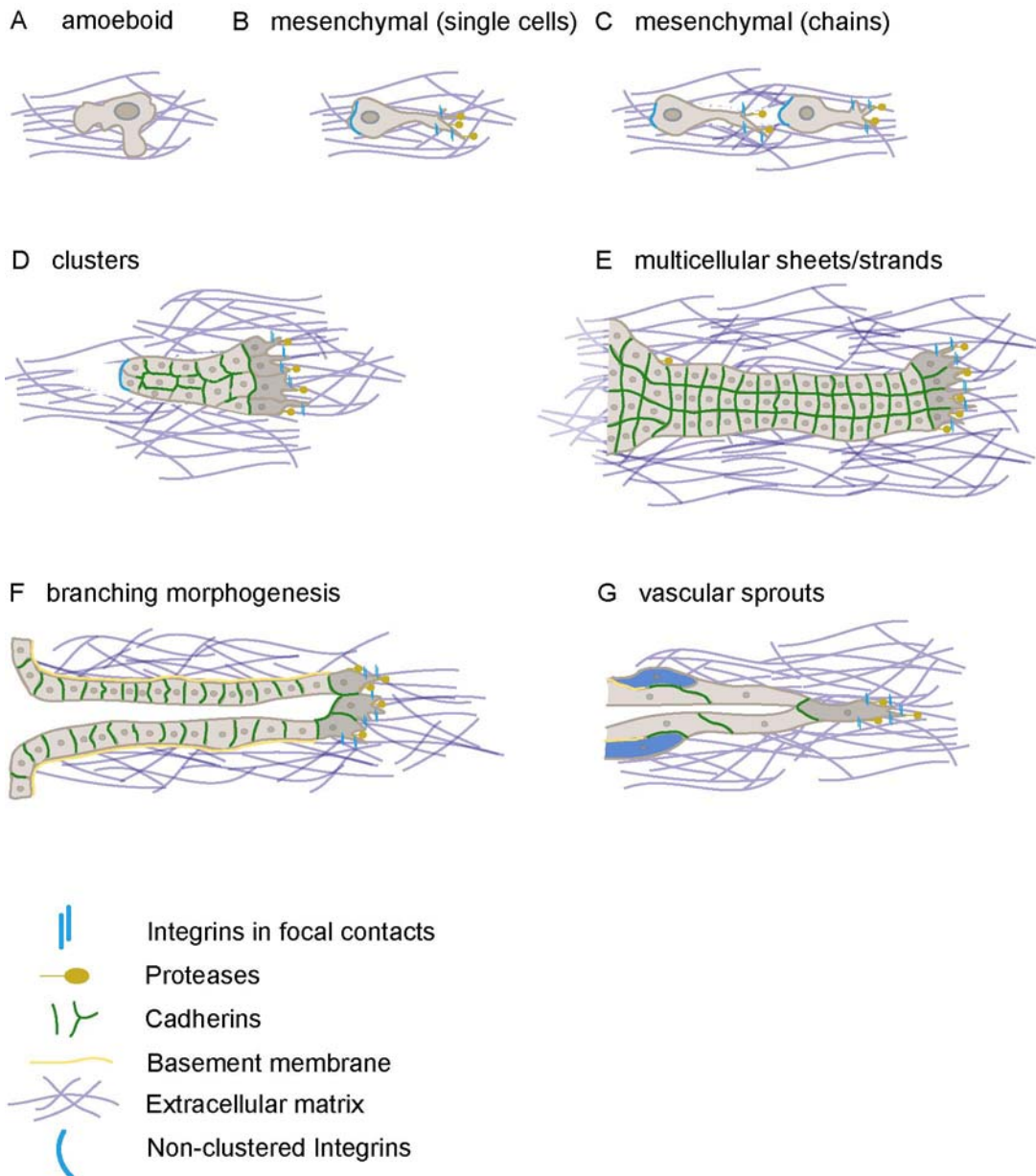


FIGURE 12:

Different types of cell migration. **A.-C.)** individual- vs. collective cell migration (**D.-G.)**.

A.) Amoeboid migrating cells develop a dynamic leading edge, rich in small pseudopodia, and a roundish or ellipsoid cell body. **B.)** mesenchymal cells show a tissue-dependent spindle-shaped elongation, form focal contacts and require proteases in order to degrade the ECM. **C.)** Chains of cells often move in proteolytic migration tracks as also seen for neural crest cells. **D.)** Clusters of cells display one or several leading cells which provide the migratory traction and pull the following group via cell-cell junctions forward. **E.)** Multicellular sheets can migrate again with a small number of leading cells and are connected to the proliferating origin via cell-cell junctions. **F.)** Branching morphogenesis is established via leading edge cells which proteolytically alter the EMC. The matrix defects are filled up by following cells, which generate a basement membrane at the interface to the EMC and an internal lumen. **G.)** Collective sprouts of endothelial cells form new blood vessels by moving and maintaining cell-cell junctions. Guided by one pathfinder cell, the chain matures into a growing strand containing a lumen. While the strand moves forward, pericytes (blue), which participate in the de novo synthesis of an encircling basement membrane, are recruited and engaged by Cadherins. Adapted from (Friedl, 2004).

3. Rho GTPases in cell migration

3.1 General aspects

Rho GTPases constitute a subfamily of the Ras superfamily of small GTPases (Luo, 2000). Rho GTPases are ubiquitously expressed and 20 members have been identified in mammals, 7 in *Drosophila melanogaster*, 5 in *Caenorhabditis elegans* and 15 in *Dictyostelium discoideum* (Raftopoulou and Hall, 2004). The best characterized Rho GTPases are RhoA (Ras homologous member A), Rac1 (Ras-related C3 botulinum substrate1) and Cdc42 (cell division cycle 42) (Luo, 2000; Raftopoulou and Hall, 2004; Ridley, 2001).

Tissue culture experiments showed that different Rho family members have different cellular functions. RhoA regulates the assembly of contractile, actin:myosin filaments (stress fibers), whereas Rac and Cdc42 are responsible for the polymerization of actin in order to form lamellipodial- or filopodial protrusions. The role of filopodia, however, is not entirely clear; it is thought that they probe the extracellular milieu, but in many cases they do not seem to be required for cell migration. In *Drosophila*, for example, loss of Cdc42 does not have any effect on peripheral glia cell migration (Sepp and Auld, 2003). However, they play a major role in controlling the direction of migration (Raftopoulou and Hall, 2004).

Cdc42 is also required for establishing cell polarity and plays a key role in epithelial cell polarity and asymmetric cell division (Macara, 2004).

3.2 Rho GTPases as molecular switches

Rho GTPases act as molecular switches by cycling between a GDP-bound inactive form and a GTP-bound active form. The cycle is tightly regulated by three groups of proteins (Fig.I3). Guanine nucleotide exchange factors (GEFs) promote the exchange of GDP for GTP to activate the GTPase. RhoGEFs are multidomain proteins consisting of a GEF domain also known as a Dbl-homology domain (DH domain) as well as a pleckstrin-homology (PH) domain. In several GEFs, the PH domain acts as an autoinhibitor of the DH domain, and binding of PIP₃ to the PH domain relieves this inhibition.

GTPase activating proteins (GAPs) negatively regulate the switch by enhancing its intrinsic GTPase activity. Similar to GEFs they are also multidomain proteins, which might be regulated through autoinhibition of the GAP activity by another part of the molecule.

Phosphorylation might be one mechanism relieving this autoinhibition to increase GAP activity.

Furthermore, some but not all Rho family proteins bind to guanine nucleotide dissociation inhibitors (GDIs). GDIs are thought to block the GTPase cycle by sequestering and solubilizing the GDP-bound form.

Once activated, Rho GTPases interact with cellular target proteins, so called effectors, to generate downstream responses (Raftopoulou and Hall, 2004; Ridley, 2001).

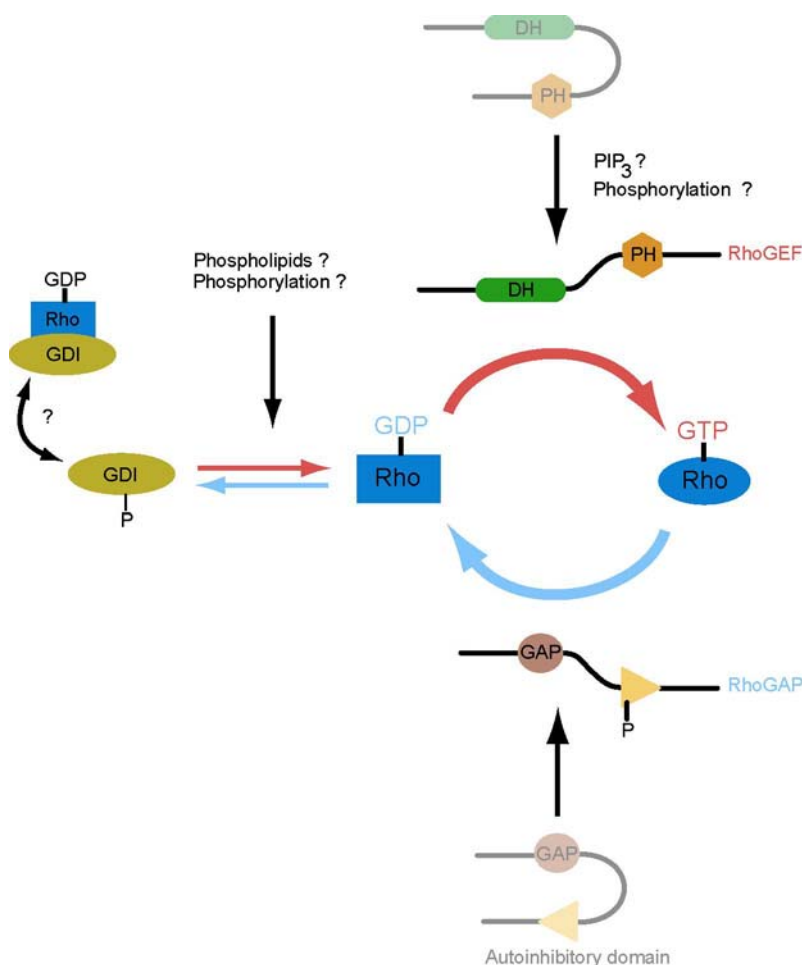


FIGURE I3:

Regulation of Rho family GTPases. Rho family GTPases cycle between an inactive GDP bound conformation and an active GTP bound form. Guanine nucleotide dissociation inhibitors (GDIs) hold the GDP bound GTPase in an inactive complex in the cytoplasm. Dissociation of this complex is required in order to activate downstream components which is achieved through upstream signaling events. Rho proteins are activated by GDP-GTP exchange factors (GEFs), multidomain proteins consisting of a GEF domain, known as a DH domain located next to a PH domain. In several GEFs, the PH domain acts as an autoinhibitor of the DH domain and PIP₃ binding to the PH domain can relieve this inhibition. GTPase activating proteins (GAPs) downregulate the Rho GTPases and like GEFs are also regulated through autoinhibition of the GAP activity by another part of the molecule. Adapted from (Ridley, 2001).

3.3 Regulators and effectors of RhoGTPases

An important regulator of Rac is PI3K, which has been widely implicated in controlling cell migration and polarity; during leukocyte chemotaxis for example, type IA PI3 kinases are required for lamellipodium extension and migration towards colony-stimulating factor. Production of PI(3,4,5)P₃ (PIP₃), leads to a local increase in GTP-bound Rac in many cell types. Moreover, expression of a constitutively activated PI3 kinase in fibroblasts generates extensive lamellipodia and membrane ruffling through Rac activation.

The mechanism through which PIP₃ works is thought to be a direct interaction with RacGEFs (Fig.13&4). Many Rac GEFs (all Dbl family GEFs) contain a PH domain and at least some of these can bind phospholipids; therefore, a major role of PIP₃ is thought to be in inducing membrane translocation. Moreover, PI3 kinase and Rac are able to directly interact with each other; Rac activation stimulates PI3 kinase leading to the production of PIP₃, which would provide an opportunity for a positive feedback loop (Raftopoulou and Hall, 2004).

Another important pathway downstream of membrane receptors required for the activation of Rac has been shown to involve a complex consisting of Dock180, the SH2/SH3 containing adaptor protein Crk, the adaptor molecule p130Cas as well as ELMO, an evolutionary conserved protein involved in cell migration, phagocytosis and cell shape changes (Fig. I4).

Genetic analysis supports a role for Dock180 and ELMO in cell migration. The fly orthologue of Dock180 is *myoblast city* (*mbc*) and has been shown to be implicated in myoblast fusion, dorsal closure and border cell migration (Duchek and Rorth, 2001a; Duchek et al., 2001b; Erickson et al., 1997; Nolan et al., 1998; Raftopoulou and Hall, 2004).

The cellular targets of Rac and Cdc42 that promote changes in the actin cytoskeleton have been the subject of intensive investigation. The Ser/Thr kinase p65PAK is commonly activated upon either Rac or Cdc42 activation and is believed to play a major role during regulation of actin dynamics and cell adhesion during cell migration. A target of p65PAK is LIM kinase (LIMK) which in turn phosphorylates and inactivates cofilin (Arber et al., 1998; Raftopoulou and Hall, 2004), (Fig.I4). Cofilin facilitates subunit dissociation from the pointed end of actin filaments and induces filament severing. Moreover it is essential for promoting filament treadmilling at the front of migrating cells.

Members of the WASp/SCAR/WAVE family of scaffold proteins are key regulators of actin polymerization (Fig.I1,I4). Upon activation, each of these proteins is able to stimulate the Arp2/3 complex, which induces actin polymerization de novo or at barbed end or sides of

preexisting actin filaments. WASp/WAVE, can also bind to profilin, which acts synergistically with Arp2/3 to speed up actin polymerization. Cdc42 can directly activate WASp or N-WASp, although the lipid PIP₂ is an essential cofactor. Rac requires the Nck-adaptor complex to indirectly activate the Scar/WAVE family proteins.

One important Rho target involved in stimulating actin:myosin filament assembly and therefore contractility is the Ser/Thr kinase p160ROCK (Fig.I4). In leukocytes Rho and p160ROCK have been shown to be essential for rear cell detachment. During migration of P-cells in the larval development of *C. elegans* as well as dorsal closure and gastrulation in *Drosophila*, p160ROCK has been shown to play an essential role. Like p65PAK, activated p160ROCK can phosphorylate and activate LIMK, which in turn phosphorylates and inactivates cofilin leading to stabilization of actin filaments within actin:myosin filament bundles. Moreover p160ROCK interacts with and phosphorylates the myosin binding subunit of myosin light chain phosphatase and thereby inactivates it. This in turn leads to increased levels of myosin phosphorylation, which can then cross-link actin filaments and generate contractile force. At the rear of the cell, this promotes movement of the cell body and facilitates detachment of the cell rear.

Since Rho activity is incompatible with membrane protrusions at the front of a migrating cell, mechanisms must be in place to inhibit its action at the leading edge. This might occur through Rac, since expression of activated Rac has been shown to inhibit Rho function in many cell types.

Another important downstream target of Rho is mDia, the mammalian orthologue of *Drosophila* Diaphanous (Fig.I4). mDia belongs to the formin-homology containing family of proteins which have been linked to actin filament assembly in both *Drosophila* and yeast (Raftopoulou and Hall, 2004).

Although the effects of Rho GTPases have mostly been investigated in the context of the actin cytoskeleton, it is now clear that they also regulate the microtubule cytoskeleton. It is unlikely that the microtubule cytoskeleton plays an essential role during cell migration or chemotaxis over short distances, however, efficient and persistent long range migration requires stabilization of cell polarity which is achieved through reorganization of the microtubule cytoskeleton (Raftopoulou and Hall, 2004).

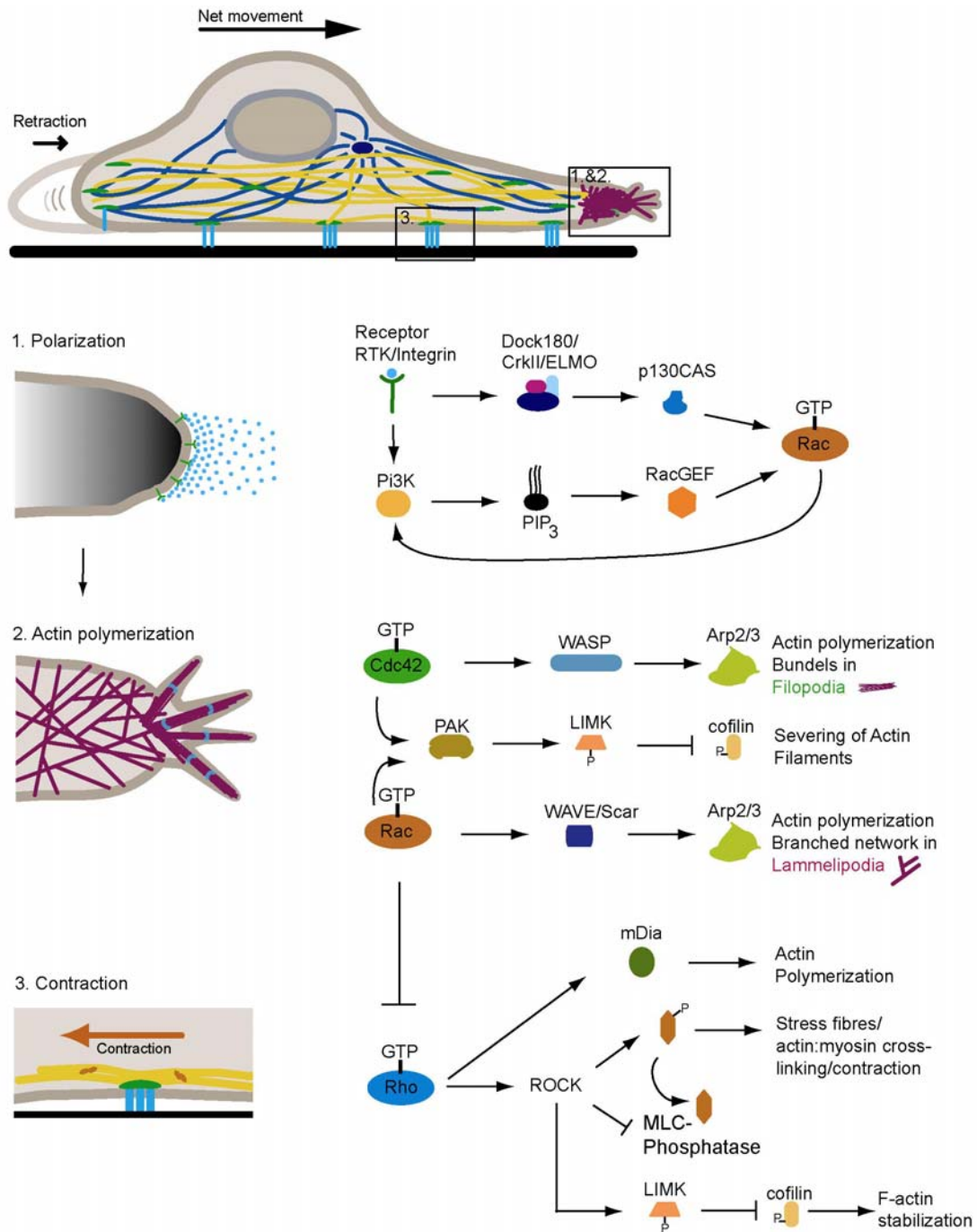


Figure 14:

Effectors and regulators of Rho GTPases. **1.)** The first response of a migrating cell to an external cue (blue dots) is to polarize the cell (shown only the very tip). A transmembrane receptor (Integrin or RTK) can activate Rac GTPases via different mechanisms. Activation of Dock180 which is thought to act in a complex consisting of CrkII/ELMO and p130CAS can lead to activation of Rac. Alternatively, DH domain containing GEFs, which are regulated via PIP₃ can activate Rac. Rac can then also act in a positive feedback loop by activating PI3 kinase which generates PIP₃.

2.) Followed by polarization, actin polymerization leads to the formation of a branched dendritic network as well as filopodia with bundled actin fibers. Both formations require the activation of the Arp2/3 complex, which in the case of filopodia is activated via Cdc42 and WASP proteins, whereas RacGTP activates WAVE family proteins. PAK can be activated via both GTPases, which phosphorylates and activates LIMK, leading in turn to the phosphorylation and inactivation of cofilin.

3.) Contractility is achieved on one hand through Rho kinase (ROCK), which phosphorylates and activates LIMK, again leading to inactivation of cofilin. Additionally, ROCK also phosphorylates and

inactivates the myosin binding unit of myosin light chain phosphatase (MLC-phosphatase) leading to an increased level of phosphorylated myosin which can cross-link actin filaments and generate contractile force. RhoGTP bound to mDia furthermore activates this scaffold protein and cooperates with ROCK in the assembly of actin:myosin filaments.

RacGTP also excludes the action of RhoGTP from the tip of a migrating cell.

Adapted from (Raftopoulou and Hall, 2004)

4. Cell migration *in vivo*: examples from *Drosophila melanogaster*

For decades, cell migration has been studied mostly in tissue culture systems. A wealth of knowledge has been gained, using these systems. Especially the intracellular events that occur as a cell moves over a substratum were studied in great detail. However, as already mentioned above, for many instances, cell migration *in vivo* differs from cell migration *in vitro*, due to the fact that the migrating cells are in contact with a number of different tissues and, therefore, exposed to extrinsic factors such as guidance cues or repellent agents (Ribeiro et al., 2003). These factors play a major role in directional migration of a moving cell. In this context, the genetic power of *Drosophila melanogaster* has proven to be extremely useful in order to study cell migration *in vivo*. As outlined in the paragraphs below, different *in vivo* systems were described and characterized in *Drosophila* with regard to cell migration and genetic analyses aiming at the identification of the major components are underway (see below). Genetic screens, which offer an unbiased approach, often initialized the study of cell migration as seen for border- or germs cells (Liu and Montell, 1999; Moore et al., 1998).

4.1 Migration of primordial germ cells (PGC)

A well characterized example of single cell migration in *Drosophila* is the migration of primordial germ cells. Like in other organisms such as zebrafish or mice, germ cells migrate through and along various somatic tissues soon after their specification to reach the somatic component of the gonad. In the gonad, specific interactions between germ cells and soma regulate sex-specific development and differentiation into either egg or sperm (Santos and Lehmann, 2004a).

In the early *Drosophila* embryo, which is a syncytium of synchronously dividing nuclei, germ cells are the first cells to form. The nuclei become surrounded by cell membranes once they reach the germ plasm at the posterior pole (Fig.I5A). In contrast to the somatic nuclei, these cells cease synchronous divisions and are committed to germ cell fate. Moreover active repression of transcriptional activation keeps the primordial germ cells transcriptional silent until stage 8-9 (3.5h AEL). During gastrulation, as the germ band extends, the PGCs are carried along the dorsal side of the embryo in close association with the posterior midgut primordium. As the primordium invaginates, the germ cells are carried to the inside of the embryo (Fig.I5 B). From there they actively migrate across the epithelium of the posterior

midgut primordium and then dorsally along its basal side (Fig.15 C,D). Finally, germ cells migrate away from the midgut toward the adjacent mesoderm, where they associate with somatic gonadal precursor cells (Fig.15E). During germ band retraction, germ cells and the associated somatic gonadal precursor cells migrate anteriorly until the somatic gonadal mesodermal cells round up to coalesce into the embryonic gonad (Fig. 15 F-H), (Santos and Lehmann, 2004a; Starz-Gaiano and Lehmann, 2001).

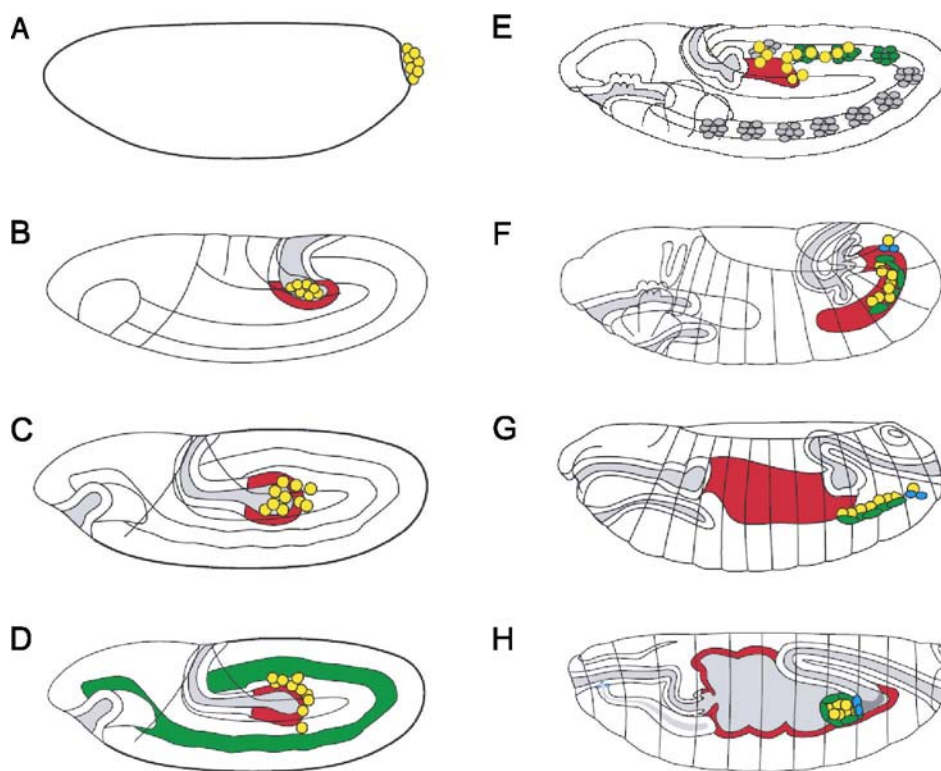


FIGURE 15:

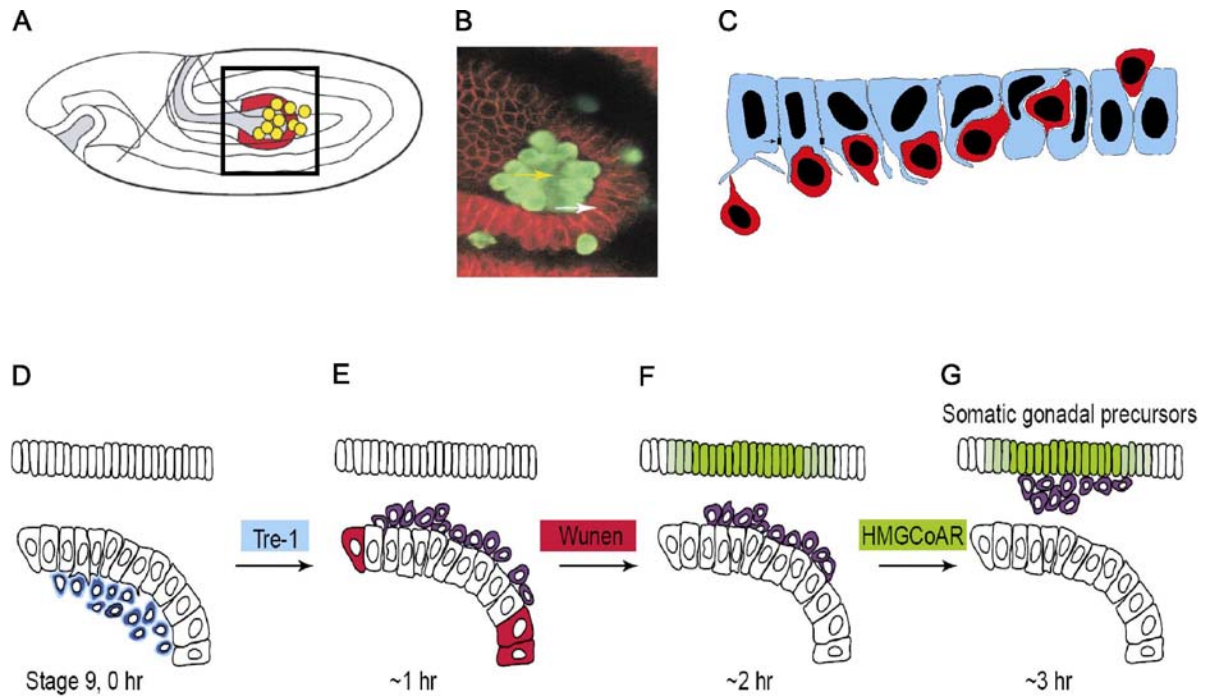
Primordial germ cell (PGC) development and migration in *Drosophila*. **A.)** At about 2.5 h after egg laying (AEL), PGCs are formed and transcriptionally silenced. **B.)** 3.5h AEL: through gastrulation movements, PGCs are swept into the embryo and adhere to the midgut. **C.)** 4.5h AEL: active migration through the midgut epithelium. **D.)** 5h 10min AEL: migration on the midgut. **E.)** 7h AEL: PGCs migrate to the mesoderm through HMGCoAR attraction. **F.)** 9h AEL: PGCs associate with the gonadal mesoderm. **G.)** 10.5 h AEL: PGCs align with the germ-line soma. **H.)** PGC coalescence. Germ cells colored in yellow, midgut in red, mesoderm in green. Adapted after (Santos and Lehmann, 2004a).

The first clear sign of germ cell migration is the crossing of the midgut epithelium (Fig. I6). Ultrastructural studies showed that, in wild-type, apical junctions of the posterior midgut dissolve and gaps are formed between cells through which germ cells are able to pass (Fig. I6 A-C). This type of cell migration is highly similar to the amoeboid cell movements in general and leukocyte cell migration more specifically (see above and (Friedl, 2004; Kunwar et al., 2003)). Until recently, only mutations affecting the midgut epithelium were isolated which prevented this active PGC migration step. In mutants, in which these intracellular gaps fail to form such as in *serpent (srp)* or *huckebein (hkb)*, the germ cells are trapped in the midgut pocket (Jaglarz and Howard, 1994; Jaglarz and Howard, 1995; Moore et al., 1998; Santos and Lehmann, 2004a). Recently a novel G-protein coupled receptor, *trapped in endoderm-1 (tre-1)* was identified, which acts germ cell autonomously (Kunwar et al., 2003). In *tre-1* mutant embryos, most of the germ cells do not transmigrate the primordial midgut and remain trapped inside. In contrast to *srp* or *hkb*, *tre-1* acts directly in the migrating germ cells. Although Rho1 as a possible downstream component was identified, the way Tre-1 mediates transepithelial cell migration remains unclear and a putative Tre-1 ligand remains elusive as well (Kunwar et al., 2003).

Once germ cells have passed through the midgut, they migrate along this epithelium to orient toward the dorsal side of the embryo. *wunen (wun)* and its homologue, *wunen-2 (wun-2)* are expressed in the posterior midgut and repel germ cells from this part of the tissue (Fig. I6 E,F). The two genes act redundantly in the soma; double mutants of *wun* and *wun-2* show a normal midgut exit of the germ cells but they subsequently fail to orient dorsally on the posterior midgut and therefore rarely reach the gonadal precursors (Starz-Gaiano et al., 2001; Zhang et al., 1997). *wun* and *wun-2* encode *Drosophila* homologs of mammalian lipid phosphate phosphatase (LPP) and are transmembrane exoenzymes which hydrolyze phospholipid substrates; however, no specific substrates have been assigned to any of the mammalian LPPs or the Wunens (Santos and Lehmann, 2004a). A very recent report furthermore provided evidence that *wun-2* but not *wun* is also expressed in germ cells and required for germ cell survival (Renault et al., 2004). Wun2 is required for the uptake of a lipid by dephosphorylation and this lipid or a metabolite is required for survival of germ cells by binding an internal or membrane bound target. A mechanism was proposed which presents a novel paradigm for cell survival and cell migration, namely that lipid phosphate signaling not necessarily occurs through G-protein coupled receptors but by means of internalization through dephosphorylation by LPPs (Renault et al., 2004).

From the midgut, germ cells migrate toward the adjacent mesoderm and attach to the gonadal mesoderm (Fig. I6 G). A protein that was shown to provide germ cells with attractive guidance cues is 3-Hydroxyl 3-Methylglutaryl Coenzyme A (HMGCoAR) encoded by the *columbus* (*clb*) gene in *Drosophila*. In *clb* mutant embryos, germ cells fail to migrate toward the mesoderm and remain associated with the dorsal region of the posterior midgut, a phenotype specific for germ cells, since the mesoderm and somatic gonad precursors seem unaffected in *clb* mutants. Furthermore, ectopic expression of *clb* is sufficient to attract germ cells (Santos and Lehmann, 2004a; Van Doren et al., 1998). Further genetic analysis of the HMGCoAR pathway revealed that two enzymes required for the production of isoprenoids, Farnesyl Diphosphate Synthase (*fpps*) and Geranylgeranyl-Diphosphate Synthase (*quemao*) control germ cell migration downstream of *clb*. Both enzymes are expressed in the mesoderm and mutants show a *clb*-like phenotype. Furthermore, another enzyme from the isoprenoid branch of the cholesterol pathway, Geranylgeranyl transferase type I, required for transferring geranylgeranyl pyrophosphate to target proteins, shows a similar phenotype as *clb* when mutated (Santos and Lehmann, 2004b). Interestingly, findings from zebrafish confirmed a role of geranylgeranylation as a critical step in cell migration (Thorpe et al., 2004). These data strongly suggest that a geranylgeranylated protein common to vertebrates and invertebrates mediates germ cell attraction downstream of *clb*. Since several enzymes required for cholesterol biosynthesis are not encoded in the fly genome, cholesterol and cholesterol modified proteins can be ruled out as mediators of PGC in *Drosophila* (Santos and Lehmann, 2004b).

Although many receptors and transducers such as FGF, EGF, Notch, Wingless, Hedgehog, PTEN, and PI3-kinase play no role during germ cell migration (Kunwar et al., 2003), *stat92E* as well as Ras signaling, both activated by Torso, seem to be implicated in germ cell proliferation and migration (Li et al., 2003). Since *Ras* as well as *stat92E* embryos lacking zygotic as well as maternal gene products show severe gastrulation defects, germ cells lacking *Ras* or *stat92E* were transplanted into wild-type embryos. Also when surrounded by wild-type tissue, the mutant germ cells failed to properly migrate, demonstrating the cell autonomous requirement of these genes during germ cell migration. *ras* mutant germ cells additionally poorly survived (Li et al., 2003).

**FIGURE 16:**

Transepithelial migration of PGCs. **A.)** At about 4.5 h AEL, PGCs actively migrate through the epithelium of the posterior midgut primordium. **B.)** Green: α -Vasa labels PGCs. Red: α -Neurotactin labels posterior midgut. **C.)** Schematic drawing of transepithelial migration. PGCs contact posterior midgut cells. Upon engulfment by midgut cells, they start to squeeze through the epithelium and exit on the other side facing the dorsal mesoderm. **D.-G.)** Factors involved in the transepithelial migration, migration on the midgut and guided migration towards the mesoderm. Adapted from (Jaglarz and Howard, 1995; Raz, 2004; Santos and Lehmann, 2004a).

4.2 Migration of hemocytes

A less well investigated type of single cell migration in *Drosophila* is the migration of hemocytes, which are the *Drosophila* blood cells and play a major role in the innate immune response and in the removal of apoptotic cells.

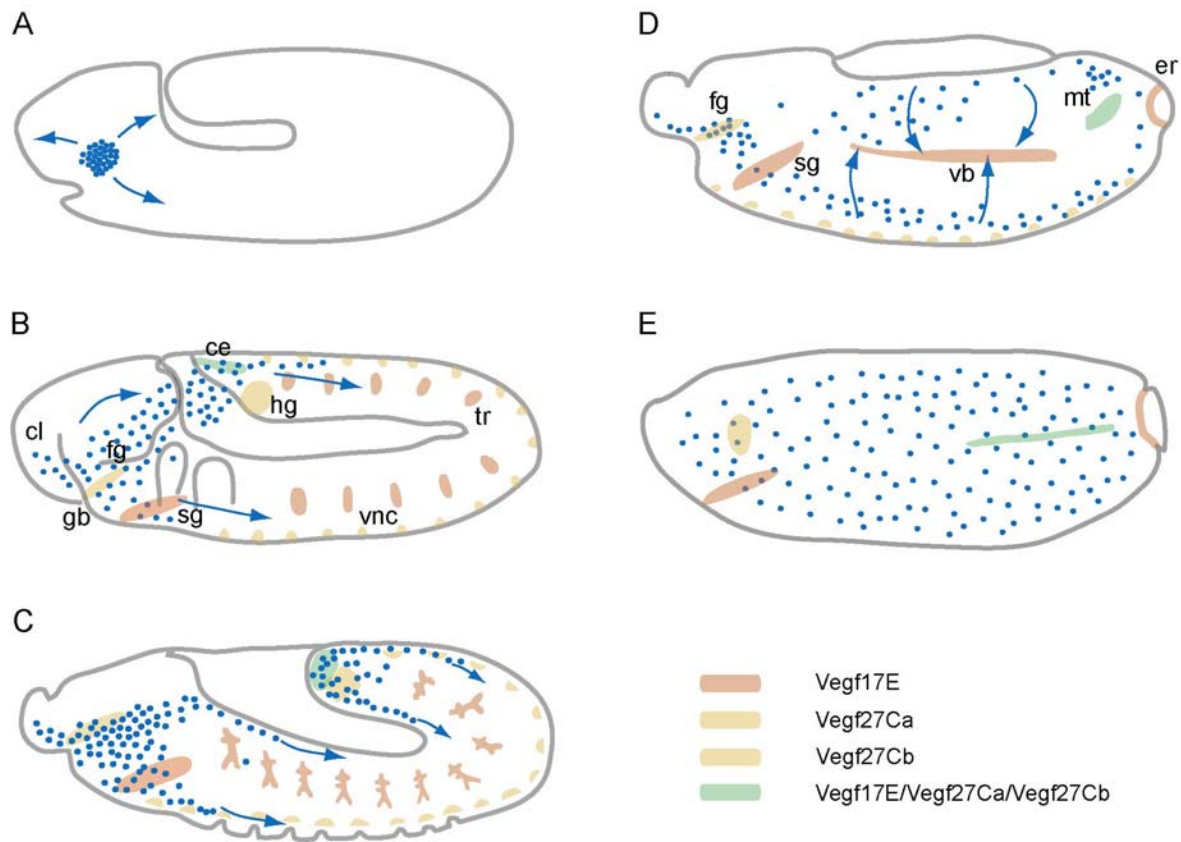
The hemocytes can first be identified approximately 2 hours after the onset of gastrulation (late stage 10) as a subpopulation of mesodermal cells located in the head of the embryo. Four mitotic cell cycles gives rise to about 600 hemocytes in the procephalic mesoderm. In addition, a small group of mesodermal cells in the lateral and midlateral part of the gnathal segments become hemocytes. Therefore, the procephalic and the gnathal mesoderm represent the only source of the approximately 700 hemocytes, which will not divide anymore after stage 11. At the beginning of germ band retraction (early stage 12), hemocytes start to spread throughout the embryo (Fig. I7 A). Moving anteriorly and ventrally, they populate the clypeolabrum and gnathal buds. Posterior migration brings them into the tail end of the germ band (Fig. I7 B,C). A substantial part of hemocytes remain in the dorsal head region.

During stages 13-14, hemocytes migrate from both ends of the embryo towards its middle (Fig. I7 D). They follow different tracks and migrate between the ventral epidermis and the ventral nerve cord, between the dorsal surface of the ventral nerve cord and the mesoderm, along the dorsal boundary of the epidermal primordium as well as along the gut primordium. By stage 14, most parts of the embryo are evenly populated with hemocytes (Fig. I7 E) with dense clusters observable in the head as well as around the fore- and hindgut (Cho et al., 2002; Tepass et al., 1994).

Hemocyte migration is guided in part by the fly homologue of the PDGF/VEGF receptor, called PVR, VEGF receptor or Stasis (Fig. I7). Upon specification, hemocytes start to express PVR (Cho et al., 2002; Heino et al., 2001). Hemocytes lacking PVR differentiate and initiate migration correctly but stall before crossing the amnioserosa and do not disperse uniformly. Remarkably, three genes coding for VEGF exist in *Drosophila*; they are expressed in cell populations along the migratory route of the hemocytes (Fig. I7). Single *pvf* genes show no effect on blood cell migration, but RNAi against all three *pvfs* show a similar phenotype as seen in *pvr* mutants. Moreover, ectopic expression of a single *pvf* results in the misguidance of hemocytes (Cho et al., 2002).

The RAS-MAPK pathway is activated in hemocytes through PVR and expression of a dominant-negative RAS protein (DRAS1N¹⁷) caused an early migration arrest, implicating RAS in the process of hemocyte cell migration (Cho et al., 2002). However, since initial migration to the caudal region as well as anterior and ventral migration but also late dispersal of hemocytes are not affected in *vegfr* mutant embryos, other signaling pathways might be involved in these early and late migration steps.

Recently another report provided evidence that VEGFR fulfils at least two important functions in the embryonic hematopoietic system, as shown already by Cho and coworkers (Cho et al., 2002). It is required for hemocyte migration but additionally PVR is also required for survival of blood cells throughout embryonic development (Bruckner et al., 2004).

**FIGURE 17**

Hemocyte migration. Expression of VEGF genes as indicated by the color code in the figure legend. Blue dots represent migrating hemocytes. **A.)** Stage 10: hemocytes migrate out in three directions. This early hemocyte migration is not guided by VEGFs. **B.)** Stage 11: Hemocytes migrated anteriorly into clypeolabrum (cl), ventrally into gnathal buds (gb), as well as posteriorly into the tail region. Vegf 17E expression can be detected in the trachea (tr), salivary gland (sg) and in a caudal ectodermal patch (ce) together with Vegf27Ca,b, which are also expressed in the foregut (fg) and ventral nerve cord (vnc). **C.)** Stage 12: Migration occurs toward middle of the embryo along the vnc, gut and dorsal epidermis. Expression as before. **D.)** Stage 13: Hemocytes reached the central region and start to spread as indicated by arrows. Expression is seen in visceral branches (vb) salivary gland (sg) and ectodermal ring (er) for Vegf17E, foregut and vnc for Vegf27Ca,b. All three ligands are coexpressed in malpighian tubules (mt). **E.)** Stage 15: Hemocytes are distributed throughout the embryo. Expression is detected as before only in the visceral branch and the vnc expression is not detected anymore. Adapted according to (Cho et al., 2002).

4.3 Border cell migration

A lot of insight into guided cell migration has been gained from the analysis of border cells. These cells consist of a group of about eight somatic cells that perform a simple, stereotypic migration during *Drosophila* oogenesis. The migration is estimated to take 6 hours. The border cells arise and delaminate from the follicular epithelium, a monoepithelial layer consisting of about 650 post-mitotic cells (Fig. I8) (Montell, 2003; Rorth, 2002).

A fascinating feature about border cell migration is that these cells migrate as a coherent group of cells and invade the germ-cell cluster, migrating on and between the giant nurse cells towards the oocyte. When the cells reach the oocyte, the border cell cluster turns and migrates dorsally to reside over the oocyte nucleus. The border cells have the essential function of making a hole in the micropyle, a specialized structure of the eggshell, so the resulting egg can be fertilized. Therefore females containing no border cells or border cells defective in migration are sterile (Montell, 2003; Rorth, 2002).

The invasive cell migration pattern of *Drosophila* border cells makes them a genetically tractable system in order studying invasive cell migration as it also occurs during cancer.

Therefore, genetic screens were performed with the aim to isolate mutations in which this cell migration pattern is disturbed (Duchek and Rorth, 2001a; Liu and Montell, 1999; Montell et al., 1992).

One of the first mutations which was isolated based on its female-sterile phenotype was the transcription factor *slow border cells (slbo)*, a member of the mammalian enhancer binding protein (C/EBP) (Montell et al., 1992). Null mutations in *slbo* are lethal and border cells fail to initiate migration. Among the known target genes of *slbo* are the FGF receptor *btl* (Murphy et al., 1995), *Jing*, a zinc-finger transcription factor (Liu and Montell, 2001), myosin VI encoded by *jaguar* (Geisbrecht and Montell, 2002), a pointed-end directed motor protein, as well as focal adhesion kinase (FAK) (Bai et al., 2000). Many of these genes are also required in other developmental- or cellular processes, thus loss-of-function mutations often lead to lethality. In order to study the function of these genes during border cell migration, wild-type or dominant-negative forms of the proteins of interest can be expressed (Rorth, 1996). Alternatively, border cells are made homozygous for the mutated gene of interest in an otherwise heterozygous animal. Such mosaic clones basically allow to study the loss-of-function effect of almost every gene of interest, of which mutants are available (Bai et al., 2000; Liu and Montell, 1999; Montell, 2003).

The egg chamber is surrounded by the follicular epithelium of which only roughly eight cells delaminate and become migratory border cells (Montell, 2003). A fascinating question is therefore what precisely is required to convert a stationary epithelial cell to a become a migrating invasive cell? It was shown that the JAK/STAT pathway (see Fig. I8) is involved in this important step (Beccari et al., 2002; Silver and Montell, 2001). As already mentioned, border cells migrate as a cluster consisting of the outer border cells and two central polar cells (Niewiadomska et al., 1999). These polar cells develop earlier during oogenesis and are themselves not able to migrate (Silver and Montell, 2001) but are passively pulled along by the outer border cells (Han et al., 2000). The cytokine ligand for the JAK/STAT pathway is encoded by the *Drosophila* gene *unpaired (upd)* and is specifically expressed in the ovary. At stage 9, when border cell migration starts, *upd* expression is restricted to the polar cells (Fig. I8 A). Outer border cells mutant for *upd* show no border cell migration defect, whereas polar cells mutant for *upd* fail to initiate border cell migration, even when all outer border cells were wild-type. This indicates that Upd is required for activating the JAK/STAT pathway in outer border cells in order to initiate border cell migration. Moreover, outer border cells mutant for *Stat92E* or hopscotch (*hop*) or the unpaired receptor *domeless*, also known as *Master of Marelle (Mom)*, failed to migrate. Thus, polar cells secrete Unpaired in order to recruit adjacent follicle cells into the cluster and causes them to become migratory. This model is also supported by the fact that ectopic expression of Upd or Hop causes additional follicle cells to become migratory (Montell, 2003; Silver and Montell, 2001). Since expression of border cell markers such as *Slbo* or *Jing* are absent or reduced in border cells mutant for *Stat92E*, the JAK/STAT pathway presumably acts upstream of *slbo* (Silver and Montell, 2001).

For border cells to initiate migration, not only correct differentiation but also the correct timing is necessary. A rise in the concentration of the *Drosophila* steroid hormone Ecdysone in the ovary precisely coincides with the timing of border cell migration. Moreover, mutations in the steroid hormone receptor coactivator gene *taiman (tai)*, which is related to AIB1 (amplified in breast cancer 1) as well as mutations in the Ecdysone receptor subunit EcR abolish border cell migration. Interestingly, DE-Cadherin was abnormally elevated at the border cell/nurse cell junctions and FAK distribution was altered in *tai* mutant border cell clusters, indicating that Tai might also affect the expression of downstream effectors implicated in the effective turnover of E-Cadherin-containing adhesion complexes (Bai et al., 2000).

Since primordial germ cells or hemocytes require attractive and in some cases also repulsive cues in order to migrate to designated locations (see above), the same principles could also apply for the directed migration of border cells. As already described, the first phase of border cells migration is directed to the oocyte. Once they reach the oocyte, border cells move dorsally towards the oocyte nucleus. In a misexpression screen (Duchek and Rorth, 2001a) it was found that EGFR signaling is required for the dorsal migration. Upon removal of the EGF-receptor (EGFR) in border cells, migration towards the oocyte nucleus was abolished. Gurken (an EGF ligand), which is secreted from the oocyte, is required for this step.

EGFR signaling appears to be specific and independent of the Raf/MAPK pathway for dorsal border cell migration. Expression of activated versions of Heartless (λ -Htl) (Duchek and Rorth, 2001a), or loss-of-function clones of *breathless* (*btl*) (*htl* and *btl* both encode *Drosophila* FGF receptors, see below) had no effect on dorsal border cell migration; also border cells mutant for *raf* migrated normally (Duchek and Rorth, 2001a; Murphy et al., 1995)

However, Ras signaling seems to be required for posterior as well as dorsal border cell migration since expression of dominant negative Ras (RasN17) or activated Ras (RasV12) moderately affected both migration steps (Duchek and Rorth, 2001a; Lee et al., 1996a). One putative candidate as a downstream effector of Ras, besides the canonical Raf/MAPK pathway, is PI3K; PI3K has been implicated as a mediator of chemotaxis in different systems. However, dominant-negative or dominant active versions of PI3K did not affect border cell migration. Moreover, RTK adaptor proteins such as Drk, Shc, Dos or PIC γ which can bind directly with their SH2 domain to RTKs, had any effect on border cell migration when mutated (Duchek and Rorth, 2001a; Duchek et al., 2001b).

In the same gain-of-function screen (Duchek and Rorth, 2001a), PVF1 was identified as a guidance molecule for posterior migration towards the oocyte. This protein is related to the mammalian platelet-derived growth factor (PDGF) and vascular endothelial growth factor (VEGF). PVF1 acts through PVR (also called Stasis or VEGFR, see above) and has a largely redundant function with EGFR. Uniform expression of PVF1 had a moderate effect on border cell migration (Duchek and Rorth, 2001a; McDonald et al., 2003) whereas expression of an activated form of PVR (λ -PVR) completely blocked border cell migration (Duchek and Rorth, 2001a). However, expression of a dominant-negative PVR (DN-PVR) as well as null mutations in PVF1 or PVR itself caused a non-penetrant migration phenotype, indicating that PVR probably acts redundantly (Duchek et al., 2001b; McDonald et al., 2003). It turns out

that border cells can use either PVR or EGFR for posterior migration. Only when both are perturbed by the expression of dominant-negative versions, migration is completely blocked (Duchek et al., 2001b).

Expression of λ -PVR in border cells showed a massive increase in filamentous actin (F-actin), changes in cell shape and Actin-rich protrusions, indicating that PVR signals to the actin cytoskeleton. Furthermore, coexpression of dominant-negative Rac suppressed the effects of activated PVR (λ -PVR), providing a link to the small Rho-GTPase Rac (Duchek et al., 2001b). It has been reported previously that border cell specific expression of activated (Duchek and Rorth, 2001a) or dominant-negative versions of Rac (Duchek et al., 2001b; Murphy and Montell, 1996) affect border cell migration. These findings were further confirmed by the analysis of *rac* loss-of-function mutants and support an involvement of Rac in border cell migration downstream of PVR (Geisbrecht and Montell, 2004).

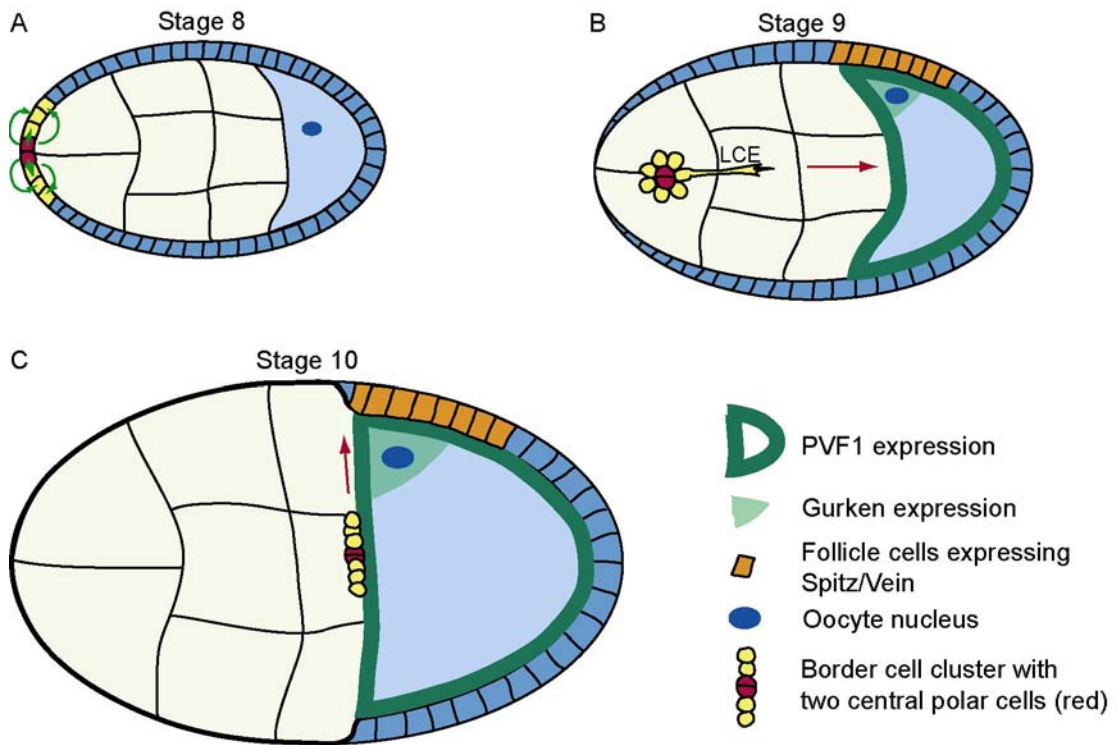
Surprisingly, it was recently found that Rac interacts with Profilin and DIAP1 to form a complex (Geisbrecht and Montell, 2004). DIAP1, *Drosophila* inhibitor of apoptosis, has been known for its role to prevent cells from dying by blocking apoptosis-inducing caspase activity (Wang et al., 1999). However, *DIAP1* loss-of-function mutants fail to migrate and suppress the effect of RacN17, indicating a novel apoptosis-independent role for DIAP1 in cell migration, which is mediated through the small GTPase Rac (Geisbrecht and Montell, 2004).

In line with these findings it was shown that *myoblast city* (*mbc*), the *Drosophila* homologue of mammalian Dock180 and *C. elegans* CED-5, which acts as an activator of Rac, was also required for border cell migration. However, *mbc* is not absolutely required for border cell migration since a small fraction of *mbc* mutant border cells were still able to migrate. *Mbc* was also shown to act downstream of PVR (Duchek et al., 2001b). Therefore border cell migration depends on an intact actin cytoskeleton, which is partially regulated through PVR, that acts on Rac to some extent through *Mbc*. Rac furthermore regulates the actin cytoskeleton with the help of profilin and DIAP1.

Another gene, identified based on its bristle phenotype and called *mal-d*, also displays an effect on the actin cytoskeleton. *Mal-d* contains an N-terminal MAL homology domain (MHD), three RPEL motifs as well as a SAP domain and a less well defined basic region (Somogyi and Rorth, 2004). Mammalian MAL family proteins have recently been found to interact with SRF and serve as transcriptional cofactors of SRF (Miralles et al., 2003). Like DSRF (Guillemin et al., 1996; Montagne et al., 1996), *mal-d* is essential for development and encodes for a SRF cofactor, so far unidentified in *Drosophila*. Both genes show the same

border cell phenotype, namely reduced migration and absence of the robust actin cytoskeleton normally visible in migrating wild-type border cells. This indicates that these genes act together during development to control specific processes that are highly dependent on the actin cytoskeleton (Somogyi and Rorth, 2004). Border cells normally produce a long actin-rich cellular extension, which is dependent on proper cell specification, EGFR and PVR signaling as well as substrate adhesion via DE-Cadherin (Fulga and Rorth, 2002). Although this extension is formed in *mal-d* mutant cells, large round cytoplasmic fragments appear to break off from the extension and perform directional migration on their own, without the cell body following (Somogyi and Rorth, 2004). Based on the levels of nuclear accumulation of the MAL-D/SRF complex, it was suggested that the activity of MAD-D and SRF was induced by tension or deformation of migrating border cells. Therefore, the physical state of a cell determines whether MAL-D accumulates in the nucleus or not with the consequence of building of a robust actin cytoskeleton when needed (Somogyi and Rorth, 2004). However the regulation of this fascinating process remains elusive.

For a cell to migrate, not only the actin cytoskeleton at the leading edge is of importance but also the polarity of the cell. In the follicular epithelium, Par-6 and Bazooka (Baz), the *Drosophila* homologue of Par3 are localized at the apical surface and this asymmetrical localization is maintained in migrating border cells. Disruption of *baz* or *par-6* function in border cells leads to a delay in migration as well as a mislocalization of membrane markers such as DE-cadherin. Thus, it was suggested that Par-6 and Baz are required for the proper distribution of membrane proteins and for efficient migration (Pinheiro and Montell, 2004).

**FIGURE 18**

A.) Border cell migration starts with the recruitment of follicular epithelial cells (green arrows) into a migratory border cell cluster through the action of unpaired (*upd*), which is expressed in two red polar cells from stage 8 on. **B.)** One border cell from the cluster, consisting of 6-10 cells including the two centrally located polar cells, extends a long cellular extension (LCE). The cluster migrates anteriorly toward the oocyte. **C.)** Dorsal migration is initiated upon reaching the oocyte and mediated through the secretion of the EGF ligand Gurken, which also induces expression of Spitz and Vein from the dorsal follicular epithelium.

Adapted from (Montell, 2003)

4.4 Mesodermal cell migration

Mesodermal cell migration takes place early during *Drosophila* gastrulation. Before the mesodermal cells can begin their journey, their fate has to be established, which is brought about by the transcription factor Dorsal. Dorsal protein concentration is highest in the nuclei on the ventral side of the embryo and activates the expression of two key factors for mesodermal determination, *twist* and *snail*. Twist is a transcriptional activator whereas Snail, which contains five zinc fingers, acts as a transcriptional repressor (Ip and Gridley, 2002; Leptin, 1999).

The mesodermal cell layer invaginates about three hours after egg laying (Fig. 19) and this process is heralded by subtle changes in the shapes of the most ventrally located blastoderm cells. These cells first flatten on their outer apical side, while their nuclei, initially positioned directly underneath the apical cell cortex, begin to migrate basally. Within the next 10-15 minutes, the apical sides constrict more progressively which results in the formation of wedge shaped cells which also shorten along their basal/apical axis. As a result of these changes, the blastoderm epithelium first forms an indentation, the ventral furrow, which is then completely internalized (Leptin, 1999).

Once inside the embryo, where the cells form an epithelial tube, the mesoderm primordium loses its epithelial character and disperses into single cells which divide, attach to the ectoderm and migrate out on the ectoderm to form a single cell layer (Leptin, 1999). By early stage 10, the mesoderm has formed a monolayer, and spans the entire dorsoventral axis on either side of the extended germ band. Subsequently, under the control of extrinsic factors such as *Dpp* or *wg*, the mesoderm is partitioned into visceral, somatic and cardiac subdomains from which a variety of organs then derived. The dorsolateral migration of the mesoderm assures the correct positioning of mesodermal cells relative to the inducing ectoderm (Michelson et al., 1998b).

The first changes in cell shape in the mesoderm are coordinated by a signaling pathway consisting of *folded gastrulation* (*fog*), probably a secreted protein, the $G\alpha$ -subunit *concertina* (*cta*) as well as more downstream regulators of the actin cytoskeleton such as DRhoGEF2, and DrhoA .

The second change in cell shape, which results in the flattening and subsequent disintegration of the tube, depends on *heartless* (*htl*), one of the two fibroblast growth factor receptors

(FGFRs) identified in *Drosophila* (Knust and Muller, 1998; Shishido et al., 1993). In *heartless* mutants, mesodermal cells fail to spread out on the underlying ectoderm (Fig.19 E, F). This is due to the fact that *htl* deficient cells fail to dissociate properly from each other, do not migrate in a dorsolateral direction and as a consequence, fail to reach the dorsal edge of the ectoderm (Michelson et al., 1998b). A recent study further subdivided mesodermal migration into three phases. Phase 1 starts after mesoderm invagination and the formation of an epithelial tube. At this stage, the mesodermal cells appear relatively smooth. After disassembly of the epithelial tube and mitosis, phase 2 begins, in which the mesodermal aggregate migrates out into dorsolateral directions. The cells at the leading edge of the aggregate are stretched along the dorsoventral axis and extend multiple cellular protrusions, which are also seen in cells immediately following the leading edge cells. Once the cells reach their final position, and form a coherent monolayer (phase 3), large extensions are absent and only few protrusions are observed (Schumacher et al., 2004).

In *htl* mutant embryos, the mesodermal epithelial tube extends further into the embryo compared to wt embryos (phase 1, Fig.19 E, F). Moreover, the leading edge cells do not extend dorsolaterally (phase 2) and the mesoderm also fails to form a monolayer configuration (phase 3). However, few protrusions are observed during phase 3 but not phase 2. Therefore, *htl* seems to be required for effective attachment of mesodermal cells to the ectoderm, which might promote the protrusive activity of mesoderm cells during migration (Schumacher et al., 2004). Another gene, which shows a similar phenotype is encoded by the *downstream-of-FGF* (*dof*) locus. *Dof* was independently identified in three labs and is also called *stumps* (*sms*) or *heartbroken* (*hbr*) (Imam et al., 1999; Michelson et al., 1998a; Vincent et al., 1998). Genetically, *dof* was placed downstream of *htl* but upstream of *ras*, since activated Ras but not Htl can partially rescue the mesodermal cell migration phenotype (Michelson et al., 1998a; Vincent et al., 1998). Signals from the FGF receptors are transmitted through the Ras/MAPK pathway (Kouhara et al., 1997) and can be monitored *in situ* with an antibody against the active, dual phosphorylated form of MAPK (dp-ERK) (Gabay et al., 1997). In wt mesodermal cells, dpERK staining can be seen in leading edge cells, whereas in *htl* or *dof* mutant cells, this staining is absent, indicating that *Dof* is required for transmitting the signal from the Htl receptor to the Ras/MAPK pathway (Michelson et al., 1998a; Vincent et al., 1998).

Recently, the endless debate concerning the existence of FGF ligands for the Htl receptor found an end. Two independent studies reported the identification of genes encoding for the FGF ligands (Gryzik and Muller, 2004; Stathopoulos et al., 2004). One gene is called *thisbe*

(*ths*) (Stathopoulos et al., 2004) or *FGF8-like1* (Gryzik and Muller, 2004) the other *pyramus* (*pyr*) (Stathopoulos et al., 2004) or *FGF8-like2* (Gryzik and Muller, 2004). The two genes have most likely arisen by tandem gene duplication and are, based on their function and homology, closely related to the vertebrate FGF8 (Gryzik and Muller, 2004; Stathopoulos et al., 2004).

ths and *pyr* are expressed in the cells that serve as substrate for mesoderm cells during migration. However, the differential expression suggests that the gene products might initially work in a redundant fashion and later serve distinct functions in mesoderm morphogenesis. Embryos deficient for both genes showed mesoderm migration defects similar to those seen in *htl* or *dof* mutant embryos. However, only injection of dsRNA against both genes or *FGF8-like2/pyr* alone did affect the differentiation of mesoderm derivatives, indicating that *FGF8-like2/pyr* has some nonredundant function during mesoderm differentiation. On the other hand, both genes seemed to be involved in cell shape changes and have therefore some redundant function in this process. Mesodermal cells that lack *FGF8-like1/ths* and *FGF8-like2/pyr* also fail to exhibit Htl-dependent activation of MAP kinase, indicating that these genes are bona fide candidate ligands for Htl receptor (Gryzik and Muller, 2004; Stathopoulos et al., 2004).

As already mentioned, DrhoA seems to be required for invagination of the presumptive mesoderm; nevertheless its function is neither needed for the actual migration step, nor for the protrusive activity (Schumacher et al., 2004). However, two recent studies reported that another RhoGEF called *pebble* (*pbl*) is required for mesodermal cell migration; mesodermal cells mutant for *pbl* showed fewer protrusions in the direction of migration. Furthermore, the cells appear to be more closely associated with neighboring mesodermal cells. The *pebble* phenotype can therefore be characterized as a failure of epithelial-mesenchymal transition and subsequent lack of dorsal migration and resembles the *htl* phenotype (Schumacher et al., 2004; Smallhorn et al., 2004). MAP kinase is still activated in *pbl* mutants arguing that Pbl is dispensable for Htl mediated MAP kinase activation and also shows that MAP kinase activation alone is not sufficient for cell shape changes in the mesoderm. Since activated forms of Ras can neither completely rescue the mesodermal cell migration defects of *htl* or *dof* mutant embryos, nor re-establish the characteristic cell shape changes in phase 1&2, it was proposed that a second signaling pathway acts in parallel to the Ras/Raf/MAPK pathway in mesodermal cell migration (Imam et al., 1999; Michelson et al., 1998a; Michelson et al.,

1998b; Petit et al., 2004; Schumacher et al., 2004; Smallhorn et al., 2004; Vincent et al., 1998).

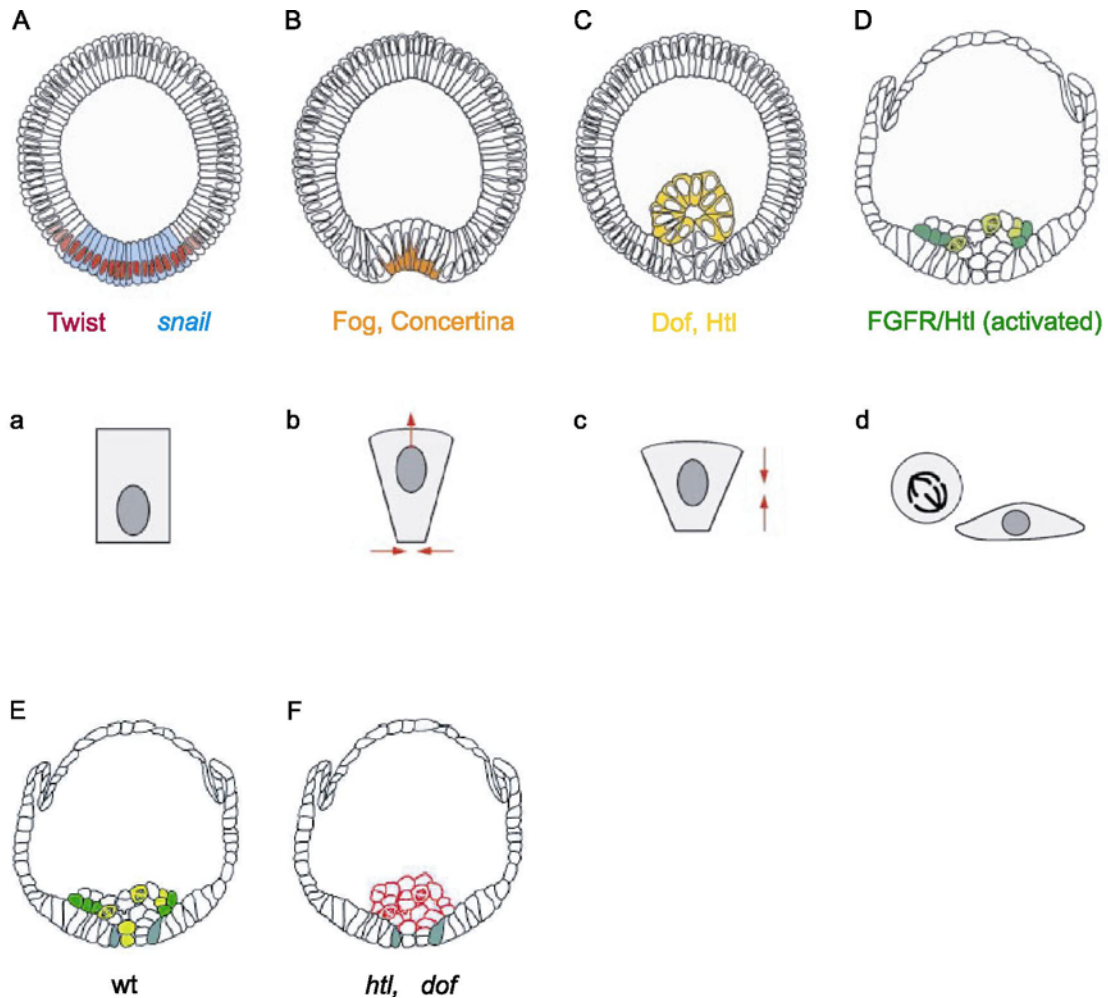


FIGURE 19

Mesodermal cell migration is initiated with the invagination of the mesoderm. The two mesodermal marker twist (nuclear protein) and snail (cytoplasmic mRNA) expression are shown. **a.)** characteristic cell shape at this early stage. **b.)** Folded gastrulation as well as concertina activity in apical constrictions. **b.)** As the mesoderm starts to invaginate, the nucleus moves basally and the apical side constricts. **c.)** The invaginated mesoderm forms a tube. Dof and htl are required for the subsequent steps. **c.)** The wedge shaped cells shorten along their apical/basal axis. **d.)** The invaginated mesoderm starts to spread and also continues dividing. Cells with highest htl activity are shown in dark green. **d.)** the mesodermal cells lose their epithelial character and disperse into single cells. **E.&F)** Compared to a wt embryo, mesodermal cells mutant for *dof* or *htl* fail to spread on the underlying mesoderm.

Adapted from (Leptin, 1999; Wilson and Leptin, 2000).

4.5 Tracheal cell migration

The *Drosophila* tracheal system contains approximately 10'000 interconnected tubes that transport oxygen and other gases throughout the body. Tracheal tubes consist of an epithelial monolayer, wrapped into a tube surrounding a central lumen through which gases flow. Oxygen enters the network at the spiracular openings and passes through primary, secondary and terminal branches to reach the target tissues (Ghabrial et al., 2003; Manning and Krasnow, 1993).

The development of the tracheal network during embryogenesis follows a highly stereotypical pattern. The 20 tracheal primordia, 10 cell clusters on each side of the embryo, are of ectodermal origin and are composed of tightly packed columnar cells between 4 and 4.5 hours after egg laying (AEL). The cells in the placode divide once before they start to invaginate (cell cycle 15) and divide one more time while invaginating (4.5-5.5 AEL) to form the 20 tracheal pits. The invagination process is incomplete, leaving a short stalk, the spiracular branch, connecting the sac to the surface. The pits contain about 80 cells, which do not divide anymore until the onset of metamorphosis (Manning and Krasnow, 1993; Samakovlis et al., 1996a). Generally, due to the presumed absence of cell death or further cell division, the tracheal cell number remains constant (Samakovlis et al., 1996a).

At 7 hours AEL, tracheal cells start to migrate in a stereotypical manner in different directions, mostly in an anterior-posterior as well as a dorsal-ventral direction, resulting in the formation of six so called primary branches (Fig. I10, A-D & E-H). At about 8 hours AEL, the main branches can be distinguished within each tracheal metamere: the dorsal trunk anterior (DTa), dorsal trunk posterior (DTp), dorsal branch (DB), visceral branch (VB) as well as the lateral trunk anterior (LTa) and lateral trunk posterior/ganglionic branch (LTp/GB) (Fig. I10 I). A few cells within the central region of the pit form the transverse connective (TC), which connects the dorsal and ventrolateral parts of the tracheal metamere (Fig. I15 B). The spiracular branch (SB), constituted by cells that have remained near the invagination site, closes during stage 12 (8-9 AEL). During their migration, several branches follow certain routes. The DTa and DTp grow in the anterior and posterior direction, respectively, and traverse fields of mesodermal cells, following a groove as they migrate (Franch-Marro and Casanova, 2000). Visceral branches grow inward to target the gut and the ganglionic branches grow ventrally towards the central nervous system (CNS) (Samakovlis et al., 1996a).

During the migration process, most but not all primary branches undergo a period of cell elongation and intercalation, in which cells initially arrange side-by-side, then intercalate and

assume an end to end configuration (Fig. I10, J-M) (Manning and Krasnow, 1993; Samakovlis et al., 1996a).

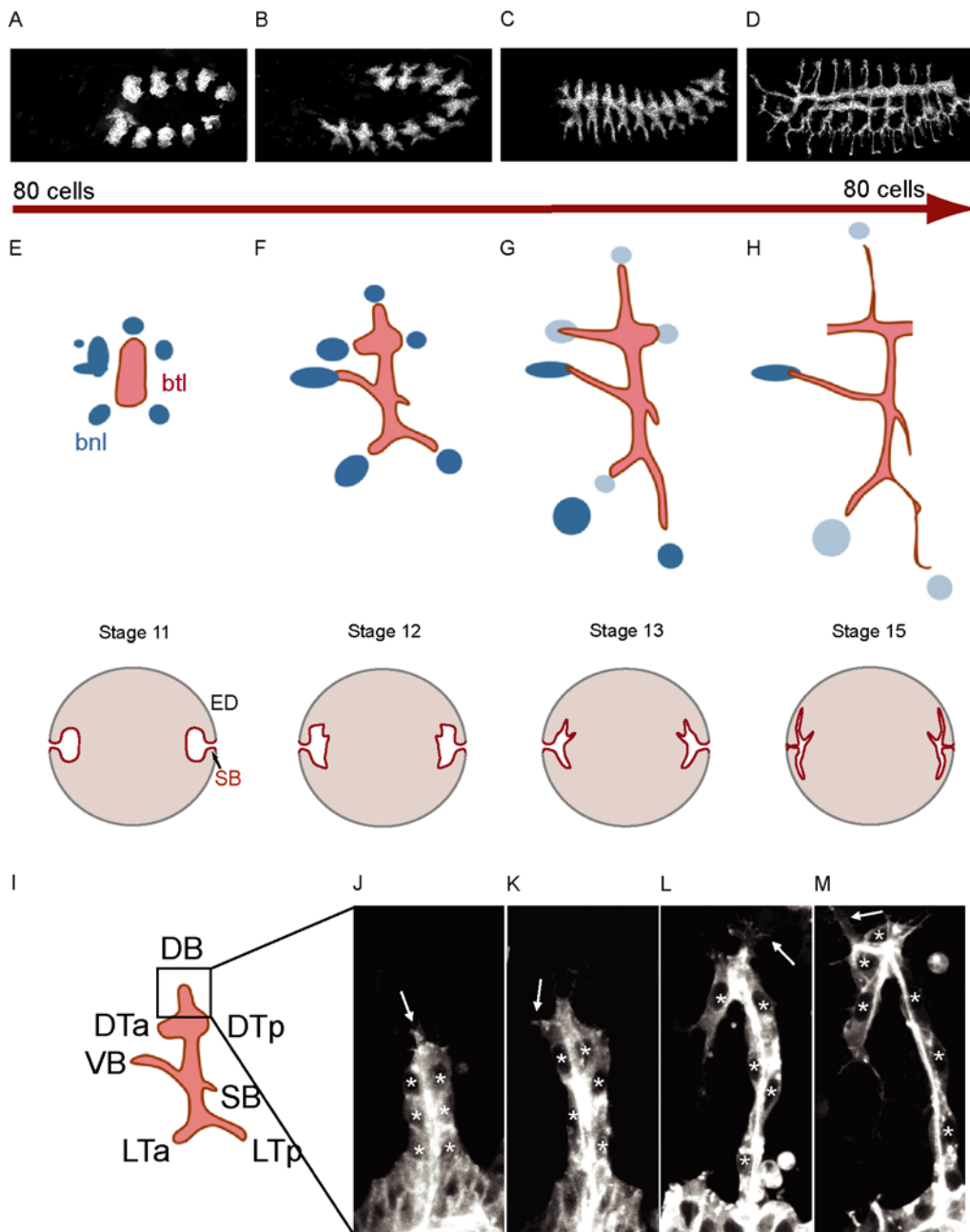


FIGURE I10

A.-D.) Development of the embryonic tracheal system. After invagination and two rounds of cell division the final number of 80 tracheal cells is achieved and remains constant throughout embryonic tracheal development. Tracheal cells start to migrate in a stereotypical fashion to elaborate into a branched tubular network. **E.-H.)** Only one metamere is schematically shown. Tracheal cells (red) express the FGF receptor *Btl* and migrate towards ectodermal cells expressing *bnl* (blue). *bnl* expression fades (light blue) as soon as tracheal cells reached the *bnl* expressing cells and reinitiates in cell clusters several cell diameters away. Cross-sections of embryos are shown below. The invaginated placode is initially still connected with the epidermis (ED) through the spiracular branch (SB). This connection will be closed in late embryonic stages. **I.)** Nomenclature of tracheal branches. DB: dorsal branch, DTa/p: dorsal trunk anterior/posterior, SB: spiracular branch, VB: visceral branch, LTa/p: Lateral trunk anterior/posterior. **J.-M.)** Cell intercalation in the DB. Asterisks mark nuclei which are at the beginning in a side-to side orientation **J**) but intercalate and elaborate in an end-to end orientation **M.** White arrows indicate filopodia. Adapted from (Cabernard et al., 2004)

Tracheal development starts with the specification of the tracheal precursor cells, which is mainly achieved through the two transcription factors, Trachealess (Trh), a basic helix-loop-helix (bHLH)-PAS domain protein and Ventral veinless (Vvl, also called drifter), a POU-domain containing DNA binding protein. Trh acts as a heterodimer with Tango (Tgo), a dARNT/HIF β (*Drosophila* aryl hydrocarbon receptor nuclear translocator/hypoxia induced factor β) homologue; this heterodimer is required for several steps during tracheal development. Trachealess expression identifies the clusters of epidermal tracheal precursor cells at stage 10 (4h AEL). In *trh* mutants, the tracheal precursors fail to undergo the cytoskeletal rearrangements necessary for their invagination and lack expression of many downstream genes necessary for branching such as *breathless (btl)*, *downstream-of-FGF (dof)* or *rhomboid (rho)* (Boube et al., 2000; Isaac and Andrew, 1996; Wilk et al., 1996).

The expression of *trachealess* is initiated by the JAK/STAT pathway, since mutations in *domeless (dom)*, an interleukin receptor homologue as well as *stat92E*, a downstream transcription factor in the JAK/STAT pathway, abolish *trh* expression (Brown et al., 2001; Chen et al., 2002).

The subsequent branching of the tracheal precursor cells as described above, is achieved through cell migration, cell intercalation and cell shape changes. In order to migrate, the tracheal cells depend on the FGF signaling pathway (which will be discussed in molecular terms in the next paragraph). The FGF ligand *branchless (bnl)* was discovered in a P transposon induced enhancer trap screen. Bnl codes for the *Drosophila* FGF homologue. *bnl* is expressed in ectodermal cell clusters around the invaginated placode and prefigures the direction of migration. In *bnl* loss-of-function mutants, tracheal cells do not migrate. Moreover, *bnl* misexpression can attract new branches towards sites of ectopic expression (Samakovlis et al., 1996a). Two other genes which basically show the same no-migration phenotype are *btl*, the *Drosophila* FGF receptor (Dossenbach et al., 2001; Klambt et al., 1992; Reichman-Fried et al., 1994; Reichman-Fried and Shilo, 1995; Shishido et al., 1993), as well as *downstream of FGF (dof/sms/hbr)*, an intracellular protein required for FGF signaling (Imam et al., 1999; Michelson et al., 1998a; Vincent et al., 1998).

Based on these findings it was proposed that FGF signaling provides spatial and temporal cues necessary for directed tracheal cell migration. Consistent with this idea was the finding that mutations in the *sugarless* as well as *sulfateless* genes, two enzymes involved in the synthesis of heparan sulfate glycosaminoglycans, result in phenotypes similar to those observed in *btl* or *bnl* (Lin et al., 1999). Moreover, using RNA interference in *Drosophila* embryos showed an involvement of the *Drosophila* heparan sulfate 6-O-sulfotransferase

(dHS6ST) in Bnl-mediated FGF signaling since RNAi injected embryos show phenotypes similar to the ones obtained from *bnl*, *sgl*, *sfl*, *btl* or *dof* mutants (Kamimura et al., 2001). Therefore, enzymes involved in the synthesis and modification of heparan sulfate proteoglycans, apparently play fundamental roles in the formation of a stable Bnl/Btl complex required for efficient signaling.

As in mesodermal cell migration, FGF signaling activates the Ras/MAPK pathway, which can be monitored by the active, dual phosphorylated form of MAPK (dp-ERK) (Gabay et al., 1997). In *bnl*, *btl* or *dof* mutants, ERK is not activated in tracheal cells. Moreover, an involvement of the canonical Ras/MAPK pathway in tracheal cell migration has been proposed since activated forms of Ras or Raf can partially rescue the *btl* or *dof* migration phenotype (Imam et al., 1999; Vincent et al., 1998). Moreover, mutations in *corkscrew* (*csw*), which codes for a Shp-2 tyrosine phosphatase, generally thought to be a positive regulator of RTK signaling, also displays tracheal cell migration defects (Perkins et al., 1996). Although a strict correlation between tracheal cell migration and MAPK activation was observed, a deletion analysis of Dof resulted in the finding that MAPK activation is not sufficient for tracheal cell migration since one particular deletion construct, which lacks the ankyrin repeats in a *dof* minimal rescue construct, is not capable of rescuing tracheal cell migration although it activates MAPK (Petit et al., 2004).

Generally, evidence was provided which showed that Dof functions as an adaptor that couples FGFR, but not other receptor tyrosine kinases, to downstream effectors in cell migration (Dossenbach et al., 2001). Biochemical analysis also revealed that Dof is recruiting a signaling complex to the activated FGF-receptor, consisting of Dof and Csw, which takes place after phosphorylation of Dof by FGFR (Petit et al., 2004; Wilson et al., 2004).

In vivo confocal microscopy showed that FGF signaling affects the formation of actin rich dynamic filopodia. Whereas in wt tracheal cells dynamic filopodia were observed, mostly in leading tip cells, these filopodia were absent in *btl*, *bnl* or *dof* mutants. Overexpression of *bnl* in all tracheal cells induced the formation of numerous filopodia in all tracheal cell (Ribeiro et al., 2002). FGF signaling is also required for expression of genes, which control subsequent branching steps in the tracheal system such as *pointed* (*pnt*) (Samakovlis et al., 1996a). In *pnt* mutants, however, no change in filopodia number or dynamics was observed indicating that FGF signaling induces cytoskeletal dynamics in the absence of transcriptional induction on any known gene and it is therefore likely that the signaling input directly influences cytoplasmic events in the absence of changes in nuclear transcription (Ribeiro et al., 2002).

These results (Ribeiro et al., 2002) as well as the findings of Valérie Petit (Petit et al., 2004) suggested the existence of additional proteins which bind either to FGFR, Dof or Csw in order to fulfill the chemotactic response and to provide a link to the actin cytoskeleton and its regulators. Up to date no clear candidates were identified although yeast-to-hybrid screens using Dof as a bait were performed (Battersby et al., 2003; Cabernard, 2000).

A number of additional genes, which show a tracheal cell migration defect, were also isolated, such as *trachea defective (tdf)* or *ribbon (rib)*. *tdf* encodes for a putative bZIP transcription factor (Eulenberg and Schuh, 1997) whereas *rib* encodes for a nuclear protein with a BTB/POZ (for Poxvirus and zinc finger) domain and pipsqueak DNA-binding motif (Bradley and Andrew, 2001; Shim et al., 2001). *tdf* is a target of Tracheless and is neither dependent nor does it interfere with FGF signaling; Tdf seems to be required for general tracheal cell migration (Eulenberg and Schuh, 1997). However, target genes of Tdf or the cellular basis for the *tdf* phenotype remain elusive.

Ribbon seems to be required rather specifically for the movement of tracheal cell bodies and the apical surface. Tracheal cells migrate with their basal side in the leading edge. Cytoplasmic processes extend from the basal surface of the lead cells, and cell bodies and the apical surface follow these extensions during migration. In *rib* mutants, the movement of the apical tracheal surface is severely defective; however the basal side is still extending filopodia and continues to extend actively. Moreover, *btl* and *bnl* expression is not affected in *rib* mutants and *rib* mutant tracheal cells are still able to respond to Bnl signaling. Since Rib is a nuclear protein with the ability to bind to DNA, it was proposed that Rib regulates the expression of target genes. However, no Rib targets, which could shed light on the cellular basis of the *rib* phenotype have been identified up to date (Bradley and Andrew, 2001; Shim et al., 2001).

Since small GTPases of the Rho family regulate the actin cytoskeleton (Raftopoulou and Hall, 2004), an involvement of *rac*, *rho* or *cdc42* during tracheal cell migration seems likely. Three *rac* genes are encoded in the *Drosophila* genome, *rac1*, *rac2* and *mig-2-like (mtl)* (Hakeda-Suzuki et al., 2002; Ng et al., 2002). Direct evidence using loss-of-function alleles of these genes in tracheal cell migration has not been shown so far. Using dominant-negative *cdc42* constructs, a reduction in filopodia extension of dorsal trunk cells and reduced ability for dorsal trunk fusion has been shown (Wolf et al., 2002). Rac on the other hand was shown to be required for cell rearrangements in the tracheal epithelium, and genetically interacts with FGF signaling (Chihara et al., 2003).

4.6 Comparison of cell migration systems in *Drosophila*

The complexity of *in vivo* systems compared to tissue culture systems with regard to the analysis of cell migration is much higher. Therefore it is not surprising that additional factors were identified, factors which only influence the migratory behavior of certain cell types. The major components required for cell migration in the systems analyzed are listed in table 1. A comparison of the different systems shows that primordial germ cells obviously rely on a different set of guidance and repellent cues than hemocytes, border-, mesodermal- or tracheal cells. However, certain molecules are repeatedly used in different contexts. The VEGF signaling pathway, for example, is first utilized for the guidance of hemocytes (Cho et al., 2002) and will be reused much later for the migration of border cells in the adult female ovary (Duchek et al., 2001b). FGF signaling is required for the mesodermal cells to contact the mesoderm (Gisselbrecht et al., 1996; Michelson et al., 1998b) and probably also for the extension of filopodia, and the same pathway is needed for filopodia induction during tracheal cell migration (Ribeiro et al., 2002). All systems most certainly rely on a set of similar actin dynamics effectors in order to fulfill the basic migratory task, such as actin bundling, treadmilling, severing, and contraction. Most progress towards elucidating these factors *in vivo* has been achieved in border cells. This simple system benefits of the broadest set of genetic tools available, including the possibility to generate mutant cells in a heterozygous tissue (clonal analysis) (Montell, 2003).

The tracheal system has been shown to be a very good system for studying branching morphogenesis (Manning and Krasnow, 1993). Until recently, most phenotypes interfering with the establishment of the interconnected tubular network were assigned as migration mutants. This picture was changed with the help of novel imaging methods, especially 4D microscopy, which allowed a more careful characterization of the available mutants (Ribeiro et al., 2002). At the moment, the most important signaling input for tracheal cell migration seems to come from FGF/Bnl. However, apart from some intracellular factors such as *csw* and *dof*, a clear picture on what components are required downstream, is lacking. In addition, the connection to the cytoskeleton, which has been shown to be involved in FGF-mediated cell migration (Ribeiro et al., 2002; Sato and Kornberg, 2002), is lacking. This has also often to do with the fact that many important genes, such as *ras*, are maternally contributed and, for this reason, cannot easily be studied in the embryonic tracheal system. Nevertheless as will be showed in the results section, the larval tracheal system, especially the air sacs, provide a novel system which facilitates the genetic analysis of tracheal cell migration. This is of major

relevance, since air sacs also respond to FGF signaling (Sato and Kornberg, 2002). For these reasons, the FGF signaling pathway will be outlined in the next paragraph and the system, based on the findings of Sato& Kornberg (Sato and Kornberg, 2002) discussed subsequently.

TABLE 1: Comparison of cell migration systems in *Drosophila*

A: GERM CELL MIGRATION

GENE	PRODUCT	FUNCTION	REFERENCE
Trapped in endoderm-1 (tre-1)	G-protein coupled receptor	Migration of PGC across posterior midgut epithelium	(Kunwar et al., 2003)
Wunen (wun)	Lipidphosphate phosphatase (LPP)	PGC repulsion	(Renault et al., 2004; Starz-Gaiano et al., 2001; Zhang et al., 1997)
Wunen 2 (wun-2)	Lipidphosphate phosphatase (LPP)	PGC repulsion and survival	(Renault et al., 2004; Starz-Gaiano et al., 2001; Zhang et al., 1997)
Hmgcr/columbus (clb)	HMGCoA reductase	PGC attraction to mesoderm	(Santos and Lehmann, 2004b; Van Doren et al., 1998)
Fpps	Farnesyl-diphosphate synthase	PGC attraction to mesoderm	(Santos and Lehmann, 2004b)
Quemao (qm)	Geranyl-geranyl diphosphate	PGC attraction to mesoderm	(Santos and Lehmann, 2004b)
GGT1	Geranyl-geranyl transferase	PGC attraction to mesoderm	(Santos and Lehmann, 2004b)
Ras	Small GTPase	Initial mitotic divisions of PGC Later for directed migration, survival and colonization of PGCs.	(Li, 2004)
Stat92E	Signal-activated transcription factor	Initial mitotic divisions of PGC Later for directed migration, survival and colonization of PGCs.	(Li, 2004)
Slow as molasses (slam)	novel	Cellularization, transition of PGCs from gut to mesoderm.	(Stein et al., 2002)

B: Hemocyte migration

GENE	PRODUCT	FUNCTION	REFERENCE
PVR/VEGFR (stasis)	PDGR/VEGF receptor	Guidance of hemocytes	(Cho et al., 2002)
PDGF-and VEGF-related factors (PVF1, PVF2, PVF3)	PDG/VEGF ligand	Guidance of hemocytes	(Cho et al., 2002)
Ras	Small GTPases	Hemocyte migration, probably downstream of VEGFR	(Cho et al., 2002)

C: BORDER CELL MIGRATION

GENE	PRODUCT	FUNCTION	REFERENCE
Slob border cells (slbo)	C/EBP homologue, Transcription factor	Activates expression of downstream genes required for migration	(Montell et al., 1992; Murphy et al., 1995; Rorth and Montell, 1992)
Jing	AEBP2 homologue (Jing) Zinc-finger transcription factor	Cooperates with C/EBP to regulate gene expression	(Liu and Montell, 2001)
Chickadee (chic)	Profilin	Stimulates actin polymerization. Maintenance of actin monomer concentration	(Geisbrecht and Montell, 2004; Montell, 2003)
Drac1	Rho-family GTPase	Actin polymerization at leading edge	(Duchek et al., 2001b; Geisbrecht and Montell, 2004; Murphy and Montell, 1996)
Shotgun (shg)	DE-Cadherin	Border-cell-nurse-cell traction	(Niewiadomska et al., 1999)
Zipper (zip)	Myosin II	Retraction of trailing edge	(Rorth et al., 2000)
Taiman (tai)	AIB1 homologue Steroid hormone receptor co-activator	Regulates timing of migration in response to Ecdysone	(Bai et al., 2000)
Ultraspiracle (usp)	RXR homologue Ecdysone receptor subunit	Regulates timing of migration in response to Ecdysone	(Bai et al., 2000)
Ecdysoneless (ecd)	Not known	Regulates ecdysone production	(Bai et al., 2000)
PDGF-and VEGF-related factor-1 (PVF1)	PVF1 or VEGF17E Secreted ligand for receptor tyrosine kinase	Guidance of border cells towards the oocyte. Might function redundantly with Grk, PVF2 or PVF3	(Duchek et al., 2001b)
PDGF/VEGF receptor (PVR)	RTK receptor for PVF1-3	Guidance of border cells to the oocyte. Might function redundantly with EGFR receptor	(Duchek et al., 2001b)
Stat92E	Signal-activated transcription factor	Causes cells to become migratory upon signal reception from polar cells	(Silver and Montell, 2001)
Unpaired (upd)	Secreted cytokine; activates JAK/STAT pathway	Stimulates follicle cells next to polar cells to cluster around polar cells and migrate	(Silver and Montell, 2001)

Hopscotch (hop)	Janus kinase homologue Non-receptor tyrosine kinase	Converts epithelial follicle cells to migratory cells	(Silver and Montell, 2001)
Domeless (dom)	Receptor for upd	Transmits upd signal to Hop kinase	(Silver and Montell, 2001)
Jaguar (jag)	Myosin VI Pointed end directed actin motor	Stabilized DE-Cadherin. Might stimulate protrusion of actin filaments	(Geisbrecht and Montell, 2002)
Epidermal Growth factor receptor (EGFR)	Epidermal growth factor receptor Receptor tyrosine kinase	Required for dorsal border-cell migration.	(Duchek and Rorth, 2001a)
Spaghetti squash (sqh)	Non-muscle myosin II light chain	Required for border cell migration.	(Edwards and Kiehart, 1996; Fulga and Rorth, 2002)
<i>Drosophila</i> serum response factor (DSRF/ blistered/ pruned)	Transcription factor	Forms a complex with it's cofactor MAL-D and is required for a robust actin cytoskeleton. Responds to physical stress to enhance the actin cytoskeleton	(Somogyi and Rorth, 2004)
Mal-d	Transcriptional cofactor of SRF	Forms a complex with SFR and is required for a robust actin cytoskeleton. Responds to physical stress to enhance the actin cytoskeleton	(Somogyi and Rorth, 2004)
Thread (th)	<i>Drosophila</i> inhibitor of apoptosis (DIAP1)	Affects border cell migration via Rac and the actin cytoskeleton. Associates with Rac and Profilin in a complex	(Geisbrecht and Montell, 2004)
Myoblast city (mbc)	Dock180 homologue	Activator of Rac. Severely impairs border cell migration although not absolutely required	(Duchek et al., 2001b)
Ras	Small GTPase	Involved in border cell migration	(Duchek and Rorth, 2001a; Lee et al., 1996a)
Par-6	PDZ domain protein	Complexed with Baz and aPKC in apical epithelial domains. Involved in border cell migration	(Pinheiro and Montell, 2004)
Baz/Par-3	PDZ domain protein	Complexed with Par-6 and aPKC in apical epithelial domains. Involved in border cell migration	(Pinheiro and Montell, 2004)

D: Mesodermal cell migration

GENE	PRODUCT	FUNCTION	REFERENCE
Heartless (htl)	FGF-receptor Receptor tyrosine kinase	Attachment of mesodermal cells to the ectoderm	(Beiman et al., 1996; Gisselbrecht et al., 1996; Michelson et al., 1998b; Schumacher et al., 2004)
Downstream of FGF/stumps/ heartbroken (dof/sms/hbr)	Intracellular component of FGF signaling	Acts downstream of htl; transmits the signal to the Ras/MAPK pathway	(Imam et al., 1999; Michelson et al., 1998a; Vincent et al., 1998)
thisbe (ths)/ FGF8-like1	FGF8-like secreted ligand	Required for mesodermal cell migration Cell shape changes	(Gryzik and Muller, 2004; Stathopoulos et al., 2004)
Pyramus (pyr)/ FGF8-like2	FGF8-like secreted ligand	Cell shape changes, mesoderm differentiation	(Gryzik and Muller, 2004; Stathopoulos et al., 2004)
Pebble (peb)	DRhoGEF	Mesodermal migration, formation of protrusions. Epithelial-mesenchymal transition (EMT)	(Schumacher et al., 2004; Smallhorn et al., 2004)
Sugarless (sgl)	Enzyme catalyzing heparan sulfate proteoglycan biosynthesis	Required for the biosynthesis of heparan sulfate glycosaminoglycans which function as coreceptors mediating formation of active FGF/FGFR signaling complexes. Required for FGF-mediated mesodermal cell migration	(Lin et al., 1999)
Sulfateless (sfl)	Enzyme catalyzing heparan sulfate proteoglycan biosynthesis	Required for the biosynthesis of heparan sulfate glycosaminoglycans which function as coreceptors mediating formation of active FGF/FGFR signaling complexes. Required for FGF-mediated mesodermal cell migration	(Lin et al., 1999)
Corkscrew (csw)	nonreceptor protein tyrosine phosphatase	Htl dependent mesodermal cell migration	(Johnson Hamlet and Perkins, 2001)

E: TRACHEL CELL MIGRATION

GENE	PRODUCT	FUNCTION	REFERENCE
Branchless (bnl)	Secreted FGF ligand	Chemoattractant for tracheal cells. Required for tracheal cell migration. Filopodia induction	(Ribeiro et al., 2002; Sutherland et al., 1996)
Breathless (btl)	FGF ligand; Receptor tyrosine kinase	Required for tracheal cell migration. Activation of the MAPK pathway. Filopodia induction	(Lee et al., 1996b; Reichman-Fried et al., 1994; Reichman-Fried and Shilo, 1995; Ribeiro et al., 2002)
Downstream of FGF/stumps/hea rtbroken (dof/sms/hbr)	Intracellular component of FGF signaling	Required for tracheal cell migration. Acts downstream of btl; transmits the signal to the Ras/MAPK pathway Filopodia induction	(Dossenbach et al., 2001; Imam et al., 1999; Michelson et al., 1998a; Ribeiro et al., 2002; Vincent et al., 1998)
Sugarless (sgl)	Enzyme catalyzing heparan sulfate proteoglycan biosynthesis	Required for the biosynthesis of heparan sulfate glycosaminoglycans which function as coreceptors mediating formation of active FGF/FGFR signaling complexes. Required for FGF-mediated tracheal cell migration	(Lin et al., 1999)
Sulfateless (sfl)	Enzyme catalyzing heparan sulfate proteoglycan biosynthesis	Required for the biosynthesis of heparan sulfate glycosaminoglycans which function as coreceptors mediating formation of active FGF/FGFR signaling complexes. Required for FGF-mediated tracheal cell migration	(Lin et al., 1999)
Heparan sulfate 6-o-sulfotransferase (dHS6st)	Enzyme catalyzing heparan sulfate proteoglycan biosynthesis	Required for the biosynthesis of heparan sulfate glycosaminoglycans which function as coreceptors mediating formation of active FGF/FGFR signaling complexes. Required for FGF-mediated tracheal cell migration	(Kamimura et al., 2001)
Corkscrew (csw)	nonreceptor protein tyrosine phosphatase	btl dependent mesodermal cell migration	(Perkins et al., 1996; Petit et al., 2004)
Ribbon (rib)	BTP transcription factor with Pipsqueck DNA binding domain	Required for cell body movement and lumen growth.	(Bradley and Andrew, 2001; Shim et al., 2001)

5. FGF signaling pathway

FGF signaling plays fundamental roles in various cellular and developmental processes in vertebrates. FGF signaling is involved in angiogenesis (Javerzat et al., 2002), wound healing, embryonic development, tumor growth and cancer (reviewed in Powers et al., 2000), limb development (reviewed in Hogan, 1999; Xu et al., 1999) and branching morphogenesis (reviewed in Affolter et al., 2003; Hogan, 1999) in the vertebrate lung. This chapter will summarize the components involved in FGF signaling in vertebrates and *Drosophila*. The importance of FGF signaling will be further highlighted with two examples, namely limb formation and lung branching morphogenesis.

5.1 FGF signaling in vertebrates

In humans, 23 FGF family members and four tyrosine kinase receptor prototypes have been described. The complexity is further increased by the existence of several isoforms (proteolytic processed derivatives) within FGF family members and the presence of spliced variants of FGF receptors (Itoh and Ornitz, 2004; Javerzat et al., 2002; Ornitz and Itoh, 2001). Like in *Drosophila*, heparan sulfate proteoglycans (HSPGs) are required as coreceptors for vertebrate FGF-FGFR interactions (reviewed in Ornitz, 2000).

Most studies of FGFR-mediated signal transduction have been carried out using FGFR-1 as the prototypical FGFR. It is assumed that the signaling pathways from different FGFRs are very similar, owing to the high degree of homology at the amino acid level between different receptor types. The principle difference between FGFRs is the strength of tyrosine kinase activity (Raffioni et al., 1999). FGFR1 is composed of three extracellular immunoglobulin (Ig)-like domains (Ig1-3), an acidic region between Ig1 and Ig2, a transmembrane domain and an intracellular tyrosine kinase domain. The intracellular cytoplasmic tail of FGFR1 contains seven tyrosine residues that can be substrates for phosphorylation. Tyr653 as well as Tyr654 are important for the catalytic activity of the activated FGFR and are essential for signaling. Tyr766 has been shown to bind the SH2 domain of phospholipase C-gamma (PLC γ). The remaining tyrosines can be mutated without loss of MAPK activity. Upon ligand binding, the FGF receptors phosphorylate specific tyrosine residues on their own and on each other's cytoplasmic tails. Phosphorylated tyrosine residues in turn recruit other signaling molecules to the activated receptors and propagate the signal through many possible transduction

pathways. Consequently, receptor dimerization is a key step for transmitting the extracellular signal intracellularly (reviewed in Powers et al., 2000)

Target proteins may be recruited to the activated receptor through the interaction of Src-homology 2 (SH2) domains of the target protein and specific phosphotyrosine residues on the activated receptor. The SH2 containing proteins may then be targets for receptor mediated phosphorylation themselves or they may act as adaptor proteins and recruit other target proteins (Powers et al., 2000).

5.2 The PLC γ signaling pathway

PLC γ is a good example of such an SH2 containing protein. PLC γ was found to be associated with FGFR1 after ligand-dependent activation. The SH2 domain of PLC γ binds to tyr766 of FGFR1. This binding is essential for phosphatidylinositol hydrolysis. PLC γ cleaves phosphatidyl-inositol-4,5-bisphosphate to inositol trisphosphate (IP₃) and diacylglycerol (DAG). IP₃ facilitates the release of calcium stores from the endoplasmic reticulum while DAG and calcium activate PKC. However, mutation of tyr766 does not affect FGFR mediated mitogenesis, neuronal differentiation or mesoderm induction in *Xenopus* animal caps. PLC γ signaling might therefore be redundant with respect to mitogenesis and differentiation or plays an important role for some other function of FGFR signaling (Powers et al., 2000) (Fig. I11).

5.3 Src & Crk

Crk is another SH2/SH3 containing adaptor protein linking FGFR to the downstream signaling molecules Shc, C3G and Cas, which may in turn propagate a mitogenic signal from FGFR. Crk binds via its SH2 domain to tyr463 of the activated FGFR. Signaling through Crk has no effect on cell motility, yet, depending on the cell type, is important for proliferation.

The non-receptor tyrosine kinase Src might link FGFR signaling to cortactin, a focal adhesion-associated protein that binds filamentous actin, which would provide an alternate pathway to that of PLC γ for FGFR-mediated cytoskeletal alterations. However, there are conflicting reports concerning the interaction of Src and FGFR (Powers et al., 2000) (Fig. I11).

5.4 SNT1/FRS2

In contrast to most other RTKs, FGFRs lack a Grb2 binding site and thus need to recruit an intermediate docking molecule to activate the MAPK pathway. This is achieved through the adaptor protein SNT1/FRS2, which links activated FGFR to the Ras/MAPK pathway. This linkage is important for growth-factor induced cell cycle progression. Activation of SNT-1/FRS2 recruits the adaptor protein Grb-2 /Sos, which in turn recruits Ras to the FGFR complex (Kouhara et al., 1997). Additionally, activated FRS2 also binds the protein tyrosine phosphatase Shp2, which also binds to the docking protein Gab-1. Recruitment of Grb2-Gab1 leads to activation of the cell survival pathway via PI3K (Hadari et al., 2001; Ong et al., 2001).

SNT-1/FRS2 is localized to the inner leaflet of the cell membrane by myristylation. FRS2 is constitutively associated with FGFR1 independent of receptor activation, in contrast to NGF receptors, which also uses FRS2 as an adaptor protein.

Thus FGFR signals by at least two independent pathways. First FGFRs utilize the traditional SH2-linked pathway joining FGFR directly to PLC γ and Crk, and probably indirectly to Src. Secondly, FGFR is linked via SNT1/FRS2 to the Ras/MAPK pathway (Powers et al., 2000) (Fig. I11).

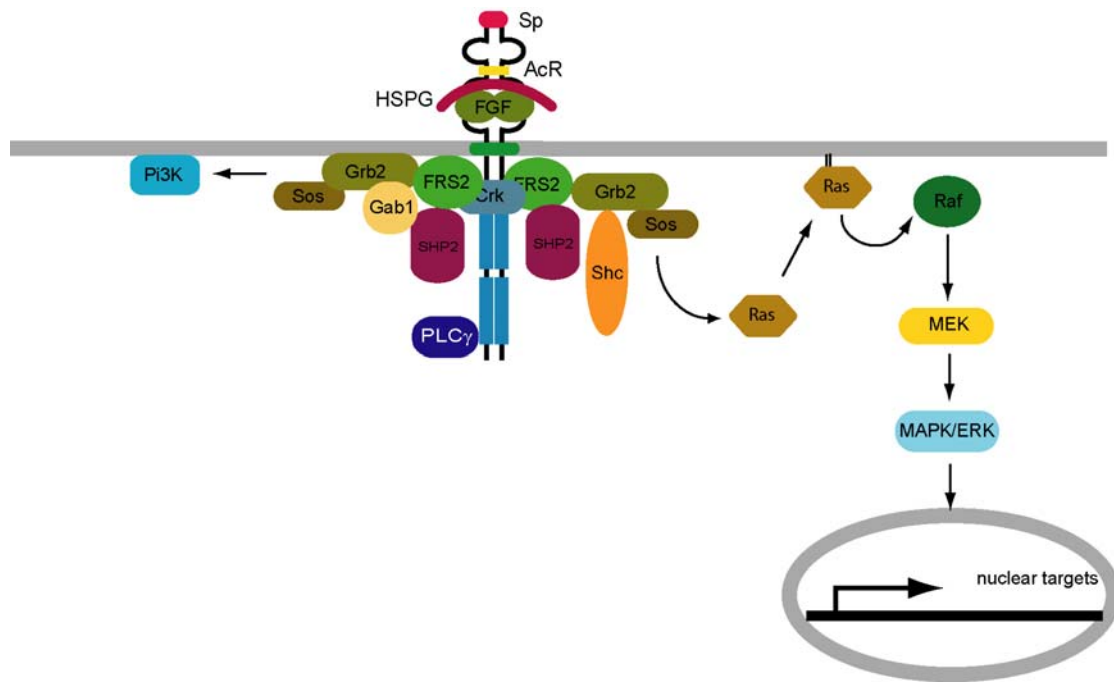


FIGURE I11

FGF signaling in vertebrates. Shown is the vertebrate FGFR1 which contains an N-terminally located signal peptide (Sp), Ig domains (black loops) as well as an acidic region (AcR, yellow box). Intracellular split kinase domains are shown by blue bars. FGF ligand binding requires the interaction of heparan sulfate proteoglycan (HSPG). In the cell, FRS2/SNT1 binds constitutively to the juxtamembrane region of the receptor and recruits a signaling complex consisting of the phosphatase Shp2, Grb2-Sos and Shc. This complex either activates Ras which triggers MAPK activation or, in a slightly altered composition consisting also of the docking protein Gab1, activates PI3K and the cell survival pathway. PLC γ also directly binds to the receptor with its SH2 domain. The SH2/SH3 domain containing protein Crk also binds to a tyrosine residue in the juxtamembrane domain and activates downstream components such as Shc. Adapted from (Javerzat et al., 2002).

5.5 FGF signaling in *Drosophila*

The *Drosophila* genome contains two FGF receptors, *breathless* (*btl*) and *heartless* (*htl*) (Shishido et al., 1993). As outlined above, *btl* is involved in tracheal cell migration (Lee et al., 1996b; Murphy et al., 1995; Reichman-Fried et al., 1994; Reichman-Fried and Shilo, 1995) whereas *htl* plays fundamental roles in mesodermal cell migration as well as in the formation of mesodermal derivatives (Michelson et al., 1998b; Schumacher et al., 2004). Up to date, there are three identified FGF ligands; *Bnl*, which signals through *Breathless* (Sutherland et al., 1996), *Thisbe* (*ths*)/FGF8-like1 and *Pyramus* (*pyr*)/FGF8-like2, which both signal through *Heartless* (Gryzik and Muller, 2004; Stathopoulos et al., 2004). Furthermore, heparan sulfate proteoglycans function as co-receptors to mediate the formation of an active FGF-FGFR complex (Kamimura et al., 2001; Lin et al., 1999).

Intracellularly, two components were identified which link the receptor to the Ras/MAPK pathway. These components are *Dof* (*Sms*, *Hbr*) (Imam et al., 1999; Michelson et al., 1998a; Vincent et al., 1998) and *Corkscrew* (*Csw*), a tyrosine phosphatase showing homology to *Shp2* (Perkins et al., 1996; Perkins et al., 1992; Petit et al., 2004).

Dof is exclusively coexpressed in tissues with either the one or the other of the two FGF receptors and is a specific adaptor for FGF in *Drosophila* (Dossenbach et al., 2001). *Dof* contains two ankyrin-repeats, a coiled coil domain, as well as eight tyrosines, which can, judged by their environment, serve as binding sites for proteins like *Grb2/drk*, *Shp2/Csw*, *PI3K* and *rasGAP* (Vincent et al., 1998). *Dof* represents the founding member of a small family of proteins including *BCAP* and *BANK*, two vertebrate proteins that have recently been identified and shown to regulate B-cell receptor specific *PI3K* activation and calcium mobilization (Okada et al., 2000; Yokoyama et al., 2002).

The intracellular domains of *Btl* and *Htl* are highly divergent from *FGFR1* in the juxtamembrane region, the region in vertebrate *FGFRs* used to recruit *FRS2*. So far, only a distant relative of *FRS2* has been identified in the *Drosophila* genome and it is thought not to be required in *Btl* signaling (Battersby et al., 2003). Therefore, in contrast to *FGFR1*, which takes advantage of *FRS2* as an adaptor, the *Drosophila* *FGFRs* build a complex with *Dof*, which binds directly onto the kinase domain of the two FGF receptors (Battersby et al., 2003; Petit et al., 2004; Wilson et al., 2004) (Fig. I12). Furthermore, upon receptor activation, tyrosine residue 515 of *Dof* becomes phosphorylated and recruits the phosphatase *Corkscrew*, which represents an essential step in FGF induced activation of the Ras/MAPK pathway (Petit et al., 2004). In contrast to *Dof*, which only acts downstream of FGF receptors (Dossenbach et

al., 2001), Csw has been shown to be required for signal propagation downstream of other RTKs such as Torso, EGFR and possibly others (Perkins et al., 1996). It is likely that other conserved RTK signaling components such as Grb2/Drk, Dshc, KSR, Cnk act downstream of FGF receptors and that some of these components could be recruited by Dof and/or Csw in an FGFR dependent manner.

Recently, it was shown that the *Drosophila* p120RasGAP orthologue RasGAP can bind to one conserved juxtamembrane tyrosine residue of FGFR when it is phosphorylated. This interaction requires the SH2 domain of RasGAP. On the other hand, the *Drosophila* dCrk, which is 49% identical with the vertebrate CrkII, does not directly bind to Btl or Htl, neither does the *Drosophila* Grb2 homologue Drk (Woodcock and Hughes, 2004). It was proposed that after ligand binding the *Drosophila* FGFRs undergo autophosphorylation on the juxtamembrane tyrosine residue, thereby providing a docking site for RasGAP. Once recruited, RasGAP becomes a substrate for the active kinase domain of *Drosophila* FGFR. However, null mutants in the gene *vacuolar peduncle* (*vap*) which encodes for RasGAP are viable and therefore *vap* is not an essential gene for development (Botella et al., 2003).

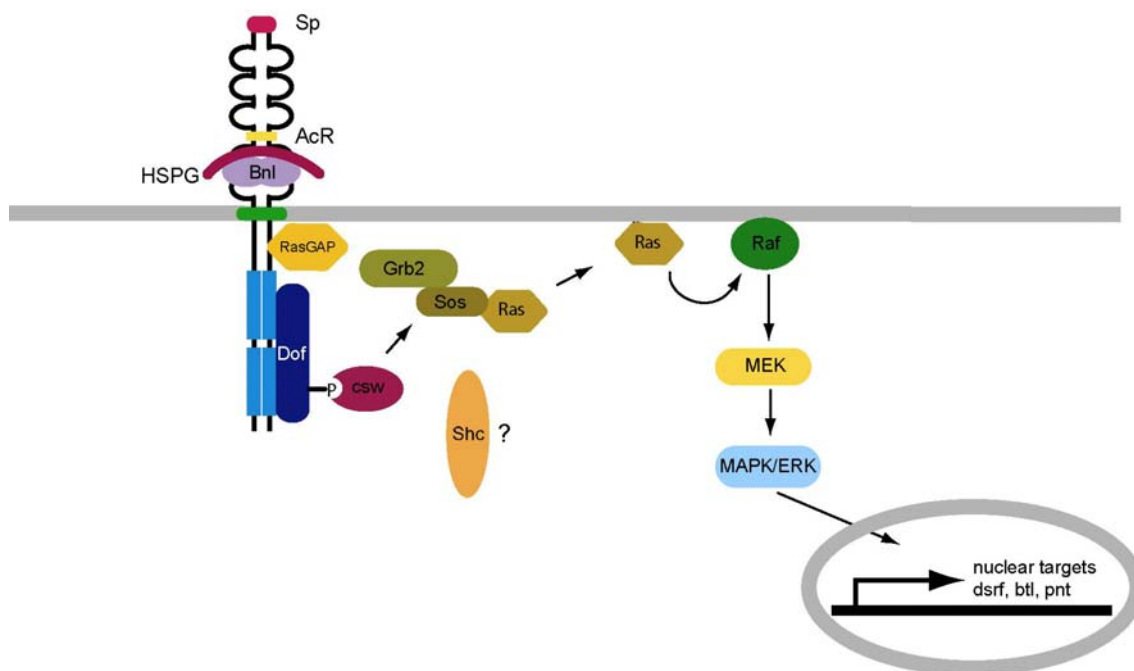


FIGURE I12

FGF signaling in *Drosophila*. Shown is the Btl receptor, similar in composition to the vertebrate FGFR1. Also efficient Btl binding requires an interaction between HSPG, Btl and Bnl. Intracellularly, Dof constitutively binds to the kinase domain and recruits Csw which binds to tyrosine residue 515 of Dof. Csw and Dof are required for activating the canonical Ras/MAPK pathway via activation of Raf. This leads to the expression FGF target genes such as *pnt* or *dsrf*. RasGAP has been shown to bind to the juxtamembrane domain of Btl via its SH2 domains. Also the *Drosophila* Grb2 homologue Drk cannot bind directly to the receptor and it is currently unknown whether it forms a complex consisting of RasGAP, Dof and Csw. Adapted from (Petit et al., 2004)

5.6 Negative regulation of FGF signaling; findings from *Drosophila* and vertebrates

RTK signaling, including and FGF signaling, has to be precisely regulated, both spatially and temporally, in order to ensure physiological appropriate outcome. Nature has invented many ways to control FGF signaling, and some of these are summarized here.

5.6.1 Abnormal wing disc (Awd)

The *Drosophila* gene *abnormal wing disc (awd)* is the homologue of the human gene *nm23*, which encodes a nucleoside diphosphate kinase (NDPK) with tumor metastasis suppressing activity . One potential role for *nm23* as a metastasis inhibitor is regulating cell motility (Steeg et al., 1988).

Using *Drosophila* loss-of-function mutants in *awd*, a recent study provided evidence that this gene is implicated in downregulation of FGF signaling (Dammai et al., 2003). *Awd* seems to attenuate Btl/FGFR activity by vesicle-transport mediated turnover. *awd* loss-of-function mutants show phenotypes that can be classified as ectopic tubule formation and aberrant migration of embryonic tracheal cells. This phenotype was alleviated by reducing the amount of Btl in tracheal cells, indicating that these two genes act in the same pathway. Moreover, Btl/FGFR overaccumulates at the cellular surface in *awd* mutants. Another protein required for vesiculation by pinching off the invaginated vesicles from the membrane is Dynamin, encoded by *shibire (shi)* in *Drosophila*. In *shi* mutants, similar defects were observed and combinations of *shi* and *awd* mutants increased the severity of the branching phenotypes. Taken together, these results suggest that internalization of membrane-bound FGFR, mediated by *Awd* and *Shi/Dynamin*, plays a major role in ensuring the proper level of the chemotactic response in tracheal cells (Dammai et al., 2003). These findings are in line with earlier studies indicating that *Awd* participates in synaptic vesicle internalization, most likely by supplying GTP required for *Shi/Dynamin* mediated endocytosis (Krishnan et al., 2001). Although the exact mechanism is not known, it is therefore assumed that *awd/nm23* act as a GEF-like activator of GTPases.

5.6.2 Cbl mediated protein degradation

Another way of regulating FGF signaling is by protein degradation mediated through the ubiquitin pathway. Cbl functions as an ubiquitin ligase, ubiquitinating and promoting the degradation of multiple cell signaling proteins. It was shown that FGF induces a ternary complex consisting of FRS2 α , GRB2 and the RING type E3 ubiquitin ligase Cbl, which results in the ubiquitination and degradation of FRS2 α and FGFR. FRS2 α therefore assembles positive, consisting of Grb2/SOS, as well as negative, Grb2/Cbl, signaling complexes in order to mediate balanced FGF signal transduction (Wong et al., 2002).

5.6.3 Similar to FGF (Sef)

Another class of FGF inhibitors, is encoded by the *similar to FGF* genes (*sef*). The Sef protein is conserved across zebrafish, mouse and humans but has not been identified in invertebrates. *sef* expression is controlled by FGFR1/Ras/MAPK-mediated FGF signaling (Furthauer et al., 2002; Tsang et al., 2002). Loss of FGF8 function in the zebrafish *acerebellar* (*ace*) mutant abolishes *sef* expression and injection of constitutively active Ras strongly induced *sef* expression. Overexpression of *Fgf8* dorsalizes the zebrafish embryo by inhibiting expression of *Bmp* genes, whereas overexpression of *sef* resulted in the opposite phenotype, a ventralization of the zebrafish embryo, indicating that Sef is an antagonist of FGF activity. *sef* loss-of-function experiments resulted in a reduction of *Bmp4* expression, consistent with an increase of FGF signaling. To show that Sef indeed interferes with FGF signaling, *sef* was coinjected with *Fgf8* and in these experiments, *Fgf8*-induced loss of *Bmp4* expression could be rescued (Furthauer et al., 2002).

Based on its amino acid sequence, Sef is a putative transmembrane protein. Indeed, it has been shown that Sef localizes in the membrane and interacts with *Xenopus* X-FGFR1 and X-FGFR2 in transfected Cos cells (Furthauer et al., 2002; Tsang et al., 2002). Injected *sef* RNA into one blastomere of the 16-cell stage embryo caused a local disruption of MAPK activation. In addition, the ectopic MAPK activation triggered by misexpression of Ras, Raf or MAPK was prevented by coinjection of *sef*. These data indicate that Sef interferes with FGF signal transduction downstream (or at the level) of MEK (Furthauer et al., 2002). However, the exact mode of action for Sef is currently not known, although a model

envisages a direct prevention of MAPK phosphorylation by MEK or indirectly through the sequestration of MAPK-phosphatases (Furthauer et al., 2002).

5.6.4 Sprouty

The inducible expression of signaling pathway inhibitors through the same signaling pathway which these inhibitors end up controlling, is a common mechanism. This also applies to Sprouty (Spry) proteins, a family of proteins found in vertebrates and invertebrates which repress RTK signaling, including FGF signaling (Kim and Bar-Sagi, 2004; Kramer et al., 1999). Sprouty was first identified in *Drosophila* as an inhibitor of tracheal branching (Hacohen et al., 1998). As is the case for *sef*, *spry* is also induced through FGF signaling; consequently, *spry* is not expressed in *bnl* or *btl* mutants (Hacohen et al., 1998). *spry* mutants show 30%-120% more branches than normal and these extra branches arise close to positions where secondary and terminal branches normally bud. The increase in branching is not due to extra cell division or suppression of cell death. Furthermore, it has been shown that Spry acts non-cell autonomously in tip cells since branch tip cell clones mutant for *spry* appear normal but the neighboring stalk cells show ectopic branching. Spry encodes for a putative secreted protein due to the presence of an amino-terminally located signal peptide. It also has a unique 124 residue cysteine-rich region. Homologues of *Drosophila* Spry were identified in *Xenopus laevis*, chickens, mice and humans (Kim and Bar-Sagi, 2004). The mouse and human genome each contain four *sprouty* genes (*spry1-4*). These homologues are considerably smaller and the sequence similarity is mostly limited to the cysteine-rich domain, only outside this region is a short sequence of similarity between *Drosophila* Spry and individual mammalian Spry proteins. This region contains a conserved tyrosine residue, which mediates the interaction of Spry with signaling molecules that contain Src-homology2 (SH2) domains (Hacohen et al., 1998; Kim and Bar-Sagi, 2004).

In the vertebrate lung, *spry2* is expressed in a subpopulation of epithelial cells which are highly responsive to FGF signaling and expression is lost when FGF signaling is compromised (Mailleux et al., 2001). As further outlined below, Sprouty2 might have a similar branching-inhibiting function during morphogenesis in the lung.

Membrane targeting is required for Spry function. This is reflected in the fact that the truncations in the cysteine rich domain of *Drosophila* Sprouty, which is required for targeting Spry to the membrane, results in lethality (Hacohen et al., 1998). Likewise, deletion mutants

of Spry2 that lack the membrane-targeting domain fail to negatively modulate cell migration, ERK/MAPK activation and cell proliferation in response to different growth factors (Kim and Bar-Sagi, 2004). The precise point at which Spry intercepts RTK signaling depends on the biological context. Epistasis studies in the *Drosophila* eye place *spry* upstream of *ras* and downstream of *EGFR*, whereas in the developing wing and ovary, Spry functions at the level of Raf or downstream of it (Casci et al., 1999; Kramer et al., 1999; Reich et al., 1999). In mouse fibroblasts Spry1&2 interfere with ERK/MAPK signaling at the level of Ras activation, whereas in human epithelial cells Spry2 functions at the level of RAF activation. *Xenopus* Spry seems to have no effect on ERK/MAPK (Kim and Bar-Sagi, 2004).

The molecular basis for Spry action is not completely understood at the moment. However, the conserved tyrosine residue in the amino terminus of Spry undergoes phosphorylation in response to growth factor stimulation and this residue functions as a binding site for the SH2 domain of the Grb2 adaptor molecule, explaining also the requirement for membrane targeting of Spry (Kim and Bar-Sagi, 2004). Grb2 binding to Spry has two consequences: it prevents binding of Grb2 to either FRS2 or SHP2 thereby preventing the coupling of stimulated FGFR with Ras (Kim and Bar-Sagi, 2004).

The *Drosophila* Sprouty protein is also able to bind Drk, which is homologous to Grb2 (Casci et al., 1999). *Drosophila* Sprouty furthermore binds to Gap1, a negative regulator of Ras *in vitro* and *spry1* and *gap1* mutants display similar eye phenotypes. Based on these findings it was proposed that *Drosophila* Sprouty recruits Gap1 to Ras containing signaling complexes, thereby accelerating the inactivation of Ras (Casci et al., 1999). Although these interactions provide a working hypothesis for the mode of Spry action, other findings such as the non-autonomous effect of *Drosophila* Sprouty during branching morphogenesis do not easily fit into this model. However, it is generally believed that there are alternative mechanisms that are used by Spry to antagonize RTK signaling (Kim and Bar-Sagi, 2004).

6. Developmental role of FGF signaling; examples from vertebrates

6.1 Fibroblast growth factors in the development of the vertebrate limb

Limb development begins when cells from lateral plate mesoderm and nearby somites migrate to the presumptive limb field. The limb bud protrudes from the lateral body wall as a consequence of continued proliferation of mesenchymal cells at the appropriate axial levels at a time of reduced proliferation of cells in the rest of the flank. It is believed that inductive signals from proliferating mesodermal cells of the initiating limb bud induce the ectoderm at the tip of the bud to form a specialized structure called the apical ectodermal ridge (AER), which is essential for maintaining continuous limb bud outgrowth along the proximodistal (P-D) axis (Fig. I13). It was found that FGF signals originating from the AER are responsible for keeping the underlying mesenchyme (a region called the progress zone) in an undifferentiated, rapidly proliferating state (Xu et al., 1999).

During the growth phase, the limb also has to establish anteroposterior (A-P) and dorsoventral (D-V) axes. A-P patterning is achieved through the action of Sonic hedgehog (Shh), a molecule produced in the zone of polarizing activity (ZPA). Shh is expressed in the posterior mesenchyme and can induce mirror-image duplications when grafted to the anterior mesenchyme underneath the AER. Specification of the D-V axis involves molecules such as *En-1*, *Wnt7a* and *Lmx-1*.

Several FGFs are expressed during limb bud initiation. FGF2, FGF4, FGF8 and FGF9 are expressed in the limb ectoderm and AER, whereas FGF2 and FGF10 are expressed in the underlying mesenchyme. FGF2 and FGF4 can substitute for AER signals and promote complete outgrowth and patterning of the chick limb. FGF1, FGF2, FGF4, FGF8 or FGF10 are capable of inducing of complete, morphologically normal limb buds when implanted in the presumptive flank of chick embryos (Xu et al., 1999). More importantly, a targeted disruption of FGF10 resulted in mutant embryos without limbs (Min et al., 1998).

However, the loss-of-function analysis of the FGF ligands is complicated by functional redundancy as well as early lethality of certain family members. Mice lacking FGFR3 or FGFR4 have normal limbs, consisting with the lack of expression of these genes in the early developing limbs. In contrast, embryos deficient for FGFR1 or FGFR2 died during embryogenesis. Only hypomorphic or partial deletion of FGFR2 showed limbless mice.

A regulatory loop between FGF8 and FGF10 was suggested based on the finding that FGF10 can induce ectopic limbs and also induces the expression of FGF8. FGF8 on the other hand

induces the expression of FGF10. During normal chick development, FGF10 expression is seen in the mesenchyme before the onset of FGF8 expression and limb outgrowth. The same was shown to be true in mice. Moreover, the regulation between FGF10 and FGF8 is mediated by FGFR2 and was disrupted in FGFR2 partial loss-of-function mutants. A model was suggested in which FGF10 is made in the mesenchyme of the limb field, diffuses into the ectoderm where it binds to the splice variant FGFR2b and induces FGF8 in the ectoderm. FGF8 in turn diffuses into the mesoderm and activates FGFR2c which causes upregulation of FGF10. Looping continues while downstream activities result in limb bud outgrowth (Xu et al., 1999).

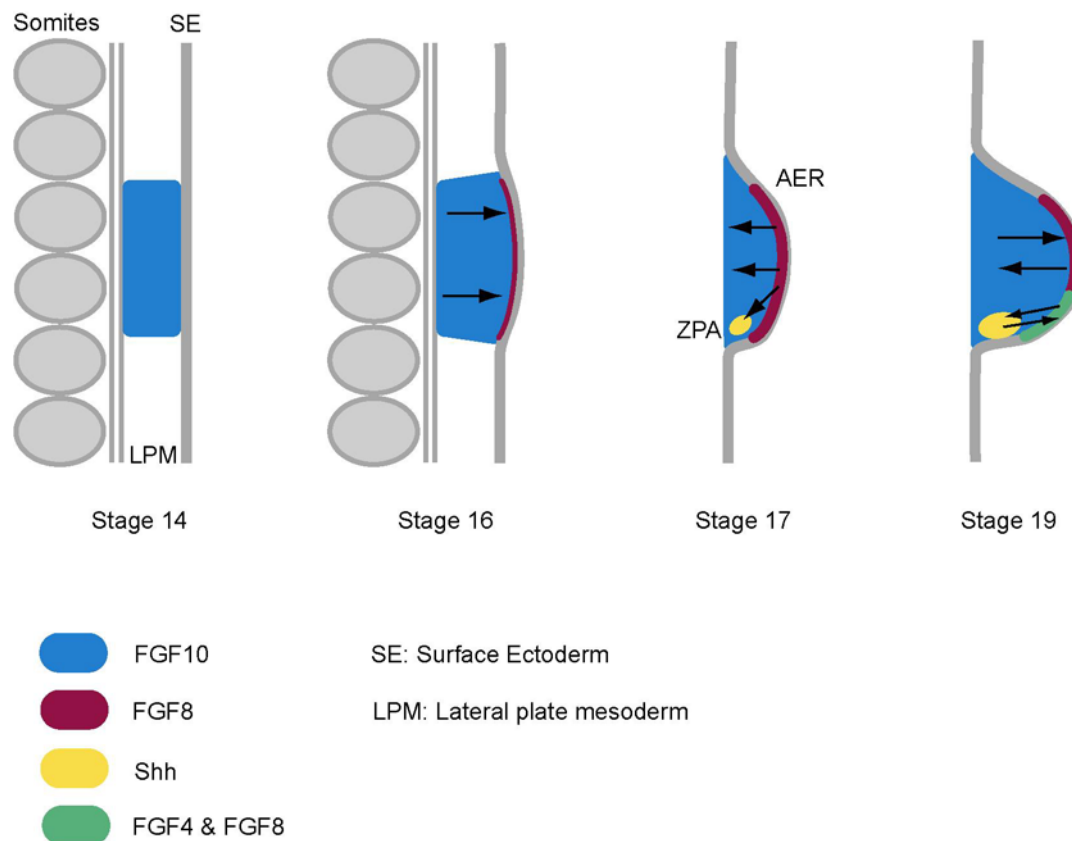


FIGURE I13

Wing bud outgrowth in the chick. Stage 14: FGF10 is expressed in the forelimb progenitor field. Stage 16: FGF10 induces the expression of FGF8 in the surface ectoderm (SE) of the presumptive apical ectodermal ridge (AER). Stage 17: FGF8 expressed from the AER acts on the underlying mesoderm and maintains FGF10 expression (arrows). Expression of Sonic hedgehog (Shh) from the zone of polarizing activity (ZPA) functions directly or indirectly as a mitogen on the mesenchymal cells and also induces FGF4 expression in the ectoderm. Stage 19: the posterior AER maintains the activity of the ZPA through expression of FGF4. Also FGF10 and FGF8 are engaged in a positive feedback loop and reciprocally maintain each others expression. Adapted from (Hogan, 1999).

6.2 Fibroblast growth factors and their roles during lung morphogenesis

Branching morphogenesis of the mouse lung is mediated through reciprocal interactions between the epithelium and its underlying mesenchyme. Similar to limb outgrowth, FGF signaling provides key information for proliferation and directed bud outgrowth. Much has been learned about the development of the vertebrate lung with the aid of suitable mice models and tissue culture systems.

The mouse lung primordium arises from the ventral foregut just anterior to the developing stomach around 9.5 days post coitum (dpc) during mouse embryogenesis. This primordium is composed of two parts: the future trachea and two endodermal buds, which give rise to the left and right lobes of the distal lung. Both components consist of an epithelial layer of endoderm surrounded by splanchnic lateral plate mesoderm cells. Initially, the primary buds grow ventrally and caudally and initiate lateral branches at invariant positions, beginning around 10.5 dpc. In this way, five secondary buds are generated, four on the right side and one on the left leading to the formation of four right lobes and one left lobe of the mature lung in mice (Chuang and McMahon, 2003). The human lung similarly originates from the primitive foregut at 5 weeks gestation and the 7-8 week old human embryo contains three lobes in the right lung and two lobes in the left lung (Warburton et al., 2000).

In humans as well as in mice, the dramatic expansion of the lung epithelium is due to dichotomous branching, a consequence of reciprocal interactions between the epithelium and the underlying mesenchyme. Since the early lung branching pattern does not vary between individuals it must be genetically hard-wired (Chuang and McMahon, 2003; Warburton et al., 2000).

FGF signaling plays an essential role in directing the outgrowth of the two primary lung buds. Although several FGFs are expressed in the mesenchyme overlying the lung epithelium, such as FGF1, 7 and 10, only FGF10 is clearly associated with early lung branching. FGF10 signals through FGFR2, which is expressed at high levels in the embryonic lung epithelium. FGF10 expression is restricted to the distal mesenchyme of the two main-stem bronchi generated from the two primary buds (Bellusci et al., 1997). In FGF10 knock-out mice, bronchial development as well as subsequent pulmonary branching is completely absent. Nevertheless, the trachea formed normally in these mice (Min et al., 1998; Sekine et al., 1999). It was shown that isolated lung endoderm in culture grows towards an FGF10 soaked bead. Since the isolated tissue moved towards the bead but also proliferated, it was concluded that FGF10 acts both as a mitogen and chemoattractant (Weaver et al., 2000). These data

indicate that, FGF10 is the key mesenchymal signal in inducing epithelial branching during early lung development.

Since FGF10 signals through FGFR2, one could assume that the receptor is equally important for branching morphogenesis in the early lung. That this is indeed true has been demonstrated with targeted disruption of different FGFR2 exons or expression of dominant negative FGFR2; targeted mice show an identical phenotype as FGF10 knock-out mice (Arman et al., 1999; De Moerlooze et al., 2000; Peters et al., 1994).

How the temporal and spatial expression of FGF10 is achieved is not known, although it is assumed that a system of coordinates likely established and specified long before the lung appears sets up a three-dimensional pattern of FGF10 in the mesenchyme (Cardoso, 2000).

Insight into how FGF10 activity is modulated during secondary branching has been gained through the analysis of Shh and BMP4 (Fig. I14). *shh* is predominantly expressed in the distal epithelium, from where Shh diffuses to form a complex with Patched (Ptc) and Smoothed (Smo) and activates signaling in the mesenchyme (Bellusci et al., 1996; Stone et al., 1996). Furthermore *shh* mutant mice show an upregulation as well as a delocalization of *FGF10* expression in the lungs, which consist of two stunted primary buds (Pepicelli et al., 1998). Shh seem to extinguish *FGF10* expression as the bud grows toward the chemotactic center. These and other data culminated in a model which proposes that Shh signaling suppresses FGF10 signaling in a spatially defined manner, resulting in focal FGF10 expression, which presumably induces secondary branching (Cardoso, 2000; Chuang and McMahon, 2003)

FGF signaling also interacts with Bmp signaling during secondary bud formation (Fig. I14). *Bmp4* expression is first detected in the ventral mesenchyme of the developing lung when the primordial lung buds are emerging from the foregut. This mesenchymal expression is maintained until 13.5 dpc. *Bmp4* expression is also detected in the distal endoderm of the developing lung bud (Weaver et al., 1999). Since *Bmp4* deficient mice die before 10 dpc, *in vitro* studies were performed which gave insight into the function of *Bmp* during secondary branching. One finding was that cultured lung buds failed to grow towards FGF10 coated beads when exogenous BMP4 protein was added to the medium, suggesting that BMP4 antagonized the action of FGF10 in inducing epithelial bud outgrowth. Extension of lung endoderm occurs by both proliferation and chemotaxis, so *Bmp4* might affect either process or both. The molecular mechanisms by which this antagonism is performed are not known, but a model has been proposed in which *Bmp4* functions as an inhibitor of lateral budding (Weaver et al., 2000). *Bmp4* is induced at the tip of the growing lung buds in response to mesenchymal FGF10. In the presence of high BMP4, FGF10 fails to induce further budding

from the growing lung bud, thus ensuring a single extending bud rather than a cluster of buds. Bmp4 therefore is induced by high levels of FGF10 and seems to cease branching probably through inhibition of proliferation as well as chemotaxis. Branching only occurs when the Fgf10 expression shifts laterally (Chuang and McMahon, 2003). Interestingly, Noggin, a Bmp antagonist is expressed in the distal lung mesenchyme and could potentially modulate Bmp signaling at the distal tip (Weaver et al., 1999). Although Shh as well as Bmp are required for dichotomous branching, they very likely function independently to regulate FGF10 signaling (Chuang and McMahon, 2003).

In addition to Bmp and Shh signaling, FGF10 could potentially induce its own inhibitor, namely *sprouty* (*spry*). Four mammalian *sprouty* genes were identified and their expression domains either overlap with, or are immediately adjacent to FGF (de Maximy et al., 1999; Minowada et al., 1999). In the lung, *sprouty1*, 2 and 4 are expressed in the distal epithelial tips and *sprouty 4* is also expressed in the mesenchyme (Zhang et al., 2001). Like in the fly, Sprouty appears to function as a FGF antagonists since reduced expression of *spry2* in cultured lungs results in an increase in branching, whereas *spry2* overexpression resulted in a lower level of branching (Mailleux et al., 2001).

Therefore, regulation of branching at the level of FGF10 signaling combines different inputs, provided by Shh, Bmp and FGF inhibitors (Fig. I14).

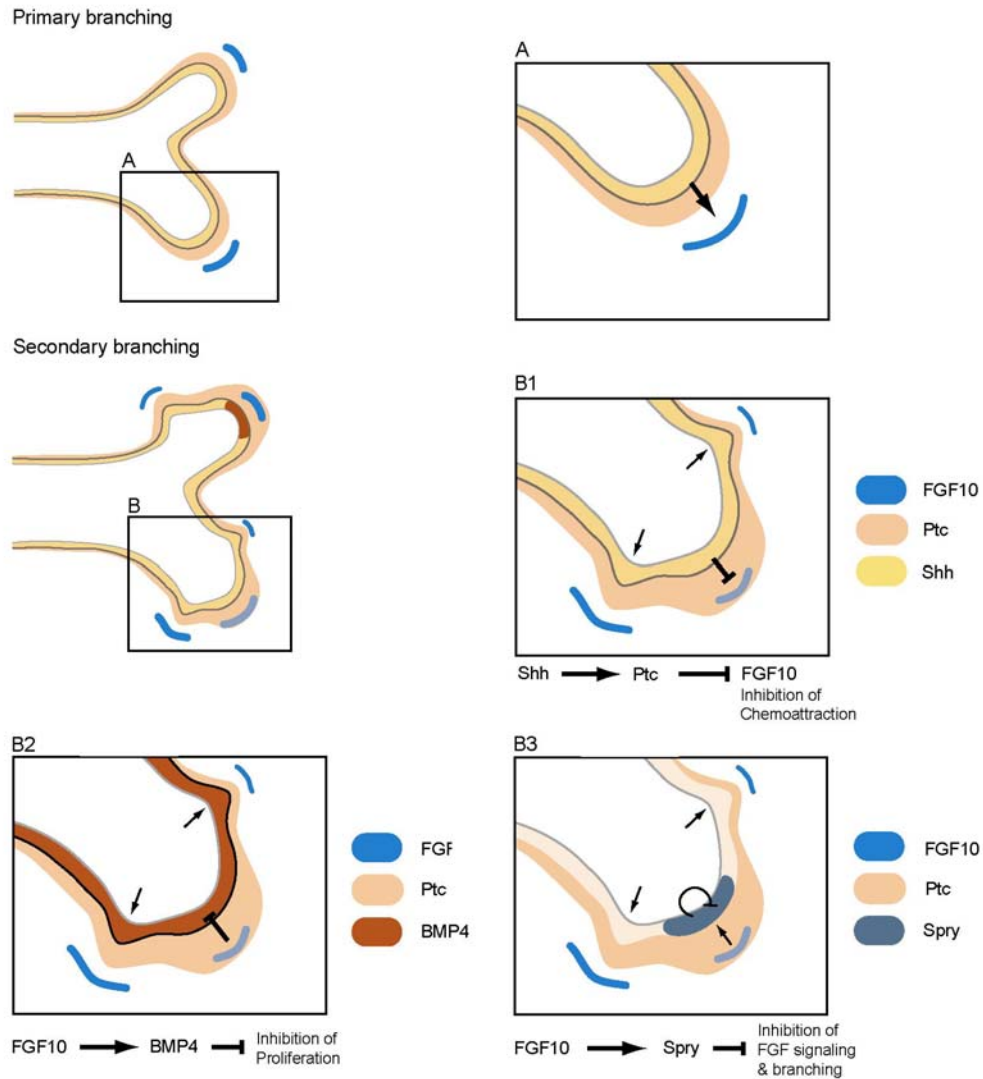


FIGURE I14

Branching morphogenesis in the vertebrate lung (Model). Interactions of different signaling pathways lead to dichotomous branching. **A)** Primary branching events lead to a first bifurcation of the outgrowing lung bud, whereas secondary branching leads to sprouting on primary branches. FGF10 is expressed in distal lung mesenchyme and induces primary as well as subsequent bud formation. FGF10 signals through FGFR2 which is expressed in the lung epithelium (not shown). Secondary branching is initiated through the activity of different signaling pathways. **B1.)** Shh is expressed in the epithelium and upregulated at distal tips of primary buds. It signals through its receptor patched (ptc), which is expressed in the subepithelial region. This signaling leads to inhibition of chemoattraction. **B2.)** Bmp4 is upregulated by FGF10 as the bud approaches the FGF10 expressing cells. Bmp4 inhibits proliferation. **B3.)** *sprouty* expression is upregulated in response to FGF10 and inhibits further branching and FGF10 signaling. Secondary bud formation is further initiated by localized FGF10 expression in the mesenchyme. How FGF10 expression is restricted in such a dynamic and locally restricted manner is currently unknown. Adapted from (Chuang and McMahon, 2003; Lebeche et al., 1999)

7. Development of larval and adult air sacs

7.1 Remodelling of the embryonic tracheal system

Much has been learned concerning the development of the tracheal system during embryogenesis. The stereotypical and genetically hardwired tracheal development starts in the early embryo and continues throughout embryogenesis. Starting from an invaginating placode consisting of genetically determined tracheal cells, an elaborate three dimensional system is built. Shortly before hatching, the tracheal system is cleared of the liquid, and becomes functional and supplies the larval tissues with oxygen. These processes take place within the first 22h after egg laying (AEL) (Manning and Krasnow, 1993). During early larval development (stages L1&L2), which lasts from 22h-72h (Fig. I15 A), the tracheal system increases in size, tubes increase in length as well as in diameter; this process also appears to be genetically controlled (Beitel and Krasnow, 2000). Moreover, fine terminal branches grow into hypoxic regions, a process triggered mainly by local oxygen concentration which regulates the expression of the chemoattractant *branchless* (*bnl*) (Jarecki et al., 1999).

However, little is known about the development and remodeling of the tracheal system during late larval, pupal and adult stages, which encompass the time window from 72h-120 on (third larval stage), 120-132h (pupation), 132-220 (pupal stage and eclosion) (see Fig I15). Some knowledge has been gathered studying related species such as *Rhodinus*, *Calliphora* and *Sarcophaga* and comparing them to *Drosophila* (Manning and Krasnow, 1993). A common theme in these species appears to be the occurrence of a series of dramatic remodeling steps such as the truncation of tracheal segments tr6-10, which are not functional in the pupa but are restored in the adult and, starting at the onset of third instar larva development (72h-120h), the proliferation of imaginal tracheoblasts. Imaginal tracheoblasts populate different regions in the embryonic tracheal system and are set aside very early during development as judged from specific enhancer trap lines (Manning and Krasnow, 1993). They are set aside mainly on the spiracular branch (SB) in tracheal segments tr2-tr9, which provide the connection between the tracheal sac and the surface of the embryo. Other locations for imaginal tracheoblasts can be observed as distinct cell clusters in the anterior region of the third instar larva (probably tr2-tr4, Fig. I15 and (Weaver and White, 1995)). It is generally believed, that imaginal tracheoblasts spread during metamorphosis, populate the tracheal

epithelium of all major branches and replace and/or remodel the tracheal epithelium (Manning and Krasnow, 1993).

A major difference between these imaginal tracheoblasts and the tracheal cells is given by their distinct histochemical staining properties as well as their smaller size compared to the tracheal cells they replace. Moreover, and most importantly, they retained the capacity to proliferate, whereas tracheal cells originating from the embryo only divide once during invagination and once more shortly afterwards (Manning and Krasnow, 1993; Samakovlis et al., 1996a). One marker which is expressed in imaginal tracheoblasts located on the spiracular branch as well as in the cell clusters in tr2-tr4 is Headcase, a cytoplasmic protein which might respond to hormonal signals by enabling imaginal tracheoblasts to reenter the mitotic cell cycle (Weaver and White, 1995).

Apart from remodeling some of the existing tubes, certain novel structures, generally termed air sacs, are established. These originate in different locations in the larva, such as the head region, giving rise to the head air sac (HAS), and in the thorax giving rise to the dorsal air sac (DAS) (Manning and Krasnow, 1993). Air sacs also originate from imaginal tracheoblasts and only very recently, the formation of the DAS, subsequently called thoracic air sac, has been studied in some detail (Sato and Kornberg, 2002).

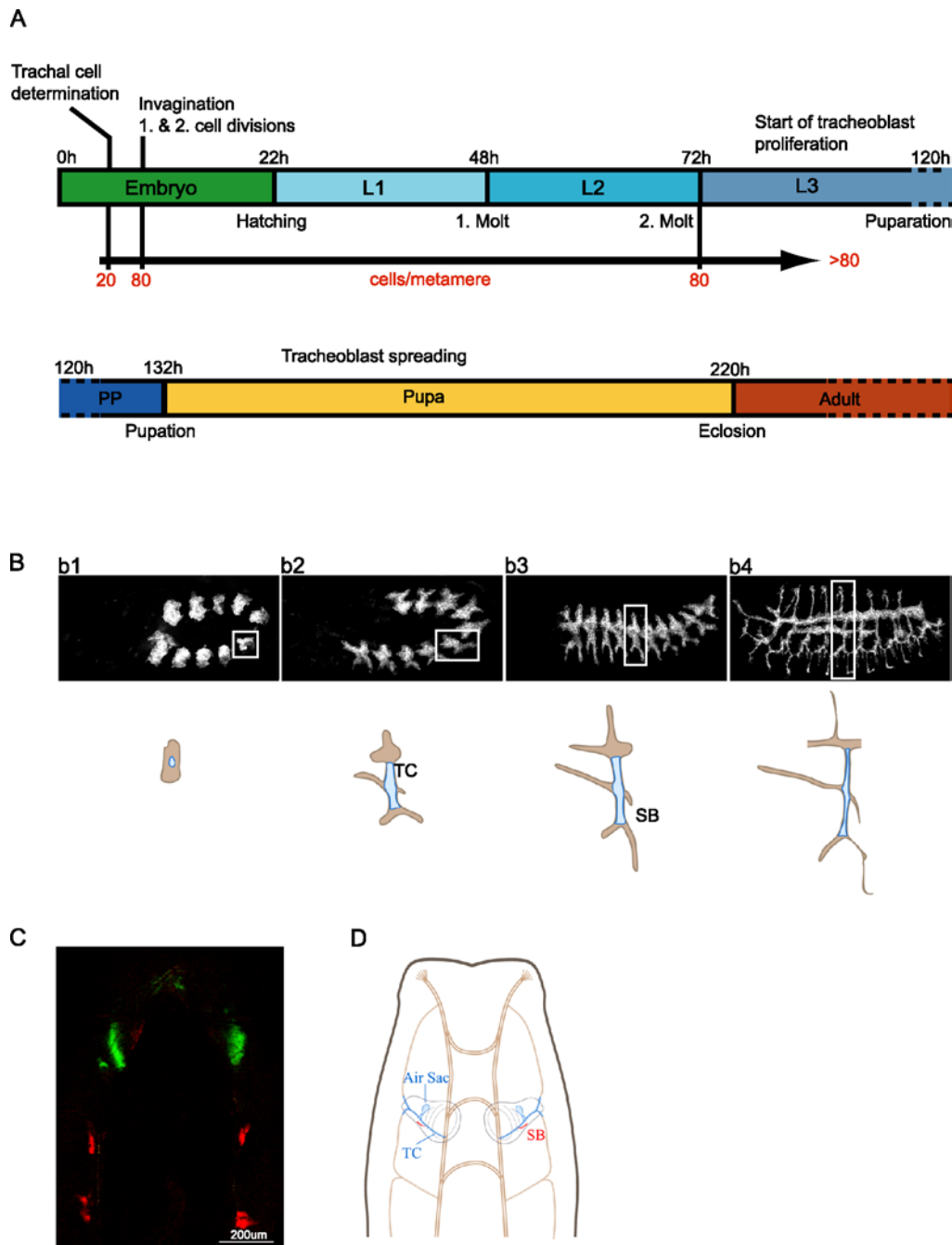


FIGURE I16

Remodeling of the embryonic tracheal system. **A.)** Overview of the life cycle of *Drosophila melanogaster* with respect to tracheal development. L1-L3: first, second and third instar larval stages. PP: prepupa. Tracheal development starts in the embryo with the determination of tracheal cells which undergo two rounds of cell division which results in the formation of 80 tracheal cells per metamere. This cell number remains constant until the third larval instar stage when imaginal- and air sac tracheoblasts re-enter the mitotic cell cycle and start to proliferate which continues throughout pupal stages. Imaginal tracheoblasts also start to spread during pupal stages. **B.)** Highlights of one tracheal metamere from stage 12 on (**b1**) until stage 15/16, (**b4**). The development and location of the transverse connective (TC) is highlighted in blue in the schematic drawing below. **C. & D.)** Both panels show a third instar larva oriented the same way, anterior is up, posterior down. Red highlights imaginal tracheoblast expression in tr3 & tr4 as outlined by RFPmoe. Green highlights the position of third instar wing imaginal discs (GFP mimics expression of *Dpp*). Imaginal tracheoblasts are nested at the junction where the dorsal trunk leads into the TC.

7.2 Formation of the thoracic air sac during *Drosophila* third instar larval development

Studying the expression pattern of the *Drosophila* FGF gene *branchless* (*bnl*) as well as the FGFR receptors *breathless* (*btl*) and *heartless* (*htl*) revealed that these genes are also expressed in the *Drosophila* wing imaginal disc (Sato and Kornberg, 2002). The wing imaginal disc arises as a tubular invagination of the epidermis and grows and flattens during larval periods. It consists of four distinct cell types, the squamous peripodial cells on one surface, a distinct group of adepithelial cells that nestle against the most proximal columnar epithelial cells, and stalk cells that connect the disc to the epidermis. The wing imaginal disc further gives rise to the majority of the adult thorax, including most of the dorsal thoracic epidermis, the wing and the flight muscles (Cohen, 1993).

bnl is expressed in 15-60 cells in early third instar wing discs and about 80-150 cells in late third instar discs straddling the anterior-posterior compartment boundary dorsal to the region of the prospective wing blade. *Btl*, on the other hand, is expressed in a tracheal branch, the transverse connective (TC), which attaches to the wing imaginal disc (Fig.I15 B, I16 A-D). Furthermore, *btl* expression is detected in a subset of adepithelial disc cells. *htl* is also expressed in the adepithelial cells but in a larger subset, which did not overlap with *btl* expressing adepithelial cells. These *htl* expressing cells also express *twist* and give rise to the adult musculature. *dof* is expressed in the *htl* adepithelial as well the *btl* positive adepithelial cells, in line with its proposed role to function downstream of both FGF receptors (Sato and Kornberg, 2002) (Fig.I16).

The *btl* expressing adepithelial cells were not detected in early third instar discs, and only cells from the TC expressed *btl*. Subsequently, at a stereotypical position adjacent to *bnl* expressing cells, *btl* positive cells were seen budding from the TC that adheres to the wing disc. During third instar development, the number of *btl* expressing cells increased and the bud expanded posteriorly towards the region of greatest *bnl* expression. As mentioned above, these cells did not express *htl* but did express *dof*. The increase in *btl* positive cells was shown to be due to cell proliferation. The TC also has a small offshoot, called the spiracular branch (SP), where imaginal tracheoblasts are located. These imaginal tracheoblasts however did not express *btl* but expressed the transcription factor *tracheiless* (*trh*) (Sato and Kornberg, 2002). Evidence was provided that the pupal and adult air sac of the thorax is derived from these *btl* positive adepithelial cells, which are distinct from imaginal tracheoblasts, and are therefore called air sac tracheoblasts (Sato and Kornberg, 2002). The air sac tracheoblasts remain as a

tight, rounded cluster of cells next to the prospective wing hinge during the first 12h after puparium formation. They then migrate dorsally between 12 and 23h after puparium formation (APF), then anteriorly and posteriorly to form three branches, the medioscutal, lateroscutal as well as the scutellar sac. At 32h APF, migration ceased and the cells elaborated into air sacs (Sato and Kornberg, 2002) (Fig.I16 F., G.)

Based on the expression of *bnl* and *btl*, it was assumed that air sac development is FGF dependent. This has been demonstrated by ectopic *bnl* expression in columnar epithelial cells. These ectopic *bnl* cells attracted tracheal cells from other locations in the TC and gave rise to ectopic branches of tracheoblast. *bnl* loss-of-function clones as well as the expression of a dominant-negative *btl* construct reduced or even abolished, in the latter case, the budding of air sac tracheoblasts. A constitutively active *btl* construct (*λbtl*) on the other hand did not interfere with branching, but caused a significant increase in the number of tracheoblast cells resulting from increased proliferation. Similar results were achieved in response to ectopic Bnl signaling. These findings indicated that FGF not only functions as a chemoattractant but also as a mitogen (Sato and Kornberg, 2002).

Using different GFP transgenes it was also observed that the migrating tracheoblasts extended numerous filopodia in the direction of migration towards the *bnl* secreting cells as well as some nonoriented filopodia. Since GFP fused to Btl also localized to these filopodia, in bright spots along their length and apparent termini, it was concluded that these filopodia serve to sense a Bnl/FGF ligand. As already shown in the embryo (Ribeiro et al., 2002), the induction of filopodia was FGF-dependent. Furthermore, ectopic *bnl* expression from columnar epithelial cells leads, as described above, to the formation of novel tracheoblast containing branches with filopodia extended in the direction of the *bnl* expressing cells.

Thus, the formation of pupal and adult air sacs depends on a so far ill-characterized group of cells, the air sac tracheoblasts, which have their origin in the TC. Based on their expression profile it was suggested that these air sac tracheoblasts are distinct from imaginal tracheoblasts, since they express *btl* while imaginal tracheoblasts located on the spiracular branch do not. Moreover, air sac tracheoblasts have the capacity to divide and migrate, presumably in response to Bnl/FGF signaling (Sato and Kornberg, 2002).

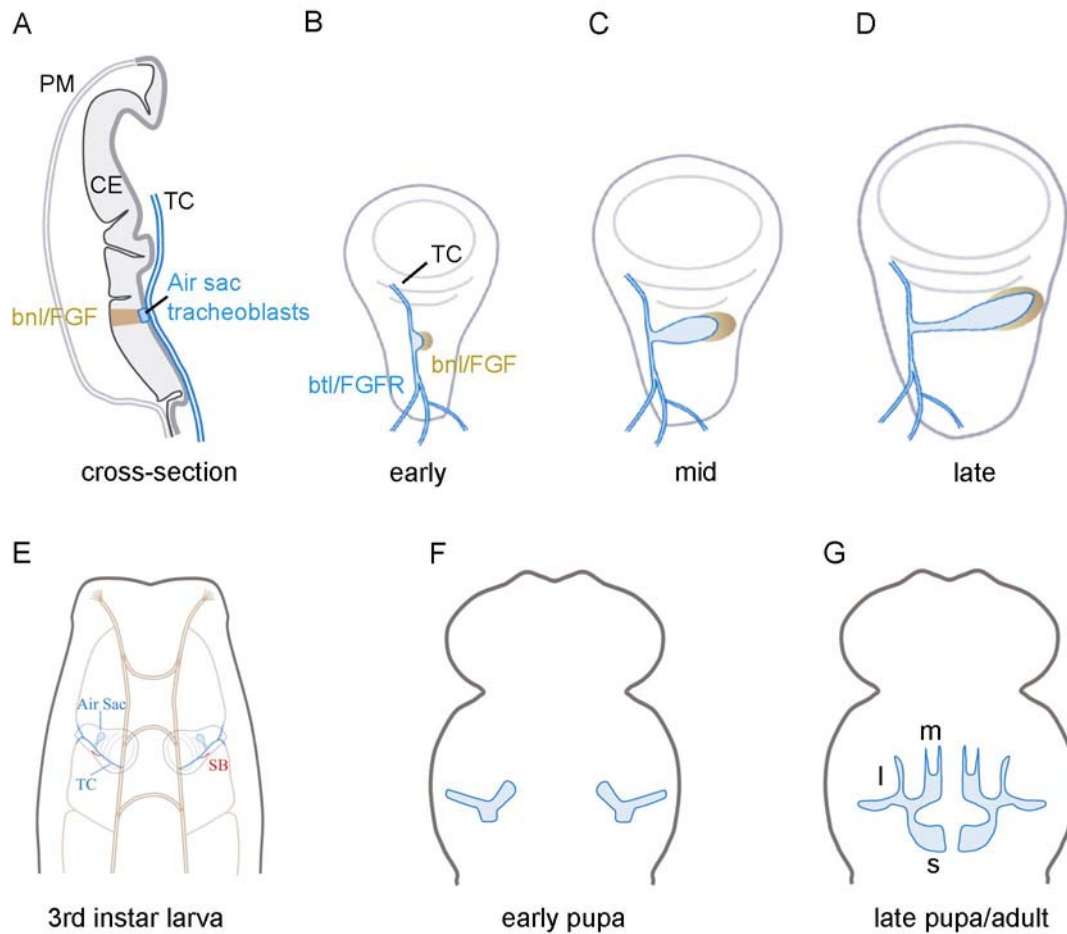


FIGURE I16

Air sac development. **A.)** Cross-section of a third instar wing imaginal disc. PM: peripodial membrane, CE: columnar epithelium, TC: transverse connective. The TC (blue) adheres to the wing imaginal disc. *bnl/FGF* (brown) is expressed in a subset of columnar epithelial cells and an air sac is formed in this area. **B.)** Early third instar wing imaginal disc with PM facing down, CE and TC facing up. *bnl* (brown) is expressed in the vicinity of the outgrowing air sac which expresses *Btl/FGFR* (blue). **C., D.)** With the growth of the wing imaginal disc, the *bnl* expressing cells increase in number and move away from the air sac tracheoblasts. Air sacs increase in size too and follow the *bnl* expressing cells. Position of wing imaginal discs and the adhering TC in third instar larva. **F., G.)** Air sac growth continues during pupal stages with the formation of the scutellar- (s), medioscutal- (m) and lateroscutal (l) air sac. Modified after (Cabernard et al., 2004; Sato and Kornberg, 2002).

8. Aim and structure of the thesis

8.1 Aim

The general aim of the thesis was to obtain a better understanding of FGF-mediated cell migration. Since Dof is a central player in the FGF signaling cascade in *Drosophila* and is required for tracheal- as well as mesodermal cell migration, we wanted to identify interacting proteins which could relay the extracellular chemotactic signal provided by Bnl into a migratory response.

Thus, the thesis started with the characterization of a putative Dof interaction partner called Receptor of activated protein kinase C (Rack1) (Vani et al., 1997) which was previously isolated in two independent yeast-two hybrid screens (Battersby et al., 2003; Cabernard, 2000).

We wanted to address the role of *rack1* by genetic means, however, *rack1* mutants have not been isolated so far. As a first aim, we sought to isolate *rack1* loss-of-function alleles which could be used to characterize the in vivo role of *rack1* during development.

However, for reasons that will be shown later, the function of *rack1* during tracheal cell migration could not be studied in the embryo. Therefore we sought for a system which would allow us to investigate the role of *rack1* and also other candidate genes for their involvement in tracheal cell migration. Many genes have pleiotropic effects and a substantial number of genes have a maternal contribution (C. Ribeiro, unpublished chip data). Therefore, the system we were looking for, should allow us to study the loss-of-function phenotype of target candidate genes in tracheal cell migration at a stage when the maternal contribution is neglectable.

Such a system is provided with the *Drosophila* third instar thoracic air sacs (Sato and Kornberg, 2002).

Therefore, a major aim of the thesis was to characterize the development of air sacs with emphasis on their cellular composition and biology. Furthermore, we wanted to develop genetic tools which allowed us to study the loss-of-function phenotype of candidate genes. Additionally, we sought for methods which would allow us to image the behavior of these air sac tracheoblasts in time laps. These tools should aid the characterization of the system in a

general way but could then also be applied for the study of the phenotype of different candidate genes such as *rack1*.

The FGF signaling pathway is used in vertebrates and invertebrates for cellular tasks such as cell migration, proliferation or differentiation. Little is known about the integration and interpretation of the extracellular information provided by FGF. The complexity of FGF signaling is greatly increased in vertebrates where several ligands as well as several receptors exist. Therefore, the analysis of conserved FGF signaling components in a simple model organism should contribute to a better understanding of this pathway. Since *Drosophila* air sac tracheoblast also respond to FGF signaling we aimed at a genetic characterization of the key FGF signaling components to test their involvement in cell migration and/or proliferation. Such an analysis has not been achieved previously and we think *Drosophila* air sacs provide the best possible system known at the moment.

8.2 Structure

The thesis consists of the characterization of the *Drosophila* thoracic air sac based on the findings of Sato and Kornberg (Sato and Kornberg, 2002).

In a first section I will outline the tools which were developed in order to analyze the cellular composition, complexity and behavior of air sac tracheoblasts. This chapter will be followed by the characterization of air sac development. Since understanding air sac development is key for the genetic analysis we undertook, this description will be detailed.

Furthermore, for the best possible understanding, the chosen genetic approach will be carefully discussed.

Since such a genetic approach with this system has not been described before, we wanted to test a number of mutants in order to be able to subclass the obtained phenotypes. For these reasons, a number of genes we tested with this system will be shown in the following chapters although these results might sometimes appear isolated. Moreover, since we and probably also the majority of the readers will focus on the FGF signaling components, these results will be shown first, followed by the results obtained with other candidates and mutants of general interest.

At the end of this thesis, an entire chapter is devoted to the work performed on *rack1*.

Since the dynamics of air sac development, captured with time laps movies, cannot be fully presented in a written report, a supplementary CD containing all the mentioned movies including legends will be available.

II Results

1. Tools to study air sac development

1.1 Live imaging

Cell migration is a dynamic process. In order to visualize the dynamics of migrating cells, the tissue under investigation must remain alive. In addition, the preservation of fine and dynamic subcellular structures such as the cytoskeleton are best achieved using non-fixed tissue (Jacinto et al., 2002a; Ribeiro et al., 2002). Air sac tracheoblasts can hardly be studied in the living larva and must be dissected. Since air sacs strongly adhere to the wing imaginal disc (shown below) and to maintain this endogenous substrate, entire wing imaginal discs are dissected and prepared for further analysis. A first goal to study the behavior of air sacs in general and air sac tracheoblasts in detail, was to keep the dissected tissue alive for several hours. After trying different media, the best results were achieved using *Drosophila* S2 schneider cell medium (see Materials and methods for composition). The protocol used for most of the presented experiments was the following: wing imaginal discs were dissected from wandering third instar larvae of the appropriate genotype in PBS buffer (see below). The discs were then put on a slide into a drop of S2 medium. The medium was surrounded by a rim of halocarbon oil. In order to support the cover glass, two spacers were added on the slide on both sides of the oil rim. Before adding the cover glass, the discs, whenever necessary, were flipped on one side with the air sac and trachea facing upwards (peripodial membrane facing down) to ensure better optical resolution (Fig R1).

Using this protocol, the discs could be maintained alive for at least 4 hours. This time window was determined by taking 5 subsequent movies of the same air sac over the mentioned time period. In all movies, dynamic behavior of the cells and air sac net movement was observed, indicating that the discs retained their ability to develop normally (see following chapters for examples). However, it was not determined whether development in this culture environment was taking place in the same time as *in vivo*. Similar procedures were used by others for imaging wing imaginal discs (Gibson and Schubiger, 2000).

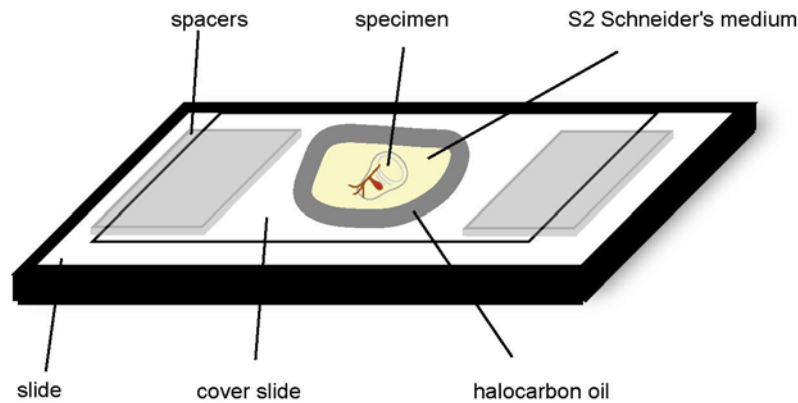
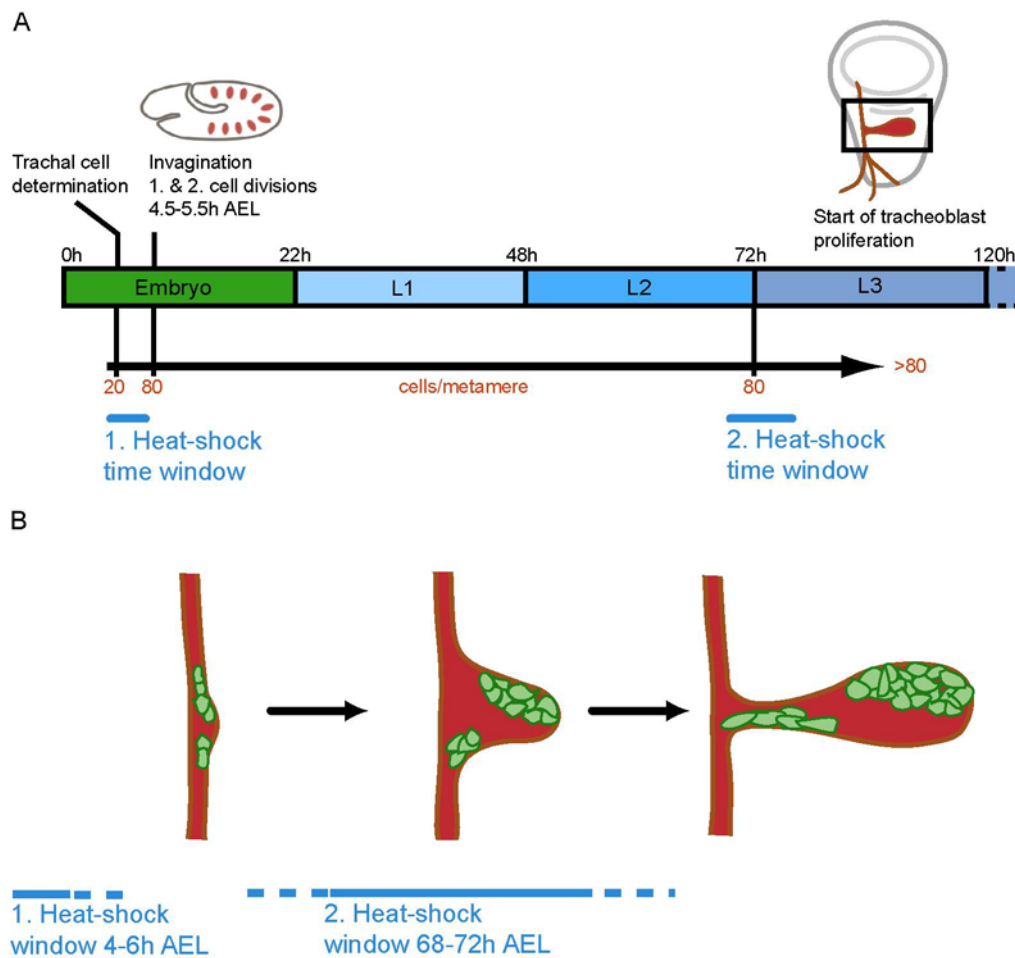


FIGURE R1:

Schematic representation of a preparation used for 3D&4D microscopy. For best optical resolution, the wing imaginal discs are placed into the S2 medium with the air sac facing upwards.

1.2 Genetic manipulations of air sac tracheoblast

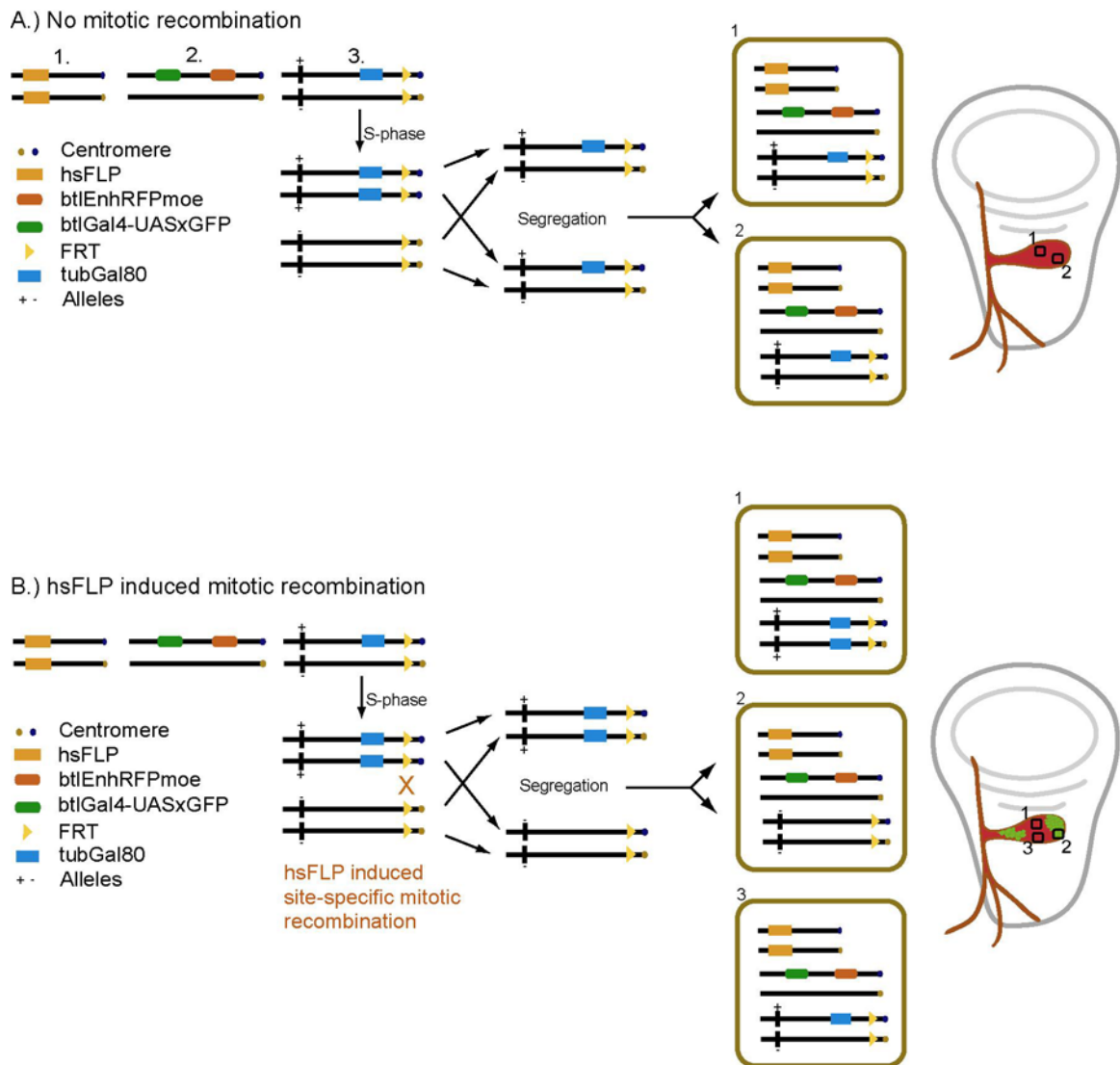
Air sac tracheoblasts, as imaginal tracheoblasts but unlike embryonic tracheal cells, re-enter the mitotic cell cycle (Sato and Kornberg, 2002; Weaver and White, 1995). Therefore we sought to take advantage of this proliferative capacity to generate mosaic air sacs using site-specific mitotic recombination (Blair, 2003; Golic, 1991; Xu and Rubin, 1993). Embryonic tracheal cells divide only twice during 4.5-5.5h AEG (Fig. R2 A) and mosaic trachea were previously generated (Samakovlis et al., 1996b) demonstrating the feasibility of the technique also in the embryo. However, we wished to study the mutant phenotype of candidate genes in a tissue-specific manner and in the absence of maternal contribution. This is best achieved in third instar larvae, when most, if not all, of the maternal products are depleted and air sac tracheoblasts start to divide. Therefore, clones induced during early embryonic development (when the tracheal cells are still dividing) result in the formation of late embryonic mosaic trachea consisting of clones with maximally 4 cells (2 cell divisions only) (Samakovlis et al., 1996a). These clones, due to their regained proliferative capacity will increase in size when they become incorporated into a growing air sac (Fig. R2 B). Thus, the behavior of these clones with regard to cell migration, cell division or rearrangement can be studied. Combined with live imaging, the behavior of such clones also be monitored in four dimensions at the cellular level.

**FIGURE R2:**

Experimental procedure for air mosaic analysis in air sacs. **A.)** Schematic life cycle of *Drosophila melanogaster* displaying the embryonic, as well as the three larval stages with the indicated time frames. Heat-shock windows for the flipase mediated site-specific recombination (FLP/FRT system) are indicated in blue as well as the approximate number of tracheal cells/metamere at these time points. **B.)** Outcome of FLP/FRT recombination. By heat-shock inducing flipase during embryogenesis (1. HS window, 4.5-5.5h AEL), marked clones are generated in random positions of the embryo. Due to two cell divisions only, clones cannot exceed 4 marked cells. If marked cells are located in the TC where the air sac starts to grow out, these clones, due to regained proliferation capacity, increase in size. Alternatively, clones can also be induced at the beginning of third instar stages, when air sac tracheoblasts start to proliferate. However, due to timing difficulties, the clones will be induced in various positions in the outgrowing air sac. Early induced clones are therefore easier to interpret in terms of cell migration.

1.2.1 Positive labeling of mutant tracheal cells using the MARCM system

In clonal analysis, one problem is to recognize the cells, which underwent mitotic recombination and are therefore mutant for the gene under study. In order to visualize such clones, a novel technique was recently developed called Mosaic Analysis using a Repressible Cell Marker (MARCM). In contrast to conventional site-specific mitotic recombination techniques, MARCM allows to positively label the mutant cells of interest (Lee and Luo, 1999; Lee and Luo, 2001) (Fig. R3). This technique relies on heat-shock inducible flipase, an enzyme that catalyses recombination between flipase recombination target sites (FRT) (Golic and Lindquist, 1989) as does the conventional FRT-mediated mitotic recombination system (Blair, 2003; Golic, 1991; Xu and Rubin, 1993). Additionally, a transgene is used, which expresses a GFP reporter under the influence of the Gal4/UAS system (Brand and Perrimon, 1993). However, the novelty is to combine these elements with a transgene containing *gal80*, that was cloned downstream of the tubulin promoter in order to generate ubiquitous expression. Gal80 antagonizes the activity of Gal4 and therefore the GFP reporter cannot be expressed when both gene products are present in the same cell. However, using heat-shock induced flipase as a mediator for site-specific recombination, the *gal80* transgene can be recombined away from *gal4*, and after cytokinesis, two genetically different sister cells are born. One cell retains the *gal80* transgene, and does not express GFP although *gal4* and the GFP reporter are present, due to the antagonizing activity of Gal80. The other cell lacks the *gal80* transgene, and is capable of expressing GFP. All other cells which did not undergo mitotic recombination retained one copy of *gal80* and thus do not express the GFP reporter (Lee and Luo, 1999). Therefore, the mutant of interest has to be recombined onto a FRT chromosome and crossed *in trans* to a *gal80* containing FRT chromosome. The flipase source as well as the GFP reporter can be combined on other autosomes and will, based on their segregation, end up with one copy in each daughter cell (Lee and Luo, 1999; Lee and Luo, 2001) (Fig. R3).

**FIGURE R3:**

MARCM applied to the tracheal system. T-MARCM stocks containing the indicated transgenes were established for the all chromosomal arms (except the 4th). The example illustrates MARCM clones generated with chromosomal arm 3L. Since the MARCM system is a combination of FLP/FRT (Golic and Lindquist, 1989) recombination and the Gal4/UAS system (Brand and Perrimon, 1993), clones can be marked with various GFP markers, indicated with UASxGFP. Only tracheal clones are marked, due to restricted expression of Gal4 in tracheal cells (btlGal4). As an air sac outline, RFPmoe fused to the *breathless* enhancer is used, which cannot be antagonized by Gal80 activity. **A.)** in case of no induced site specific mitotic recombination, two genetically identical cell types are generated, both of which contain one copy of *gal80* and therefore antagonize *gal4* activity. No GFP positive cells are visible. **B.)** Upon Flipase induction, site specific recombination creates three cell types, two *gal80* containing cells (type 1&3) as well as one without *gal80*. The other used transgenes segregate as indicated, therefore only cells without Gal80 protein express the GFP marker and are therefore the only GFP labeled cells (cell type 2). Due to perdurance of Gal80 protein, cell type 2 starts to express GFP within 48h (Lee and Luo, 1999; Lee and Luo, 2001).

The MARCM system was originally developed for studies in the nervous system of *Drosophila*. Application of this technique in the larval tracheal system required the generation of suitable stocks. In order to positively mark only mutant air sac tracheoblasts, the heat-shock inducible flipase was combined with GFP reporter lines, which are under UAS control and recombined with *breathless-Gal4* (*btlGal4*). This driver line shows very specific expression in (almost) all tracheal- and some glia cells. The following reporters fusions were used as GFP markers: CD8:GFP, actinGFP, tauGFP and α cateninGFP. These lines, when expressed with *btlGal4*, showed no misexpression phenotypes in the embryonic or larval tracheal system. They also labeled all air sac tracheoblast cells but did not show any obvious phenotype in the air sacs.

The integration of these markers into MARCM strains allowed to label exclusively those tracheal cells, that underwent mitotic recombination, whereas the rest of the air sac tracheoblasts will not be labeled. To visualize all tracheal cells with a different marker, a direct fusion of the *breathless* enhancer (Ohshiro and Saigo, 1997) with the monomeric red fluorescent protein (mRFP, (Campbell et al., 2002) fused to Moesin (btlEnhRFPmoe) was constructed and provided by Marc Neumann. Flies bearing this construct express mRFPmoesin under the control of the *breathless* enhancer and show ubiquitous RFPmoesin expression in the tracheal system. These flies also show RFP expression in the air sac tracheoblasts and can therefore be used to outline the entire air sac. The direct fusion to the tracheal specific enhancer makes this construct independent of the Gal4-UAS system and inaccessible for the antagonizing activity of Gal80. Therefore, *btlGal4-UASxGFP* (x stands for any of the mentioned reporters), *btlEnhRFPmoe*, *hsFLP*, as well as the *tubGal80* bearing FRT chromosomes were crossed together in order to generate the stocks used for generating marked clones in tracheal cells; henceforth these stocks will be called T-MARCM stocks (see Fig. R3, Table 1 and materials and methods).

TABLE 1: T-MARCM stocks**1. CHROMOSOME**

hsFLP tubGal80 FRT19A/hsFLP tubGal80 FRT19A; btlEnhRFPmoe-btlGal4-UASactGFP

2. CHROMOSOME

2L: hsFLP/hsFLP; tubGal80 FRT40A/tubGal80 FRT40A; btlEnhRFPmoe-btlGal4-UASCD8:GFP/TM6C

2L: hsFLP/hsFLP; tubGal80 FRT40A/tubGal80 FRT40A; btlEnhRFPmoe-btlGal4- α catGFP/TM6C

2R: hsFLP/hsFLP; tubGal80 FRTG13/tubGal80 FRTG13; btlEnhRFPmoe-btlGal4-UASCD8:GFP/TM6C

2R: hsFLP/hsFLP; tubGal80 FRTG13/tubGal80 FRTG13; btlEnhRFPmoe-btlGal4- α catGFP/TM6C

2R: hsFLP/hsFLP; tubGal80 FRT42B/tubGal80 FRT42B; btlEnhRFPmoe-btlGal4-CD8:GFP/TM6C

2R: hsFLP/hsFLP; tubGal80 FRT42B/tubGal80 FRT42B; btlEnhRFPmoe-btlGal4- α catGFP/TM6C

3. CHROMOSOME

3L: hsFLP/hsFLP; btlEnhRFPmoe-btlGal4-UAS-actinGFP/CyO; tubGal80 FRT2A/tubGal80 FRT2A

3L: hsFLP/hsFLP; btlEnhRFPmoe-btlGal4-UAS- α catGFP/CyO; tubGal80 FRT2A/tubGal80 FRT2A

3L: hsFLP/hsFLP; btlEnhRFPmoe-btlGal4-UAS-tauGFP/CyO; tubGal80 FRT2A/tubGal80 FRT2A

3L: hsFLP/hsFLP; btlEnhRFPmoe-btlGal4-UAS-actinGFP/CyO; tubGal80 FRT80/tubGal80 FRT80

3L: hsFLP/hsFLP; btlEnhRFPmoe-btlGal4-UAS- α catGFP/CyO; tubGal80 FRT80/tubGal80 FRT80

3L: hsFLP/hsFLP; btlEnhRFPmoe-btlGal4-UAS-tauGFP/CyO; tubGal80 FRT80/tubGal80 FRT80

3R: hsFLP/hsFLP; btlEnhRFPmoe-btlGal4-UAS-actinGFP/CyO; tubGal80 FRT82/tubGal80 FRT82

3R: hsFLP/hsFLP; btlEnhRFPmoe-btlGal4-UAS- α catGFP/CyO; tubGal80 FRT82/tubGal80 FRT82

3R: hsFLP/hsFLP; btlEnhRFPmoe-btlGal4-UAS-tauGFP/CyO; tubGal80 FRT82/tubGal80 FRT82

2. Development of air sacs

2.1 Air sac development during third instar larval stage

The development of air sacs in *Drosophila* has been described previously (Manning and Krasnow, 1993; Sato and Kornberg, 2002). However, still very little is known concerning the cellular architecture and dynamics of air sac formation. Since we wished to use this system for the analysis of mutant cells, mostly with regard to cell migration, we reasoned that a better understanding of the development as well as the cellular- and tissue architecture of third instar and pupal air sacs is a prerequisite.

I started with imaging studies of third instar- as well as pupal air sacs (Fig. R4-R6). Fig.4 shows three late wing imaginal discs and illustrates the position of the tracheal air sac as well as the stereotypic growth. Wing disc cells are marked with a ubiquitously expressed protein-trap line which tethers GFP to the membrane. Tracheal cells are outlined with RFPmoe under the control of the *breathless* enhancer. Suggested by previous studies (Sato and Kornberg, 2002), also the direct fusion of the *btl* enhancer does not outline imaginal tracheoblast cells of the spiracular branch (SB), which can be detected with the GFP signal. The transverse connective (TC) branch adheres to the wing disc; this adhesion is strongest in the region of air sac formation, since dissection never removes the TC in the region of the air sac. Moreover, air sacs always seem to bud more or less at the same position, as has been observed previously (Sato and Kornberg, 2002).

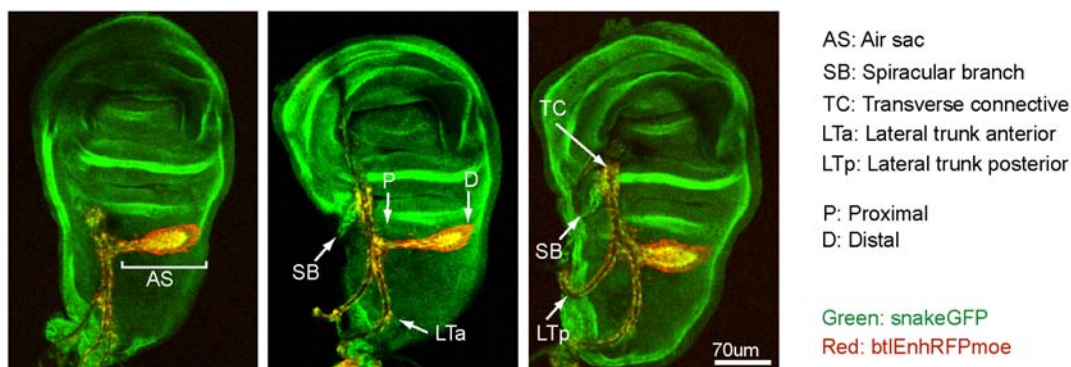
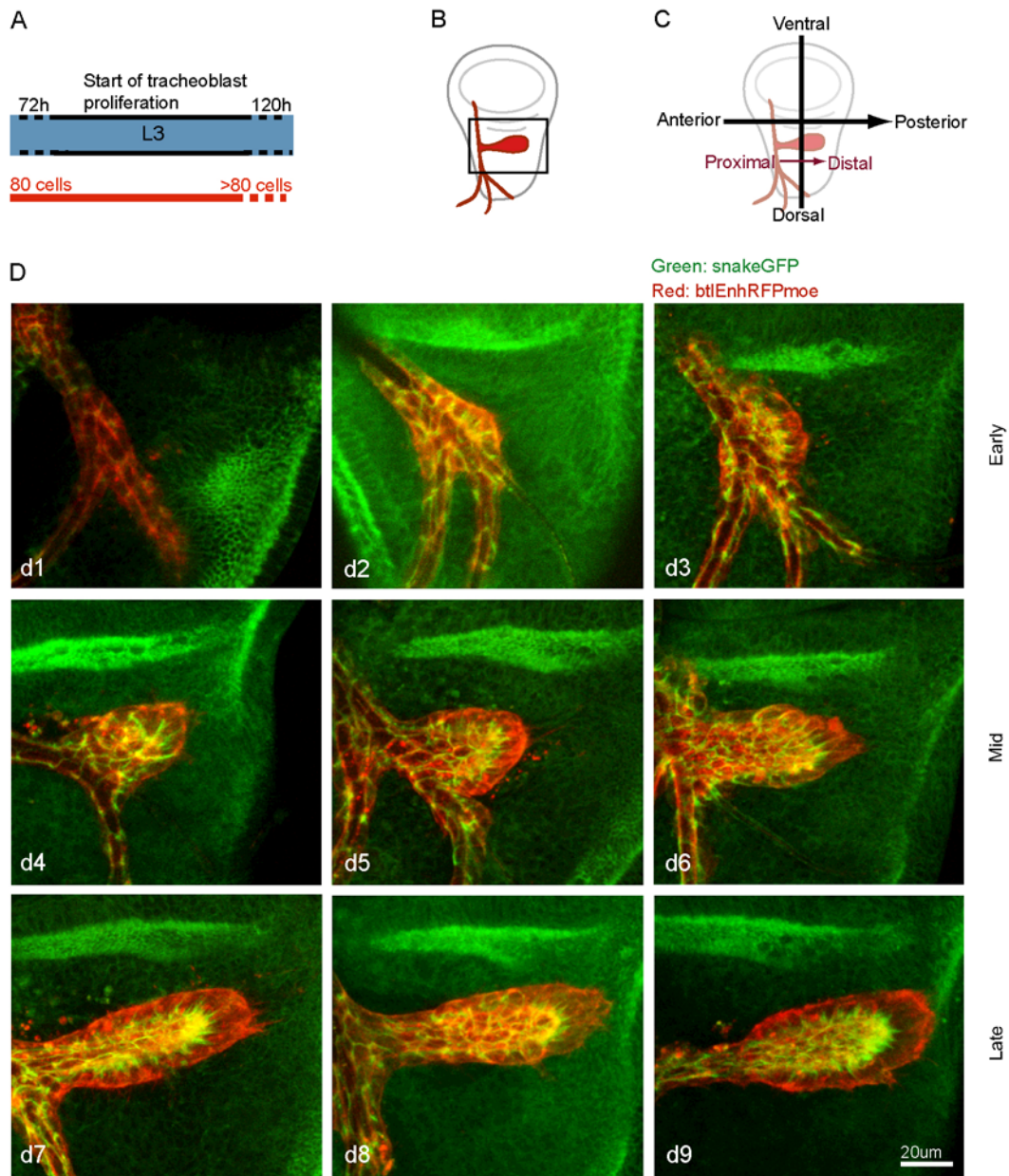


FIGURE R4:

Air sac development and nomenclature (partially adapted from (Manning and Krasnow, 1993; Samakovlis et al., 1996a; Sato and Kornberg, 2002)). Three different late third instar wing imaginal discs are shown. Air sac development shows, although stereotypical, some variability. All wing disc cells are outlined with a protein-trap tethering GFP to the membrane, providing morphological landmarks. Air sac tracheoblasts and TC cells are outlined with the expression of RFPmoe fused to the *breathless* enhancer. Note that that RFPmoe is not expressed in the spiracular branch (SB).

Air sac tracheoblasts as well as imaginal tracheoblasts start to proliferate about 70-72h AEL, which coincides with the start of the third instar larval stage (Fig. R5A), and ends at about 120h AEL when the larva starts to pupariate. Wing imaginal discs, dissected from individual early third- to late third instar larvae can be sorted into three developmental stages. In the early stages (70h AEL onwards, Fig. R5d1-d3), the TC can be seen without any outgrowth.. Air sac outgrowth is initiated in the TC at a position usually above the junction of the lateral trunk anterior (LTa) and lateral trunk posterior (LTp). However, in some cases the air sac also buds from the LTa (see Fig. R4, third disc). Budding, as well as wing disc growth, continues during third instar development (Fig. R5d4-d6) and air sac tracheoblasts start to target the margin of the wing imaginal disc. In late third instar wing imaginal discs, the proximal part (see Fig. R4&R5 for nomenclature) starts to rearrange and forms a stalk, which connects the TC with the bulk of air sac tracheoblasts located more distally (Fig. R5, d7-d9). Thus, the final position of the air sac in late third instar wing imaginal discs is the following: it abuts the most dorsal wing hinge, outlined by the strong GFP signal, and reached the posterior end of the wing imaginal disc. At this late stage, the most proximal air sac tracheoblasts often also turn ventrally and target a region located on the same level as the most dorsal wing hinge, although slightly posterior to it (not shown).

**FIGURE R5:**

Development of third instar air sacs. **A.)** Wing imaginal discs were dissected from third instar larvae from the indicated time window. **B.)** Schematic drawing of a third instar wing imaginal disc. Boxed area highlights the area seen in pictures **d1-d9**. **C.)** Overview of the used nomenclature. The black coordinates are adapted from (Klein, 2001). **D.)** Unfixed early, mid and late third instar wing discs were mounted as schematized in Fig. R1. As reference points, wing imaginal disc cells express membrane tethered GFP (see Fig. R4). Air sac tracheoblasts are marked with RFPmoe expressed in tracheal cells only. See text for description.

2.2 Air sac development during pupal stages

Air sac development continues throughout pupal stages (Sato and Kornberg, 2002). In order to examine the process of late air sac development, Actin fused to GFP was expressed in the tracheal system with *btlGal4*, a trachea-specific driver. The pupal case of mounted pupae was opened to achieve better optic resolution. Covered with a drop of halocarbon oil and a cover slide, the pupae were analyzed under the confocal microscope.

Wandering third instar larvae, once they have crawled out of the food, will start to form pupae within the next ten hours. Pupal development continues for about 4 days (132-220h AEL, Fig. R6, A). Within this period, the thoracic air sac, originating from the TC as described before, grows laterally upwards under the thorax of the developing fly (Sato and Kornberg, 2002). Air sac tracheoblasts continue to grow towards the center of the thorax but are slightly oriented towards the abdomen of the pupa (Fig. R6, b3). The air sac starts to split for the first time; one part of the air sac grows anteriorly towards the head, whereas the other part, the future scutellar air sac, continues to grow posteriorly (Fig. R6, b3, b4). The scutellar sac bends slightly and targets the middle of the thorax where it meets the future scutellar sac from the other side. The initial loose contact is lost again in older pupae (Fig. R6, b4-b6). The cells which grow towards the center of the thorax will form the medioscutal air sac. The region at the tip of the future medioscutal air sac broadens and branches once more to give rise to two lobes, both of which extend anteriorly (Fig. R6, b4-b6). The lateroscutal air sac is more difficult to image since it develops mostly in the lateral region of the thorax. It seems to also start growing anteriorly as the scutellar and medioscutal air sac begin to take shape (Fig. R6, b4-b6). Initially only a small offshoot can be seen at the very lateral side of the pupa (Fig. R6, b4) which, elongates in a symmetrical manner anteriorly and broadens in older pupae (Fig. R6, b6-b8). This also applies for the medioscutal- as well as the scutellar air sac, which, once the main branched structure is established, just grows and broadens. Pictures b2-b8 show the thoracic region highlighted in the inner small box of panel b1. Picture b9, however, shows a less detailed view encompassing also the head region of the pupa (outer box in panel b1). Three main air sacs can be distinguished. First the thoracic air sac described here, consisting of the three main branches: scutellar-, medioscutal- and lateroscutal air sac. Second, there is a huge air sac formed in the head region (HAS) that grows from a relative central position laterally in a symmetrical fashion. Third, another lobe can be seen just posteriorly of this head air sac, which could represent an offshoot of the thoracic or the head air sac, although the former seems more likely. We find, as previously reported (Sato and Kornberg, 2002), that

the main structure of the thoracic air sac is established about three days after puparium formation.

Higher magnification also reveals additional details. At the tip of growing air sacs, a number of fine extensions can be observed (Fig. R7 A,D) which, the older the air sac becomes, increase in length and diameter (Fig. R7, B,E). We currently do not know whether they exhibit a similar dynamics like filopodia in the embryo or do we know what their assigned function is. Confocal recordings over time did not show any dynamics, which could be due to two reasons; surgical manipulations destroyed the tissue or the tissue simply does not show any dynamics. However, future experiments would have to be performed in order to draw any further conclusion.

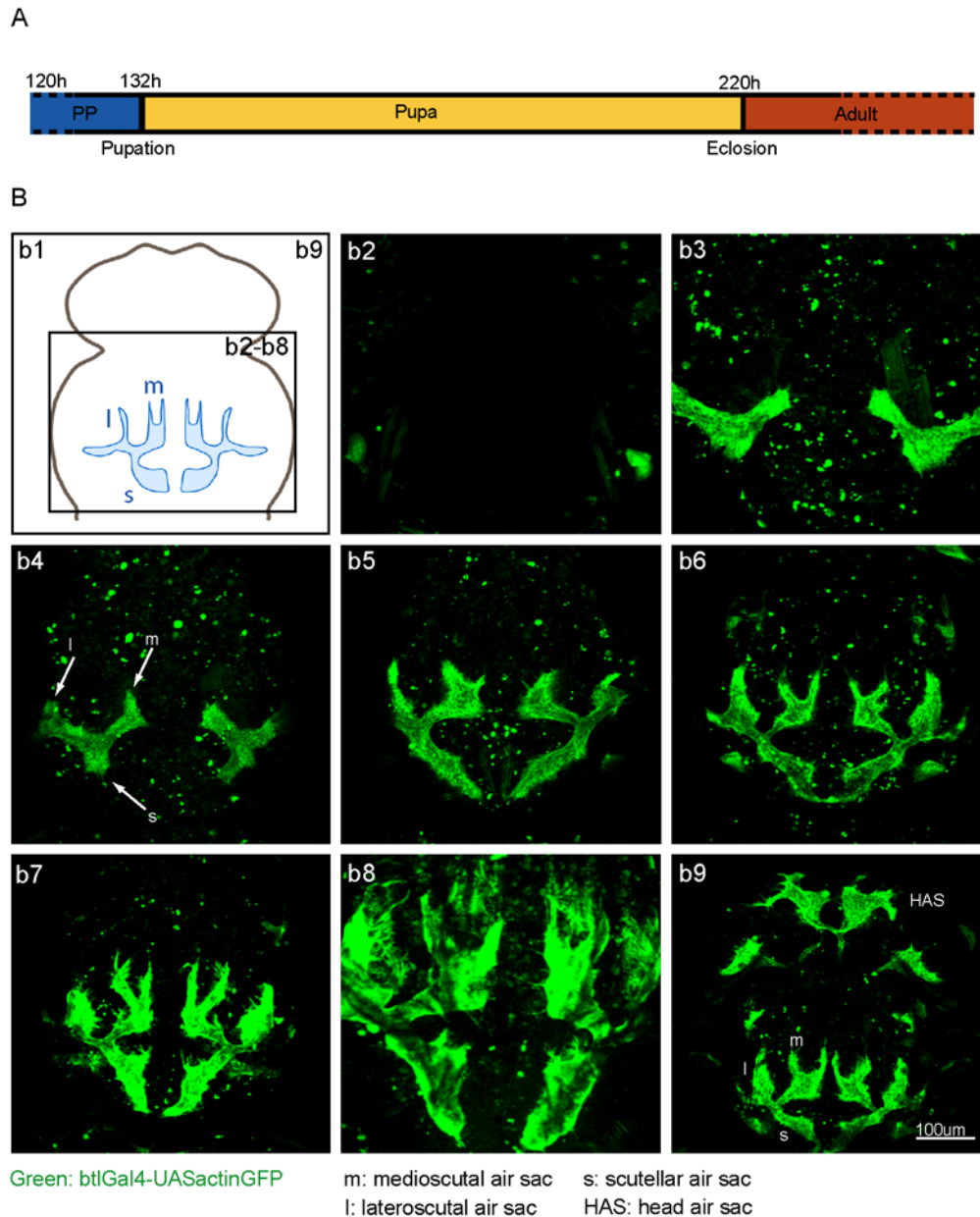
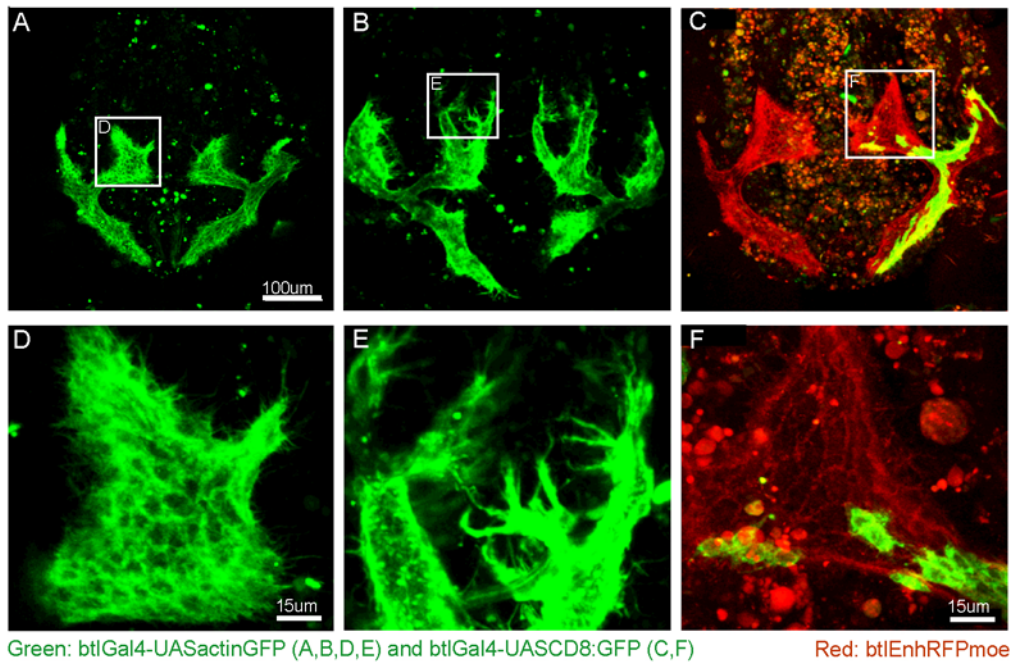


FIGURE R6:

Air sac development in pupal stages. **A.**) Pupae from the indicated time window (132-220h AEL, yellow bar) were imaged. ActinGFP outlines all tracheal cells due to tracheal specific expression (*btlGal4*). **B.**) b1: Schematic overview of the imaged area. Pictures **b2-b8** were taken from the area represented in the inner small box. **b9** represents the area outlined with the outer, big box. For description see main text. Nomenclature according to (Sato and Kornberg, 2002).

We did not observe tracheal bundles in late pupae as described previously (Sato and Kornberg, 2002). On the contrary, higher magnification revealed a mesh like pattern, resembling the outline of individual cells (Fig. R7 D, F). In order to confirm this finding, a subpopulation of air sac tracheoblast cells were genetically marked. MARCM clones were induced early during embryonic development (4-6h AEL) and pupae containing clones were analyzed under the confocal microscope. Fig. R7C & F shows a large clone, as well as a small subclone in the posterior region of the future medioscutal air sac, expressing the membranous marker CD8:GFP (Lee and Luo, 1999). Higher magnification (Fig. R7F) shows several individual cells, best seen at the margin of the clone, indicating that this mesh like pattern indeed represents air sac tracheoblast cells. This implies that the growth of the structure also largely depends on cell proliferation, since the number of cells seen at this late pupal stage by far exceeds the number of cells observed at the end of third instar air sacs. The existence of large MARCM clones supports this statement.

Therefore, I conclude that air sac tracheoblasts continue to divide during pupal stages. Furthermore, the elaborate and stereotypic branched structure of pupal air sacs suggests that air sac tracheoblasts migrate and do so under the influence of a guidance cue. The existence of filopodia-like structures in leading air sac tracheoblasts supports this observation, but direct evidence for guided cell migration in late air sac tracheoblasts is lacking.

**FIGURE R7:**

Detailed analysis of pupal air sacs. **A.-C.)** overview pictures are provided for orientation. **D.-E.)** Higher magnifications from the boxed areas in **A.-C.)**. Colors according to the legend. Note that air sacs are marked with two different GFP markers. Air sacs in **A, B, D, E** express actinGFP, whereas **C.& F.** express CD8:GFP, which, according to (Lee and Luo, 1999) is localized to the membrane. In tracheal cells, also perinuclear and cytoplasmic localization is observed.

3. Cell division in larval air sacs

It has been reported previously that imaginal tracheoblasts undergo extensive proliferation (Manning and Krasnow, 1993). Air sac enlargement was also shown to be a consequence of an increase in cell number due to cell proliferation of air sac tracheoblasts (Sato and Kornberg, 2002). This has mainly been shown using anti-phospho-histone H3 antisera, an antibody which recognizes specifically mitotic phase histone H3 (Sato and Kornberg, 2002). However, the question remained whether all air sac tracheoblast cells are capable of dividing or whether prepatterned mitotic domains exist in the air sac. This question was asked in the context of air sac development since we wanted to study mechanisms contributing to the growth, shape and morphology of air sacs. The main question was whether cell division occurs in a spatially restricted fashion or randomly.

3.1 Entry into mitosis in third instar air sacs; expression of *stringLacZ*

In order to gain insight into the distribution of mitotically active cells and to look at the dynamics, different experimental strategies were performed. I first looked at the expression of the *Drosophila cdc25* homologue *string*, a mediator of mitosis (Edgar and O'Farrell, 1989). Since *string* expression precedes cell division, it was assumed that the distribution of *string* expressing cells should indicate which cells are capable of dividing. I mostly researched mid and late stages of air sac development since the early stages were rare. However, it can be assumed that the results are also representative for early stages. The results are displayed in figure R8. *btlGal4-UASactinGFP* was crossed to *stringLacZ^{P[w+]STGβ6C}*, a transgenic line reflecting expression of *string* most prominently in tracheal cells (Hacohen et al., 1998) as well as in some other wing disc cells. As seen in figure R8, β Galactosidase expression is uniform in the air sac (Fig.R8 B,E,H) indicating that all tracheoblasts could undergo cell division. Very prominent *string* expression was also seen in the spiracular branch (Fig. R8 B,C), the location of imaginal tracheoblasts. This was not surprising since these cells are known to proliferate. However, as can be seen in Fig. R8A, *btlGal4* does not label these particular cells.

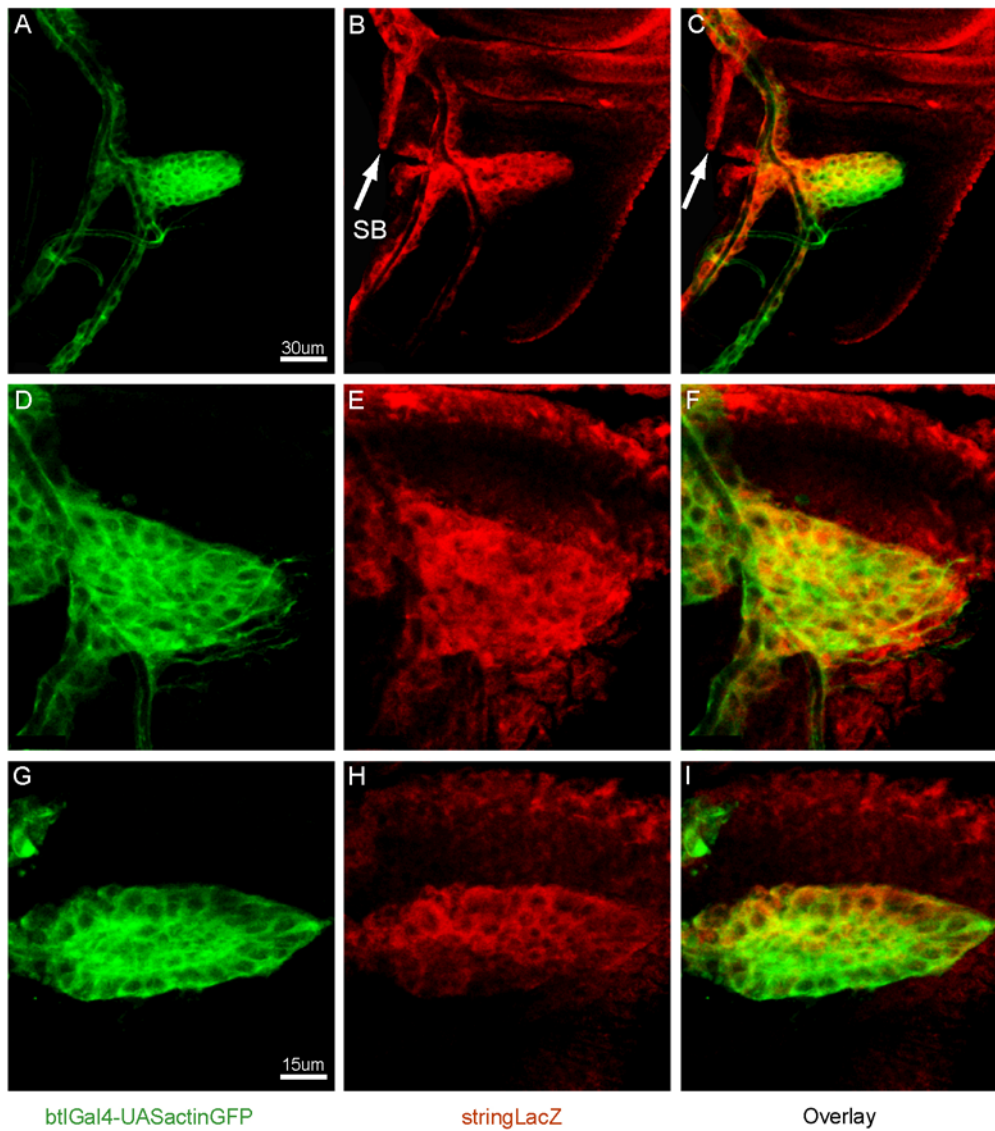
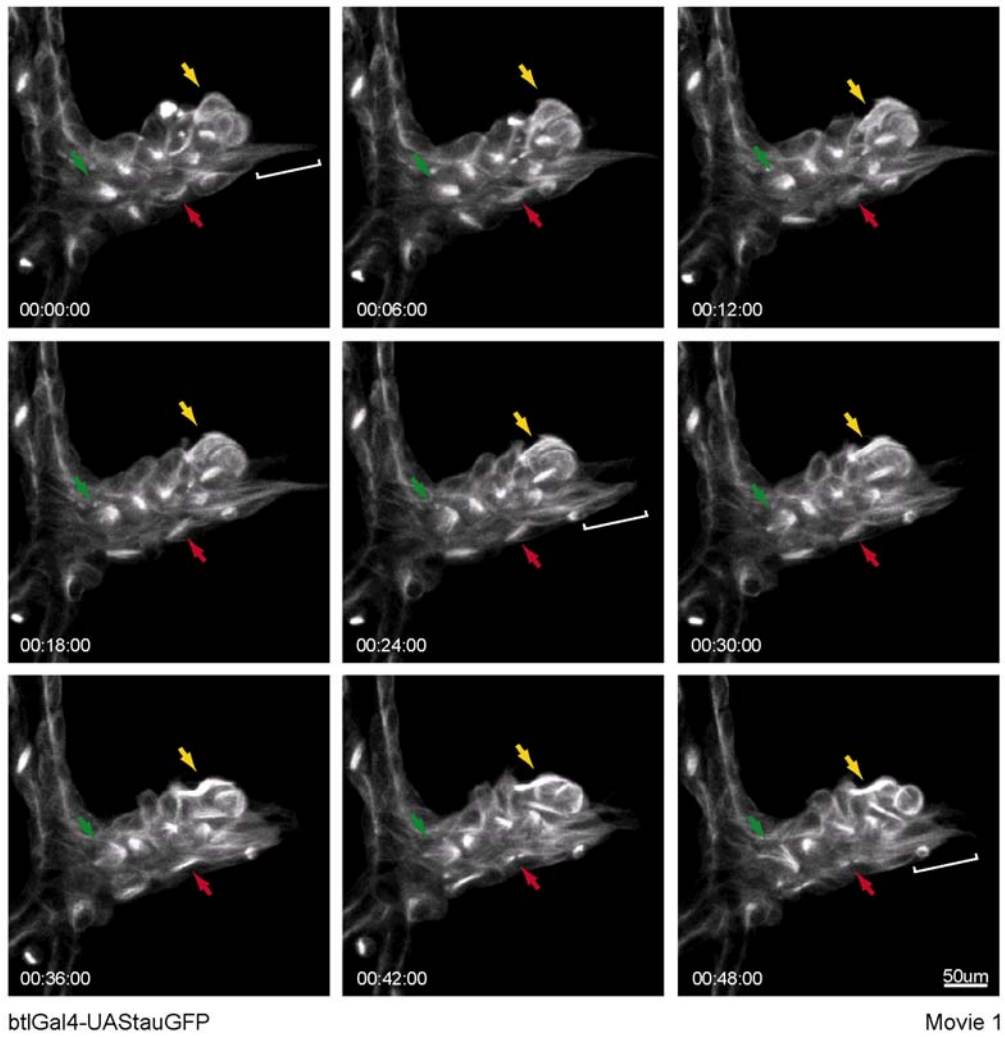


FIGURE R8:

String expression in air sac tracheoblasts. **A.-C.)** provide overview pictures. **D.-I.)** present higher magnifications. **A., D., G.)** only the GFP (ActinGFP) channel is shown, **B., E., H.)** only string expression, **C., F., I.)** Overlay. String expression was visualized using the transgenic line $stringLacZ^{P[w+]STG\beta6C}$ (Hacohen et al., 1998). Note that the spiracular branch is only outlined by β gal expression but not with $btIGal4-UASactinGFP$.

3.2 Patterns of cell division in early/mid stage air sacs

To show dividing cells directly, the microtubule binding protein Tau fused to GFP (tauGFP) (Brand, 1995) was misexpressed in air sacs and analyzed with 4D microscopy. Pictures from such a movie (movie1) can be seen in figure R9. The movie nicely illustrates the occurrence of cell division in various locations of this early/mid stage air sac. Dividing cells can be recognized according to the formation of mitotic spindles in proximal as well as distal areas of the air sac (Fig. R9, see green, yellow and red arrows for examples). The movie also shows the formation of extensions at the tip of the air sac (brackets in Fig.9). This particular extension forming cell was not observed to undergo cell division. However, other tip cells can undergo cell division as shown in Fig. R9 (yellow arrow and cell below). Further evidence for random cell division comes from movie 2, represented by snap shots in figure R10. In this experiment, MARCM clones were labeled with tauGFP, which enables the evaluation of individual cells. For a precise location of MARCM clones, RFPmoe fused to the *breathless* enhancer was recombined onto the btlGal4-UAStauGFP chromosome; the outline of the entire air sac as well as individual clones can be observed simultaneously. A distal cell as well as a more proximal cell can be distinguished in this early/mid stage air sac, which both form mitotic spindles and therefore are in the process of dividing.

**FIGURE R9:**

Picture series of movie 1. Not all time points are represented. Colored arrows show examples of mitotic spindles. White brackets illustrate the extension formed at the tip. For complete movie see movie1 on supplementary CD.

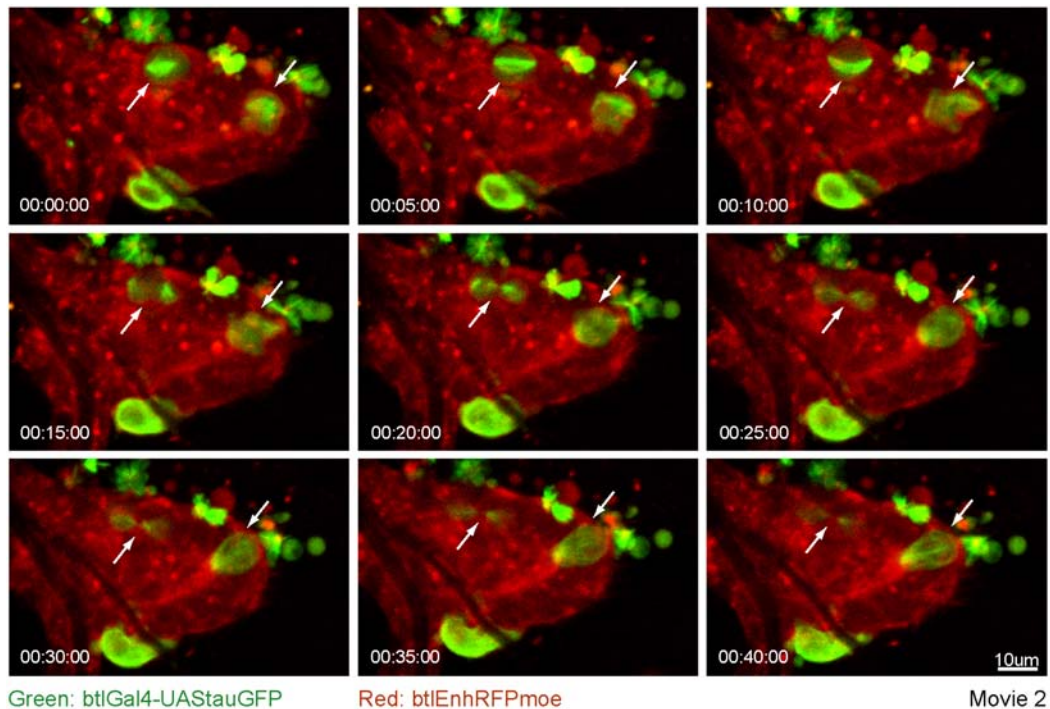


FIGURE R10:

Cell division of single air sac tracheoblasts. MARCM clones were labeled with tauGFP. All air sac tracheoblast cells express RFPmoe. Selected time frames are presented. White arrows show examples of dividing cells. For the entire movie see movie 2 on supplementary CD.

3.3 Cell division rates in late air sacs

The experiments shown above demonstrate that air sac tracheoblasts do not divide in a spatially restricted manner. A specialized subpopulation of air sac tracheoblasts within the air sac could not be distinguished. Nevertheless, studying late air sacs, provided evidence that air sac tracheoblasts do not divide uniformly in all stages. As already shown in figure R5 d8-d9 the most proximal cells elaborate into a stalk-like connection similar in appearance and cellular complexity to the TC. On one hand, formation of this stalk is not in agreement with uniform cell division. On the other hand, extensive cell rearrangements in the air sac could contribute to the formation of this stalk. However, as will be shown later, no extensive rearrangement was observed with the tools used so far. Imaging late air sacs, which express tauGFP and RFPmoe simultaneously in air sac tracheoblasts, shows that cell division is excluded from the stalk region and spatially restricted to more distal areas of the air sac, based on the formation of mitotic spindles (Fig. R11, A-C). The air sac shown represents just one of

several that demonstrate the same phenomena. I have observed previously that dividing air sac cells round up, which can be seen by cortical RFPmoe localization. The spindles, outlined with tauGFP, usually sit in the center of these round cells and appear as blots if the spindle is oriented in the x-z axis (Fig. R11, B, white arrow).

These observations are confirmed by analyzing the distribution of MARCM clones (Fig. R11D-I) induced in the early embryo (1. heat-shock window, see fig. R2). We assume that such clones consist of a maximum of four cells at the beginning of third instar air sac development since only two tracheal cell divisions occur during embryonic development and no further cell division is reported until the onset of third instar stages. Clones labeled with CD8:GFP can be seen in various locations in the air sac (see also subsequent chapters). In late air sacs, proximal clones usually appear to consist of fewer cells than clones located in more distal areas (compare fig. R11 D with E, F, H). Although some clones (shown in fig. R11H) populate the entire stalk region they do not further increase in size, at least not to an extent as more distally located clones. These cells also show an elongated shape, different from more distally located cells (fig. R11I).

Nevertheless, also small clones can be observed at the very tip of the outgrowing air sac (see fig. R11 F,G, broken boxes). These could arise via two mechanisms. First, they could become separated from a big founder clone. Second, they could represent independent clones and thus reflect reduced proliferation rates. Since we find independent isolated small clones in proximal and distal locations, indicates that some clones are subject to altered division rates. We also suggest the involvement of cell migration for the location of small clones at the tip (see later).

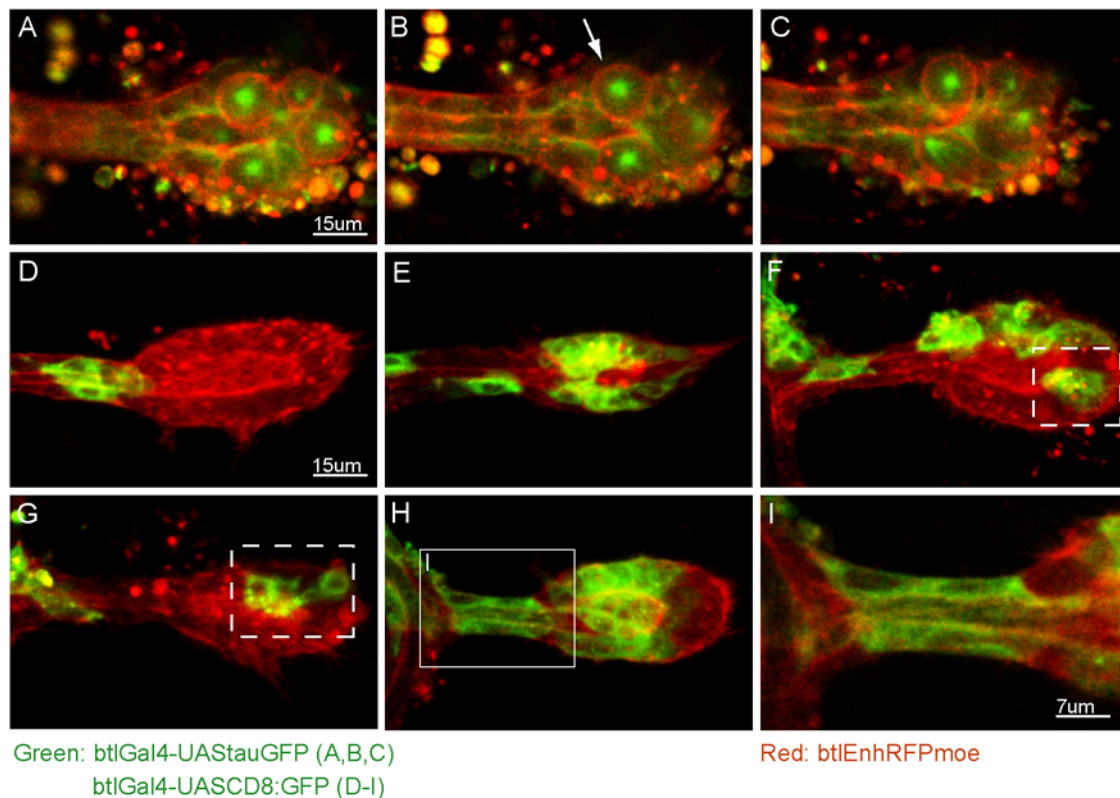


FIGURE R11:

A.-C.) Three sections through the same air sac are shown. RFPmoe as well as tauGFP are simultaneously expressed in this air sac to correlate mitotic spindle formation with air sac tracheoblast shape. Dividing cells round up as seen with cortical RFPmoe localization and the mitotic spindle is outlined as a green spot when seen from a specific angle. **B.)** white arrow points to a dividing cell. **D.-I.)** MARCM clones labeled with CD8:GFP. Small clones are usually located in the stalk as seen in **D, E, F.** **E.&H.)** Clones located in the main air sac body increased in size compared to clones in the stalk (compare clones within air sac in **E.**). Boxed areas in **F.&G.** highlight small clones at the tip. **I.)** represents a clone in the stalk. All stalk cells are labeled and display the characteristic elongated shape. See text for further explanation and interpretation.

Imaging data suggest that air sac tracheoblasts in later stages mostly divide in distal areas of the air sac. Clonal analysis supports this observation based on the occurrence of small individual clones in proximal, but also in distal locations of the air sac.

The distal clones could either be separated through cell rearrangement events from their founder clone or represent independent clones that did not divide as often as other founder clones. Since the development of an early-induced clone in an early air sac cannot be imaged over very long time periods, it is difficult to test this hypothesis.

However, based on these observations, I speculate that the position of the founder cell of a clone can probably determine the proliferation rate and therefore the final clone size.

Therefore, the original location and size of an embryonic born clone relative to the site of air sac outgrowth could determine its final size (see also discussion).

4. Third instar air sac morphology

4.1 Polarity of air sac tracheoblasts

Tracheal cells are epithelial cells and therefore have an intrinsic polarity with an apical and a basal side (Manning and Krasnow, 1993; Samakovlis et al., 1996a; Tepass et al., 2001). Embryonic tracheal cells extend their basal side towards the Bnl/FGF signaling centers and the cell body as well as the apical surface then follow (Shim et al., 2001).

We wanted to investigate whether air sac tracheoblasts also display this characteristic polarity. We took advantage of the subapical marker α -Catenin, which localizes at the apical junctions of *Drosophila* tracheal cells (Jazwinska et al., 2003).

Studying air sac tracheoblasts which express *Drosophila* α -Catenin fused to GFP (Oda and Tsukita, 1999) from early- to late third instar stages reveals that air sac tracheoblasts are also polarized from very early on. Moreover, this polarization is maintained throughout third instar development (Fig. R12). In very early third instar air sacs, α -Catenin is already subapically localized and displays the characteristic mesh-like pattern, as reported previously in the embryonic tracheal system (Jazwinska et al., 2003). This pattern was also observed in TC. However, the budding zone can be distinguished based on its position in the TC as well as from the outgrowth of a number of cells. These cells clearly protrude with their basal side since the subapical marker α -Catenin is localized towards the lumen of the TC (Fig. R12 A). In subsequent early stages (Fig. R12, B, C), the subapical localization of α -Catenin can be observed. However, the cells are not yet as regularly arrayed as they are in later stages (Fig. R12, D-I). This might reflect the fact that cell division precedes cell rearrangement. Although proliferation is maintained in later stages, these two processes are probably better coordinated.

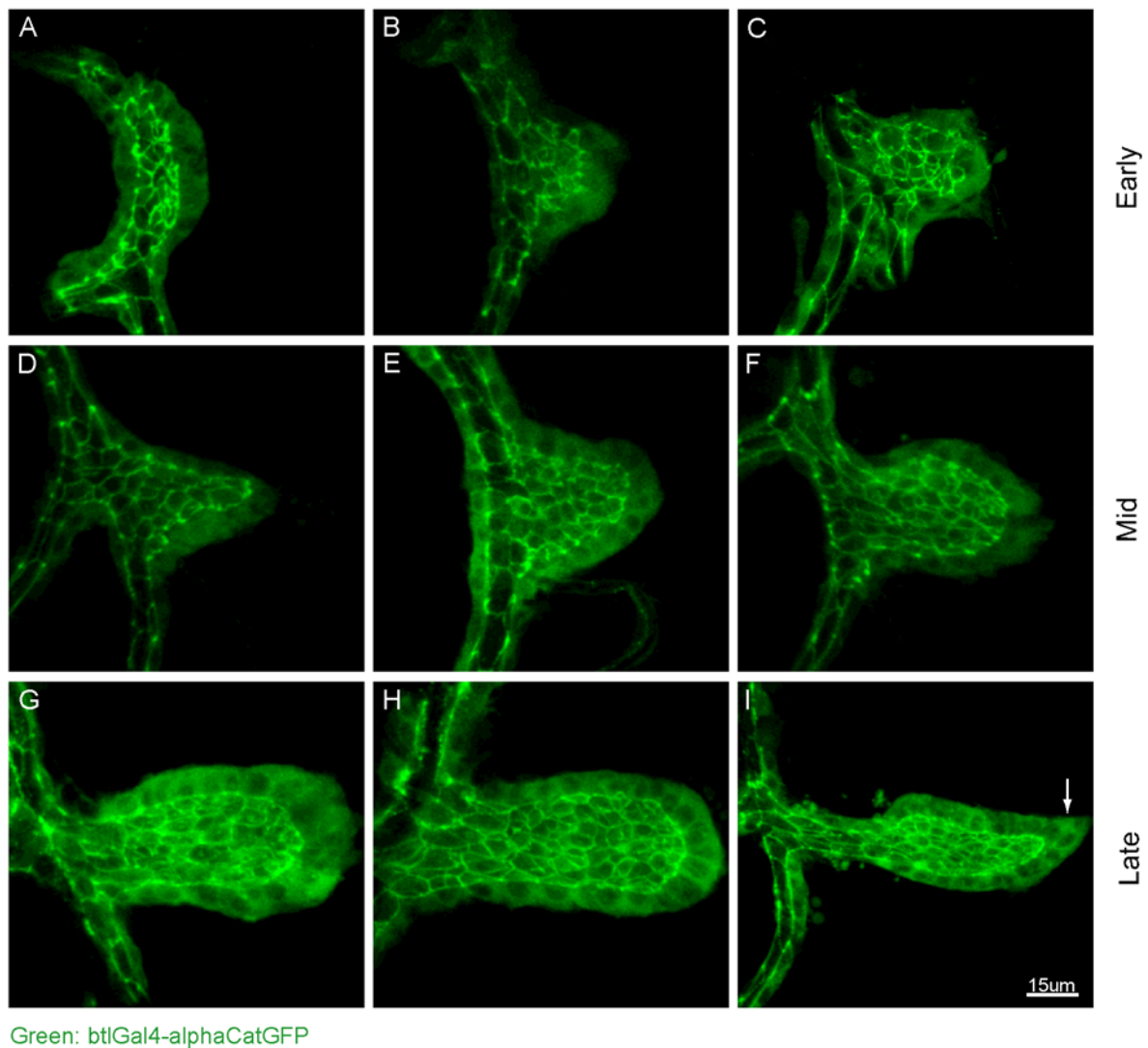


FIGURE R12:

Polarity of air sac tracheoblasts as seen with α CateninGFP localization. **A.-C.)** From early third instar stage on, α CateninGFP is subapically localized. **A.)** Budding zone in the TC. **B., C.)** air sac tracheoblast arrangement appears unorganized in early air sacs. **D.-F.)** Mid air sac stages display a regular organization of the air sac tracheoblasts into a monoepithelial layer. **G.-I.)** Regular organization is maintained, although in late air sacs, two distinct zones can be observed. **I.)** In the stalk, cells elongate and probably rearrange. In the very tip (white arrow), the regular organization seems interrupted.

4.2 Air sac architecture

Figure R12 shows the architecture of third instar air sacs. As in the TC, which consists of a lumen surrounded by a tracheal monoepithelium, a similar complexity can be seen in the air sac. A monoepithelial cell layer seems to wrap around a luminal space. In almost all stages and in all positions of the air sac, just one cell can be seen at the outer rim of the air sac with its apical side facing inwards and the basal side directed outwards (best seen in fig. R12, E-I).

However, especially in later stages (see fig. R12, I), this organization seems altered at the most distal position of the air sac, the air sac tip. It appears as if two cells are arranged in an end-to-end fashion; one cell containing an apical side, whereas the other cell does not.

In order to confirm this observation as well as to characterize air sac tracheoblasts based on their shape with respect to their position and stage, MARCM clones were specifically labeled with α -CateninGFP. Examples of clones can be seen in figure R13. Cells located in the main air sac body region labeled with α -CateninGFP, overlap completely with RFPmoe which is expressed in tracheal cells only. The apical side can be distinguished from the nucleus as well as unlocalized cytoplasmic α -CateninGFP as a bright ring facing inwards. The nuclei are located basal to the adherens junctions (fig.13, E, F). These cells usually have a narrow apical- but a broad basal surface, resulting in wedge shaped cells. Cells located at the most proximal end of the air sac display larger apical sides as well as elongated cell shapes (fig. R13, K,L). Other clones located in the stalk wrap around it and show the elongated, but narrow, apical side (fig. R13, G). The most interesting clones, however, are located at the most distal part of the air sac. As mentioned above, clones can be distinguished where α -CateninGFP is not (yet) subapically localized. Two examples are seen in Fig. R13 F&J. In both cases (best seen in fig. R13, J), two cells are located in a row as judged from the position of the nuclei, but only one cell abuts the apical luminal side, which can also be identified based on the strong RFPmoe localization.

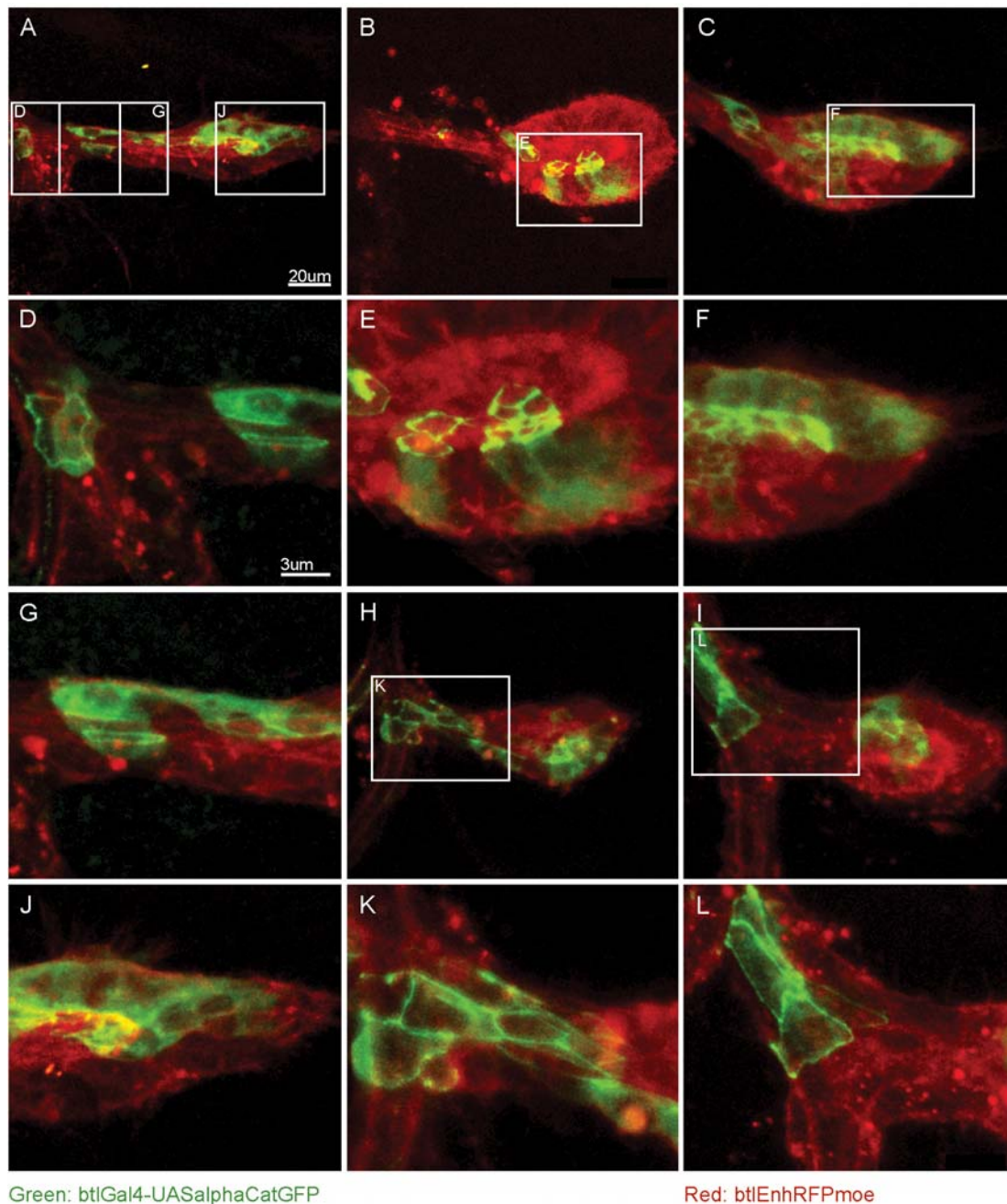


FIGURE R13:

Cell shapes of individual air sac tracheoblasts. MARCM clones marked with α CateninGFP were induced in the early embryo. Air sacs are outlined with RFPmoe. **A.-C.)** Overview pictures. Clones were recovered in different positions in the air sac. **D.)** A rare single TC clone showing a different orientation than clones in the stalk. Stalk clones wrap around the stalk and show elongated cell shape with the nucleus located above the adherens junctions. **E.)** Clones in the main air sac body to demonstrate the monoepithelial character of the air sac tissue. The apical side is marked with a bright green ring, whereas weak unlocalized cytoplasmic α CateninGFP can be extending basally and overlaps with RFPmoe. **F.)** as in E. clones located closer to the tip. **G.)** Stalk cell clones as in D. **H.&I.)** Overview pictures. **J.)** Tip cell clone. One cell adjoins the apical side as outlined with the bright red internal ring, the neighboring cell more distally does not show α CateninGFP localized to adherens junctions. **K.&L.)** Very proximal clones at the interception of stalk and TC. These cells usually display a larger apical side compared to cells located more distally in the main air sac body (compare with E.).

To get further insight into cellular dynamics at the tip, a movie was taken of an air sac containing MARCM clones marked with α -CateninGFP (fig. R14, movie 3). At time-point zero, two to three cells alongside each other and abutting the apical side can be observed. Over time, the center cell (marked with a white asterisk) of this three cell cluster seems to elongate, and another cell appears (blue asterisk, time point: 6 min), in which only unlocalized cytosolic α -CateninGFP can be detected. Since the position of the neighboring cells of this three cell cluster does not appear to be altered, I conclude that this cell appears either from the other side of the air sac or is a new born daughter of the middle cell (white asterisk). The latter explanation is more likely, since the two cells are in the same focal plane. Based on these observations, the architecture of a third instar air sac can be described as a monoepithelial layer consisting of an inward-facing apical side as well as an extending basal side. Cells located proximally, elongate and wrap around the stalk which contains fewer cells than the main body of the air sac. At this position, the apical side of air sac tracheoblasts is constricted and the basal side enlarged, resulting in wedge shaped cells. At the tip, cells have been observed that do not abut the apical side of the air sac and extend basally.

Thus, it is very likely that cell rearrangements play an important role in establishing such a structure. However, the occurrence of cell division does not facilitate the analysis. Movies 4, 5 & 6, show the summarized observations in motion. The three movies represent 4D imaging from just one air sac, expressing α -CateninGFP in all air sac tracheoblast cells. Snap shots of the three movies are shown in figure R15. In the first time frame, the air sac appears as an elongated bud that over time elongates even further. Cells in proximal locations are stretched and elongated whereas cells at the tip interrupt the regular monoepithelial organization.

Currently, we neither understand how air sac tracheoblasts organize themselves in such a regular fashion nor do we know how specialized regions such as the stalk or the tip are established. It will be of major interest to address these questions in the future.

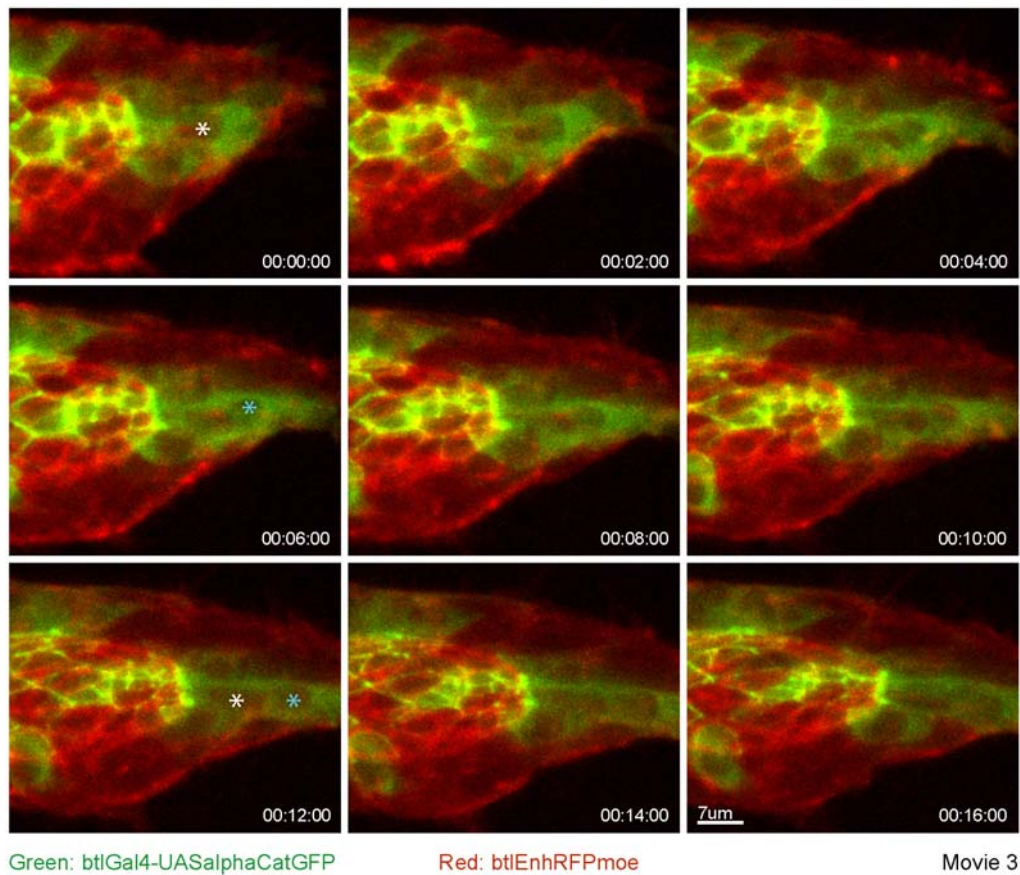


FIGURE R14:

Picture series of movie 3. MARCM clones labeled with α CateninGFP. Distal area of a late third instar air sac was imaged. A clone consisting of at least three cells adjoin the apical side of the air sac (bright red ring located internally in the air sac). The center cell was marked with a white asterisk. Note the appearance of a fourth cell (blue asterisk) distally to the highlighted one. After about 12 min. both cells can be seen arranged in an end to end orientation. Only one cell contains a narrow apical side as judged from the bright green α CateninGFP signal, whereas in the other cell α CateninGFP is only localized cytosolic.

See supplementary CD for complete movie sequence (movie 3).

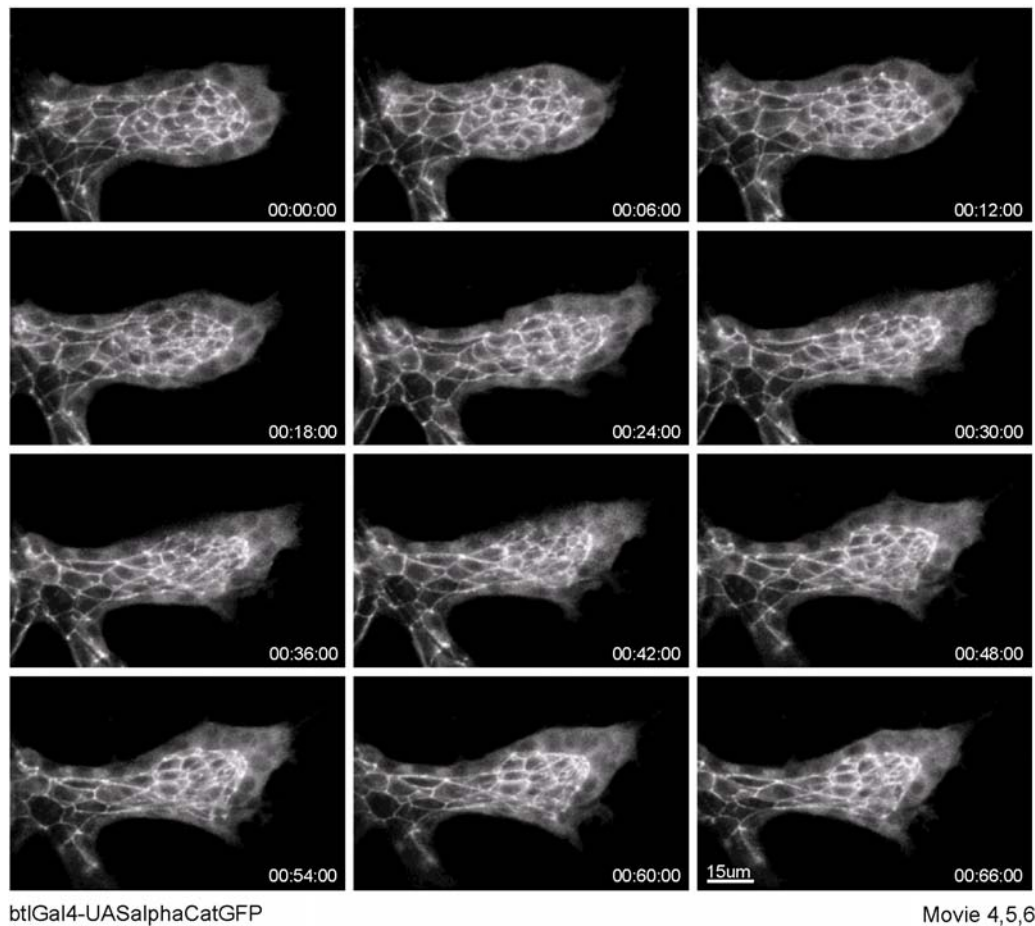


FIGURE R15

Picture series of movies 4,5,6. Individual time points from all three movies are combined in this figure. The organized mesh-like pattern is due to the subapical localization of α CateninGFP, highlighting adherens junctions. Note that at the tip, the regular monoepithelium is interrupted from time point 00:24:00 on. Moreover, cells in the proximal region start to organize themselves into a stalk. See supplementary CD for complete movie sequences (movies 4-6).

4.3 Air sac lumen formation

As already mentioned, air sac tracheoblasts seem to be organized around a luminal space. This observation is based on the analysis of confocal sections through third instar air sacs as well as studying air sacs expressing α -CateninGFP (see also movie7&8, representing 3D reconstructions of mid & late third instar air sacs). Confocal sections through air sac tracheoblasts revealed the existence of a region devoid of cells (not shown). To further investigate the composition of this lumen, third instar wing imaginal discs were incubated with an antibody against Pio, an apically secreted luminal protein and component of the extracellular matrix (Jazwinska et al., 2003). In early air sacs (fig. R16, A-C), Pio protein can

be detected in air sac tracheoblasts, although the expression is weak. In mid stages, expression increases and Pio becomes localized into a lumen that is best visible in late stages of third instar air sacs (fig. R16, G-I). Therefore, air sac growth and lumen formation take place simultaneously.

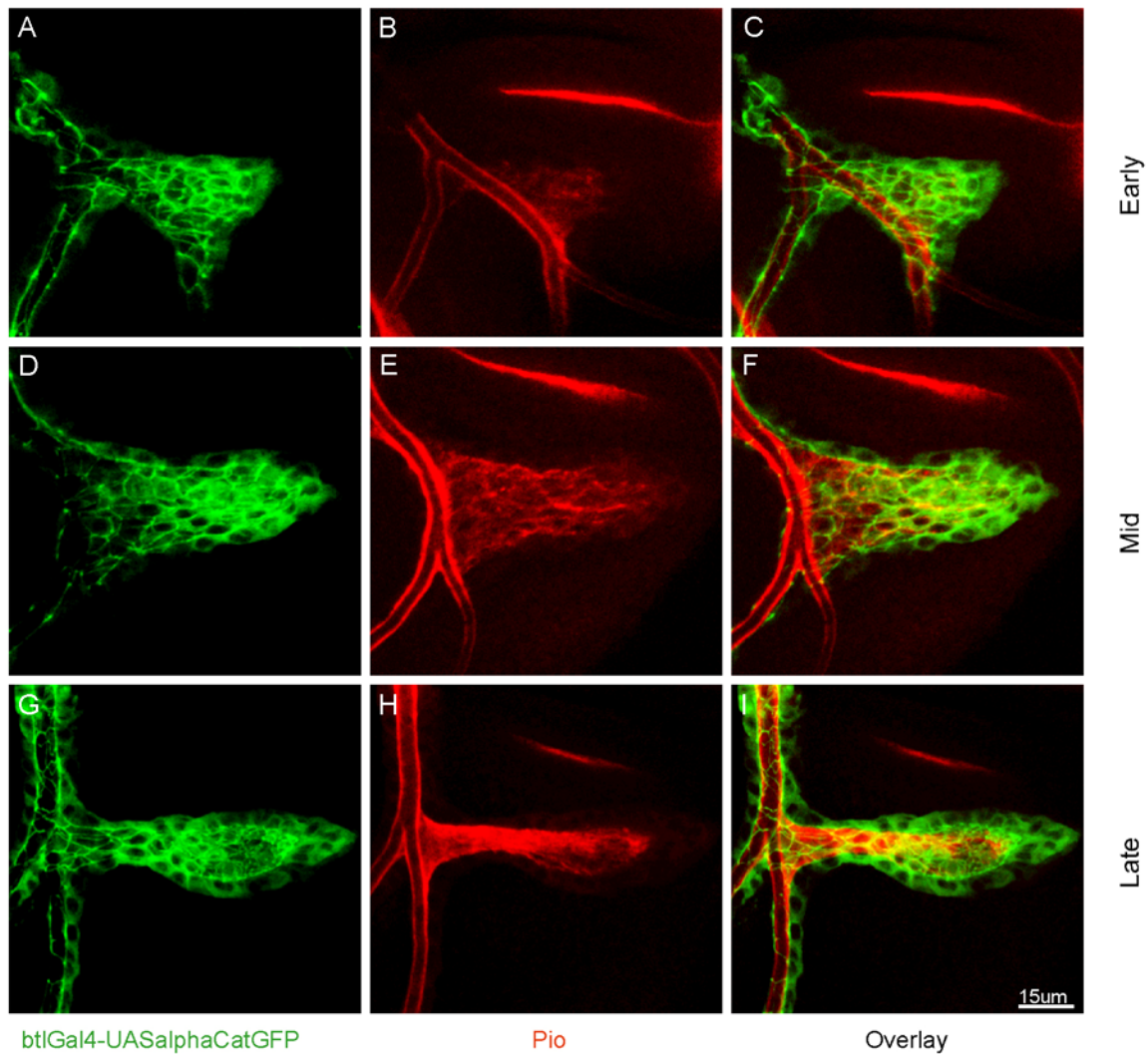


FIGURE R16:

Lumen formation as highlighted with the localization of Pio (Jazwinska et al., 2003). **A.,D.,G.)** Only GFP channel is shown. **B.,E.,H.)** Pio localization in red. In early third instar air sacs Pio is localized in air sac tracheoblasts. Later Pio is mainly detected in the lumen. **C.,F.,I.)** Overlay.

We further asked whether the lumen contains a connection with the transverse connective (TC), which is at this stage already functional and filled with gas. However, higher magnifications of late third instar air sacs do not reveal a connection between the lumen of the TC and the lumen of the air sac (fig. R17). The TC furthermore shows no intraluminal Pio staining, whereas in air sac lumen, Pio is equally distributed (fig. 17 B&E). The different localization of Pio in the TC and the air sac is very likely due to the fact that the air sacs are liquid filled, which enables Pio to spread, whereas spreading in the air-filled TC is limited. Therefore, to prevent the air sac lumen from collapsing during development, this structure must be stabilized with liquid and extracellular matrix proteins until it is ready to carry out its function. I assume that the air sac lumen is opened towards the TC during pupal stages, or shortly before eclosion. Although we imagine the existence of a “plug cell”, we currently have no concept of how the separation and reconnection of the different lumens are established.

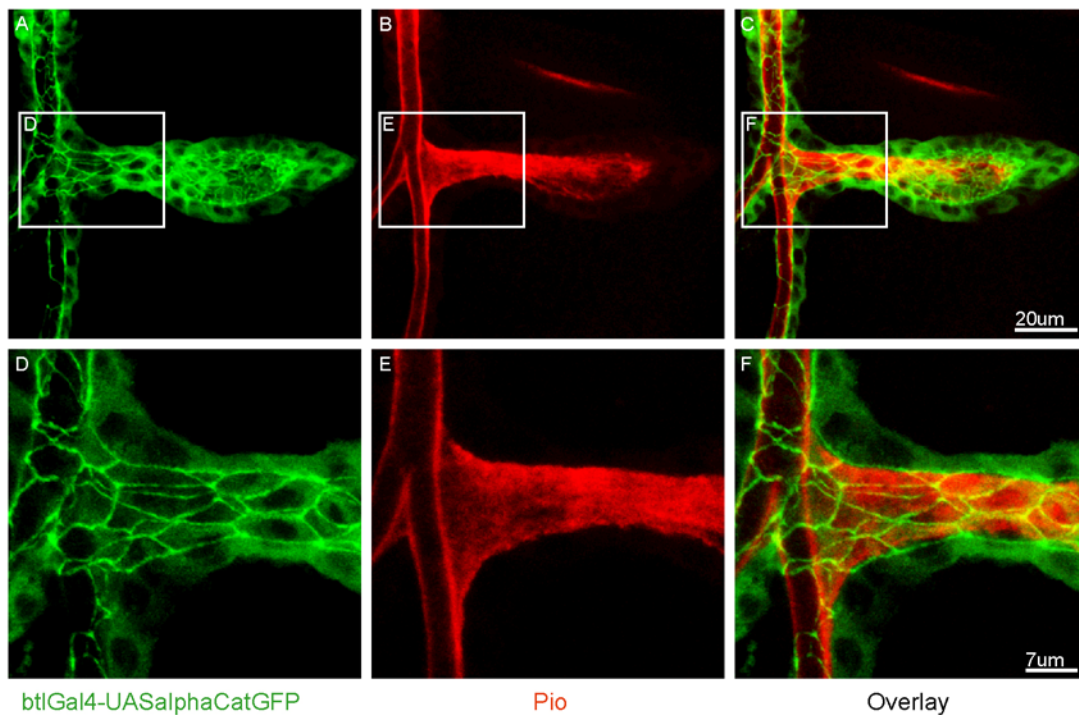


FIGURE R17:

Connectivity of the air sac lumen. **A., D.)** α CateninGFP expression to outline the adherens junctions at the apical side. **B., E.)** Highlight of Pio staining. Note that Pio is localized in the lumen of the air sac but not in the TC. **C., F.)** Overlay.

5. Guided cell migration of air sac tracheoblasts

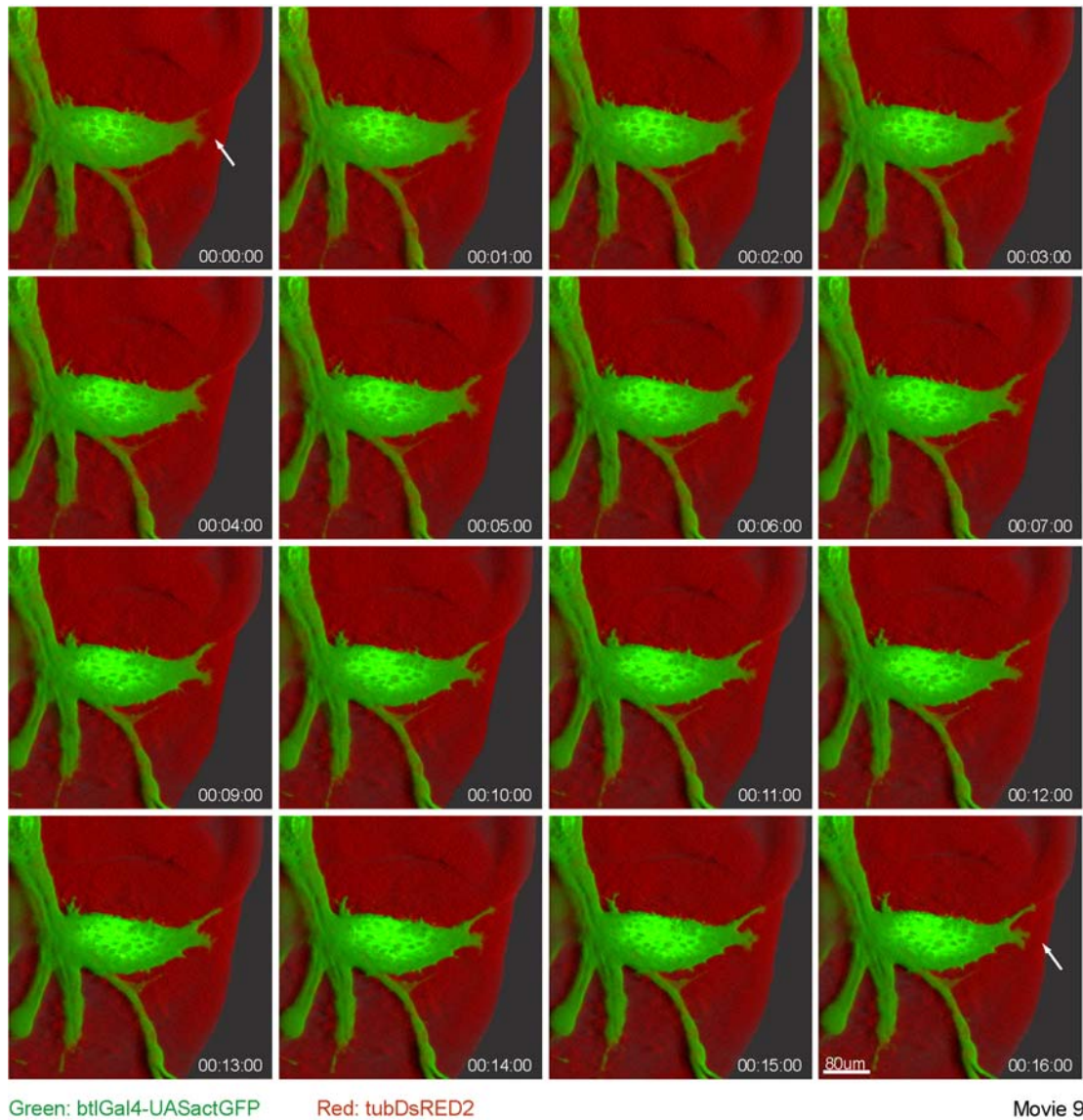
5.1 Guided cell extensions and cell migration of air sac tracheoblasts

It has been suggested that air sacs also develop via cell migration, which is supported by the expression of the FGF ligand *bnl* in cell clusters of the columnar epithelium and *btl/FGFR* expression in air sac tracheoblasts (Sato and Kornberg, 2002) and Fig. I17). Gain-of function as well as loss-of-function experiments only support this suggestion to a certain extent. Expression of dominant-negative *btl* constructs abolished the formation of an air sac, which could be due to the absence of cell migration, cell proliferation or both. On the other hand, it was shown that *bnl* loss-of-function clones in the columnar epithelium stalls air sac tracheoblast migration, whereas ectopic *bnl* clones induce the formation of novel air sacs (Sato and Kornberg, 2002). Based on these experiments, it was concluded that air sac tracheoblasts migrate in response to FGF signaling.

Tracheal cells extend dynamic filopodia at the tip of migrating branches (Ribeiro et al., 2002; Shim et al., 2001; Wolf et al., 2002). It is assumed, although not directly proven yet, that filopodia are required for tracheal cell migration. In addition, air sac tracheoblasts extend filopodia-like protrusions at the tip (Sato and Kornberg, 2002).

We intended to gain further insight into the process of cell migration of air sac tracheoblasts by first studying wild-type air sac tracheoblasts with regard to migration. Since cell migration is a dynamic process, 4D imaging seemed to be the method of choice to investigate the migratory behavior of air sac tracheoblasts.

Movie 9 (fig. R18) shows a 4D reconstruction of a low resolution movie. As a reference point, all wing imaginal disc cells are outlined in red, due to ubiquitous DsRED2 expression (Sato and Kornberg, 2002). Air sac tip cells, expressing actinGFP show extensions, one of which seems to be stabilized and targets the fold of the posterior wing margin. A slight net forward movement can be observed.

**FIGURE R18:**

Picture series of movie 9. Tracheal cells are outlined with actinGFP, the wing disc with DsRED2 (direct fusion with tubulin promoter (Sato and Kornberg, 2002)). White arrows highlight the extension at the tip of the outgrowing air sac. Note the fold in the wing disc which is targeted by this extension. See supplementary CD for complete movie sequence (movie 9).

More detailed 4D analysis with the expression of tauGFP in air sac tracheoblasts showed that the initial extension is followed by the cell body as described in the cell migration cycle. TauGFP allows for the differentiation between dividing and non-dividing cells, since the dividing cells round up and display characteristic mitotic spindles. As shown in figure R19, which represents snap shots of movie 10 & 11, the cell(s) at the tip form an initial extension (highlighted with a green arrow at time 00:00:00). About 10 minutes later, the connected cell body propels forward (red arrows, fig. R19). Moreover, the extension, as well as the

following cell target to a predefined location, indicating that this movement is directly guided, most likely by FGF/bnl. A retraction of this cell has not been observed in subsequent movies. Therefore, this event reflects the classical migration cycle; the cell polarizes due to an external agent, extends a protrusion in the direction of migration and moves the cell body forward.

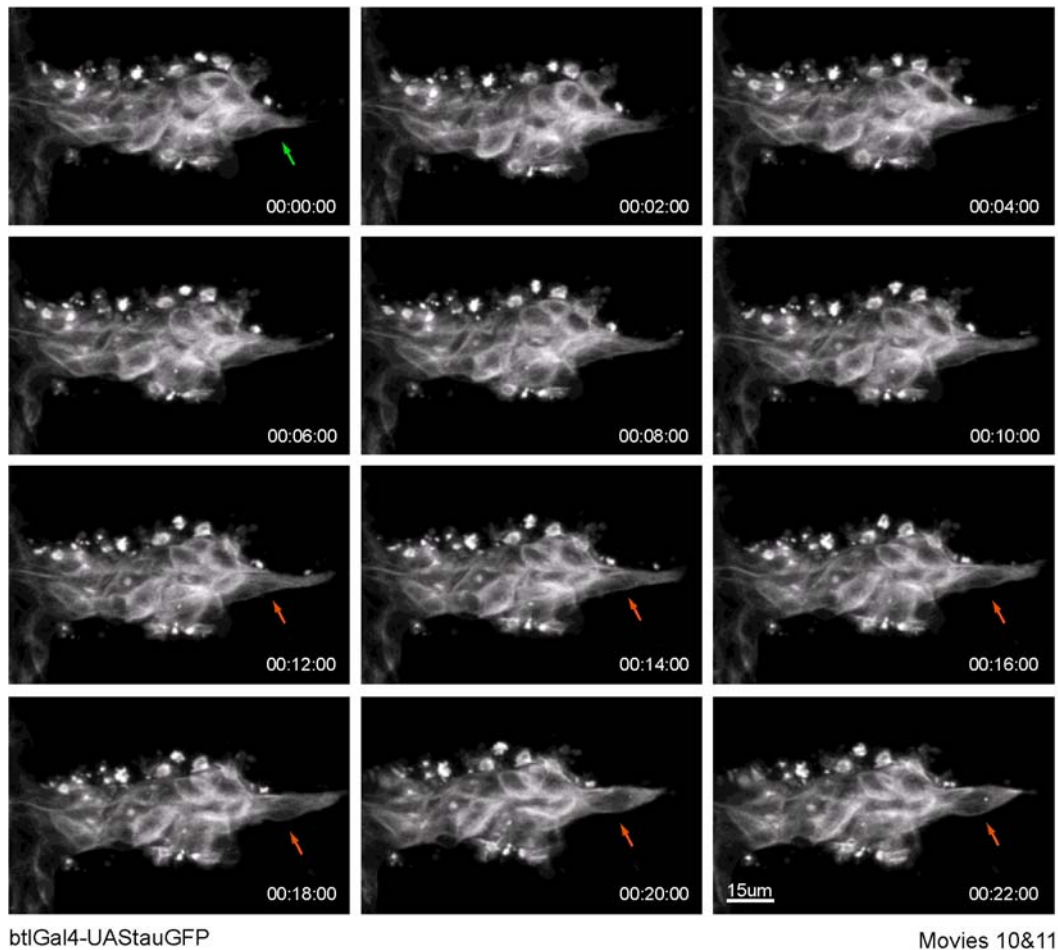


FIGURE R19:

Picture series of movies 10&11. Tracheal cells are outlined with tauGFP. The initial protrusion at the tip is highlighted with a green arrow. Note how the extension broadens after about 12 min (red arrows) and a cell body moves forward. See supplementary CD for complete movie sequence (movie 10 & 11).

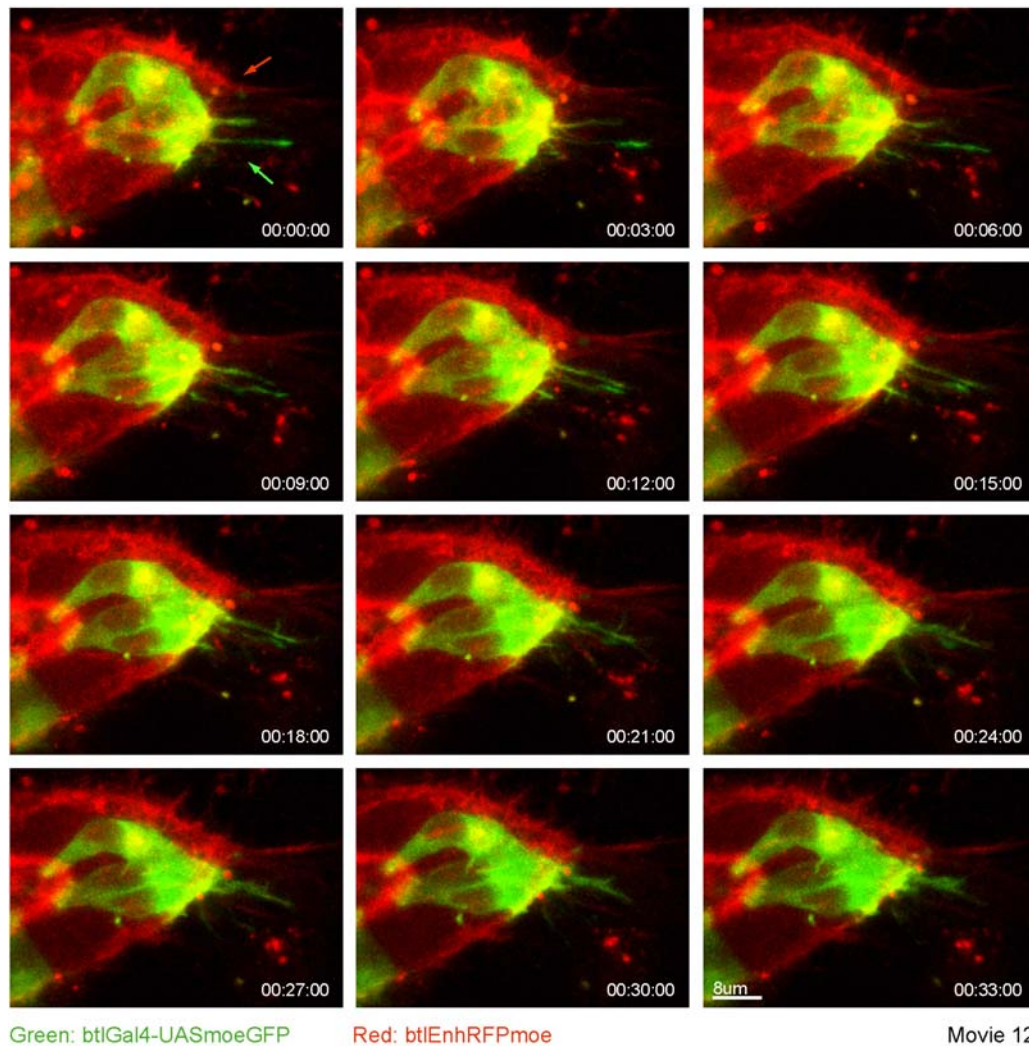
However, the observed leading air sac tracheoblast is embedded in a tissue. For cells to follow, several scenarios can be envisioned. In the first one, only the leading cell(s) is actively moving, whereas the others are passively pulled along. In the second scenario, cells several cell diameters away from the tip also actively migrate and collectively contribute to net forward movement of the entire tissue. In a third scenario, migration in a graded manner could occur, which means that cells initially actively migrate but slow down and halt, whereas

cells located further ahead are still moving. Genetic analysis provides preliminary evidence (see later) for the third model, however, a conclusive answer can currently not be provided.

5.2 Cellular extensions in tip- and proximal cells

To further characterize the extensions seen at the tip of migrating cells, a double labeling experiment was performed. The basic question behind this experiment was whether there is only one cell or several tip cells that can form extensions. Since only one cell in the migrating border cell cluster forms a long cellular extension (LCE) (Fulga and Rorth, 2002) but several tracheal cells form filopodia, both scenarios could be imagined.

Figure R20 shows snap shots of movie 12 which answers this question. In order to differentially label two cell populations, flip-out clones were generated and labeled with Moesin fused to GFP. Flip-out clones are generated by the removal of a spacer sequence via FLP/FRT mediated recombination (Golic and Golic, 1996). Only cells that have undergone site-directed recombination in cis (see materials and methods) are labeled in green, whereas all air sac tracheoblast cells are labeled with Moesin fused to monomeric RFP (mRFP). As can be seen in figure R20/movie 12, cells from the flip-out clone as well as cells where the flip-out cassette was not removed, form dynamic extensions. These extensions furthermore are very similar to the observed dynamic filopodia in tracheal branches (Ribeiro et al., 2002). Therefore, this experiment confirmed the finding of filopodia-like extensions at the tip of migrating air sac tracheoblasts (Sato and Kornberg, 2002) and further shows that these extensions are formed by several cells.

**FIGURE R20:**

Picture series of movie 12. A flip-out experiment was performed in order to differentially label two cell populations. Green cells express moesinGFP, all air sac tracheoblasts express RFPmoe. Filopodia-like extensions can be distinguished (green & red arrows) which originate from GFP- or RFP labeled cells respectively.

See supplementary CD for complete movie sequence (movie 12).

Is this process only restricted to tip cells, or are air sac tracheoblast cells located more proximally also forming filopodia-like extensions? MARCM clones, marked with GFP fused to monomeric actin (actinGFP), were generated in order to answer this question. Small clones are particularly instructive, since they show best the distribution of filopodia-like extensions surrounding the cell (figure R21). Generally, all clones seem to form filopodia-like extensions, however, clones located more distally (compare fig. R21, J with L), show longer and more branched extensions. Proximally located clones exhibit short, spike-like extensions (fig. R21, D, E, J) as compared to the long and branched extensions that are found more

distally (fig. 21, L). The movie sequence shown in figure R22 (movie 13) further demonstrates the dynamics of these protrusions. Although some extensions also face away from the tip and extend proximally, the distal extensions show a higher order of branching and appear longer as well as more numerous.

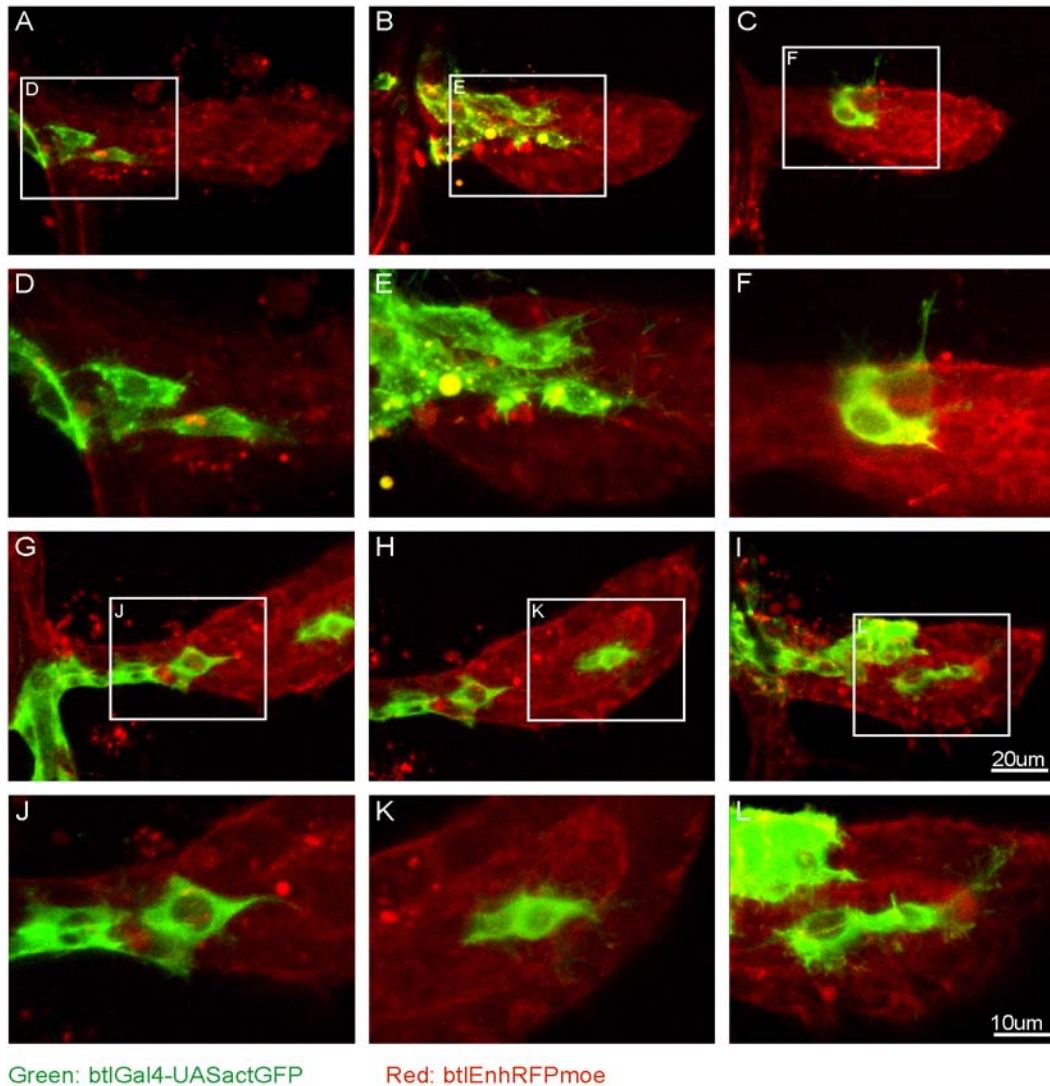
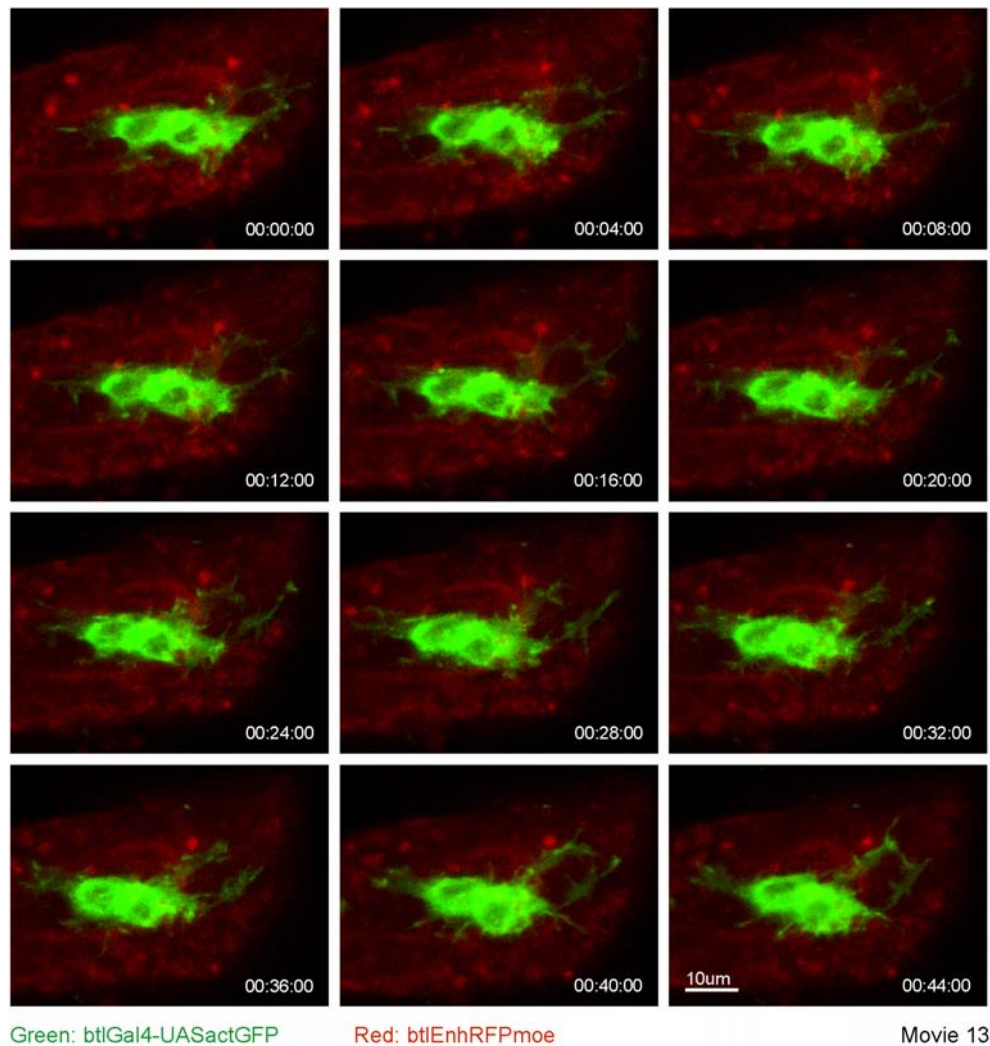


FIGURE R21:

Visualization of actin based cellular extensions. MARCM clones labeled with actinGFP were generated in order to visualize actin based extensions. **A., B., C., G., H. & I.)** provide overview pictures for location of the clones. **D.& J.)** Most proximal clones show spike-like extensions. **E., F. & K.)** Clones positioned more distally. These clones show longer and finer extensions. **L.)** Two-cell clone located in the middle of the air sac. Cellular extensions can be distinguished, which protrude proximally as well as distally. Distal protrusions seem to be longer and to display a higher branching pattern.

**FIGURE R22:**

Picture series of movie 13. MARCM two-cell clone positioned as shown in figure R21, K. The clone is marked with actinGFP. Note the formation of dynamic and branched extensions, projecting distally as well as proximally. Proximal extensions however seem longer and display a higher degree of branching.

See supplementary CD for complete movie sequence (movie 13).

I next investigated the tubulin cytoskeleton to visualize tubulin-rich extensions. Again, MARCM clones were generated in order to label small- or individual groups of cells with the microtubuli binding protein Tau (Brand, 1995). Clones marked in such a manner display several characteristics as seen in figure R23. They also show long and broad but unbranched extensions even from cells in more proximal locations (fig. R23, A&E). Some extensions also face away from the distal tip towards the lateral side (fig. R23, I&L), whereas cells in the stalk appear elongated with microtubuli arrayed in bundles (fig. R23, I&J). Furthermore, as previously described, cells located distally as well as proximally form mitotic spindles and round up (best seen in fig. R23, C&G, note the RFPmoesin rich cortex surrounding the cells).

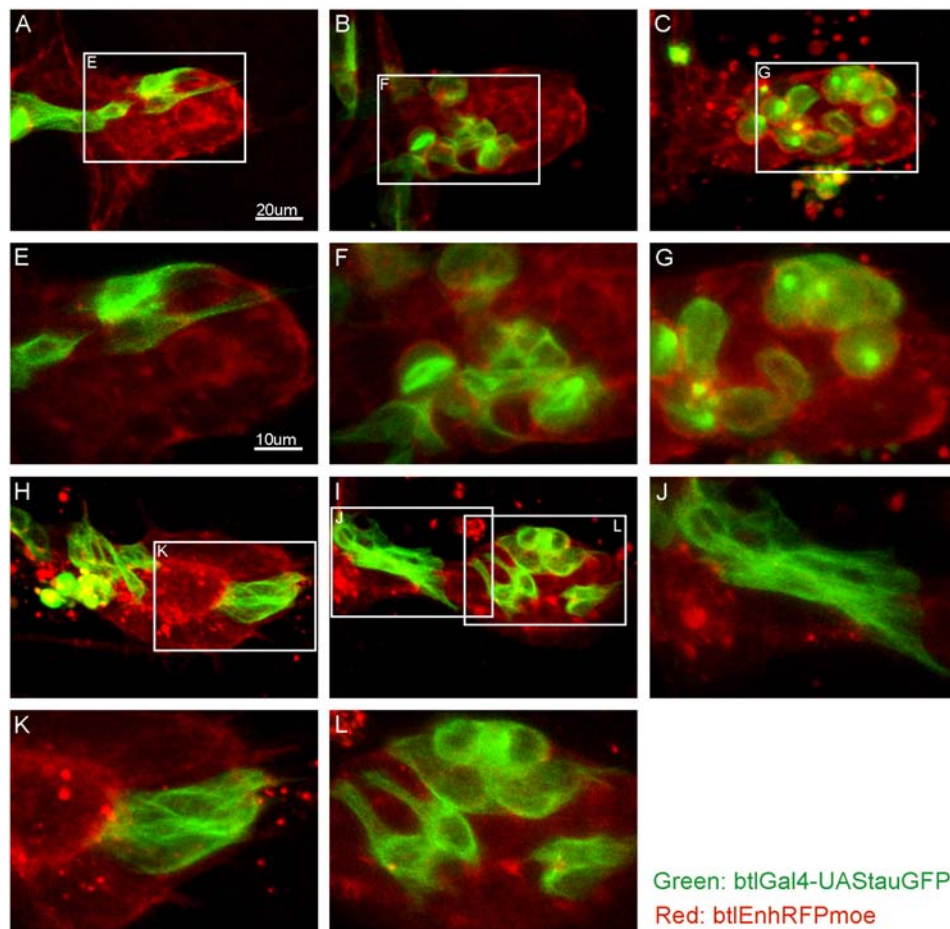


FIGURE R23:

Visualization of tubulin based cellular extensions. MARCM clones are labeled with tauGFP, a microtubule binding protein. **A.-C.)** Overview pictures provide information of clone localization. **E.)** Unbranched, long tubulin based extensions can be seen in proximal located clones. **F.&G.)** Dividing cells labeled with tauGFP. **H.&I.)** Two air sacs with clones located at the base as well as at the tip. **J.)** Proximal located clones in late air sacs display an elongated shape as observed previously with other markers. Note the bundled organization of microtubuli. **K.)** In tip cell clones, microtubules seem not to be very strictly arrayed. **L.)** Clones in the main air sac body also display extensions facing in other directions.

The dynamics of the long extensions were studied using 4D microscopy on dissected wing imaginal discs. Figure R24/movie14 shows several cells marked with tauGFP, of which one shows a long unbranched extension (fig. R24, time point 00:00:00, white arrow). This extension retracts and the cell starts to reorient itself. Finally another extension projects from a different cell in this clone with the angle of the projection slightly altered (fig. R24, time point 00:40:00, white arrow).

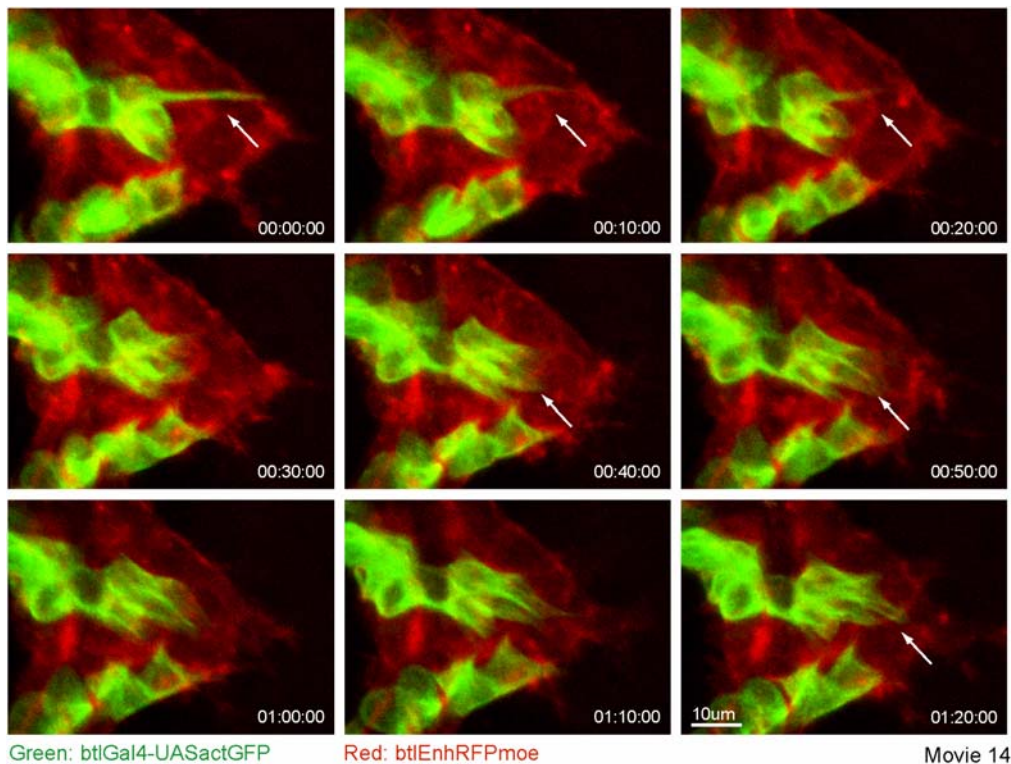


FIGURE R24:

Picture sequence of movie 14. MARCM clones labeled with tauGFP were imaged in this early air sac. Note the long unbranched cellular extension (white arrow) from a cell located in the middle of the air sac. After retraction and reorientation of the cell, the neighboring cell starts to project an extension aiming in a slight different direction.

See supplementary CD for complete movie sequence (movie 14).

These observations can be summarized as follows. First, filopodia-like extensions do not only occur in one tip cell but several. Moreover, filopodia-like extensions occur not only in tip cells but also in more proximal cells, although with a lower degree of branching. As already

observed in the embryonic tracheal cells, the actin cytoskeleton shows higher dynamics compared to microtubuli (Marc Neumann, personal communications). Microtubuli too, are not entirely static, as is seen with the extension of tau-rich protrusions. However, these protrusions have not been observed to show any degree of branching. These data are in agreement with a model that suggests that filopodia-like extensions first probe the environment of the cell. Once the cell has decided which path to follow, an actin-rich extension will be stabilized with unbranched microtubuli in the direction of migration (see also fig. R19, movie 10&11).

We currently do not know what functional role these extensions have. However, this and further studies of wild-type cells combined with loss-of-function studies should allow further insight into these and similar questions. The MARCM system, as seen later, is of great value for answering such questions, since it not only allows for the labeling of cells with different markers but also serves to generate marked mutant cells in an otherwise heterozygous tissue of interest.

6. Cellular interactions of air sac tracheoblasts with the surrounding tissue

6.1 Expression of *ovo/shavenbaby* in wing imaginal discs

The transcription factor Ovo/Shavenbaby (Svb) is required for the formation of ventral denticles in *Drosophila melanogaster*. It was shown that Svb triggers early F-actin redistribution and is able to initiate the entire process of cytoskeletal remodeling (Delon et al., 2003; Payre et al., 1999). Since *svb* is also expressed in the embryonic tracheal system (I. Delon, personal communication) and codes for a transcription factor involved in F-actin redistribution, I wanted to investigate whether expression persists in third instar air sacs. A *svbGal4* line (provided by H. Dechanut) was crossed to *UASmoeGFP*. In order to outline the air sac, monomeric RFP fused to Moesin under direct *btl*-enhancer control was also crossed into this background. As seen in fig. R25 A, *svb* is broadly expressed in the notum of the wing imaginal disc. Furthermore, *svb*-expressing cells, probably adepithelial cells, seem to partly engulf the air sac tracheoblasts (Fig. R25, B, F). Confocal sectioning reveals that *svb*-expressing cells closely adjoin the air sac on the lateral sides (Fig. R25, C&F, and Fig. R26 A-F) and some even grow over the air sac and contact *svb*-expressing cells from the other side (Fig. R25, B&E, Fig. R26, A).

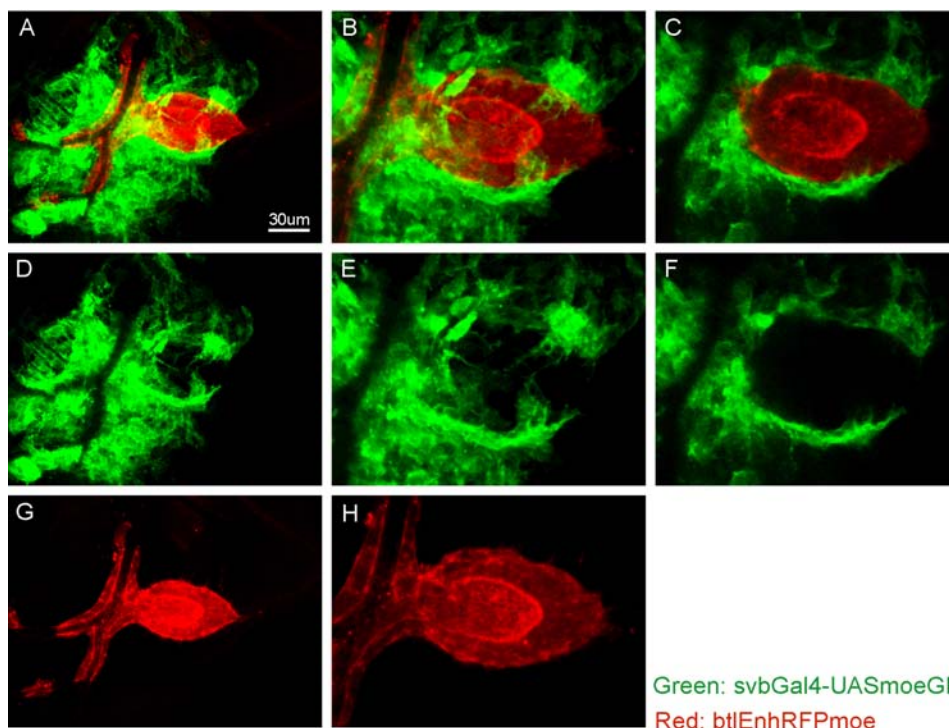
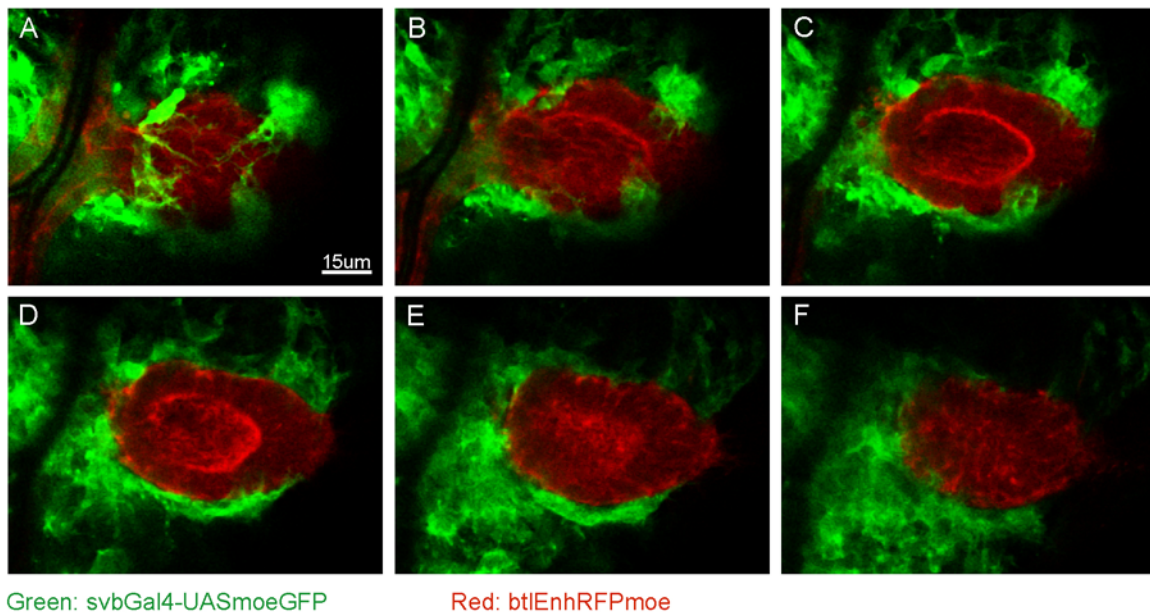


FIGURE R25

svbGal4 expression in third instar wing imaginal discs. **A.)** Overview picture. *svbGal4* was crossed to the actin binding protein Moesin (*UASmoeGFP*). RFPmoe outlines the air sac. **B.)** Projection. **C.)** Only one section is shown. **A.-C.)** Overlay. **D.-F.)** green channel only. **G., H.)** Red channel only. Note how the *svbGal4* expressing cells adjoin (**C., F.**) but also clasp around the air sac (**B., E.**).

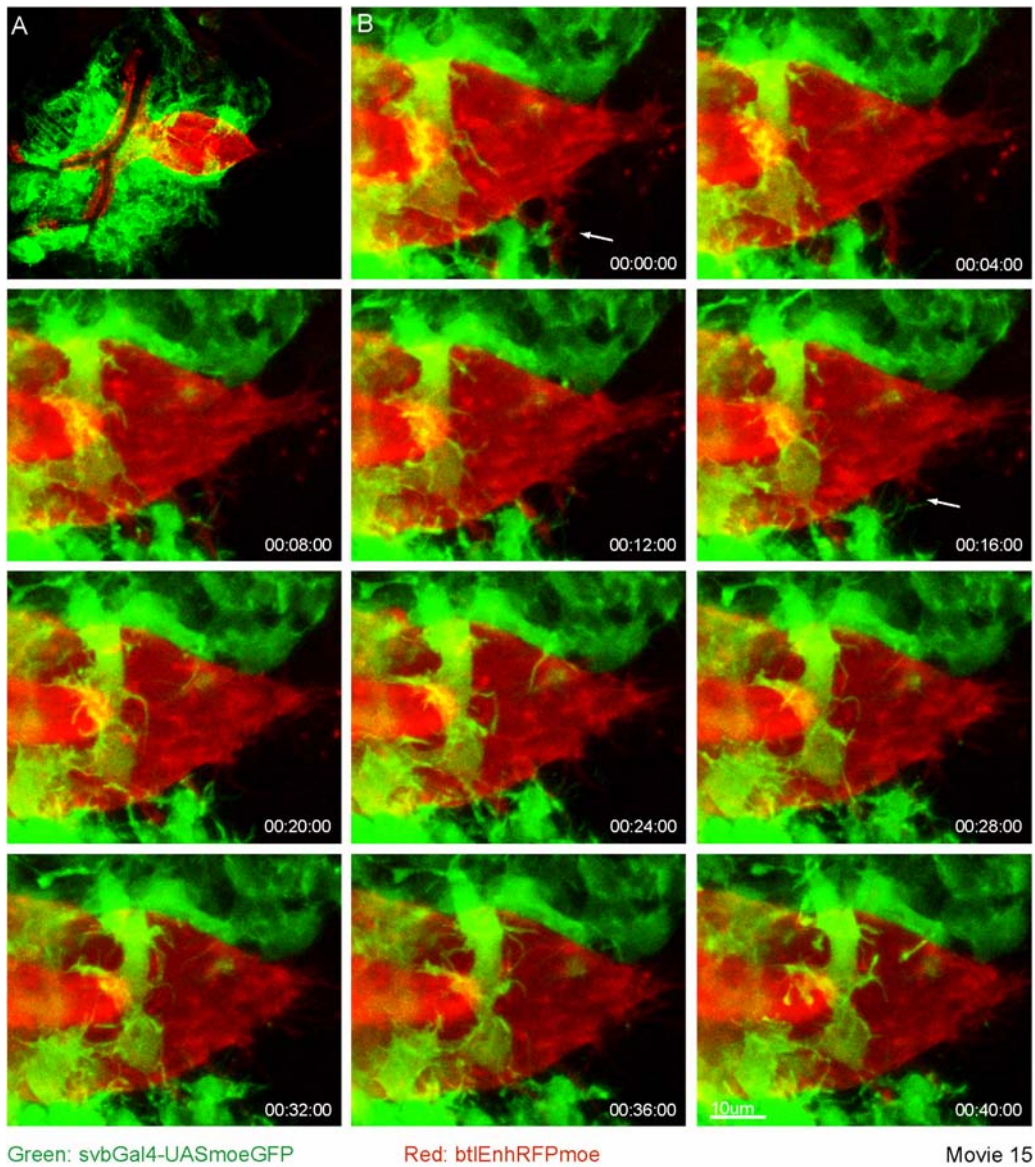
Green: *svbGal4-UASmoeGFP*
Red: *btlEnhRFPmoe*

**FIGURE R26**

Confocal sections of a late third instar air sac, enclosed by *svbGal4* expressing cells. Sectioning started at the top of the wing disc (adepithelial layer) and progresses towards the peripodial membrane. **A.)** Top section. Only few tracheal and *svbGal4* expressing cells are seen. **B.-E.)** Middle sections. The lumen of the air sac becomes visible with the bright red internal RFPmoe ring. Also here, the surrounding tissue forms a mould for the air sac. **F.)** Bottom section. Distance between each section is about 0.5-0.8µm.

Higher magnification as well as 4D microscopy revealed a very dynamic behavior of these adjoining cells. Figure R27 shows time frames of movie 15 to illustrate this point. A distal portion of an air sac is shown (see Fig. R27, A for an overview). *svb* expressing cells growing over the air sac extend a number of dynamic protrusions. *svb* cells located more laterally, project protrusions, which seem to contact filopodia-like structures originating from the air sac (Fig. R27, white arrow in B and subsequent frames).

However, *svb* does not seem to be expressed in air sac tracheoblasts, which was to some extent surprising. We currently investigate the expression and localization of Svb using an antibody. Nevertheless, the *svbGal4* line illustrates the interaction of the air sac with the surrounding tissue. It can be speculated that the shape of an air sac is also regulated and maintained by physical constraints and tissue boundaries (see also discussion).

**FIGURE R27**

Picture series of movie 15.

A.) Overview picture. **B.)** Picture series. White Arrows highlight interactions of air sac protrusions as well as filopodia-like extensions from the *svbGal4* expressing cells. Note how some of the *svbGal4* expressing cells wrap around the air sac.

See supplementary CD for complete movie sequence (movie 15).

7. Genetic analysis of FGF-mediated cell migration using site-specific mitotic recombination

7.1 General considerations

Air sac development depends, to a large extent, on cell migration as well as cell proliferation (Sato and Kornberg, 2002). Mitotically active cells are a prerequisite site specific mitotic recombination, since homologous chromosomes need to pair in order to exchange loci on chromosomal arms and need to segregate afterwards. Since many genes have pleiotropic effects, loss-of-function mutations, abolishing the function of the gene under study in all tissues, often lead to dramatic defects. The analysis of tissue-specific phenotypes is therefore hindered. In order to circumvent this problem, different strategies can be used. The expression of RNAi or dominant-negative constructs in a tissue-specific manner, with the use of the Gal4/UAS (Brand and Perrimon, 1993) system, is one possibility. However, this implies the existence of an appropriate Gal4 line which mimics, timely and spatially, the desired expression of Gal4. Furthermore, RNAi as well as dominant-negative constructs often lead to hypomorphic phenotypes, also due to position dependent integrations, and cannot always be compared to complete loss-of-function phenotypes. The use of tissue-specific alleles would be an alternative, but for obvious reasons such alleles are not readily available. Therefore, the generation of a mosaic tissue consisting of cells that completely lack the gene under study mixed with wild type cells is considered as one of the better solutions to circumvent the pleiotropic effects and to study the gene of interest in a tissue-specific manner.

As already mentioned, the most straightforward way to generate mosaics is by site specific mitotic recombination using the FLP/FRT system (Blair, 2003; Golic, 1991; Xu and Rubin, 1993).

In the embryonic tracheal system, clonal analysis has been performed to a very limited extent (Hacohen et al., 1998; Samakovlis et al., 1996a). However, since embryonic tracheal cells divide only twice, the clones generated in the embryo from a single cell do not consist of more than four cells. The translated proteins of the gene of interest are thus not diluted to a large extent. Moreover, maternally supplied products, such as RNA or proteins, can still interfere with the analysis of the gene of interest. Therefore, we envisaged a system for the study of genes putatively involved in tracheal cell migration, in which the problem of maternal contribution can be largely overcome and that allowed us to study the loss-of-function phenotype in a tissue-specific manner.

We think the third instar air sacs are suitable for the analysis of guided cell migration, since this tissue combines all the mentioned advantages (or rules out the mentioned disadvantages). Moreover, in contrast to border cells, a system which helped substantially to establish a clearer picture of guided cell migration *in vivo*, FGF signaling plays a fundamental role during air sac tracheoblast migration (Sato and Kornberg, 2002).

In the following paragraphs, I will present the results of my genetic analysis of air sac tracheoblast migration. In order to do so, the established T-MARCM stocks were used. Generally, very little is known about air sacs and a genetic analysis has not been performed so far. Thus, as a starting point, the analysis was focused on two main characteristics; clone position and clone size. The mutants analyzed should follow a logic scheme and were selected according to the following aspects. First, we wanted to learn more about RTK components putatively involved in FGF-mediated cell migration. Second, we looked at components involved in cell migration in other systems, mainly border cells. Furthermore, our attention was drawn to genes involved in the regulation of the cytoskeleton. However, a number of components so far unlinked to cell migration but involved in other important cellular processes were tested.

Unless stated otherwise, the clones were induced in early embryogenesis by inducing the expression flipase with a heat-shock pulse (1. HS window, see Fig. R2). The clones were then analyzed in third instar stages with regard to clone size and clone position. Clone size always refers to the actual size of the clone, not the size of the labeled cells. Clone position refers to the relative position of the labeled cells with regard to the defined axes of the air sac (see Fig. R4, R5).

For detailed experimental procedures as well as more information regarding the alleles used, the reader is referred to materials & methods.

7.2 Distribution and size of wild-type MARCM clones in third instar air sacs

To test the feasibility of the system as well as to learn more about the distribution and relative size of early-induced clones, MARCM clones, labeled with the membranous marker CD8:GFP (Lee and Luo, 1999) were generated with an unmutagenized wild-type chromosome (FRT 40A, 2L). A total of 38 air sacs containing clones were analyzed and representative examples are displayed in figure R28 (and Table R1 for absolute numbers). Generally, clone size as well as clone distribution are variable. However, closer examination allowed me to subgroup the clones into different classes. In terms of size, three classes were defined; small-, medium- as well as large clones. Small clones usually consist of only very few cells with regard to the entire air sac. Examples are given in figure R28, a1-a3 (tip clone in a3). Medium clones populate between 20-50% of the entire air sac (Fig. R28, a4-a6) whereas large clones populate almost and sometimes even the entire air sac (Fig. R28, a7-a12). The distinction of these clones under the aspect of size does not rely solely on the total amount of cells in a given clone but orients itself on the relative size of the clone with regard to the rest of the air sac (a small air sac containing 25% of labeled cells falls into the same class as a big air sac containing 25% of labeled cells, although the number of labeled cells in the big air sac is higher compared to the number of labeled cells in the small air sac). Nevertheless, it has to be mentioned that such a distinction is arbitrary. Furthermore, whereas the distinction between small clones and medium/large clones is straightforward, distinguishing between medium- and large clones is not always easy. Clone position is a means by which to express the ability of the labeled cells to move in a labeled tissue. It is assumed, and will be shown in the next paragraph, that cells that retain normal migratory function have a tendency to populate the region of the tip of the air sac. By looking at wild-type clones, this can be clearly observed. Clones of variable size can migrate at the leading edge of the air sac. Small clones can either populate the stalk region (Fig. 28, a1) or the tip (Fig. 28, a2, a3). Medium sized clones or even large clones behave similarly. However, for obvious reasons, large clones have a greater tendency to reach the tip. Figure R28 B displays the statistics and summarizes clone position as well as clone size. It can be observed that 70% of all clones, independent of their size, reach the tip under wild-type conditions. With respect to clone size, the majority of clones are medium or large. However, a certain amount of small clones were also recovered, in the given experiment around 30%. In summary, under wildtype conditions, I observed that in about 70% of the cases, the labeled cells reached the tip. In addition, around 70% of the clones were medium- to large-sized.

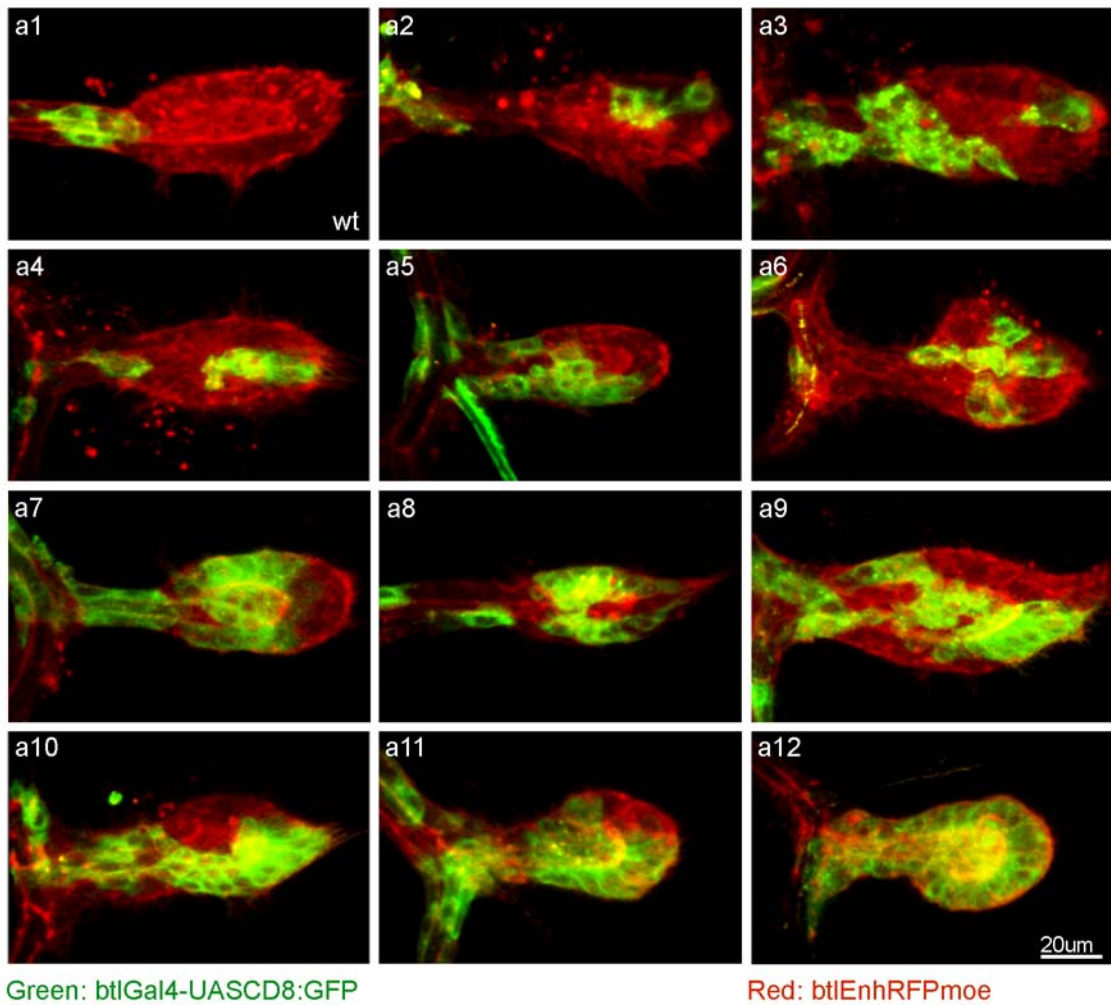
Next I analyzed whether small clones have a reduced probability to reach the tip. In order to do so, I only considered the small clones and counted the amount of clones that reached the tip within this selected group. About half of these small clones populated the tip whereas the other half did not reach the tip. The same is true for medium-sized clones. Large clones, as already mentioned, have a higher probability to reach the tip. Based on these results, I concluded that the final position of the clone is not strongly biased by clone size, or stated differently: clone size does not determine clone position. Intuitively, one would assume that the bigger the clone, the higher the probability to reach the tip of the air sac. Although this is confirmed with the obtained data, it is important to note that a medium or small wild-type clone has a 50% chance to reach the tip.

This also implies that certain positions (as well as clone size) in the very early air sac favor the rate of proliferation. Unfortunately, since the performance of clones cannot (yet) be followed over the entire third instar stage, clear knowledge concerning this aspect is lacking (see also discussion).

Table R1: Absolute numbers of wild-type clones with respect to size and distribution

ALLELE	N	ABSOLUTE NUMBER OF CLONES AT TIP	LARGE CLONES	MEDIUM CLONES	SMALL CLONES	LARGE CLONES AT TIP	MEDIUM CLONES AT TIP	SMALL CLONES AT TIP
<i>wt</i>	38	27	19	11	8	17	6	4

A



B

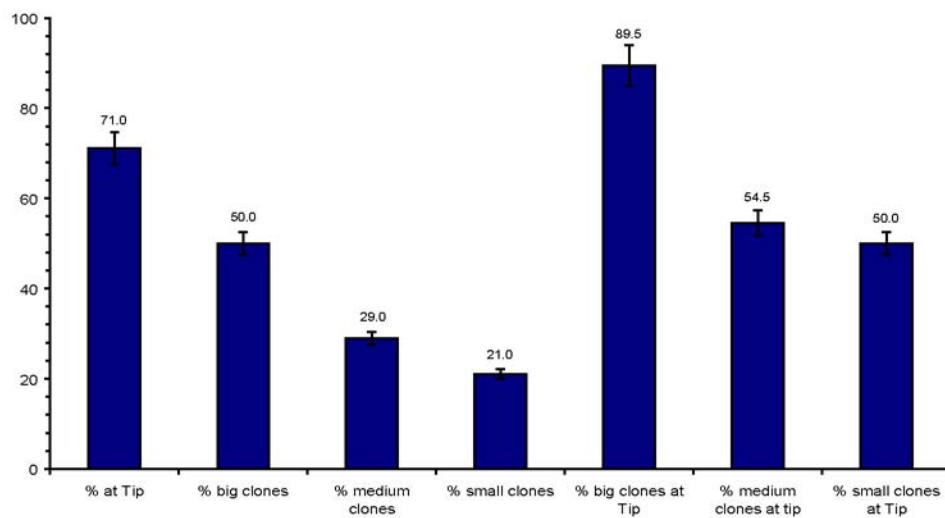


FIGURE R28

Wild-type MARCM clones: Clones generated with FRT40A (2L), labeled with CD8:GFP

A.) a1-a3: representative small wild-type clones located at the back (**a1**) or the tip (**a2,a3**).

a4-a6: medium sized wild-type clones. **a7-a9:** wild-type clones of medium/large size. **a10-a12:** large wild-type clones.

B.) Quantification with regard of clone size and position.

Numbers and scale bar are in percent. Columns 2, 3 & 4 indicate clone size. Columns 5, 6 & 7 represent the percentage of large-, medium-, or small clones at the tip in relation only to the amount of clones in the respective size group. Thus, regarding all small clones as a separate group, 50% of these are positioned at the leading edge of the air sac.

7.3 *dof* & *btl* mutant clones

Having established the fact that wild-type clones have a high probability to populate the tip of the air sac, it appears that this assay could be applied to the analysis of mutant clones. As a first test, we wondered how clones mutant for a gene that we know is involved in tracheal cell migration performs. For obvious reasons, we looked at *downstream of FGF (dof)* mutant clones first. Dof protein is detected in air sac tracheoblasts as well as in the adepithelial tissue (Sato and Kornberg, 2002). In the embryo, *dof* has been shown to be required for tracheal- as well as mesodermal cell migration (Imam et al., 1999; Michelson et al., 1998a; Vincent et al., 1998). The loss-of-function allele *dof*^{P1740} was used for generating mosaic air sacs. Since the phenotype of hemizygous (*dof*^{P1740} over deficiency) is indistinguishable from that of embryos homozygous for *dof*^{P1740}, the latter is assumed to represent a strong loss-of-function or even amorphic allele (Imam et al., 1999). Furthermore, a *dof*-RNAi line, constructed by Alain Jung, was tested for air sac defects. As reported previously, expression of dominant-negative *btl* (*btl*^{DN}) in the tracheal system abolishes air sac formation. By expressing *dof*-RNAi in the tracheal system, the same result was obtained; the formation of an air sac was completely inhibited (Fig. R29, a1).

It is, however, elusive whether the absence of air sacs resulted from abolished proliferation or cell migration.

Ten independent air sacs containing *dof*^{P1740} mutant clones were analyzed with regard to clone size and position. In contrast to *dof*-RNAi, air sac development proceeded normally, although the mutant cells always clustered at the back of the air sac (Fig. R29, a3-a6). In one instance, the region where the air sac originates was populated with *dof* mutant cells and the air sac developed between two clusters of *dof* mutant cells.

With respect to clone size, the majority of clones could be assigned to the group of medium to large clones. Independent of clone size, the mutant cells never reached the tip. I therefore conclude that cells deficient in the strong loss-of-function allele of *dof*^{P1740} have a reduced or lack the ability to migrate. Proliferation, on the other hand, appears to be normal.

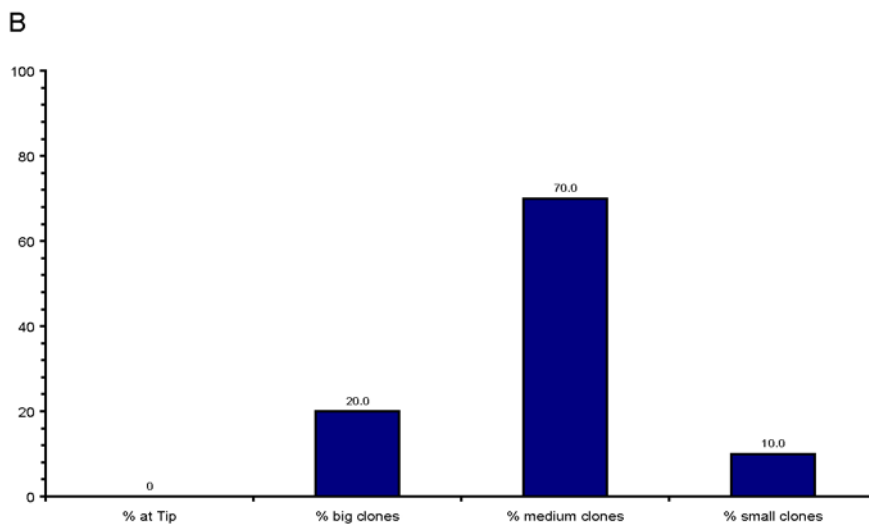
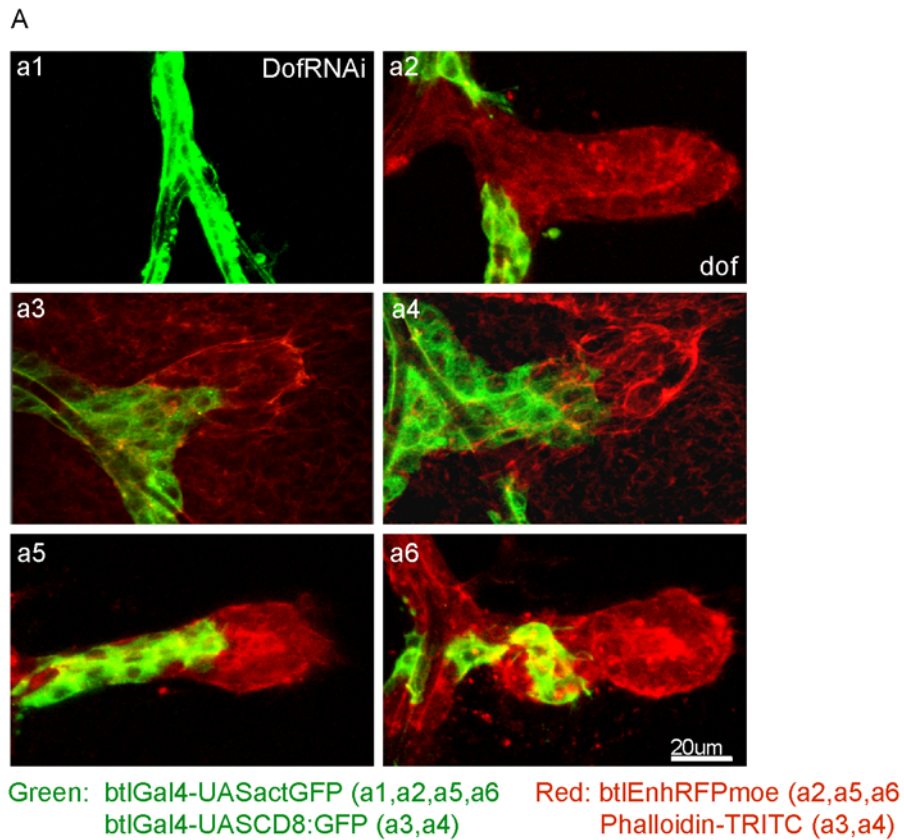


FIGURE R29

DofRNAi & MARCM clones mutant for *dof*^{P1740}.

A.) **a1:** DofRNAi expressed in all tracheal cells using *btlGal4-UASactGFP*. Note that in late third instar larva, no air sacs are formed. **a2:** *dof* MARCM clones in the transverse connective. Clones were not incorporated into the air sac. **a2,a3 & a6** represent medium sized clones. **a5:** big *dof* mutant clone. **B.)** Statistics as in previous figure. Since no clones were found at the tip, the last three columns are not shown. Note that the majority of *dof* mutant clones is represented by medium sized clones. Labeling as indicated.

A similar result was obtained with the strong loss-of-function allele *btl*^{H82Δ3}. This allele was generated by imprecise excision and lacks 500bp of *btl* flanking DNA upstream of the *btl* coding region (Murphy et al., 1995). Of the total 16 recovered clones, none reached the tip. The majority of *btl*^{H82Δ3} mutant clones represent primarily medium sized clones with a few small and large clones. In summary, these clones are indistinguishable from *dof*^{P1740} mutant clones (Fig. R30 A, B and table R2).

In two instances, air sacs were recovered that showed an interesting detail. Adjacent to the air sac containing a medium-sized *btl* clone, a small ectopic air sac developed (Fig. R30, a6&a7). Furthermore, in a few instances, *btl* clones were recovered which showed filopodia-like extensions. Since this allele has been used to demonstrate that the absence of FGF-receptor signaling causes embryonic tracheal cells are to be devoid of filopodia (Ribeiro et al., 2002), the occurrence of these structures was surprising. As will be discussed later, formation of filopodia-like structures could require additional factors in air sac tracheoblasts.

Table R2: Absolute numbers of *dof*^{P1740} & *btl*^{H82Δ3} clones with respect to size and distribution

ALLELE	N	ABSOLUTE NUMBER OF CLONES AT TIP	LARGE CLONES	MEDIUM CLONES	SMALL CLONES	LARGE		MEDIUM		SMALL	
						CLONES AT TIP	AT CLONES TIP	AT CLONES TIP	AT CLONES TIP		
<i>dof</i> ^{P1740}	10	0	2	7	1	0	0	0	0	0	0
<i>btl</i> ^{H82Δ3}	16	0	4	11	1	0	0	0	0	0	0

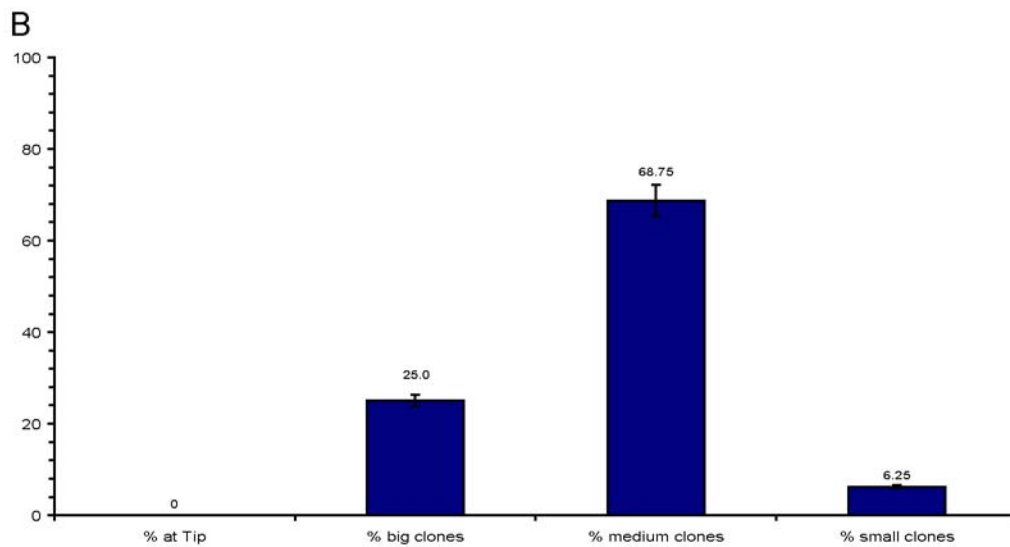
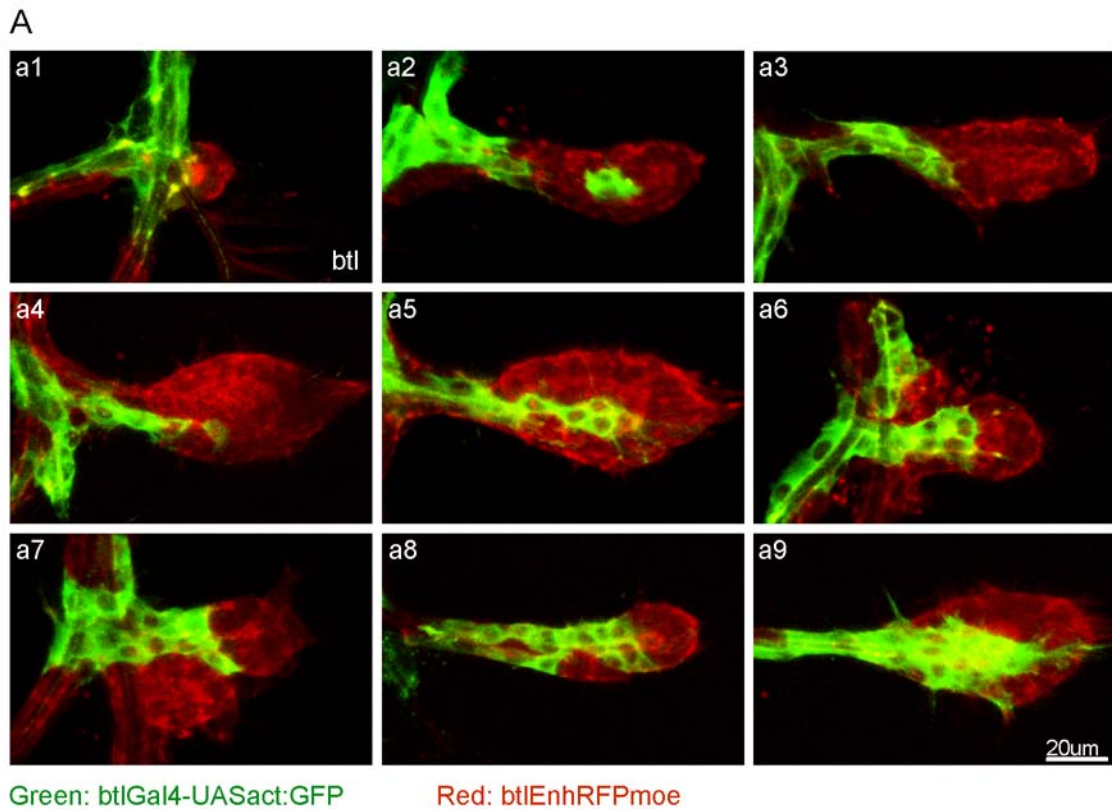


FIGURE R30

MARCM clones mutant for *btI*^{H82Δ3}.

A.) Representative *btI* clones. **a1-a3**: small clones. **a4-a6**: medium clones. **a7-a9**: medium to large clones. Note the “twin-air sac” in **a6** & **a7**. **a9**: large clone displaying filopodia-like extensions at the tip and at the margin.

B.) Statistics as in previous figures. No *btI* mutant clone was ever found at the tip. Note that the distribution with regard to clone size is almost identical as seen with *dof* mutant clones. Labeling as indicated.

7.3.1 *dof* & *btl* mutant clones in third instar larval branches

Early-induced clones distribute randomly in the embryonic and later the larval tracheal system. These clones can also be analyzed in third instar larval branches, which allowed us to make certain statements about the fate and developmental history of mutant tracheal cells (Fig. R31, A). *wt* clones, in third instar larvae, mark all the different tracheal cells, such as dorsal trunk-, dorsal branch-, terminal- or fusion cells to name just a few. As observed previously, clones do not exceed a maximal number of four cells, due to only 2 early cell divisions, but they can disperse from each other. Therefore, single cell clones can be frequently found (not shown and Samakovlis et al., 1996a).

Larvae containing *btl* or *dof* clones never had marked, and therefore mutant, terminal cells. However, mutant cells can be found in a position just behind the terminal cell. The main morphological characteristic of the terminal cell is that it forms long cytoplasmic extensions emerging from the cell body. Figure R31 shows such a *wt* terminal cell (B), as well as examples of cells mutant for *btl* (C, C', D, D') or *dof* (E, E', F, F'). In the given examples, light microscopy pictures (C', D', E', F') help to position the mutant cells. Terminal cells are never marked with GFP and are therefore always wild-type. The terminal cell is the leading cell in all major branches. It was therefore assumed that this leading edge cell requires *btl* or *dof* for guided cell migration. The occurrence of cells lacking Dof or Btl in the cells following the leading cell indicates that this cell is not required for guided cell migration. Moreover, the tip cell can either differentiate into a terminal- or into a fusion cell. Also the fusion cell is not marked with GFP in the example given in figureR31, E, E' (white arrow).

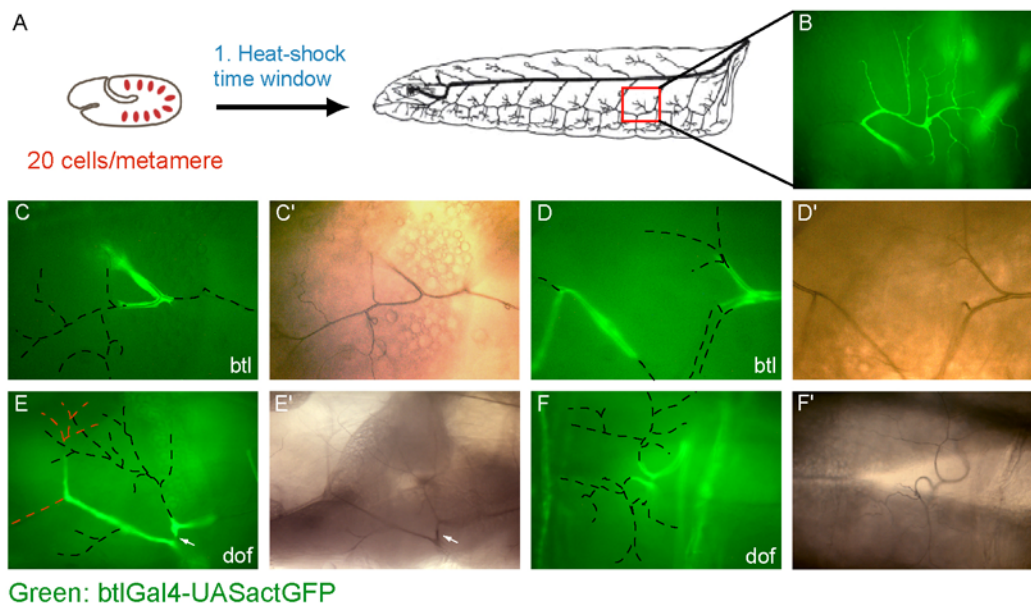


FIGURE R31

MARCM clones mutant for $btl^{H82,\Delta 3}$ or dof^{P1740} in third instar larva.

A.) Schematic heat-shock protocol. 4-6h AEL old embryos were heat-shocked for 1h at 38°C (see also Fig. R2). Prior to wing disc dissection, third instar larva were screened for clones. The boxed area in the schematic third instar larva highlights one location of a terminal cell. **B.**) wild-type terminal cell marked with actGFP. Terminal cells contain several long cytoplasmic extensions. **C. & C'**): $btl^{H82,\Delta 3}$ mutant cell. The dashed lines indicate the branching of the terminal cell as inferred from C'. **D. & D'**): Another example for a $btl^{H82,\Delta 3}$ mutant cell.

E. & E'): cell mutant for dof^{P1740} . The red dashed line indicates a second terminal cell as inferred from E'. White arrows indicate the position of a fusion cell, which is not marked and therefore wild-type. **F. & F'**): Another example for a clone mutant for dof^{P1740} . Note that no terminal cells mutant for either dof^{P1740} or $btl^{H82,\Delta 3}$ were ever found.

Labeling as indicated.

7.4 *drk* & *shc* mutant clones show a migration phenotype similar to *dof* and *btl*

In order to further characterize components downstream of the FGFR/Btl receptor, clones mutant for *drk* and *dshc* were analyzed. *drk* is the *Drosophila* homologue of the vertebrate adaptor protein Grb2 and contains SH2/SH3 domains (Olivier et al., 1993; Simon et al., 1993). In the *Drosophila* eye, Drk has been found to bridge the RTK receptor Sevenless (SEV) to Son of sevenless (Sos), a guanine nucleotide release factor that activates Ras, by directly binding to activated SEV as well as Sos (Raabe et al., 1995). Dshc, the *Drosophila* homologue of the vertebrate SHC, is another adaptor protein and contains a PTB and SH2 domain. Dshc lacks the high-affinity Grb2 binding domain common to the vertebrate Shc, and no binding of Dshc to Drk was observed in coimmunoprecipitation experiments (Lai et al.,

1995; Luschnig et al., 2000; van der Geer et al., 1995). Genetically, *dshc* was found not to act downstream of *sev* but is required for EGFR and Torso signaling. Furthermore, Dshc acts in parallel with Drk and Dos to transduce the Torso signal (Luschnig et al., 2000).

An involvement of these two adaptors in FGFR/btl signaling in *Drosophila* has not been shown to date. Since both adaptors are required for multiple developmental events, the method of choice was to look at mosaic air sacs. I analyzed the function of both proteins in clones mutant for one or the other gene. In both cases amorphic alleles were used; *drk*^{AP24} (Hou et al., 1995) and *dshc*^{BG} (Luschnig et al., 2000). Both genes show similar phenotypes. *drk* as well as *dshc* mutant clones show a reduced ability to migrate since they were found only in about 16% (vs. 70% in wt) at the tip. With regard to clone size, both mutants do not display a reduction in proliferation, since the majority of clones were medium- to large sized (Fig. R31 A, B).

Table R3: Absolute numbers of *drk*^{AP24} & *dshc*^{BG} clones with respect to size and distribution

ALLELE	N	ABSOLUTE NUMBER CLONES AT TIP	LARGE OF CLONES	MEDIUM CLONES	SMALL CLONES	LARGE CLONES AT TIP	MEDIUM CLONES AT TIP	SMALL CLONES AT TIP
<i>drk</i> ^{AP24}	18	3	4	9	5	0	2	1
<i>dshc</i> ^{BG}	18	3	9	8	1	2	1	0

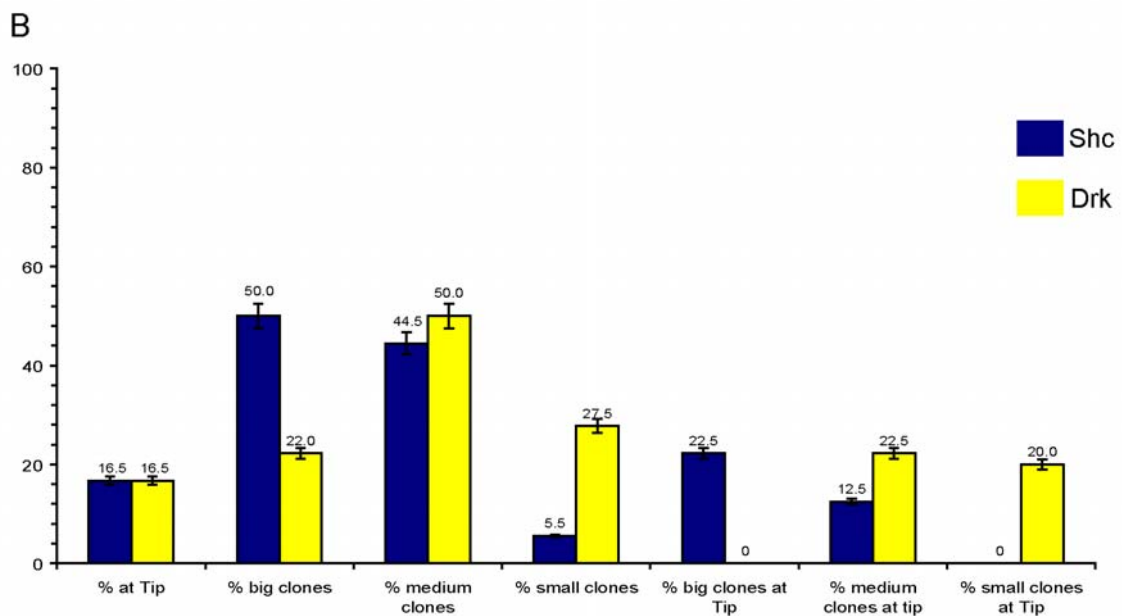
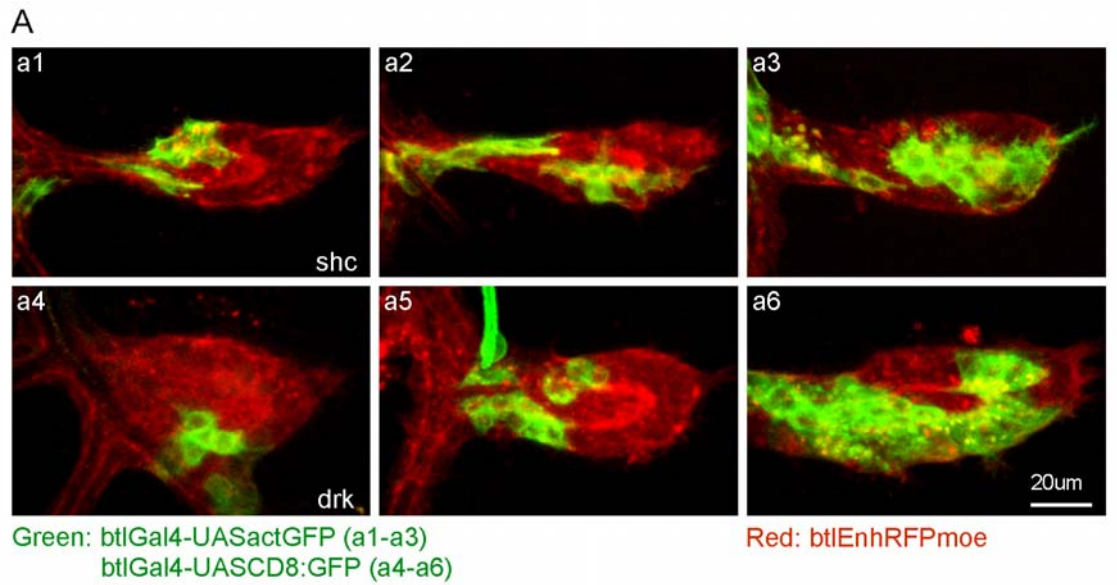


FIGURE R32

MARCM clones mutant for *shc*^{BG} or *drk*^{P Δ 24}.

A.) a1-a3: representative clones mutant for *shc*^{BG}. A small, medium and large clone is shown.

a4-a6: clones mutant for *drk*^{P Δ 24}. Clones shown represent small-, medium & large clones.

B.) Statistics as indicated before. Note that only a small fraction reaches the tip (column 1). Most of the clones are large or medium sized.

7.5 *ras, sos, cnk, ksr* mutant clones

We next investigated the role of Ras signaling in tracheal cell migration. Ras has been implicated in border-, hemocyte- and likely also germ cell migration in *Drosophila* (Cho et al., 2002; Duchek and Rorth, 2001a; Lee et al., 1996a; Li et al., 2003). To a certain degree, activated versions of Ras rescue tracheal cell migration defects in a *dof* or *btl* mutant background (Imam et al., 1999; Vincent et al., 1998). Thus, it was assumed that Ras signaling is also important for the migration of tracheal cells. The same results were obtained with activated versions of Raf, indicating that the MAPK module is required for tracheal cell migration (Imam et al., 1999; Vincent et al., 1998). However, loss-of-function experiments with strong or amorphic alleles for these genes cannot be performed in the *Drosophila* tracheal system. This is due to the fact that these two molecules are central players in many developmental events and have thus pleiotropic effects. Moreover, a substantial fraction of RNA as well as proteins of these genes is maternally contributed. *ras* germline clones lacking maternal as well as paternal gene product show dramatic developmental defects (data not shown), and it is not surprising that the embryonic tracheal system is not properly formed.

Therefore, we reasoned that the analysis of *ras* or *raf* mutant clones in *Drosophila* air sacs should provide insight into the function of these proteins with regard to tracheal cell migration. *ras* loss-of-function clones with the strong *ras*^{X7b} allele, a deletion which starts 18bp upstream of the transcription start and ends 198bp downstream of the putative polyadenylation signal (Halfar et al., 2001) of *ras*, result in the formation of predominantly small clones, which always cluster at the most proximal part of the air sac (Fig. R33, a1-a3 & B, table R4). These clones were rather difficult to obtain, which explains the small number of recovered clones. However, the phenotype shows hardly any variation between these seven clones. In order to confirm this result, mutations in *son of sevenless* (*sos*), which codes for the rasGEF, were analyzed. Sos exchanges GDP for GTP and thereby activates the catalytic activity of Ras. It was expected that air sac tracheoblasts lacking *sos* should display a similar phenotype as *ras* mutant clones since Ras activation is diminished. Indeed, the amorphic allele *sos*^{X122}, as well as *sos*^{SF15} show indeed almost identical phenotypes compared to *ras*^{X7b} clones. Mutant cells cluster at the most proximal part of the air sac and the clones only consist of very few cells, indicating that these cells undergo reduced rates of proliferation (Fig. R33, a4-a6).

A primary response to Ras is the activation of the Raf kinase and the subsequent activation of MEK and MAPK (reviewed in Rommel and Hafen, 1998). We therefore wanted to know whether the Raf/MAPK pathway is responsible for the observed *sos/ras* phenotype. Again, we aimed at doing this in air sac tracheoblast clones mutant for *raf* as well as MEK or MAPK. MAPK is encoded by the *Drosophila* locus *rolled* (*rl*). This gene, however, is not located within the range of available FRT chromosomes (E. Hafen, personal communication), and could therefore not be tested by FLP/FRT mediated recombination. Unfortunately *raf* as well as *MEK/dsor* clones could not be recovered so far due, to unsolved technical problems. To circumvent these difficulties, two related mutants, *kinase suppressor of ras* (*ksr*) and *connector enhancer of KSR* (*cnk*) were tested instead. KSR is a conserved protein and contains a putative kinase domain (Therrien et al., 1995). Functionally, KSR acts as a scaffold bridging Raf and MEK in a Ras-dependent manner. It was reported that KSR participates in the phosphorylation of MEK by Raf. Furthermore, *ksr* dsRNA inhibited phosphorylation and activation of MEK in *Drosophila* S2 (Roy et al., 2002). Depletion of KSR in *Drosophila* S2 cells also impaired catalytic Raf function (Anselmo et al., 2002). Therefore, KSR is a component of the MAPK pathway required for the activation of MEK and MAPK. Also CNK, which was found in a genetic modifier screen (Therrien et al., 1998), is required for the activation of Raf. Genetic epistasis experiments placed *cnk* upstream of *raf* but downstream of *ras*, suggesting that CNK might regulate Raf activity. CNK was found to associate with the catalytic domain of Raf and depletion of endogenous CNK by RNAi in S2 cells abolished insulin-induced RAF as well as MEK and MAPK activation (Anselmo et al., 2002; Douziech et al., 2003). Therefore clones mutant for *ksr* or *cnk* should mimic the loss-of-function effect of *raf* as well as *dsor* and abolish the activation of the MAPK pathway.

Clones homozygous mutant for *cnk*⁽²⁾¹⁶³¹⁴, a strain containing a P-element insertion in the first intron of *cnk* (Therrien et al., 1998), showed a phenotype very similar to clones mutant for *ras* or *sos*. Clones predominantly clustered at the proximal part of the air sac and were for the most part of small size (Fig. R33, a7-a9 & B). Moreover, clones using *ksr*^{S-638}, a strong *ksr* loss-of-function allele (Therrien et al., 1995) were recovered. Also these clones show a dramatic reduction in clone size as well as proximal clone clustering (Fig. R33, a10-a12). The defects seen with *ksr*, especially in regard to clone size, were the strongest so far observed. With this allele, only 5 clones were obtained, but all showed the same phenotypic effects. Taken together, the data showed that activation of Ras signaling is required for proliferation of air sac tracheoblasts. This finding was not entirely surprising, since Ras has been associated with proliferation, cell survival and growth (reviewed in Rommel and Hafen,

1998). Furthermore, the Raf/MAPK pathway, an effector pathway of Ras, seems to be important for this particular function of Ras. However, the stringent correlation between clone size as well as clone position suggested that proliferation and/or growth defects might be causally linked with migration defects of air sac tracheoblasts. Therefore, in other words, the absence of cell migration could be a secondary consequence of reduced proliferation, growth or even survival. At the moment we cannot rule out this possibility. However, experiments were performed and are underway which aim at specifically addressing this point (see following paragraphs as well as discussion). Despite the appearance of small and proximally located clones, long cellular extensions were observed in some instances (Fig. R32, a5&a11) indicating that the remodeling of the cytoskeleton is not affected in these mutants. In order to address this point more profoundly, further experiments are necessary.

Table R4: Absolute numbers of ras^{x7b} , sos^{X122} , $cnk^{(2)16314}$ & ksr^{S-638} clones with respect to size and distribution

ALLELE	N	ABSOLUTE NUMBER CLONES AT TIP	LARGE OF CLONES	MEDIUM CLONES	SMALL CLONES	LARGE CLONES AT TIP	MEDIUM CLONES AT TIP	SMALL CLONES AT TIP
ras^{x7b}	7	0	0	1	6	0	0	0
sos^{X122}	10	0	0	2	8	0	0	0
$cnk^{(2)16314}$	12	0	0	4	8	0	0	0
ksr^{S-638}	5	0	0	0	5	0	0	0

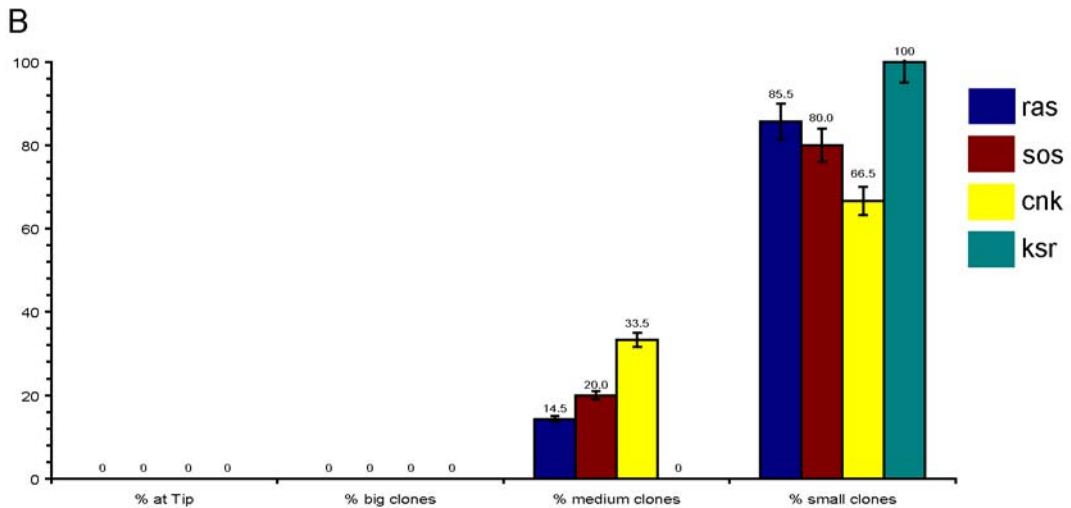
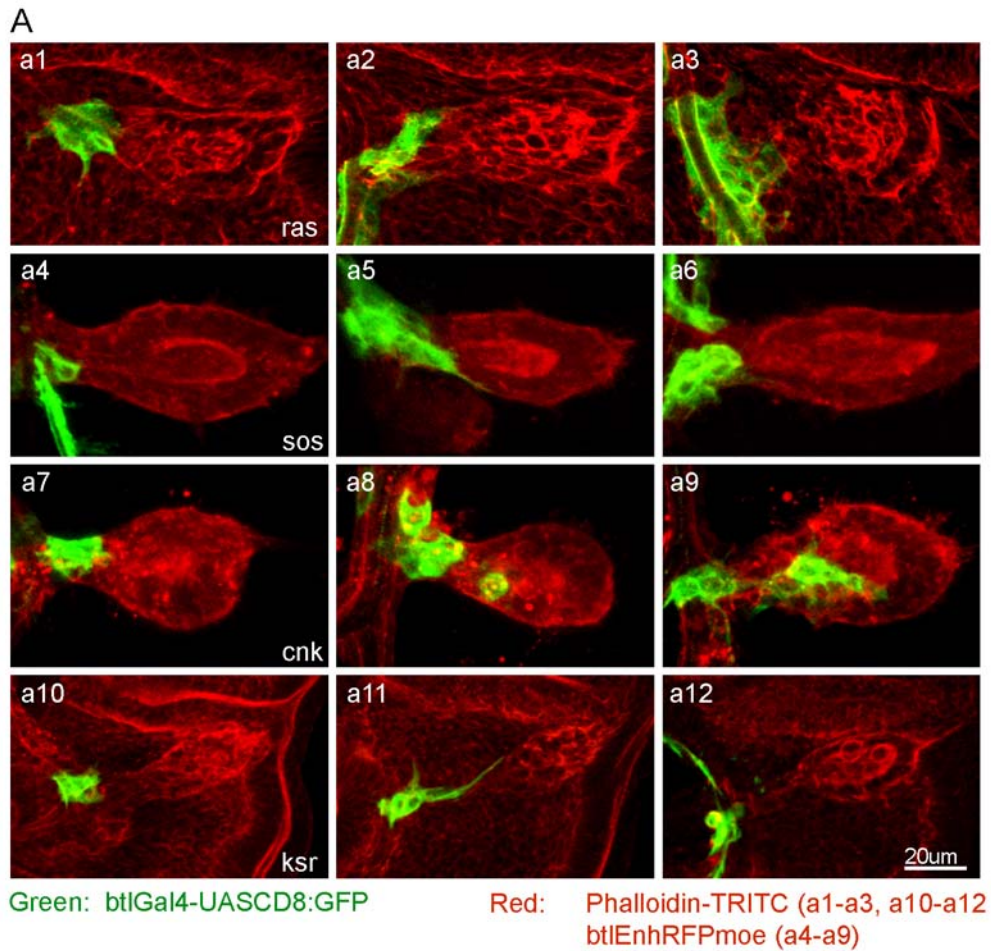


FIGURE R33

MARCM clones mutant for *ras*^{x7b}, *sos*^{X122}, *cnk*⁽²⁾¹⁶³¹⁴ & *ksr*^{S-638}.

A.) **a1-a3:** clones mutant for *ras*^{x7b}. Air sacs are outlined with phalloidin-TRITC. **a4-a6:** clones mutant for *sos*^{X122}. **a7-a9:** clones mutant for *cnk*⁽²⁾¹⁶³¹⁴. Air sacs are outlined with btlEnhRFPmoe in **a4-a9**. **a10-a12:** clones lacking *ksr*^{S-638}. Note the long cytoplasmic extension in **a11**.

B.) Statistics as indicated in previous figures. Note the representation of the clones with regard of the different size groups. Most of the clones fall into the small clone class.

7.5.1 *sos*, *ras*, *cnk* & *ksr* mutant clones in third instar larval branches

In order to further characterize this group of mutants, I also looked at terminal cells in third instar larva. Again, the logic predicted that cells unable to migrate should not be capable of forming terminal cells. Surprisingly enough, clones mutant for *sos*, *ras*, *cnk* or *ksr* were found to set up normal terminal cells (Fig. R34 A-D). However, terminal cells are established already during embryogenesis. Therefore, maternal contribution could suffice for the migration of leading tip cells and the formation of terminal cells despite the lack of de novo synthesis of protein.

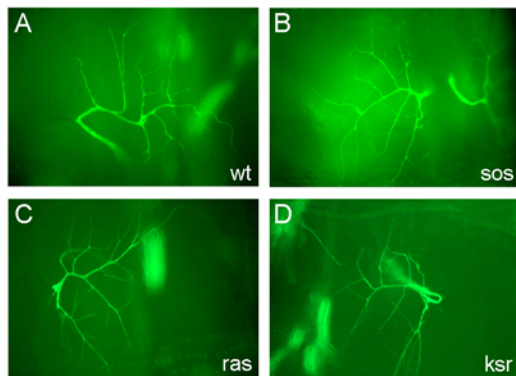


FIGURE R34

MARCM clones mutant for *sos*^{X122}, *ras*^{x7b} & *ksr*^{S-638} in third instar larva.

A.) wt terminal cell clone. **B.)** *sos*^{X122} mutant clone. **C.)** *ras*^{x7b} mutant clone. **D.)** *ksr*^{S-638} mutant clone.

Note that actGFP labeled terminal cells were found in all three instances.

Green: *btlGal4-UASactGFP*

7.6 *rca1* & *cdc2*, two genes implicated in the cell cycle.

The phenotype of *sos*, *ras*, *cnk* and *ksr* is both interesting and puzzling. Since such a clear correlation between clone size and position is observable in these mutants, we cannot confidently state that these genes are involved in air sac tracheoblast cell migration. Therefore, we designed several tests in order to distinguish between real cell migration phenotypes as well as secondary consequences associated with this class of mutants. One reason why these mutants fail to migrate could be that the cells are trapped in a particular state of the cell cycle which renders them inactive to receive or respond to external cues. In order to test this hypothesis directly, I looked at effector genes required for mitosis. Two genes were tested in a clonal manner: *rca1* as well as *cdc2*. Mutants in *regulator of cyclin A* (*rca1*) are embryonic lethal and arrest in G2 of cell cycle 16 with a phenotype similar to *cyclin A* loss-of-function mutants (Dong et al., 1997). Furthermore, in the absence of *rca1*, mitotic cyclins are prematurely degraded and cells fail to enter mitosis (Grosskortenhaus and Sprenger, 2002). Since clones mutant for *rca1* in third instar wing imaginal discs also fail to proliferate (Grosskortenhaus and Sprenger, 2002), we wanted to see first whether air sac tracheoblasts show reduced rates of proliferation and, second, whether this would have any effect on the migratory performance of these clones.

Indeed, as seen in figure R35 A (a1-a3), clones lacking *rca1* have a very severe phenotype with respect to clone position and size. Clones usually consist only of 2 to 3 cells and always cluster at the back of the air sac. Of the 10 clones tested, all were clustered at the back of the air sac and were classified as small clones (Fig. R35, B, and table R5). Furthermore, individual cells mutant for *rca1* appear bigger. The entire cell body and the nucleus look enlarged compared to wt clonal cells (Fig. R35, a1-a3).

Since we did not want to base any conclusion on this experiment alone, another cell cycle component was tested, namely *cdc2*. *cdc2* encodes for a protein kinase that regulates entry into mitosis upon dephosphorylation and thereby activation through the Cdc25 tyrosine phosphatase String (Edgar et al., 1994; Edgar and O'Farrell, 1989).

Clones mutant for the amorphic allele *cdc2*^{B47} show a phenotype similar to *rca1* mutants. Clones are located in proximal parts of the air sac and also consist of only about 2 to 4 cells (Fig. R35, a4-a6).

These experiments suggest that cell cycle entry and/or cell cycle progression are somehow linked with clone position and thereby very likely with cell migration. Clearly, cell division and cell migration use much of the same cytoskeletal machinery and must therefore be

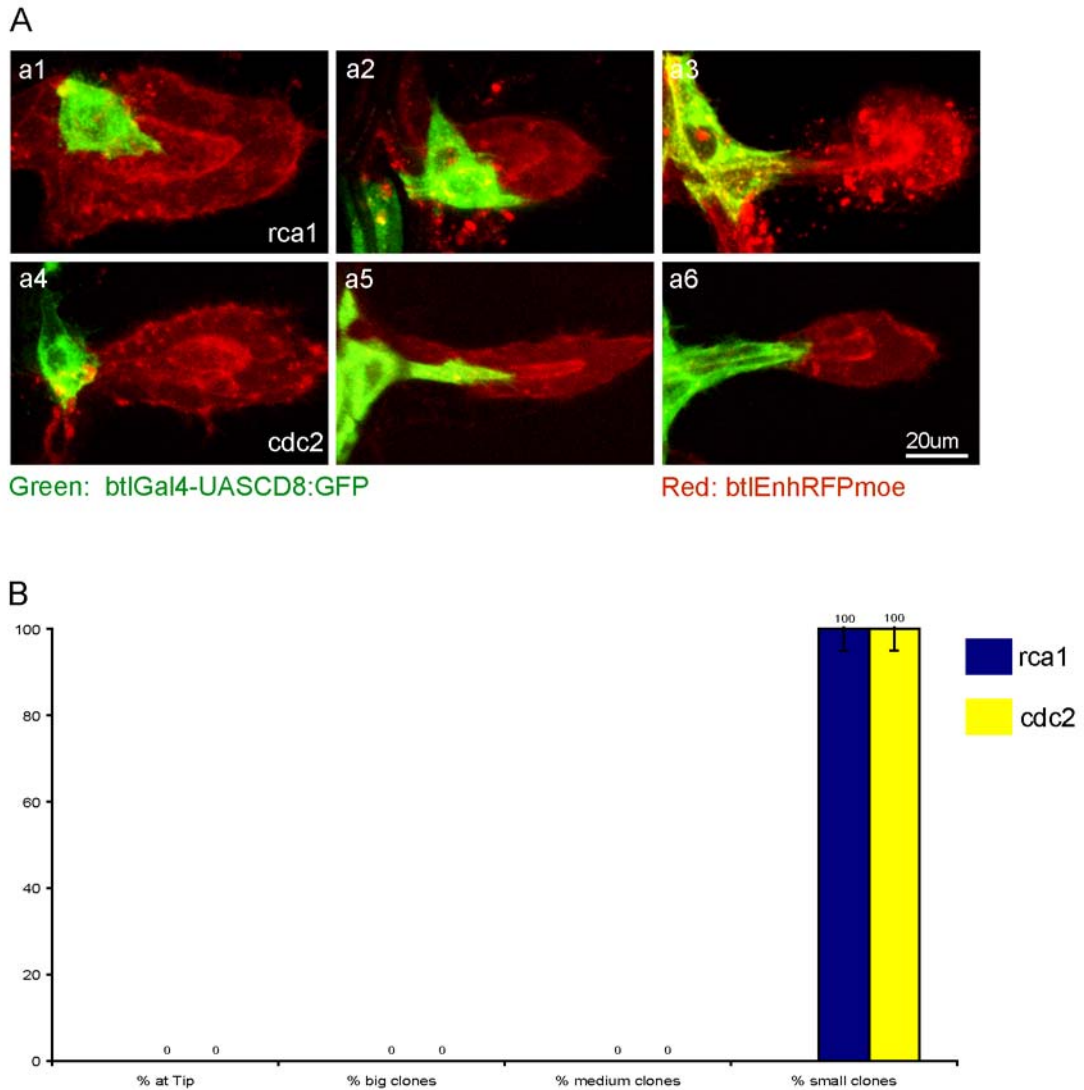
temporarily separated. In the case of *cdc2*, a recent report provided evidence that $\alpha_v\beta_3$ integrin expression in LNCaP (beta3-LNCaP) prostate cancer cells causes increased *cdc2* mRNA- as well as Cdc2 protein and kinase activity levels. Cdc2 inhibitors furthermore reduced migration (Manes et al., 2003).

However, terminal cells also mutant for these two genes under investigation were frequently recovered in third instar larvae.

Therefore, it is likely that inhibition of cell cycle entry or progression is one reason why cells lacking *sos*, *ras* and/or *ksr* show this strong correlation between clone size and position (see also discussion). Nevertheless, additional reasons could cause the failure of cells deficient for these factors to migrate.

Table R5: Absolute numbers of *rca1*² & *cdc2*^{B47} clones with respect to size and distribution

ALLELE	N	ABSOLUTE NUMBER CLONES AT TIP	LARGE OF CLONES	MEDIUM CLONES	SMALL CLONES	LARGE CLONES AT TIP	MEDIUM CLONES AT TIP	SMALL CLONES AT TIP
<i>rca1</i> ²	10	0	0	0	10	0	0	0
<i>cdc2</i> ^{B47}	5	0	0	0	5	0	0	0

**FIGURE R35**

MARCM clones mutant for *rca1*² & *cdc2*^{B47}.

A.) a1-a3: clones lacking *rca1*². Note the appearance of small clones containing large cells. All scored clones do not contain more than two to three cells. **a4-a6:** *cdc2*^{B47} mutant clones. These clones are also small in size and cells within the clone look enlarged too.

B.) Statistics as in previous figures.

7.7 The *son-of-sevenless* allele *sos*^{XMN1025} shows normal clone size but reduced cell migration

Another way of discriminating between cell cycle entry/progression, cellular growth or survival as a cause for reduced cell migration in the absence of the Ras/Raf pathway would be to look at an allelic series. The logic behind this approach is based on the fact that proteins usually contain different domains which also often exert different cellular functions. Sos for example is a multidomain protein, consisting of a DH domain, which is the catalytic guanine nucleotide exchange factor motif for Rho/Rac/cdc42 family GTPases (RhoGEFs), a PH domain as well as the Ras exchanger motif (REM), which is important for full RasGEF function. Moreover, Sos harbors a cdc25 homology region, encoding the catalytic RasGEF activity (Fig. R36 A, reviewed in Silver et al., 2004).

Alleles were isolated which specifically alter only one of the described domains. Two of these alleles were tested. *sos*^{M98} contains a point mutation in the DH domain, the site of RacGEF activity. The residue in *sos*^{M98} is not only conserved in Sos homologues from *Drosophila* to humans but also in the DH domains in distantly related GEFs such as Tiam-1 and Trio. The other allele tested is *sos*^{XMN1025} and it contains a missense mutation in the REM of Sos, likely impairing RasGEF function (Silver et al., 2004).

As already shown, *sos*^{SF15} or *sos*^{X122} alleles show severe phenotypes with respect to clone position as well as clone size (Fig. R33, a4-a6, and Fig. R36, b1-b3). However, the alleles *sos*^{M98} as well as *sos*^{XMN1025} appear similar to wild-type clones in terms of clone size (Fig. R36, b4-b9, C). About 80% of the clones represent medium- to large clones for the alleles *sos*^{XMN1025} and *sos*^{M98} (Fig. R36, C and table R6). However, with respect to clone positioning, *sos*^{M98} appears normal, since about 60% reached the tip. In contrast, *sos*^{XMN1025} mutant cells show a clear preference for the proximal locations of the air sac. Only 30% of *sos*^{XMN1025} were found to be at the tip. Furthermore, small clones can be found with both alleles at the tip (Fig. R36, b4, b7, C.).

This experiment shows that the mutation in the REM motif does not completely abolish Ras activation based on the fact that clones still reach a moderate size in contrast to complete *sos* loss-of-function alleles. It can therefore be speculated that the intensity of Ras signaling leads to different readouts as has been demonstrated for Ras signaling in the *Drosophila* eye (Halfar et al., 2001) (this point will be further addressed below as well as in the discussion).

This experiment does not prove that *sos* and phenotypically related genes such as *ras*, *cnk* or *ksr* are involved in cell migration, the existence however of alleles in the case of *sos* which

affect clone positioning but not clone size shows that clone size and clone position can be separated to some extent.

Table R6: Absolute numbers of sos^{X122} , sos^{M98} & $sos^{XMN1025}$ clones with respect to size and distribution

ALLELE	N	ABSOLUTE NUMBER OF CLONES AT TIP	LARGE CLONES	MEDIUM CLONES	SMALL CLONES	LARGE		MEDIUM		SMALL	
						CLONES	AT TIP	CLONES	AT TIP	CLONES	AT TIP
sos^{X122}	10	0	0	2	8	0	0	0	0	0	0
sos^{M98}	25	14	9	11	5	6	6	6	2		
$sos^{XMN1025}$	24	7	3	16	5	1	4	2			

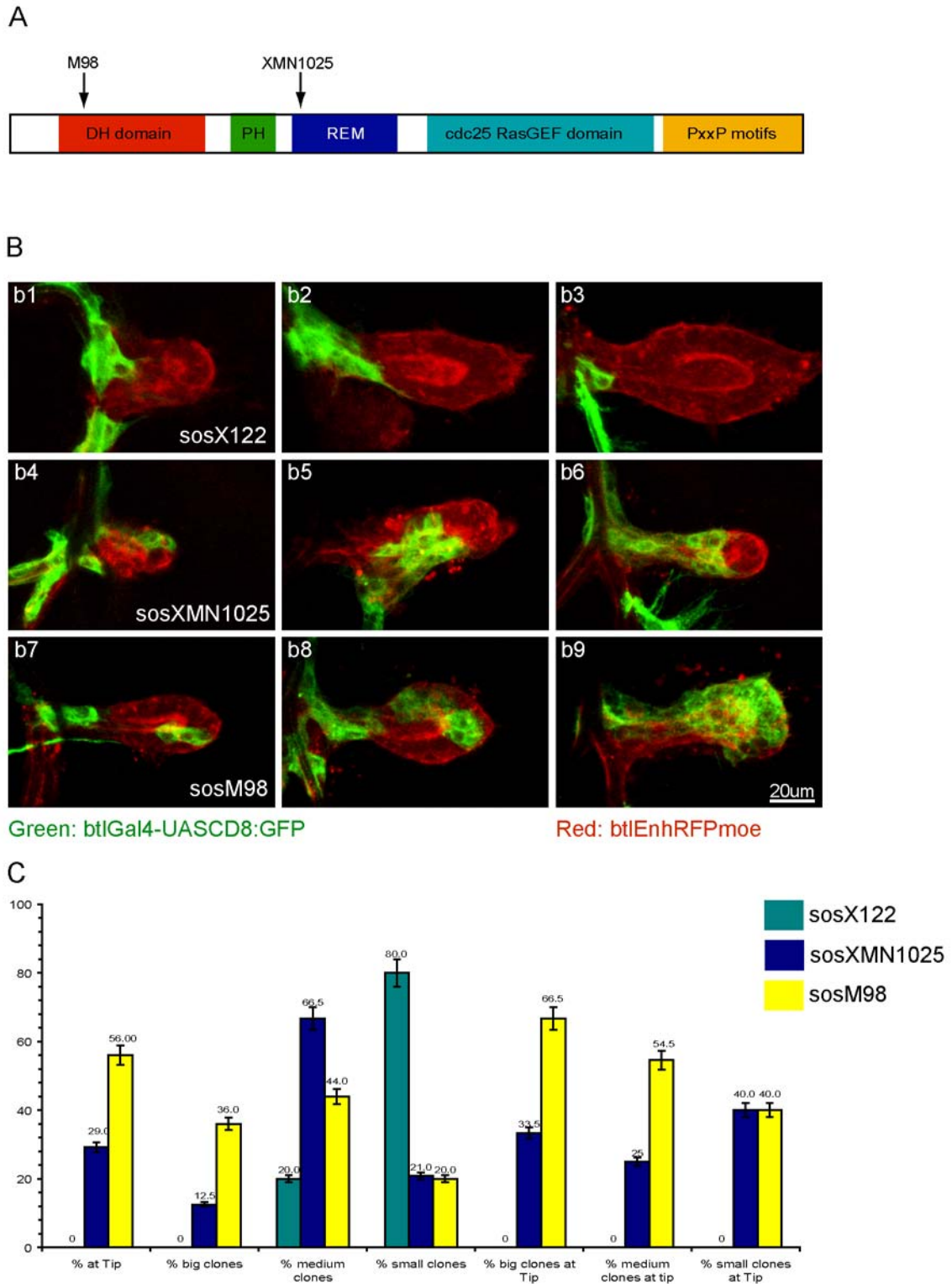


FIGURE R36

MARCM clones mutant for sos^{X122} , sos^{M98} & $sos^{XMN1025}$.

A.) Schematic representation of the Sos protein. Domains are indicated as well as the sites of lesion in the two EMS alleles. Sites of lesion for sos^{X122} are not reported **B)** **b1-b3:** sos^{X122} mutant clones (see also Fig. R34). **b4-b6:** $sos^{XMN1025}$ mutant clones. A small and two medium clones are shown. **b7-b9:** small, medium and large sos^{M98} mutant clones.

C.) Statistics as in previous figures.

7.8 Negative regulators of RTK signaling; *gap1* & *sprouty*

As shown above, the *sos*^{*XMN1025*} allele contains a point mutation in the Ras exchanger motif and thus might reduce the level of activated Ras. Thus, the observed phenotype could also be due to reduced Ras signaling activity. It has been previously reported that wing imaginal disc clones lacking *ras* completely are reduced in size compared to wild-type clones (Prober and Edgar, 2000). Also in the eye wing imaginal disc the same phenotype was observed. However, low Ras activity was reported to be sufficient to increase the size of a clone (compared to no Ras activity). Moreover it was shown that different thresholds of Ras/MAPK activate distinct cellular responses (Halfar et al., 2001). In order to further test this hypothesis, activated levels of *ras* were altered using the *Drosophila* RasGAP (*Gap1*).

Early induced clones deficient for *gap1* using the amorphic allele *gap1*^{*B2*} (Gaul et al., 1992) were analyzed with respect to clone size and clone position. *gap1* clones were predominantly medium- to big sized. (Fig. R37, a1-a3, B, table R7). Only about 30% of the clones however were positioned in distal locations of the air sac, indicating that these cells also have a reduced ability to move up to the front of migrating air sac tracheoblasts. Since 13 *gap1*^{*B2*} clones were analyzed, this result can be regarded with a certain confidence. Interestingly, the *sos*^{*XMN1025*} allele shows a reduction of migration in the same range.

Additionally, *sprouty*, a negative regulator of FGF/RTK signaling (Hacohen et al., 1998; Kramer et al., 1999) was analyzed as well. *sprouty* is expressed in air sac tracheoblasts of third instar wing imaginal discs as well as in the ad epithelial cell layer (not shown). However, in contrast to *gap1*, *spry* loss-of-function clones performed normal with regard to clone size and position (Fig. R37, a4-a6, B, table R7). However, it has to be noted that only 5 clones were analyzed so far and the obtained results are therefore based on weaker grounds.

Gap1 acts as a negative regulator of Ras. Removal of this negative regulator likely prolongs signaling activity of Ras. Comparing the clone positions of *gap1*^{*B2*} or *sos*^{*XMN1025*} could indicate that altered Ras signaling levels and/or duration have an influence on clone position and thus cell migration. However, this hypothesis has to be tested.

Table R7: Absolute numbers of *gap1*^{*B2*} & *spry* clones with respect to size and distribution

ALLELE	N	ABSOLUTE NUMBER CLONES AT TIP	LARGE OF CLONES	MEDIUM CLONES	SMALL CLONES	LARGE CLONES AT TIP	MEDIUM CLONES AT TIP	SMALL CLONES AT TIP
<i>gap1</i> ^{<i>B2</i>}	13	4	4	5	4	3	1	0
<i>spry</i> ^{<i>D5</i>}	5	4	2	1	2	2	0	2

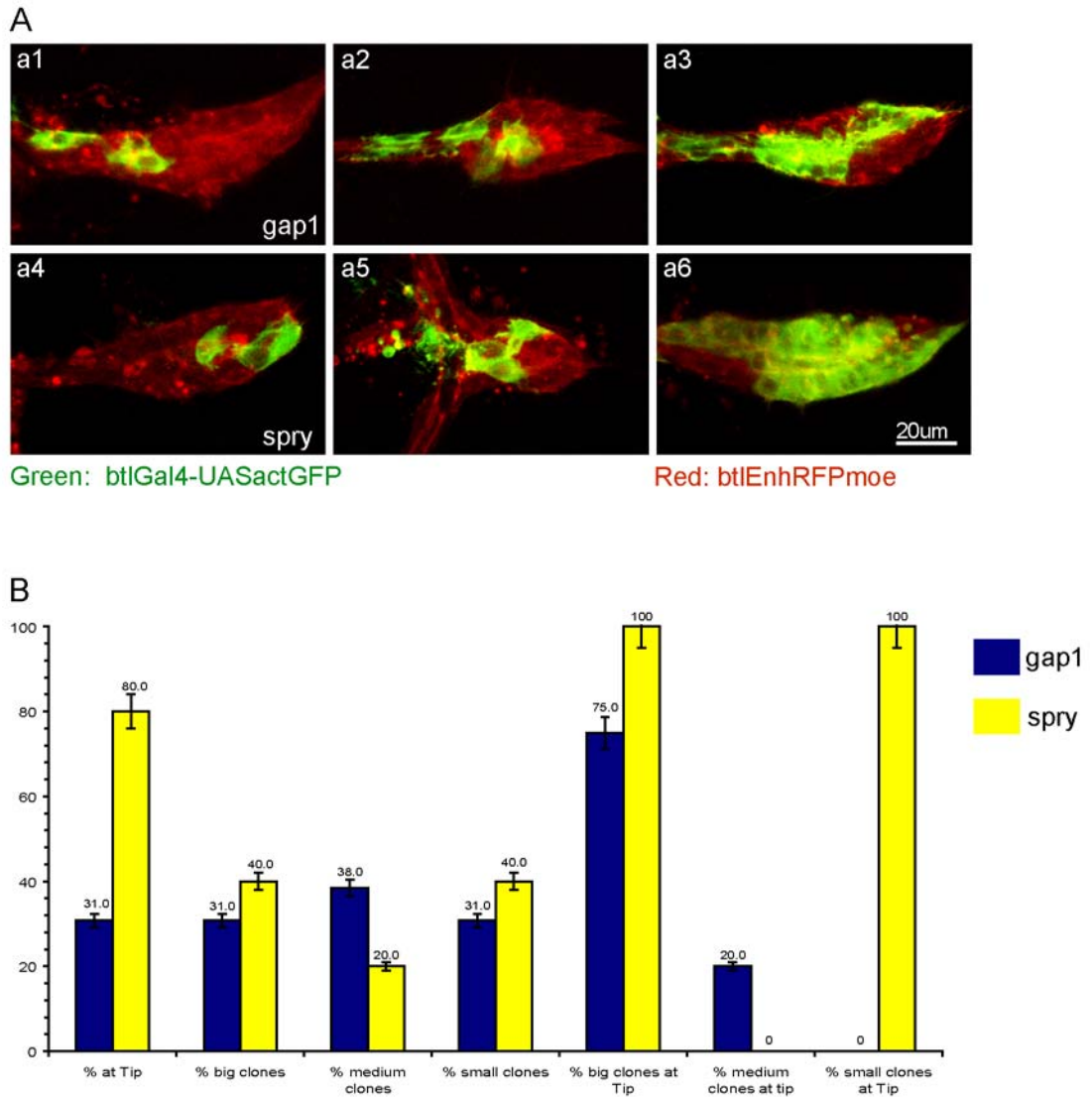


FIGURE R37

MARCM clones mutant for *gap1^{B2}* or *spry*.

A.) a1-a3: *gap1^{B2}* mutant clones. Representative small-, medium- and large clones are shown. **a4-a6:** representative *spry* clones. For both alleles, medium- and large clones represent the majority.

7.9 *PI3K* and *pten* mutant clones show air sac migration phenotypes

Another Ras-effector molecule is PI3K. In response to growth factors, PI3K catalyzes the production of phosphatidylinositol-3,4,5-trisphosphate, which sets in motion a coordinated set of events including cellular growth, cell cycle entry, cell migration and cell survival. PI3K consists of a regulatory (p85) as well as a catalytic (p110) subunit. The catalytic subunit is kept in a low-activity state by p85, which also mediates its activation by direct interaction with phosphotyrosine residues of activated growth factor receptors or adaptor proteins. Furthermore, direct binding of p110 to activated Ras protein in response to activated growth factor receptors further stimulates PI3K activity. With respect of cell migration, the generation of PIP₃ is clearly of importance, since local production of PIP₃ activates RacGTPases required for actin cytoskeleton remodeling. The production of PIP₃ leads to an increase in GTP-bound Rac in many cell types which is thought to be promoted through a direct interaction of PIP₃ with the DH domain of RacGEFs (reviewed in Cantley, 2002; Raftopoulou and Hall, 2004; Rommel and Hafen, 1998; Stocker and Hafen, 2000).

In contrast to PI3K, the phosphatase PTEN dephosphorylates PI(3,4,5)P₃ to produce PI(4,5)P₂. Loss of *pten* has been found in a large fraction of advanced human cancers. Pten is also able to dephosphorylate other substrates, such as Focal adhesion kinase (FAK) or the adaptor protein Shc. PTEN is further involved in insulin signaling to control cellular growth and counteracts the activity of PI3K (reviewed in Cantley, 2002; Stocker et al., 2002).

For these reasons, the analysis of *PI3K* as well as *pten* in air sac tracheoblasts was of major interest. Clones lacking functional *PI3K* were generated first. Similar to *ras* or *ksr* clones, very few clones were found in third instar air sacs. However, in the larval branches, *PI3K* clones did not seem underrepresented in comparison to wild-type clones. Furthermore, also terminal cells, mutant for *PI3K*, were found in the larva (not shown). Air sac tracheoblast clones on the other hand showed a very severe phenotype. These clones consisted of not more than two to three cells and were usually clustered at the very back of the air sac. Only one clone was identified, which was positioned at the margin of the main air sac body (Fig. R38, a3 and a1,a2). Nevertheless, extensions were observed in most of these clones (Fig. R38, a3, white arrow). From 7 analyzed clones, 6 were clustered at the very back (as examples a1,a2 in Fig. R38), whereas only one was positioned closer to the tip but still far away from it (Fig. R38, a3).

Next I analyzed *pten* loss-of-function clones, which occurred very frequently. Interestingly, of 19 analyzed clones only 2 were found at the tip. Both of these were in addition large clones.

However, all the other 17 clones never reached the tip in air sacs. With regard to clone size, only very few small clones were recovered, the majority was medium to big sized (Fig. R38, a4-a6, B). In total, only about 10% of *pten* mutant clones reached the tip of third instar air sacs. Interestingly, from the large clones alone, 30% managed to reach the tip, whereas in wild-type, 90% of large clones reach the leading front. Therefore, although normal conditions with respect to proliferation are established, the majority still does not reach the tip, similar to clones generated with the *sos*^{*XMN1025*} allele.

A difference in cell size of clones mutant for *PI3K* or *pten* was not observed.

Table R8: Absolute numbers of *PI3K*^{*5w3*} & *pten*^{*1*} clones with respect to size and distribution

ALLELE	N	ABSOLUTE NUMBER CLONES AT TIP	LARGE OF CLONES	MEDIUM CLONES	SMALL CLONES	LARGE CLONES AT TIP	MEDIUM CLONES AT TIP	SMALL CLONES AT TIP
<i>PI3K</i> ^{<i>Dp110A</i>}	7	0	0	0	7	0	0	0
<i>Pten</i> ^{<i>1</i>}	19	2	6	12	1	2	0	0

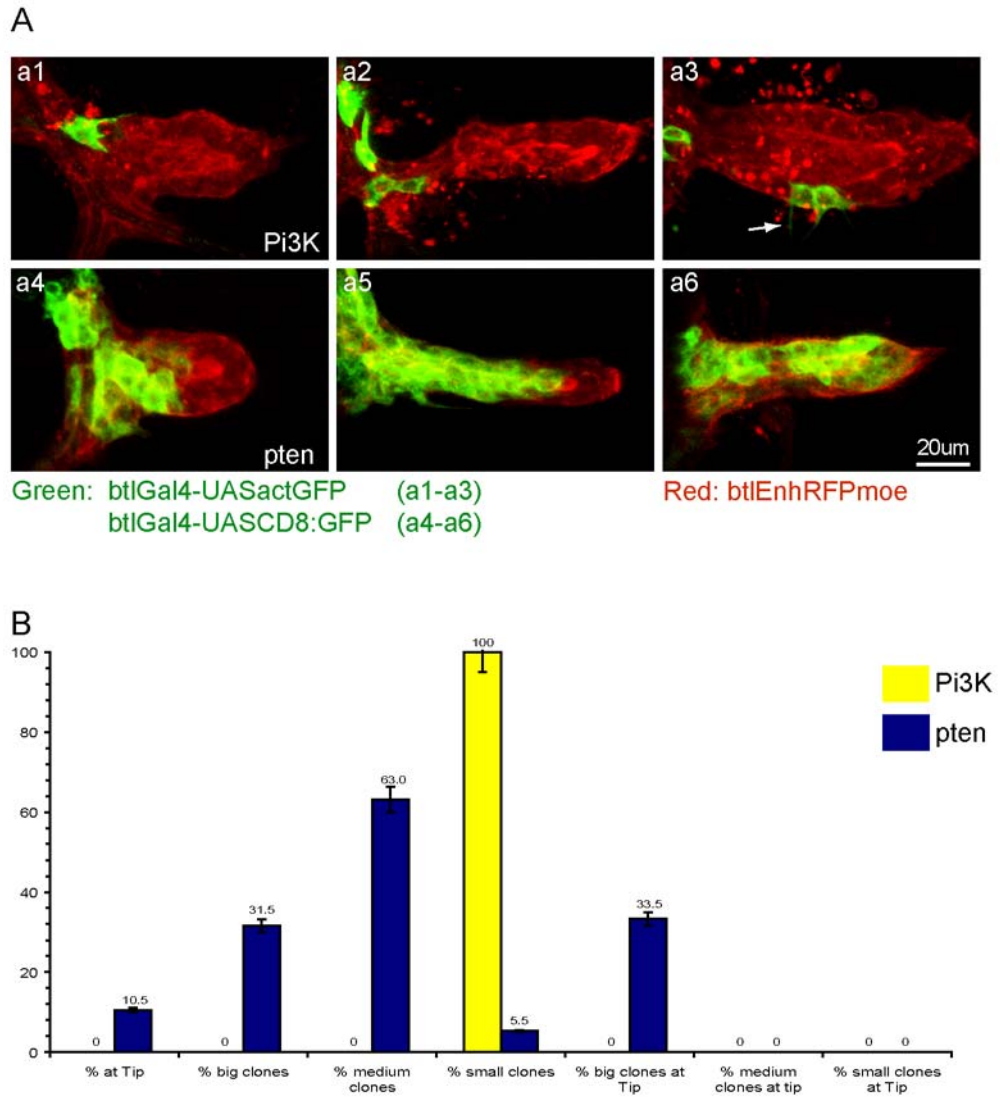


FIGURE R38

MARCM clones mutant for *Pi3K^{Dp110A}* or *pten¹*.

A) a1-a3: *Pi3K^{Dp110A}* mutant clones. All recovered clones are similar in size and position. Note the clone in a3 displays an actin rich extension (white arrow). **a4-a6:** *pten¹* mutant clones display the opposite phenotype in terms of size but not position. **B.)** Statistics as in previous figures. Note that only large clones were found at the tip.

7.10 Regulators of the actin cytoskeleton; *rac*, *mbc*, *pak*, *chic*.

As mentioned already in the introduction, the Rho GTPases are fundamental regulators of the Actin cytoskeleton. Cell migration, but also other cellular processes, rely on an intact and robust cytoskeleton. In order to integrate extracellular stimuli into a cellular response, Rho family GTPases require to interplay with upstream regulators and downstream effectors. Due to multiple cellular functions of Rho family GTPases, loss-of-function mutations are not easy to analyze due to global effects. *cdc42* mutants, for example, severely affect the embryonic tracheal system (Dossenbach, 2004), however other developmental defects such germ band retraction or dorsal closure are also affected (Genova et al., 2000). Clear evidence for the involvement of Rac in cell migration *in vivo* came from border cell studies, as mentioned above (Duchek et al., 2001b; Geisbrecht and Montell, 2004; Murphy and Montell, 1996). It was further found that *mbc*, the *Drosophila* Dock180 homologue and activator of Rac, is also involved in border cell migration, although not absolutely required since about 10% of *mbc* deficient border cells still reached the oocyte. Pak, a Rac effector, did not show any border cell migration defects (Duchek et al., 2001b). In the *Drosophila* embryonic tracheal system, reduction of Rac displayed an inhibition of epithelial cell rearrangement as well as tracheal cell migration phenotypes. Similar findings were reported for Pak. Furthermore, a genetic interaction between FGF and *rac* as well as FGF and *pak* was found (Chihara et al., 2003).

Three *rac* genes are encoded in the *Drosophila* genome, *rac1*, *rac2* and *mig-2-like* (*mtl*) (Hakeda-Suzuki et al., 2002; Ng et al., 2002). Clones homozygous mutant for *rac1* and *rac2* were generated. Two different *rac1* alleles were used, *rac1^{J11}* as well as the weaker *rac1^{J10}* (Ng et al., 2002). For *rac2*, the amorphic allele *rac2^A* (Ng et al., 2002) was used in both instances. Since both *rac* genes are on the same chromosomal arm (3L), double mutants are generated with relative ease. However, *mtl* is located on 3R and we have thus not yet generated *rac1*, *rac2*, *mtl* triple mutants. Nevertheless, we made clones genotypically double mutant for *rac1^{J11} rac2^A*, or *rac1^{J10} rac2^A mtl/+*, the latter also lacking one copy of *mtl*.

The clones of the above genotype show no defects in size (Fig. R39, a1-a6, B). Although clones containing two wild-type copies of *mtl* are generally a bit larger; nevertheless, this difference is small (Fig. R39, B). With regard to clone position, clones are generally located at the back of the air sac in both instances. By reducing the amount of Mtl to 50%, clones have an even smaller probability of reaching the tip. Of 16 analyzed clones lacking *rac1, rac2* as well as one copy of *mtl*, only 1 clone was found to be at the tip. Not surprisingly, this was a clone of large size.

In contrast, *mbc* clones show a similar distribution with regard to clone size, compared to *rac* clones; however, they appear to display improved clone positioning. About 20% of *mbc* clones reached the tip (Fig. R40, a1-a3). Of these clones capable of reaching the leading edge, the majority was also big in size (Fig. R40, B). The downstream effector Pak on the other hand, also shows no effect on clone size and more than half of the *pak* clones reached the tip. I would therefore conclude that these clones display only a very weak migratory phenotype and that this gene is not absolutely required for air sac tracheoblast migration (Fig. R40, a4-a6, B).

Furthermore, mutants in the *Drosophila* gene *chickadee* (*chic*), encoding for Profilin, were analyzed. *chic* mutant clones show very severe phenotypes. First of all, clone recovery was poor. Some of the detected air sac clones displayed signs of apoptosis such as fragments of GFP without any recognizable cell body (Fig. R40, a7). Furthermore, in some instances, Moesin fused to RFP, which is used as a marker to outline the entire air sac, was also absent in the mutant clone. This result can be explained with the fact that Moesin binds to Actin filaments; if these cannot be properly formed due to the absence of Profilin, binding and proper localization is abolished. However, this has only been observed once in the biggest detected clone (Fig. R40, a9). Generally, with regard to clone size, most of the clones are small. No clone was ever found at the tip but also only 5 clones were analyzed so far. Therefore, the absence of tip cell clones in the case of *chic*, which was investigated with the amorphic allele *chic*^{05205a}, could be due to an absence in cell migration and/or a secondary consequence of apoptosis.

In sum, several regulators of the Actin cytoskeleton, which were previously implicated in cell migration, also display clone positioning defects and therefore, very likely, reduced cell migration. Interestingly, Pak mutants do not show a strong reduction in migration, which is consistent with findings in border cell migration (Duchek et al., 2001b).

However, the question still remains whether the defects observed in the case of *mbc*, *rac* or *chic* are linked with FGF signal transduction. Future experiments will specifically address this question.

Table R9: Absolute numbers of *rac1^{J11}rac2^Δ*, *rac1^{J10}rac2^Δ mtl/+*, *mbc^{D11.2}*, *pak¹* & *chic^{05205a}* clones with respect to size and distribution

ALLELE	N	ABSOLUTE NUMBER OF CLONES AT TIP	LARGE CLONES	MEDIUM CLONES	SMALL CLONES	LARGE CLONES AT TIP	MEDIUM CLONES AT TIP	SMALL CLONES AT TIP
<i>rac1^{J11}rac2^Δ</i>	9	2	3	4	2	1	1	0
<i>rac1^{J10}rac2^Δ mtl/+</i>	16	1	4	6	6	1	0	0
<i>mbc^{D11.2}</i>	14	3	3	6	5	2	1	0
<i>pak¹</i>	9	5	4	3	2	3	2	0
<i>chic^{05205a}</i>	5	0	0	1	4	0	0	0

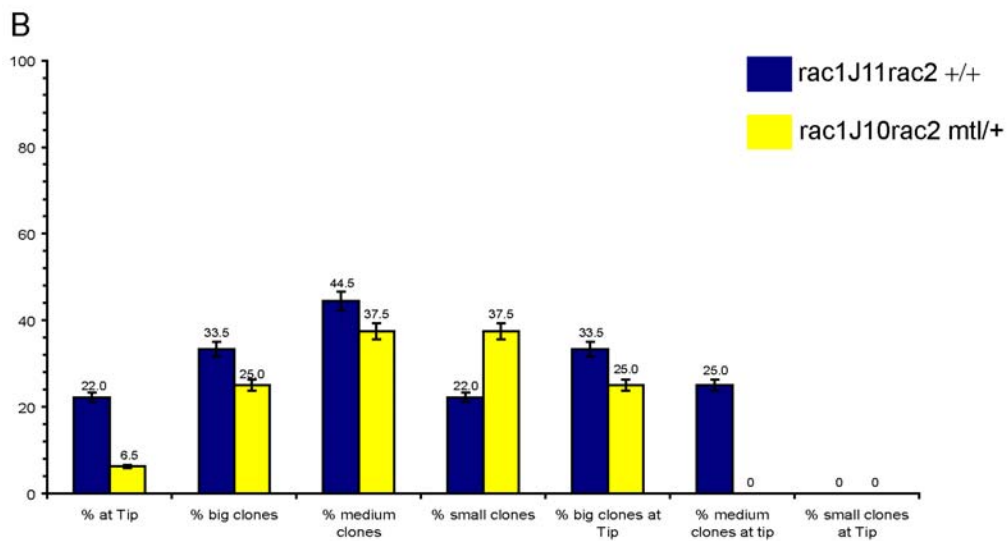
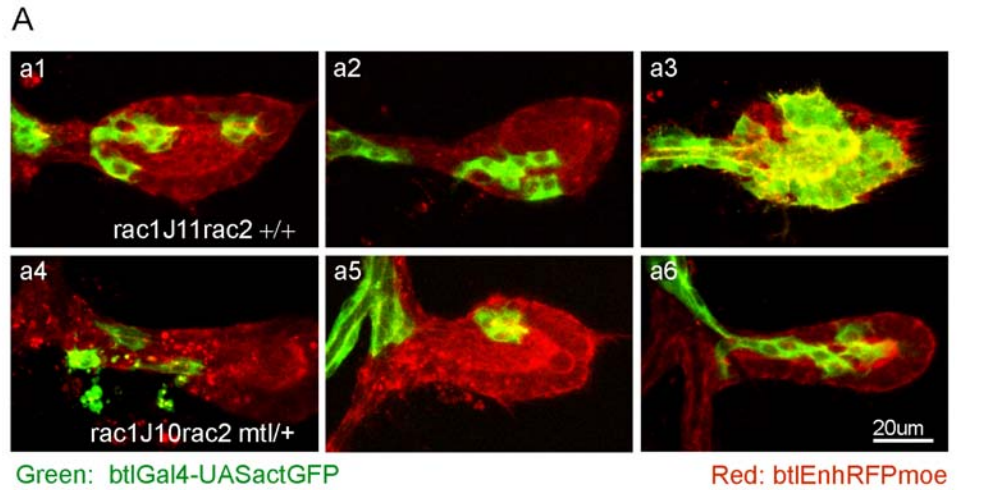


FIGURE R39

MARCM clones mutant for *rac1^{J11}rac2^Δ* or *rac1^{J10}rac2^Δ mtl/+*

A.) a1-a3: representative clones mutant for *rac1^{J11}rac2^Δ*. These clones contain two copies of wild-type *mtl*. **a4-a6:** representative *rac1^{J10}rac2^Δ mtl/+* clones. Note that these clones lack both copies of *rac1* and *rac2*. In addition, they contain only one copy of *mtl*. **B.)** Statistics as in previous figures. Note that a higher fraction of small clones was recovered with *rac1^{J10}rac2^Δ mtl/+* compared to *rac1^{J11}rac2^Δ*. The *rac1^{J10}rac2^Δ mtl/+* allelic combination also results in less large- or medium sized clones.

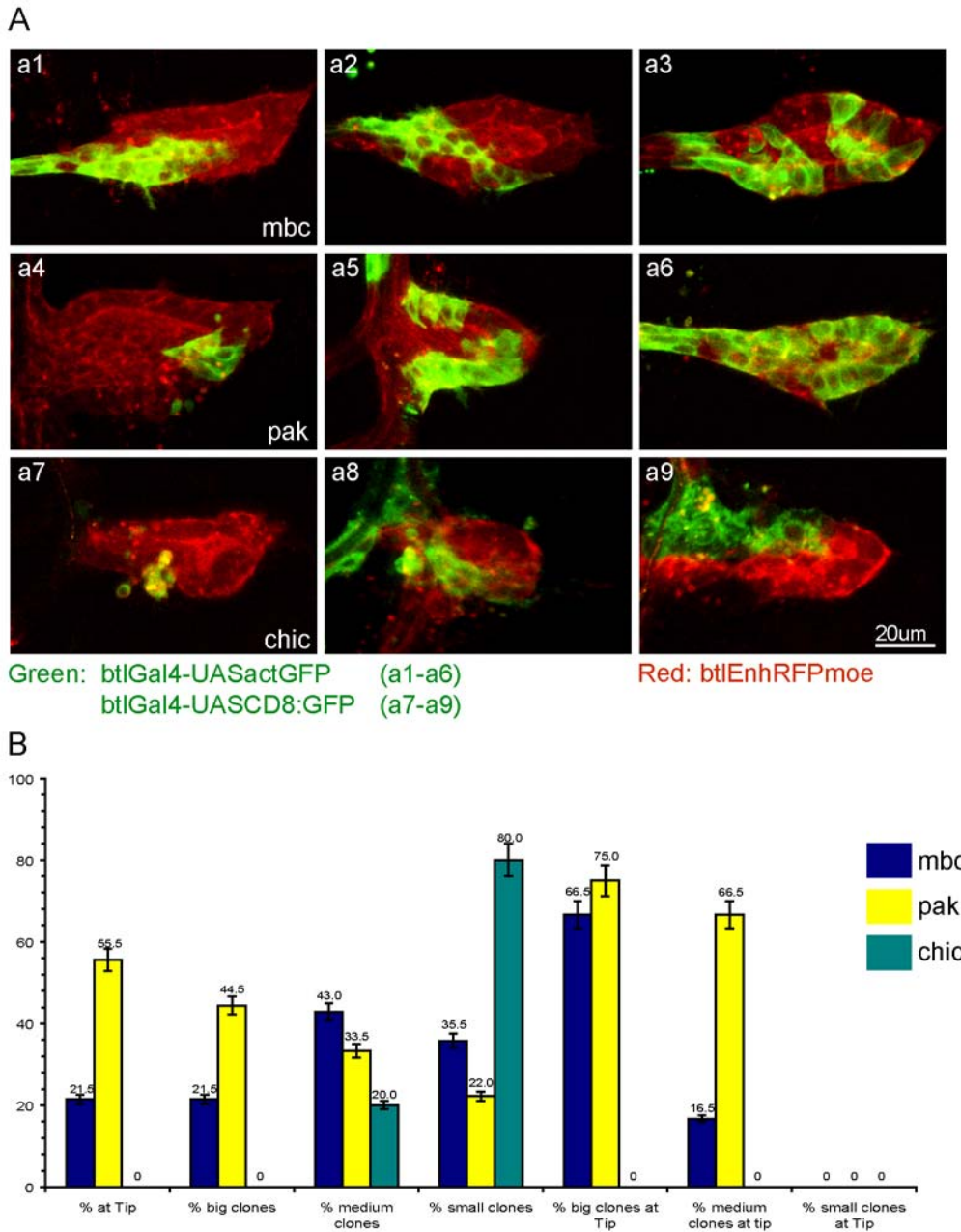


FIGURE R40

MARCM clones mutant for *mbc*^{D11.2}, *pak*¹ & *chic*^{05205a}.

A.) **a1-a3:** representative *mbc*^{D11.2} clones. Although the majority of these clones do not reach the tip, including medium- or large clones, some clones can still be found at the tip. **a4-a6:** representative *pak*¹ clones. **a7-a9:** Clones mutant for *chic*^{05205a} show severe phenotypes. Clones are often small, look fragmented or do not coexpress RFPmoe.

B.) Statistics as in previous figures. Note that *pak*¹ clones show a wild-type like distribution with respect to size. *chic*^{05205a} clones are predominantly small.

7.11 Role of RhoGEFs in air sac

RhoGEFs are major regulators of Rho GTPases. In contrast to Rac or cdc42, Rho acts via Rock in the assembly of stress fibers required for contraction (reviewed in Raftopoulou and Hall, 2004; Ridley, 2001). RhoGEFs have also been shown to be involved during *Drosophila* cytokinesis, gastrulation as well as mesodermal cell migration (Barrett et al., 1997; Hacker and Perrimon, 1998; Prokopenko et al., 1999; Schumacher et al., 2004; Smallhorn et al., 2004; Somers and Saint, 2003).

We were interested in the function of two RhoGEFs, Pebble (Pbl) as well as RhoGEF2. The latter has been shown to be involved in cell shape changes during gastrulation movements (Barrett et al., 1997; Hacker and Perrimon, 1998). Pebble has been found to be involved in cytokinesis (Prokopenko et al., 1999; Somers and Saint, 2003) as well as mesodermal cell migration (Schumacher et al., 2004; Smallhorn et al., 2004).

By analyzing clones mutant for *rhoGEF2* in third instar air sacs, only very weak phenotypes can be seen. Clone size appears normal whereas clone position is only very weakly affected. Roughly 50% of clones lacking rhoGEF2 are located in distal parts of the air sac (Fig. R41, a1-a3, B, table R10).

In the case of *pbl*, however, the situation is much more dramatic. No single clone has been discovered at the tip of air sacs so far. However, since clones mutant for the amorphic allele *pbl⁵* were difficult to recover, a weaker allele *pbl¹¹* was used. In case of *pbl⁵*, clones were often seen to undergo apoptosis. Only fragments of GFP were detected. Furthermore, these fragments were excluded from the air sac (Fig. R41, a4). Nevertheless, also with the hypomorphic allele, strong phenotypes were observed. The cells migrated poorly and as seen in example a6 in Fig. R41, displayed a strange shape. In total, only 4 clones were recovered, with both alleles. At the moment, we cannot rule out whether the observed defects are due to cytokinesis defects or reflect an intrinsic migration problem.

Unfortunately, no allele exists which only affect migration but not cytokinesis (Arno Müller, personal communication).

Table R10: Absolute numbers of *rhoGEF2^{4,1}*, *pbl^{5&11}* clones with respect to size and distribution

ALLELE	N	ABSOLUTE NUMBER OF CLONES AT TIP	LARGE OF CLONES	MEDIUM CLONES	SMALL CLONES	LARGE CLONES AT TIP	MEDIUM CLONES AT TIP	SMALL CLONES AT TIP
<i>rhoGEF2^{4,1}</i>	15	7	5	7	3	5	2	0
<i>pbl^{5&11}</i>	4	0	0	1	3	0	0	0

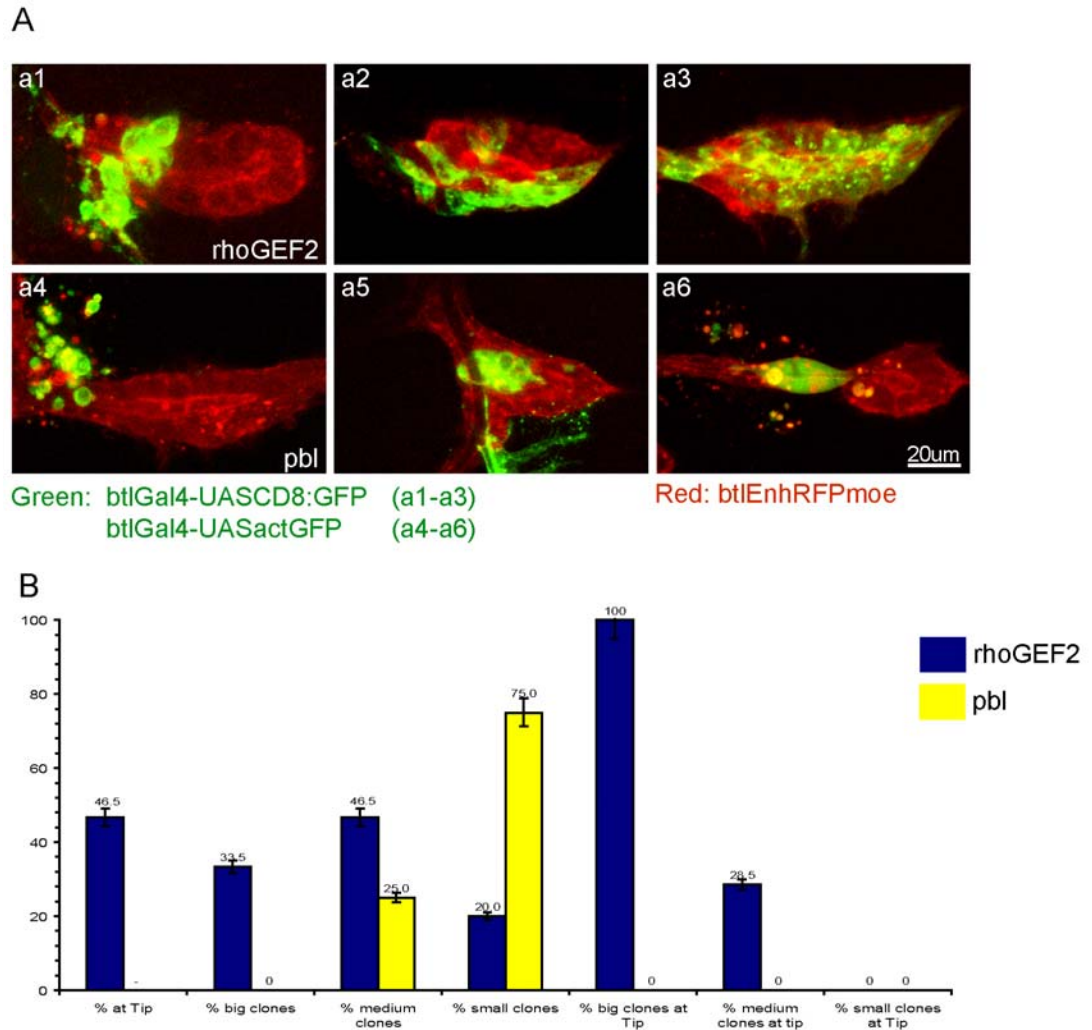


FIGURE R41

MARCM clones mutant for *rhoGEF2*^{4.1}, *pbl*^{5&11}.

A.) a1-a3: *rhoGEF2*^{4.1} clones display weak migration phenotypes. Some clones as the example in a1 also look fragmented. However, medium or large tip clones can be found. **a4-a6:** *pbl*^{5&11} clones show very severe phenotypes. **a4** represents a clone mutant for the amorphic allele *pbl*⁵. Note the exclusion and severe fragmentation of this clone representative for null *pbl* alleles. **a5, a6:** clones mutant for the weaker allele *pbl*¹¹.

B.) Statistics as described previously

7.12 Air sac tracheoblasts mutant for different signaling components

Although FGF signaling was central in our analysis of guided cell migration, we also asked whether other signaling pathways play important roles during air sac formation. Taken into account that air sac tracheoblasts mutant for *btl* or *dof* can still proliferate, whereas *ras* deficient cells divide poorly, we assumed that other signaling pathways might be responsible for air sac tracheoblast proliferation. In order to test this assumption, components of different signaling pathways were tested, such as Smoothed, one of the two Hedgehog (Hh) receptors (Alcedo et al., 1996), the EGF-receptor (EGFR/DER) (reviewed in Shilo, 2003), Thick veins (Tkv), one of the two Dpp receptors (Nellen et al., 1994) as well as Spalt, a context dependent target for EGFR and/or Dpp signaling (reviewed in Affolter et al., 2001; Ghabrial et al., 2003).

Clones lacking *smo* show no signs of reduced proliferation. *smo* clones are often positioned in distal parts of the air sac. However, as reported previously (Dahmann and Basler, 2000), these clones show a rounded morphology based on the endeavor to minimize contact with the surrounding tissue. In terms of size, the majority of *smo* clones falls into the class of the medium to big sized clones (Fig. R42, a1-a3, B, table R11). However, not all clones display this rounded morphology. Next, I looked at clones lacking the *Drosophila* EGF-receptor (DER). As reviewed already in the Introduction, EGFR plays a major role during the guided migration of border cells. Furthermore, this EGFR/ErbB family receptor displays a multitude of diverse functions during *Drosophila* development (reviewed in Shilo, 2003).

First of all, clones deficient for an amorphic *egfr* allele appear to survive poorly, as indicated by signs of apoptosis (Fig. R42, a4, a5). Again, the yield of clones recovered in the air sac was poor and only small clones were found (Fig. R42, a4-a6, B., table R11). Additionally, only one out of eight clones was positioned at the tip. Nevertheless, in contrast to *ras*, or *ksr* clones, which also appear very small in size, *egfr* clones were not entirely located in the very proximal part of the air sac. They are also found in the main air sac body and therefore do not perform as poorly as *ras* or *ksr* clones (compare Fig. R42, a4-a6 with Fig. R33, a1-a3 & a10-a12). This is also reflected in the fact that one clone was found at the tip, whereas this never happened in *ras* or *ksr*. Thus, I assume that the poor survival of *egfr* cells contributes to the position of the clone.

At last *sal* or *tkv* clones behave as wild-type clones with regard to clone position (Fig. R42., a7-a12). In terms of clone size, a difference is seen between *sal* and *tkv*. *sal* clones display a like-like distribution of big, medium and small clones. Few big *tkv* clones however were

found, the majority of tkv clones represent medium sized clones and also about one third can be regarded as small (Fig. R42., a10,-a12).

In sum, clones lacking functional EGFR display the strongest phenotype in the light of clone position as well as clone size. EGFR also signals through Ras and the Raf/MAPK pathway and also influences proliferation as well as cell survival (Shilo, 2003).

However, other major signaling pathways such as Notch, Wingless or JAK/STAT have not been tested so far.

Table R11: Absolute numbers of *smo*, *egfr*^{K35}, *Df(2L)sal*⁵, *tkv*^{Q12} clones with respect to size and distribution

ALLELE	N	ABSOLUTE NUMBER OF CLONES AT TIP	LARGE OF CLONES	MEDIUM CLONES	SMALL CLONES	LARGE CLONES AT TIP	MEDIUM CLONES AT TIP	SMALL CLONES AT TIP
<i>smo</i> ³	25	14	4	14	7	3	9	2
<i>egfr</i> ^{K35}	8	1	0	0	1	0	0	1
<i>Df(2L)sal</i> ⁵	16	12	7	6	3	7	5	0
<i>tkv</i> ^{Q12}	17	13	1	10	6	1	9	3

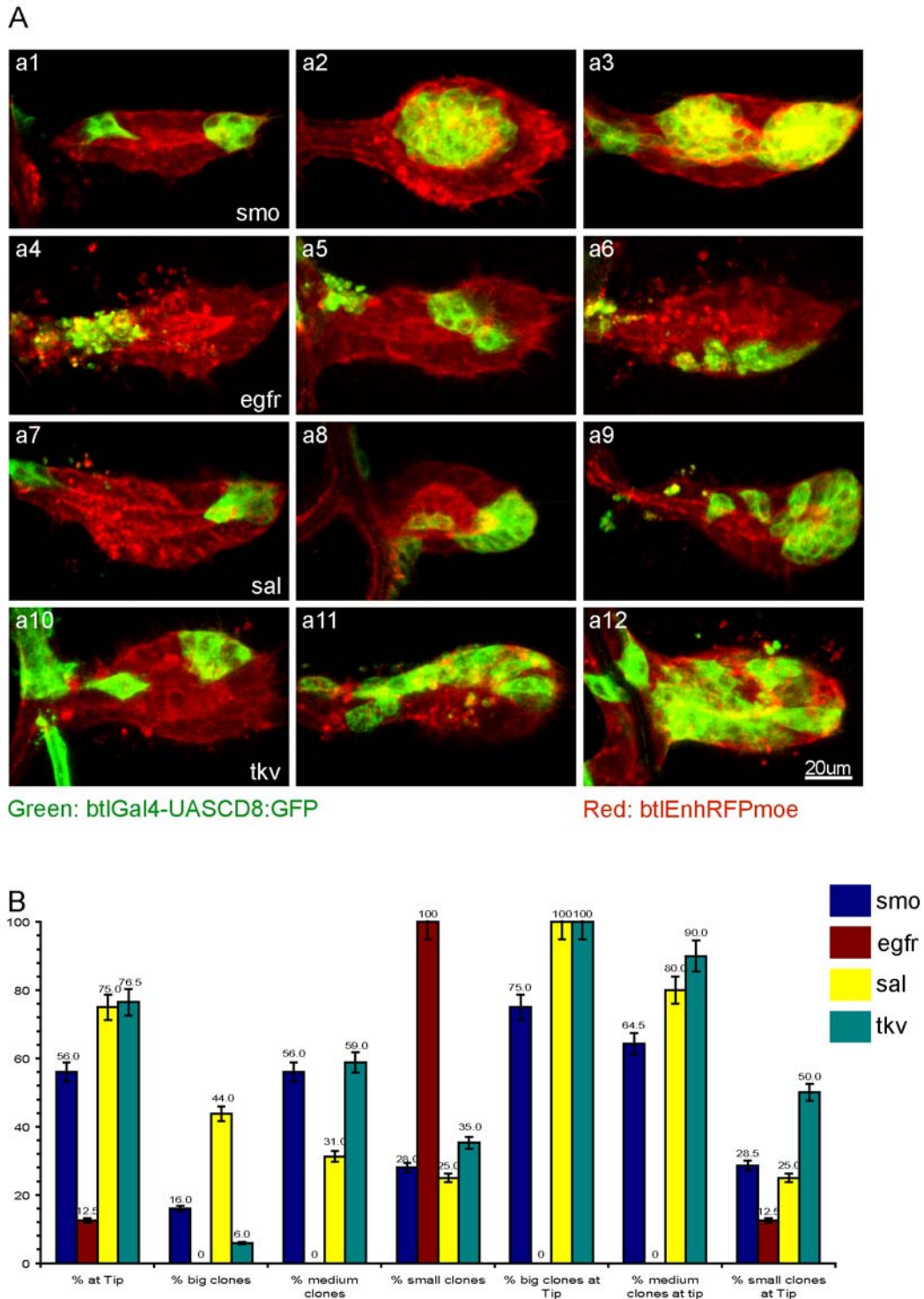


FIGURE R42

MARCM clones mutant for *smo*³, *egfr*^{K35}, *Df(2L)sal*⁵, *tkv*^{Q12}.

A.) a1-a3: clones lacking Smo function. Note the tendency of the clone to minimize contact with the surrounding tissue. **a4-a6:** clones mutant for the allele *egfr*^{K35}. Clones often undergo apoptosis as judged from the appearance of GFP positive fragments. Clones however do not only cluster at the back but can also be found in more distal regions. **a7-a9:** Clones mutant for *spalt major* and *spalt related*. The small deficiency *Df(2L)sal*⁵ uncovers both genes. These as well as *tkv*^{Q12} clones **a10-a12** do not show phenotypes with regard to clone size or position.

B.) Statistics as in previous figures.

7.13 Clones deficient for genes implicated in border cell migration

A lot of progress concerning guided cell migration *in vivo* came from the study of border cells. These cells very likely take advantage of the same basic cellular migration machinery as other cell types. However, in contrast to tracheal cells, border cells do not respond to FGF signaling. Although the FGF receptor is a target of the transcription factor Slbo, border cells mutant for *btl* show no impairment in border cell migration (Murphy et al., 1995). The same is true for border cells lacking *dof* or the second FGF receptor Heartless (Duchek and Rorth, 2001a).

I was wondering whether air sac tracheoblasts show an impairment with regard to cell migration if they lack the most prominent components involved in border cell migration such as Slbo, PVR, Tai, DE-Cadherin or SRF (see table 1C in the introduction). Due to the mentioned advantages, these factors were again tested in the third instar air sac by generating loss-of-function clones.

As expected, none of the tested components show a reduction in air sac tracheoblast proliferation. The majority of clones were medium sized, with some big as well as some small sized clones (Fig R43&44). *slbo* clones were predominantly found at the tip. From 28 analyzed clones, 19 were found at the tip which corresponds to about 70%. The same percentage was found with *wt* clones. Also *pvr* clones were mostly found at the tip albeit at a slightly reduced ratio (60%) (see also Fig. R43, a1-a6, B., table R12). Since in both cases strong alleles were used, I conclude that neither *slbo* nor *pvr* are required for air sac proliferation or migration. This result was not entirely anticipated, since as already mentioned, Slbo is a transcription factor and induces directly the expression of *btl*. Also *pvr* was found to be ubiquitously expressed in wing imaginal discs (not shown and (Rosin et al., 2004). Moreover, PVR was shown to have a strong effect on the Actin cytoskeleton in border cells (Duchek et al., 2001b).

The other components tested, *tai*, *DE-Cadherin* (encoded by *shotgun* (*shg*)) and *bs*, do not show severe defects in this clonal assay. Only *tai* clones show a slight reduction in migration, since 50% reached the tip compared to 70% in wild-type. *Shg* as well as *bs* clones both reach the tip with frequencies comparable to wild-type clones.

Albeit the fact that *Shg* clones migrated normally, they show another interesting detail. Similar to *smo* clones, *shg* deficient clones appear roundish in morphology and try to minimize contact with the surrounding tissue (Fig. R44, a4-a6) although the effect is not as strong as seen with *smo* clones. Furthermore, clones marked with α CateninGFP displayed no

apical side and the marker was completely dislocalized (not shown). In several instances, it was also observed that *shg* clones, which located at the tip, break off from the air sac (Fig. R44, a5). Since *shg* encodes for the *Drosophila* DE-Cadherin, a homophilic cell adhesion molecule, this phenotype can be explained with the lack of adhesion. Furthermore, α Catenin connects the E-Cadherin- β Catenin complex to the Actin cytoskeleton (reviewed in Kobiela and Fuchs, 2004), and the mislocalization of α CateninGFP was thus not surprising.

In addition, terminal cells mutant for all these investigated genes were recovered in third instar larva with the exception of *bs*, the major terminal cell fate determinant (Affolter et al., 1994; Guillemin et al., 1996).

Another intriguing detail concerning SRF is based on the fact that antibody stainings failed to detect any SRF protein in third instar air sacs. However, certain transgenic LacZ expression lines containing SRF enhancer fragments do express β Gal uniformly in air sac tracheoblasts (U. Nussbaumer, personal communication). Furthermore, a SRFGal4 line was found, which crossed to UASGFPmoe, expresses GFP in air sacs although in a patchy and very weak manner (not shown).

However, based on the finding that SRF does not show any detectable phenotype with respect to clone size or clone position, we argue that this protein is not required in these late stages.

Table R12: Absolute numbers of *slbo*^{E7B}, *pvr*⁵³⁶³, *tai*^{61G1}, *shg*^{IH}, *bs* clones with respect to size and distribution

ALLELE	N	ABSOLUTE NUMBER OF CLONES AT TIP	LARGE OF CLONES	MEDIUM CLONES	SMALL CLONES	LARGE CLONES AT TIP	MEDIUM CLONES AT TIP	SMALL CLONES AT TIP
<i>slbo</i> ^{E7B}	28	19	4	20	4	4	12	3
<i>pvr</i> ⁵³⁶³	20	12	2	16	2	1	10	1
<i>tai</i> ^{61G1}	35	18	2	29	4	2	14	2
<i>shg</i> ^{IH}	22	16	1	20	1	1	14	1
<i>bs</i> ¹⁴	19	12	5	13	1	4	8	0

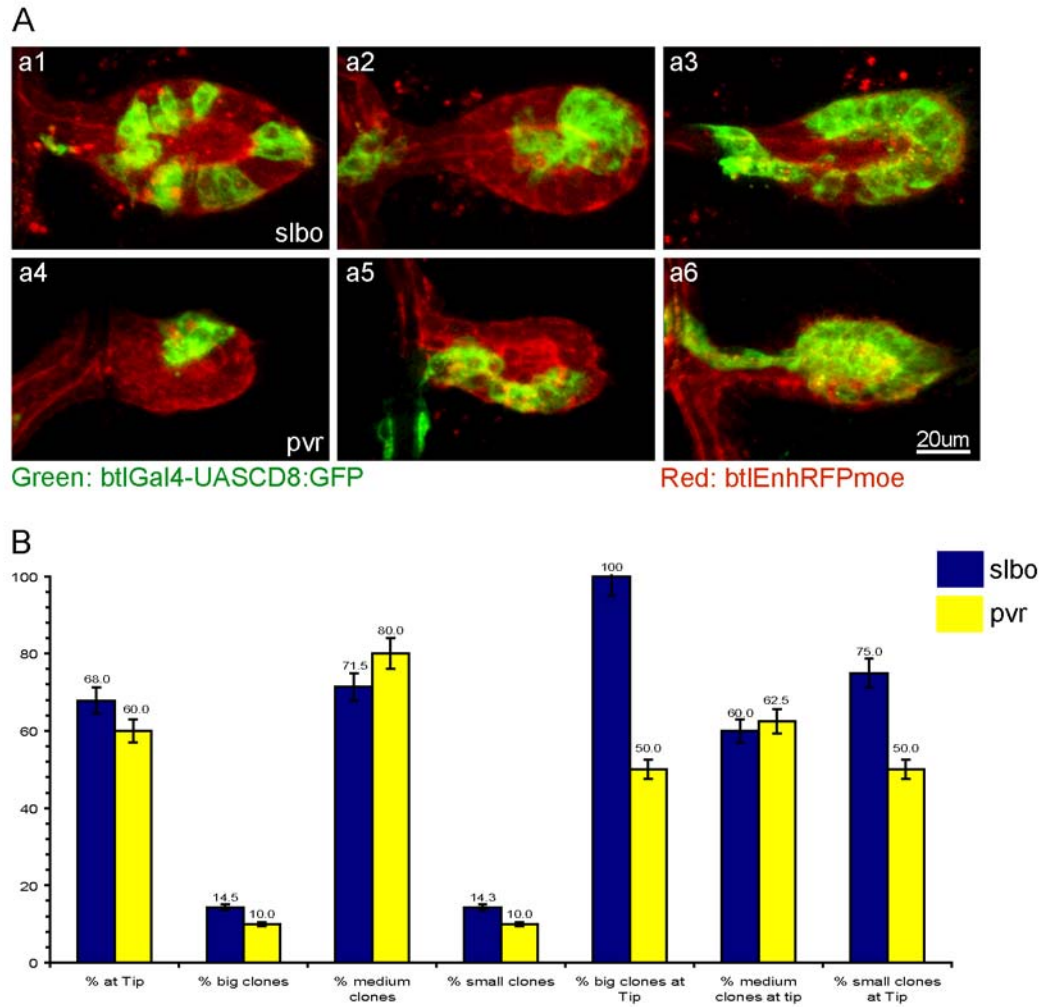


FIGURE R43

MARCM clones mutant for *slbo*^{E7B}, *pvr*⁵³⁶³.

A) a1-a3: representative clones lacking *slbo*. The majority of clones are found at the tip. **a4-a6:** clones lacking *pvr* are also predominantly found at the tip.

B.) Statistics for both alleles. A similar distribution with regard to clone size can be seen.

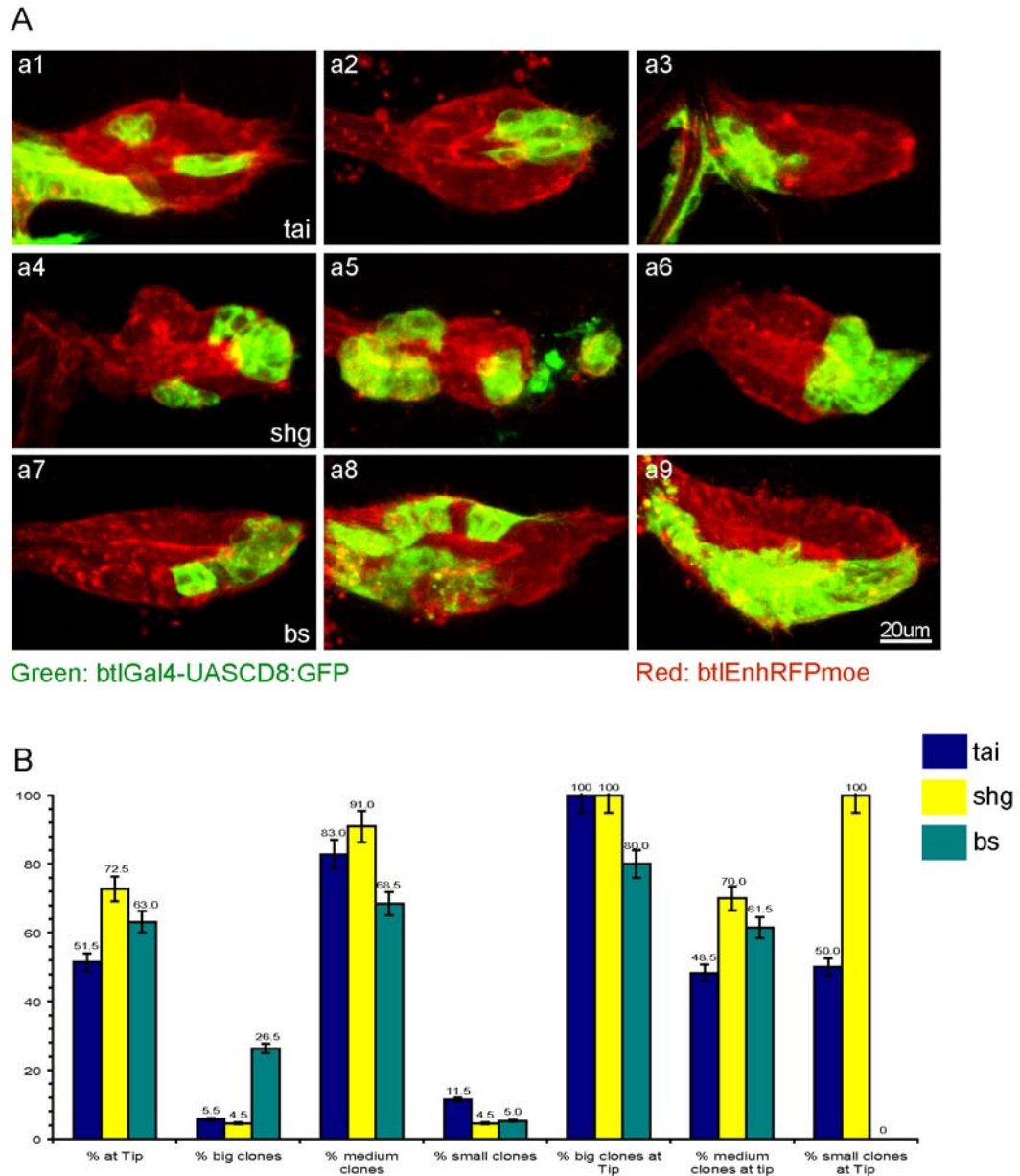


FIGURE R44

MARCM clones mutant for , *tai*^{61G1}, *shg*^H, *bs*¹⁴ .

A.) **a1-a3:** representative *tai* clones found at the tip or at the back. **a4-a6:** clones lacking DE-Cadherin have a similar tendency as *smo* clones to round up and minimize contact with the surrounding tissue although not to the same extent. Tip clones breaking off (a5) can be found sometimes. **a7-a9:** clones lacking SRF show no obvious phenotypes.

B.) Statistics as in previous figures. All clones show a similar distribution in terms of clone size.

7.14 Air sacs deficient for *bsk*, *dock* and *lgl*

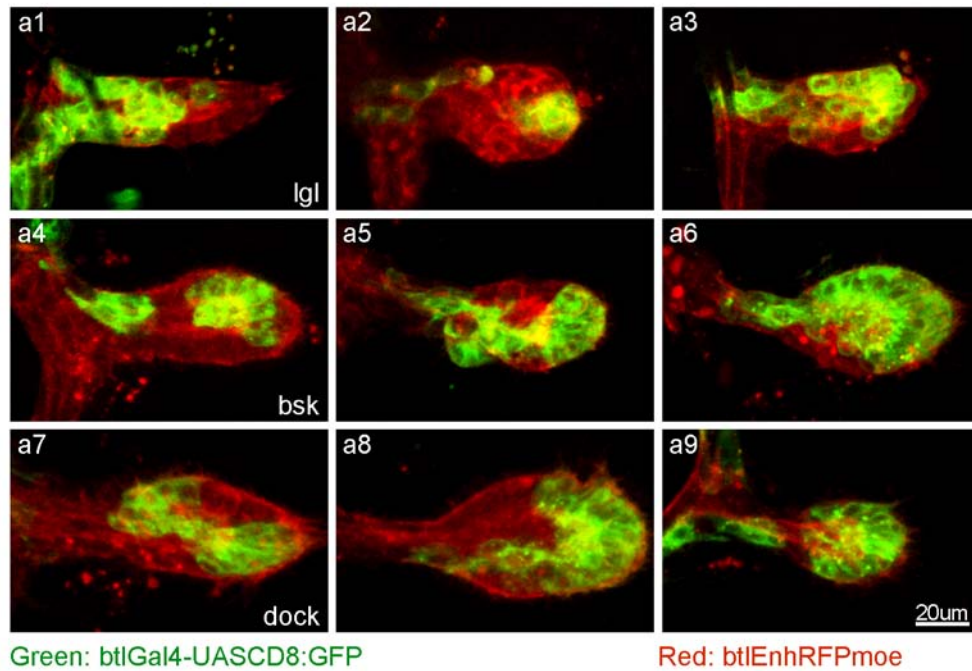
Apart from genes involved in border cell migration, components implicated in other biological processes might be instructive in terms of air sac tracheoblast migration. I tested three molecules, which were not associated with tracheal- or cell migration in general so far. These include *basket* (*bsk*), the *Drosophila* homologue of mammalian Jun-N-terminal kinases (DJNK) (Riesgo-Escovar et al., 1996), the SH2/SH3 containing adaptor protein Dreadlocks (Dock) (Garrity et al., 1996; Riesgo-Escovar et al., 1996), as well as the WD40 containing tumor suppressor protein Lethal giant larva (Lgl) (reviewed in Humbert et al., 2003).

These three components are involved in different biological processes; *bsk* is involved in dorsal closure (Riesgo-Escovar et al., 1996), *dock* has been reported to be important for axon pathfinding and guidance (Ang et al., 2003; Garrity et al., 1996) and *lgl* is required for establishing epithelial cell polarity (Bilder et al., 2000; Humbert et al., 2003; Hutterer et al., 2004). Therefore it was interesting to see whether any of these components display a distinct phenotype in air sac tracheoblasts. As seen from figure R45 a1-a9 as well as panel B, only *lgl* shows a reduction in distal clone positioning. Compared to wild-type clones, clones mutant for the amorphic allele *lgl^f*, show a 20% reduction in distal clone positioning (Fig. R45, a1-a3, B, Table R13). *bsk* as well as *dock* clones performed completely like-like (Fig. R45, a4-a9, B., table R13). In terms of clone size, all three genes are not required for proliferation, growth or survival, since the majority of the clones were medium- to big sized. Furthermore, in all three cases, terminal cells deficient for one of the genes under study, were recovered.

Table R13: Absolute numbers of *lgl^f*, *bsk* & *dock⁰⁴⁷³²* clones with respect to size and distribution

ALLELE	N	ABSOLUTE NUMBER OF CLONES AT TIP	LARGE OF CLONES	MEDIUM CLONES	SMALL CLONES	LARGE CLONES AT TIP	MEDIUM CLONES AT TIP	SMALL CLONES AT TIP
<i>lgl^f</i>	19	9	2	12	5	2	5	2
<i>bsk^f</i>	15	11	6	8	1	6	5	0
<i>dock⁰⁴⁷³²</i>	13	10	3	10	0	3	7	0

A



B

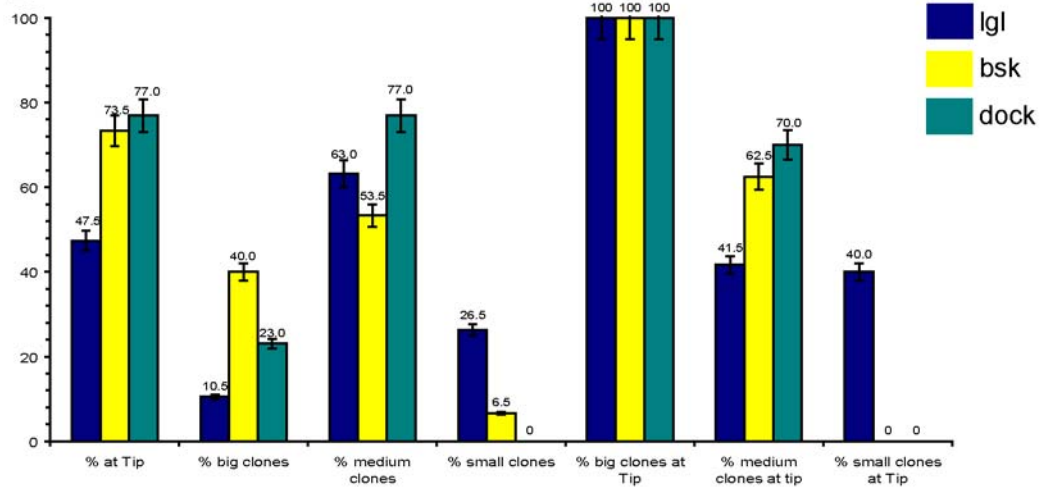


FIGURE R45

MARCM clones mutant for *lgl*^A, *bsk*¹ & *dock*⁰⁴⁷³².

A.) **a1-a3:** representative *lgl*^A clones. RFP fragments can sometimes be seen when a *lgl*^A mutant clone is at the tip (**a2**, **a3**). **a4-a6:** clones lacking *bsk* are normal in clone size and position. The same is true for air sac tracheoblasts deficient for *dock* **a7-a9**.

B.) Statistics as previously described. Note that *lgl*^A shows ~20% less tip cell clones compared to *bsk*, *dock*⁰⁴⁷³² or *wt*.

Nevertheless, since *lgl* is implicated in the establishment of epithelial cell polarity (Humbert et al., 2003), I was wondering whether air sac tracheoblast polarity is still properly maintained. As shown in preceding chapters, the polarity of air sac tracheoblasts is maintained from very early third instar stages on. Moreover, the epithelial character can be visualized with the α Catenin marker, which also localized subapically in tracheal cells (Jazwinska et al., 2003; Oda and Tsukita, 1999). Figure R46 A-C, shows again the localization of α CateninGFP in mid- to late stage third instar air sac tracheoblasts. Uniformly expressed α CateninGFP (Fig. R46. A) outlines the cellular junctions nicely. *lgl* mutant clones show a mislocalization of α CateninGFP especially in tip cell tracheoblasts (compare Fig. R46, A, B, C (wt) with D-I). In some tip cell clones, α CateninGFP becomes localized basally (white arrow in G&M), or can be seen in a spot like pattern (white arrow in H). Wild-type clones abutting the lumen display properly localized α CateninGFP as well as some unlocalized cytoplasmic α Catenin (C). As shown earlier, wt clones at the tip often only display cytoplasmic α CateninGFP. Therefore, the occurrence of basal localized GFP or the clustering of α Catenin in spots indicated that the polarity of these cells is disturbed. Furthermore, in some instances, cells at the very tip seemed to become excluded from the air sac, judged from the appearance of GFP/RFP positive fragments. Nevertheless, other cells displayed a more or less regular localization of α Catenin (D, N, M).

Taken together, mostly cells located at the tip of the air sac deficient for *lgl* displayed a mislocalization of the marker.

However, and somewhat surprisingly, the lack of correct epithelial polarity in these tip cells did not interfere with proper cell migration. It could also be that initially, *lgl* mutant tip cells were correctly polarized and only in later stages, due to increased physical stress, the lack of Lgl protein resulted in a mislocalization of α CateninGFP. Thus, it is possible, that in later stages, these tip cells are either displaced or taken over by wild-type cells. Evidence for this assumption is the occurrence of normally polarized air sac tracheoblast cells as well as the visible cell fragments.

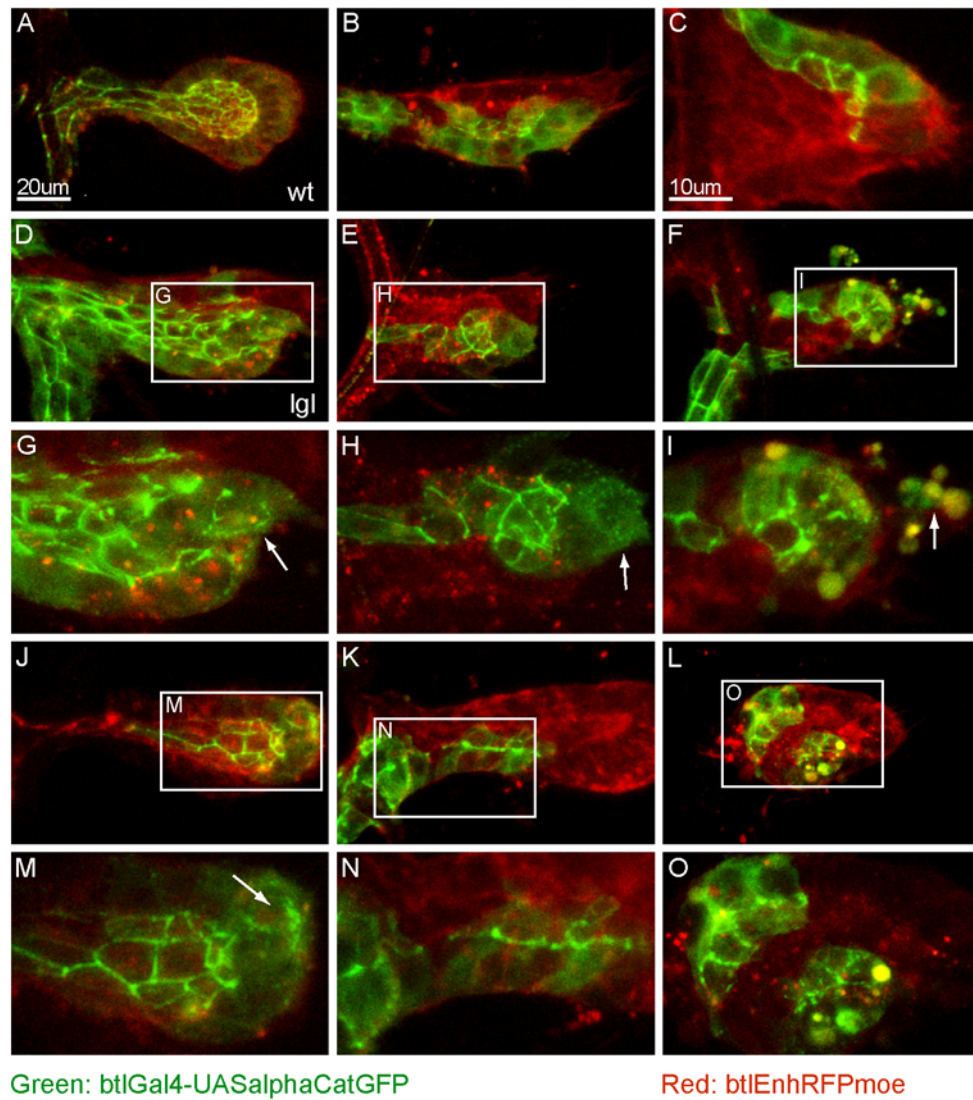


FIGURE R46

MARCM clones mutant for *Igf1* and labeled with α CateninGFP. All clones in panels A.-C., are wt, clones in panels D.-O. are mutant for the amorphic allele *Igf1*.

A.) α CateninGFP expressed in the entire air sac. **B.) & C.)** wild-type clones labeled with α CateninGFP. Note the regular subapical localization of α CateninGFP as well as weak unlocalized cytoplasmic GFP. **D.-F., J.-L.)** Overview pictures of clones mutant for *Igf1*. **G.)** α CateninGFP can be seen also on the basal side of air sac tracheoblasts in this *Igf1* tip cell clone (white arrow). **H.)** α CateninGFP appears in dots. **I.)** GFP/RFP containing fragments are excluded from tracheal cells (white arrow). **M.)** α CateninGFP extending to basal sides of the air sac. **N.)** A *Igf1* clone located not at the tip, similar to wt clones in terms of α CateninGFP localization. **O.)** A distally located *Igf1* clone.

8. Characterization of *receptor of activated protein kinase C (rack1)* during *Drosophila* development.

8.1 What the papers say

Receptor of activated protein kinase C (Rack1) has originally been identified as an anchoring protein for protein kinase C (Verheyen and Cooley, 1994). Rack1 is a 36-kDa protein containing seven internal Trp-Asp 40 (WD40) repeats. The best studied case of a WD40 protein is the β -subunit of G proteins, to which Rack1 shows 42% identity. The crystal structure of the β -subunit of G proteins has been solved (Garcia-Higuera et al., 1998). Inferring from the structure of this protein, the WD40 repeats of Rack1 can be predicted to form a seven-bladed propeller structure with each blade made up of β -sheets (Fig. R49, B., C.) (reviewed in McCahill et al., 2002). The family of WD-repeat proteins comprises many different proteins and they fulfill many different cellular functions, involved in processes such as signal transduction, transcription, pre-mRNA splicing, cytoskeletal organization and vesicular fusion (reviewed in Garcia-Higuera et al., 1996). Rack1 is also highly conserved among different species (Fig. R47) and is expressed ubiquitously in the tissues of higher mammals and humans, including brain, liver and spleen, suggesting that it has an important functional role in most if not all cells (reviewed in McCahill et al., 2002).

The propeller structure, likely common to most of the WD40 proteins (Garcia-Higuera et al., 1996), contains three potential interacting surfaces: the top, the bottom and the circumference (Smith et al., 1999). Therefore it is not surprising that a lot of proteins were found to interact with Rack1 (reviewed in McCahill et al., 2002; Schechtman and Mochly-Rosen, 2001).

Originally, it was found to interact with active conventional PKC isoforms, of which PKC β II seemed to be the preferred binding partner. Conventional PKCs are calcium- and diacylglycerol (DAG)-dependent protein kinases that are activated after the receptor-stimulated hydrolysis of plasma membrane phosphatidylinositol 4,5-bisphosphate, which yields both DAG and calcium elevation (Liu and Heckman, 1998). However, Rack1 is also able to interact with members of calcium-independent “novel” PKCs as well as the atypical PKCs, which are calcium- as well as DAG-independent (Liu and Heckman, 1998). The interaction of Rack1 with PKC is believed to be stimulus-dependent. Upon stimulation of the cell, Rack1 anchors PKC and shuttles it intracellularly to bring it into the vicinity of target proteins (Schechtman and Mochly-Rosen, 2001) such as myrostylated alanine-rich C kinase

substrate (MARCKS) protein, a direct target of PKC. MARCKS proteins bridge the plasma membrane and the actin cytoskeleton (reviewed in Keenan and Kelleher, 1998).

Furthermore, Rack1 has been found to interact with a number of other proteins, including Phospholipase C γ (PLC γ), rasGAP, Dynamin-1, Src, PTP μ , Integrins or Phosphodiesterase 4D5 (reviewed in McCahill et al., 2002; Schechtman and Mochly-Rosen, 2001).

The physiological role of Rack1 has been addressed in a number of different systems, mostly tissue-culture but also some genetically amenable organisms such as yeast. A fission yeast homologue of mammalian Rack1, cross-pathway control (Cpc)2, with 77% similarity to mammalian Rack1, has been isolated. Although mutant *S. pombe* lacking Cpc2 are viable, cell cycle abnormalities were found, such as mitotic delay, cell elongation as well as defects in conjugation and meiosis. Such defects could be rescued with the mammalian Rack1 (McLeod et al., 2000). It was also shown that Cpc2 interacts with Pck2, one of the known PKC homologs *in vivo* and *in vitro*. Single mutants in both genes show abnormal morphology, whereas the double mutant, although viable, has an even more aberrant cell morphology. It was further proposed that Cpc2 acts as a receptor of Pck2 in the regulation of the actin cytoskeleton (Won et al., 2001). Similar findings, which also provide a link of Rack1 and cell migration were found in tissue-culture experiments. Overexpression of Rack1 resulted in an increase in actin stress fibers and focal contacts, leading to a decrease in cell migration (Buensuceso et al., 2001). The organization of focal adhesions through Rack1 are established through an interaction with the non-receptor kinase Src. Furthermore, via its Src binding site, Rack1 was also found to regulate cell protrusions and chemotactic migration (Cox et al., 2003). Experiments using antisense oligonucleotides against *rack1* in NIH 3T3 cells, resulted in a more contracted and less spread cell morphology. Fewer stress fibers and focal adhesions were also found in cells treated in this manner. Moreover, proliferation of antisense RNA-expressing cells was reduced (Hermanto et al., 2002).

Interestingly, Rack1 has been found to be present on ribosomes and to interact with eIF6, a protein which is bound to free 60S ribosomal subunits. Upon release of 60S by eIF6, the 40S and 60S subunits join to form the 80S ribosome, an event that is rate-limiting for translation. This release, and thus the establishment of the 80S ribosome could be achieved through a Rack1-PKC β II pathway (Ceci et al., 2003; Sengupta et al., 2004).

Although the literature about Rack1 is vast, little *in vivo* data from higher model organisms are available. Hardly nothing is known about the role of Rack1 during development. In one study, Rack1 has been found to be locally induced by FGF in the interlimb lateral plate. Furthermore PKC activity was increased and blocking of PKC with inhibitors resulted in the

prevention of Shh expression and thus the formation of truncated wings. Therefore it was therefore concluded that in the limb bud, PKC, through FGF induced *rack1*, plays a role in *shh* expression (Lu et al., 2001).

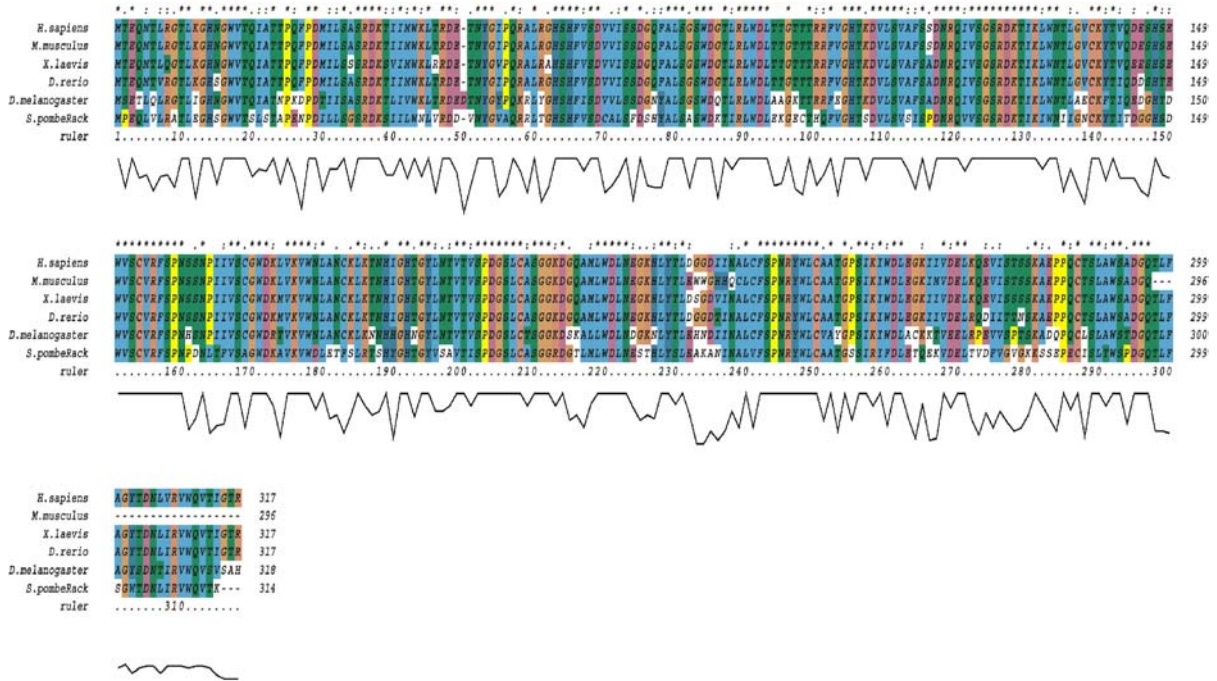


FIGURE R47

Rack1 full length protein alignment. Note the very high conservation between Rack1 from human, mouse, frog, fish, fly and yeast. Asterisks indicate region of perfect match.

8.2 Isolation and characterization of *Drosophila rack1* mutants

We and others independently found Rack1 in a yeast two-hybrid screen using Dof as a bait (Battersby et al., 2003; Cabernard, 2000). *Drosophila rack1* has previously been cloned (Vani et al., 1997) and shows 76% identity to rat Rack1 as well as high homology to Rack1 from other vertebrates. Rack1 from human, zebrafish as well as mouse are almost identical (Fig. R47). Furthermore, the fact that *rack1* was reported to be expressed in the *Drosophila* tracheal system (Vani et al., 1997) (Fig. R48) further enhanced our interest in this gene.

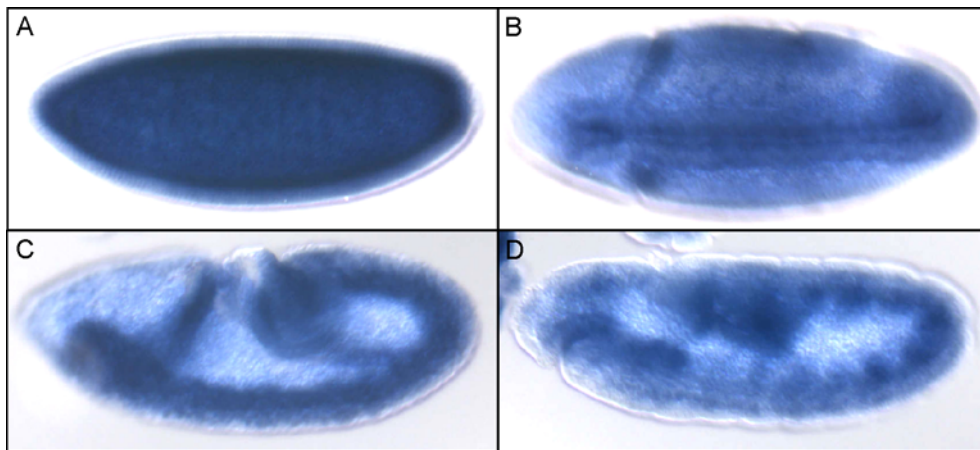


FIGURE R48

Embryonic *rack1* expression pattern.

A.) *Rack1* RNA is highly maternally provided. **B.)** Transcription occurs in the mesoderm and cephalic furrow just prior to gastrulation. **C.)** Cephalic furrow and mesoderm expression.

D.) Upregulation of *rack1* mRNA is seen in the anterior and posterior midgut as well as in the tracheal pits.

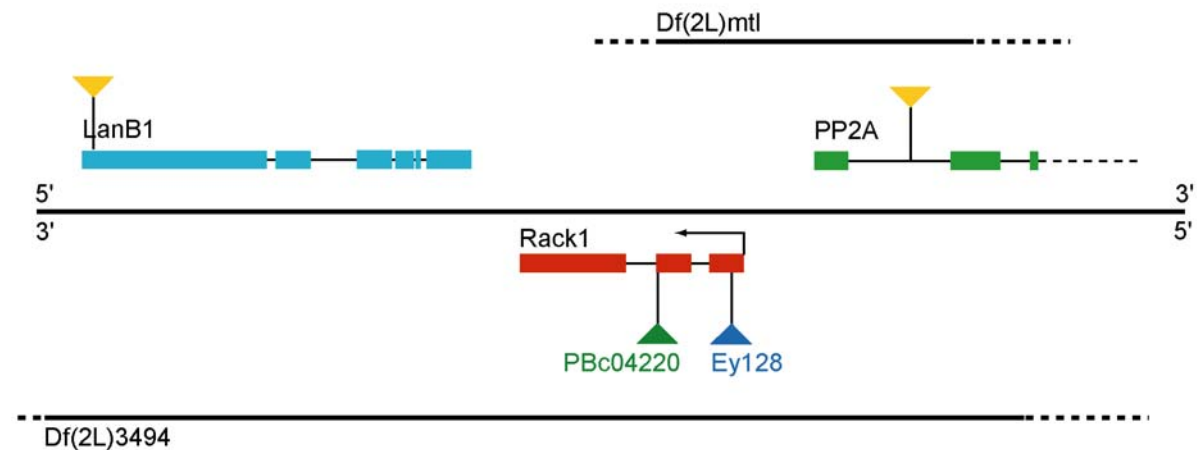
As a first step to genetically characterize the *in vivo* role of *rack1*, we aimed at isolating mutants. *rack1* is located on the left arm of the second chromosome on cytological position 28D1-3. Initially, we unsuccessfully screened this locus for P-element insertion lines. However, with the ongoing gene disruption project from the Berkeley *Drosophila* Genome Project (BDGP) (Bellen et al., 2004) we could finally retrieve a novel P-element (*Ey128*, henceforth *rack1^{Ey128}*) inserted into the transcribed region of *rack1*. Independently of this line, we obtained a second piggybac insertion line from Exelixis (thanks to Walther Gehring) (PB_c04220, henceforth *rack1^{PB_c04220}*), as well as an EMS induced *rack1* mutant from Jennifer Chapin (*rack1^{EMS1-8}*). Furthermore, a large deficiency, Df(2L)3494, putatively removing *rack1* as well as other loci in the indicated region was obtained (Fig. R49A). In order to test whether this deficiency removes the *rack1* locus, complementation tests were performed using lethal P-element insertions in genes neighboring *rack1*. *rack1* is immediately flanked by the two genes *PP2A* as well as *LanB1*. In both genes, lethal P-element insertion lines were reported. Crossed over the deficiency Df(2L)3494, complementation was neither achieved with *LanB1* nor *PP2A*, indicating that these two genes are uncovered by the deficiency and therefore most likely also the *rack1* locus, which lies between *LanB1* and *PP2A* (Fig. R49).

In order to test whether mutants in *rack1* were lethal, the corresponding alleles were crossed over Df(2L)3494 and tested again for complementation. All three alleles were found to be lethal over the deficiency as well as lethal inter se. Furthermore, the transallelic combinations were found to be lethal too (Table R14). Since all three alleles originate from independent sources, lethality associated with second site mutations can be ruled out. However, in order to proof that lethality is due to a disruption of the *rack1* locus, a rescue construct was made. Full length Rack1 cDNA was cloned into a transposition vector containing a heat-shock inducible promoter (hsRack1) and recombined onto the P-element insertion line *rack1^{Ey128}*. The recombinant *rack1^{Ey128}*-hsRack1 was then crossed again over the alleles *rack1^{PB_c04220}* and *rack1^{EMS1-8}*. Moderate heat-shocks applied several times during development resulted in a rescue frequency of 15% when crossed to *rack1^{Ey128}* (the others were not counted), whereas without heat-shock, no viable transallelic offspring was found (Table R14). Thus, the lethality of the alleles *rack1^{Ey128}*, *rack1^{EMS1-8}* as well as *rack1^{PB_c04220}* is due to disruption of the *rack1*. Furthermore, *rack1* is an essential gene.

Table R14: Summary of complementation tests

Allele	<i>Df(2L)3494</i>	<i>rack1^{Ey128}</i>	<i>rack1^{EMS1-8}</i>	<i>rack1^{PB_c04220}</i>	<i>rack1^{Ey128}</i> -hsRack1 with HS	<i>rack1^{Ey128}</i> -hsRack1 without HS
<i>rack1^{Ey128}</i>	lethal	lethal	lethal	lethal	15% viable	0%
<i>rack1^{EMS1-8}</i>	lethal	lethal	lethal	lethal	Not counted	0%
<i>rack1^{PB_c04220}</i>	lethal	lethal	lethal	lethal	Not counted	0%
<i>Df(2L)3494</i>	lethal	lethal	lethal	lethal	Not done	Not done

A



B



C



FIGURE R49

Genomic organization of *rack1*, protein cartoon and inferred structure.

A.) *rack1* is located on 2L at 28D1-3 and is flanked by the two genes *PP2A* and *lanB1*. Lethal insertions in the genes *PP2A* and *lanB1* as well as the deficiency *Df(2L)3494* were used for complementation tests. A smaller deficiency, *Df(2L)mts* (provided by J. Chapin) confirmed the complementation results (not shown). Colored triangles indicate transposons insertions.

B.) Rack1 consists of 7 WD40 repeats which are thought to fold into a propeller fold, containing 7 β sheets which serve as protein-protein interaction interfaces.

C.) Inferred structure of Rack1.

8.3 Molecular characterization of the *rack1* alleles

The insertion site of the two P-elements was mapped by inverse PCR. The BDGP provided flanking sequence of the insertion site of the Ey128 P-element and the integration site was confirmed by our own experiments. Ey128 integrated in the transcribed region about 50 nucleotides upstream of the initiation start methionine (Fig. R50). Characteristic for P-element insertions, an 8bp duplication occurred at the site of integration. Inferred from several

cDNAs, the transcription start site lies about 8 nucleotides upstream of the Ey128 integration site (Fig. R50). The *rack1*^{EMS1-8} allele contains a stop codon in the 6th amino acid after the start methionine (J. Chapin, personal communication). The piggybac insertion line *rack1*^{PB_c04220} contains a lesion associated with the second exon. This transposon is, according to the information of Exelixis, inserted at the end of the second exon. Since all alleles do not complement each other and the fact that the lethality is in all cases associated with the disruption of *rack1*, this information has not been verified.

Based on the molecular nature of these alleles, it is assumed that all three mutants are strong loss-of-function alleles. However, since our attempts to generate an antibody failed, probably due to the very high conservation of Rack1, we are not able to confirm this by directly checking the protein levels.

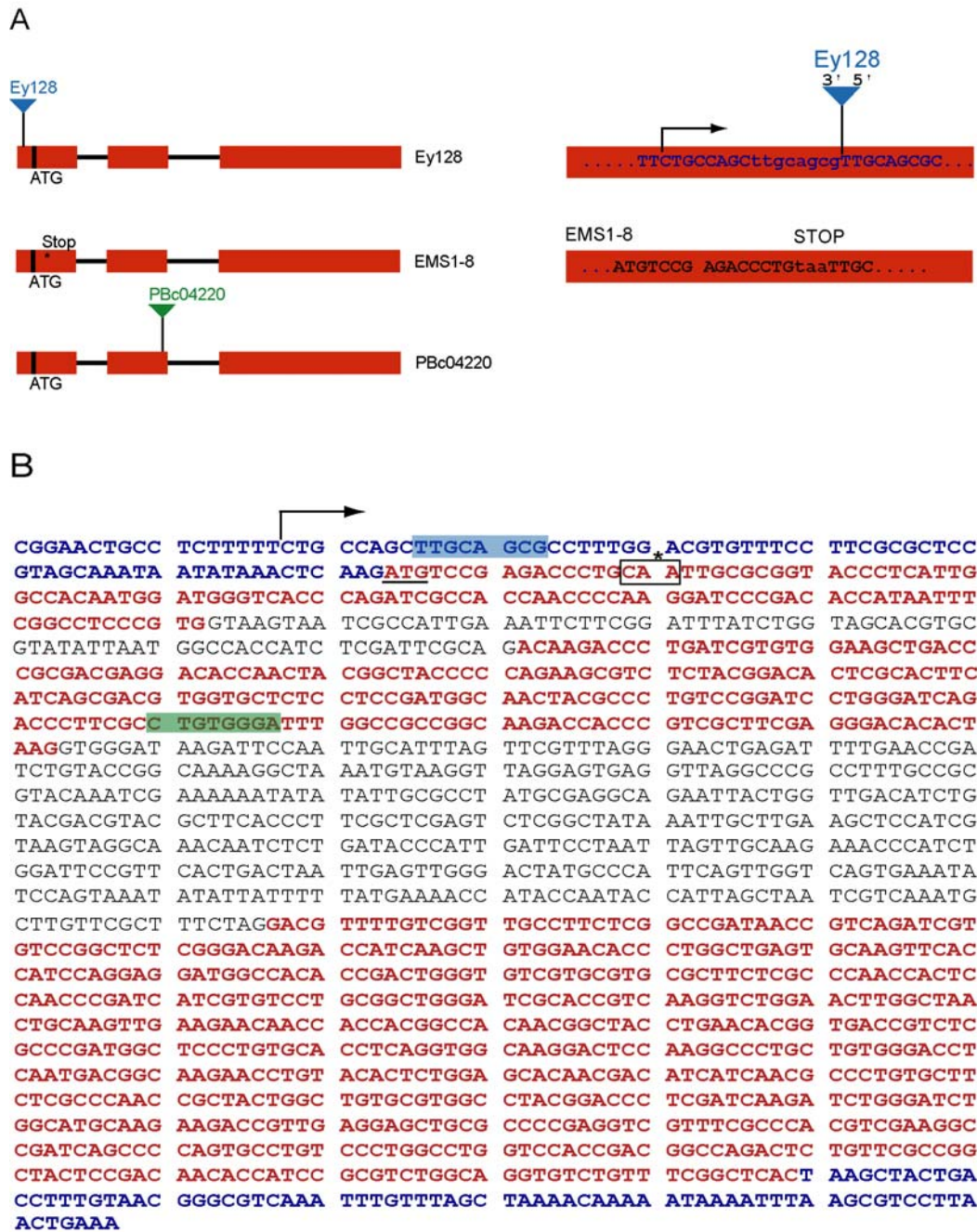


FIGURE R50

rack1 alleles and molecular lesions

A.) Schematic overview of insertion sites. Colored triangles indicate transposon insertions (P-element/Ey128, piggybac/PB_c04220). Asterisk refers to the EMS induced stop codon. The altered sequence is shown for the Ey128 insertion and the EMS allele.

B.) *rack1* transcription unit. Blue sequence indicates 5'/3'UTR region. Black arrow indicates transcription start site. Red sequence represents protein coding sequence, start codon is underlined. The blue and green underline sequence refers to the insertion of the transposons. The black box highlights the EMS affected codon (wt sequence shown here).

8.4 Phenotypic analysis of *rack1* mutants

8.4.1 Embryonic phenotypes and lethal phase

Since *rack1* mutants are lethal, we wanted to see whether there are any embryonic phenotypes detectable. Transallelic embryos were collected and stained with 2A12, an antibody which highlights the lumen of the tracheal system, α FasIinIII, which marks the visceral mesoderm as well as the epidermis, as well as α HRP recognizing an antigen in the central nervous system of *Drosophila*. With none of these markers, any embryonic phenotypes were detected (Fig. R51). Also other markers highlighting the PNS (22C10) or the migrating primordial germ cells failed to detect any phenotypes.

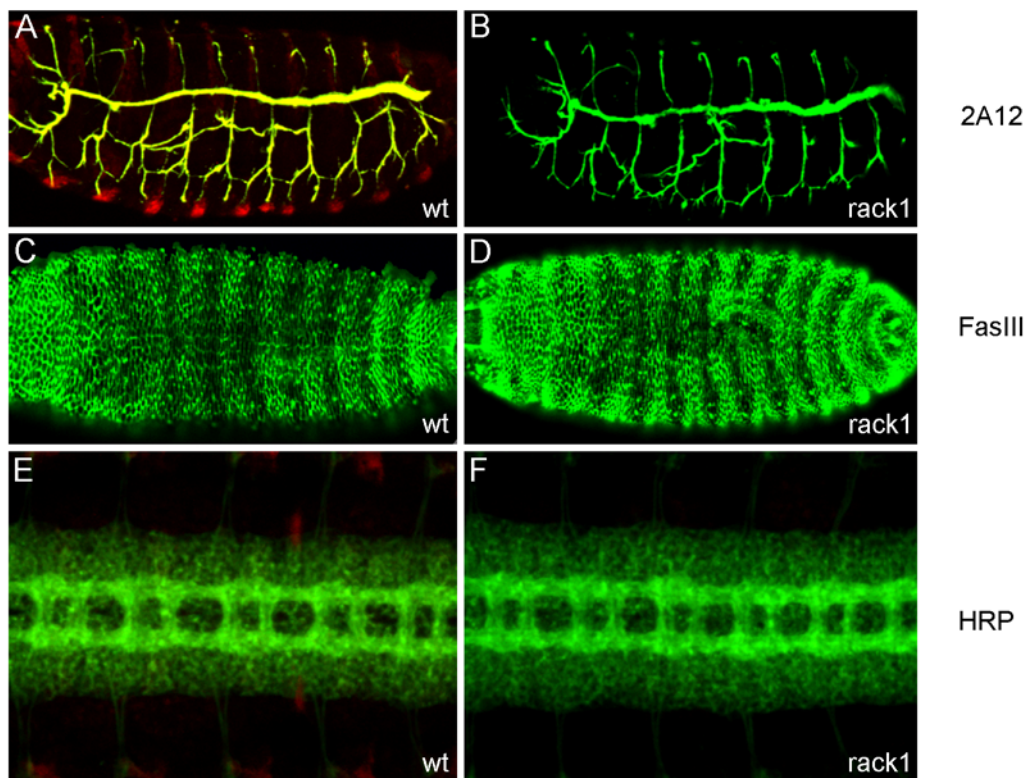


FIGURE R51

Embryonic phenotypes of *rack1*^{Ey128}/*Df(2L)3494*.

Embryos A., C., E., are wild-type, B., D., F., mutant for *rack1*.

A.) No difference between *wt* and mutant embryos can be detected using α 2A12, a late tracheal marker.

B.) Neither aberrant dorsal closure or epidermis can be detected with α FasIII **C.)** nor any visible phenotype with α HRP, a marker for the CNS.

It was further found that all three alleles are late pupal lethal but failed to hatch. Therefore, the lack of embryonic phenotypes was not very surprising. However, *rack1* mRNA is contributed maternally in very big quantities (Fig. R48, and C. Ribeiro, unpublished chip data). Thus, germline clones were generated using the FLP/DFS technique (Chou and Perrimon, 1996). Only embryos which underwent recombination in the female germ-line lack the dominant female-sterile mutation *ovoD* and eventually develop into an oocyte which upon fertilization can give rise to an embryo (Fig. R52 A).

Embryos devoid of maternal product generated with the allele *rack1*^{*Ey128*} and fertilized with either a wild-type- or *rack1* deficient sperm (see Materials and Methods for cross) failed to develop. Even very early markers such as α Evenskipped did not show a visible expression pattern (not shown). Control crosses generating germ-line clones with an unmutagenized FRT chromosome resulted in viable offspring. By examining the embryos we could detect two prominent phenotypes. A big fraction of embryos had fused dorsal appendages, indicating a failure in dorsal-ventral specification during oogenesis. Furthermore, these embryos displayed a reduction in size compared to wild-type embryos (Fig. R52, B., C.).

As mentioned already, all allelic combinations could be rescued with the *hsRack1-rack1*^{*Ey128*} flies, by applying heat-shock. It was further found that by backcrossing rescued females, to *rack1*^{*Ey128*} flies, embryos were laid but did not develop, hence resulting in a classical female-sterile phenotype. Thus we demonstrate that oogenesis is affected in *rack1* mutant flies. However, additionally, due to lethality of *rack1* mutant flies, this gene must also play a role in other processes during *Drosophila* development.

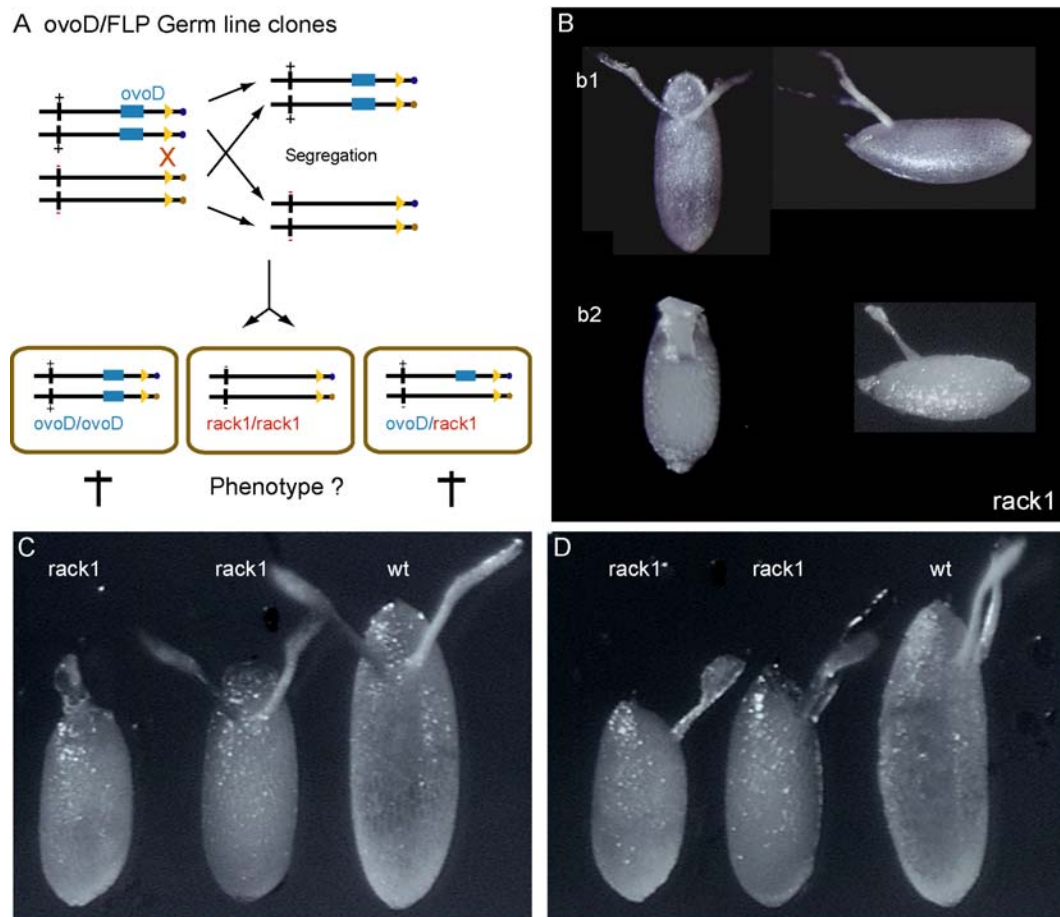


FIGURE R52

rack1 germline clones (GLC)

A:) Principle of FLP/DFS method. Only eggs survive, which do not contain a copy of the dominant female-sterile mutation *ovoD*.

B.) only *rack1* GLC are shown; top and side view. Some variation in size and fused dorsal appendage phenotype can be seen between different *rack1* GLC.

C.& D.) Size comparison of *rack1* GLC and *wt* embryo; **C.)** top views. **D.)** side views.

8.4.2 Mosaic analysis of *rack1* in the *Drosophila* female germline

Since *rack1* alleles are lethal we generated mosaic clones in the *Drosophila* female germline in order to study the cell autonomous effect of *rack1* mutant loss-of-function clones. *rack1*^{*Ey128*} was recombined onto FRT40A and crossed into a background consisting of the head-shock inducible Flipase enzyme (hsFLP) as well as FRT chromosome containing a GFP reporter under the tubulin promoter. Clones generated in this manner are negatively labeled since the *rack1*^{*Ey128*} mutant cells recombined away from the GFP reporter.

Clones generated in such a manner can be found in the *Drosophila* ovary in basically all stages of egg chamber development, indicating that the *rack1*^{Ey128} mutant clones survive over several days (Fig. R53, A.). Thus *rack1* does not seem to be required for cell viability in the *Drosophila* female germ-line. The egg chamber is also surrounded by an epithelial monolayer, the follicular epithelium (reviewed in Montell, 2003). Follicle clones mutant for *rack1* can be found at high frequencies. Since these clones are large, an involvement of *rack1* in cell proliferation or growth in the *Drosophila* ovary seems unlikely. Phalloidin and α -Spectrin stainings furthermore did not indicate any cell shape or actin cytoskeleton abnormalities (Fig. R53, B-D.). Since *rack1* has been associated with cell migration, we also looked at border cell clones deficient for *rack1*^{Ey128}. Egg chambers were found in which border cells as well as nurse cells were wt, nurse cells were wild-type but border cells mutant or basically all cells were mutant for *rack1*^{Ey128}. In all cases, at least anterior migration took place, judged from the position of the border cells in later egg chambers (Fig. R53, E-G). We did not further investigate dorsal border cell migration nor did we determined whether migration was normal in terms of timing or in terms of frequency. However since late egg chambers consisted of a micropyle, a structure established through border cells, we infer that border cell migration is normal.

The only phenotypes detected in egg chambers containing clones lacking *rack1* were seen in late stages. At the end of oogenesis, egg chambers undergo a process called nurse cell dumping. During these last stages of egg chamber development, the polyploid nurse cells start to rapidly transfer proteins and RNAs into the oocyte. This rapid transport phase is initiated by a cue to enter a modified apoptotic program (reviewed in Hudson and Cooley, 2002b). The apoptotic cue leads to the formation of a network of actin bundles in the nurse cells followed by the disassembly of the nuclear envelopes of the nurse cells, which allows the nurse cell nuclear contents to mix with the cytoplasm. Finally the nurse cells actively contract, expelling their remaining cytoplasmic contents into the oocyte. The cytoplasmic actin bundles are required to restrain the nurse cell nuclei during rapid transport, as mutations that compromise bundle formation still contract but fail to transfer cytoplasm, due to the movement of the large polyploid nuclei into the ring canals, blocking further transport. Ring canals are cytoplasmic bridges resulting from 4 asymmetric, incomplete and synchronous cell divisions. The contractile force appears to be generated by cytoplasmic myosinII (reviewed in Hudson and Cooley, 2002b).

Late egg chambers containing *rack1* mutant nurse cells display a typical nurse cell dumping phenotypes (Fig. R53, H.& I). Nurse cells fail to undergo apoptosis and are still connected at

the anterior pole with the oocyte. Dorsal appendages as well as the micropyle can often be seen in these eggs. Furthermore, the oocyte is smaller in size compared to egg chambers consisting of wild-type nurse cells.

This nurse cell dumping phenotype is also seen in mutations affecting the actin cytoskeleton or related processes. Mutations in Profilin (*chic*) (Cooley et al., 1992; Verheyen and Cooley, 1994), the arp2/3 complex (Hudson and Cooley, 2002a), or myosinII (*sqh*) (Wheatley et al., 1995) also display such a dumping phenotype.

Thus the reduction in size of the unlaidd- as well as the laid eggs (seen with FLP-FDS germline clones) can be explained with incomplete nurse cell dumping. In the following we tried to elucidate the reason for this phenotype associated with *rack1*.

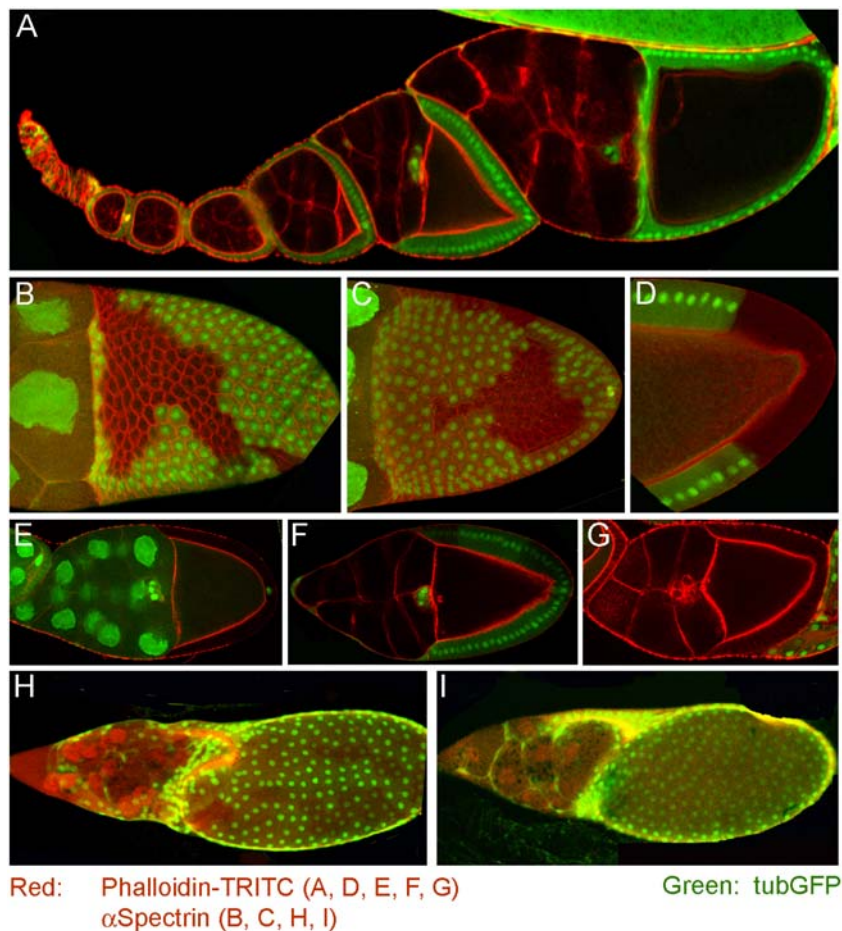


FIGURE R53

rack1 clones in the germline and the soma. Mutant tissue is marked by absence of GFP.

A.) *rack1* clones can be recovered in the germline. Mutant clones are able to proliferate and to survive. **B-D.)** *rack1* follicle cell clones are able to proliferate and show no detectable phenotype. **E.)** *wt* germ- border- and polar cells; mutant follicle cell clone covering the oocyte. Border cells migrate normally and overall egg chamber morphology appears normal. **F.)** Germline clone. Border cell migration is not affected. **G.)** Complete follicle and germ cell clone. Border cells did migrate. **H&I.)** Nurse cell dumping defects are observed in mutant germ cell clones. Note the appearance of dorsal appendages as a sign for completed oogenesis. The nurse cells however did not undergo apoptosis and are still attached to the oocyte. **Analyzing the *rack1* dumpless phenotype**

In order to rule out that the observed dumpless phenotype is due to a second site mutation on the *rack1*^{*Ey128*}-FRT40 chromosome, ovaries were analyzed from transallelic combinations. We took advantage of the fact that the lethality can be rescued by crossing in the hsRack1-*rack1*^{*Ey128*} transgene to *rack1*^{*PB_c04220*} as well as *rack1*^{*EMSI-8*}. Ovaries of such rescued females were dissected and analyzed with regard to the dumpless phenotype. Indeed, in all transallelic combinations, the dumpless phenotype was observed (Fig. R54). In addition, these females were also female sterile since the eggs they laid did not develop. Furthermore, eggs obtained in this experiment displayed the same phenotype as eggs derived from germ-line clones. They also appeared to be smaller than wild-type eggs (Fig. R54, F.). Thus, the dumpless- and

associated female-sterile phenotype are due to the characterized disruptions of the *rack1* locus.

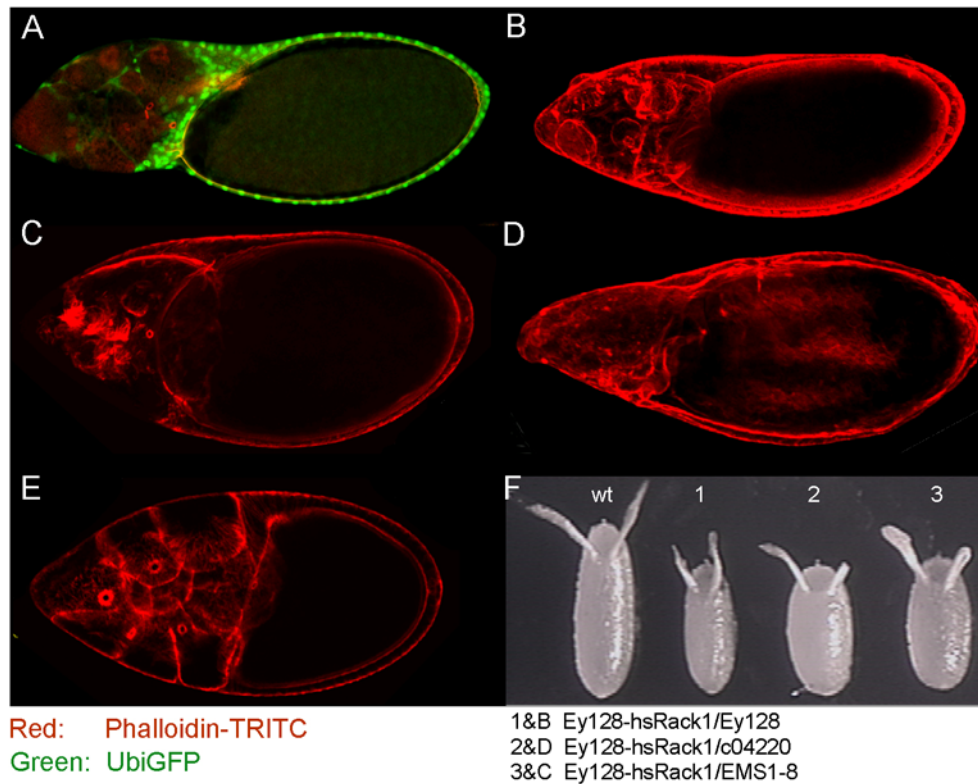


FIGURE R54

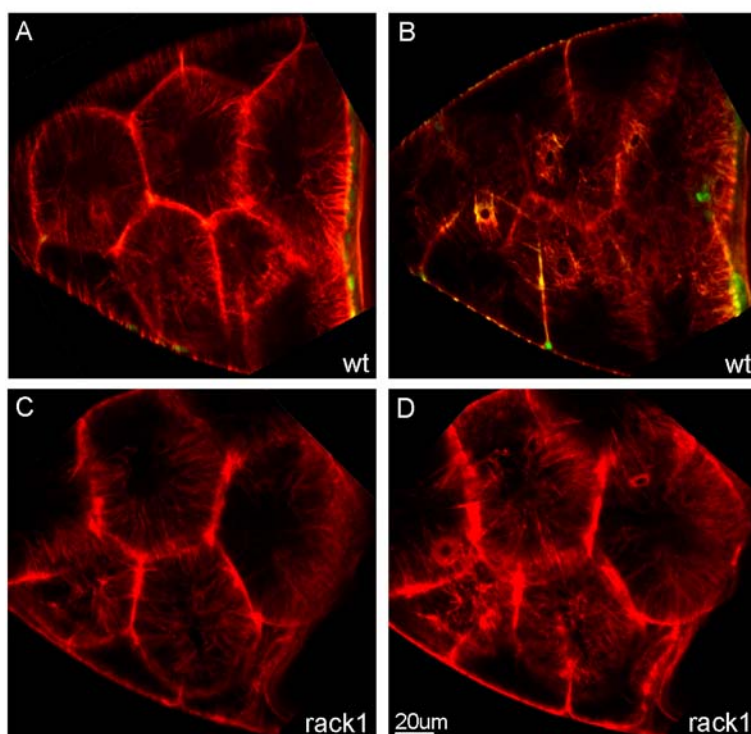
rack1 transallelic combinations.

A.) *rack1* germ cell clones **B., C., D.)** Dissected follicles of *hsRack1* rescued females with the indicated transallelic combinations. See legend for genotype. The phenotypes are identical to the germline clones seen in A.) and Fig. R53.

E.) Stage 9/10 egg chamber, displaying an intact actin cytoskeleton. **F.)** Embryos laid by *hsRack1* rescued females of the indicated genotypes. Apart from the fused dorsal appendage phenotype, the size differences can be seen again. Compare to Fig. 52

Next we wanted to investigate the cause for the dumpless phenotype. As mentioned previously, dumpless mutants are often associated with defects in the actin cytoskeleton. Rapid dumping involves the contraction of nurse cells, which requires the formation of bundled actin filaments, which cage the nurse cell nucleus and prevents the physical blocking of the ring canals. Such cables consisting of bundled actin filaments appear in the cytoplasm prior to dumping and extend inward from the plasma membrane (Guild et al., 1997). Mutants displaying defects in the formation of the ring canals, also an actin rich structure (Robinson et al., 1994; Warn et al., 1985), often show reduced fertility due to incomplete nurse cell dumping (Dodson et al., 1998).

Thus, we looked at the occurrence of bundled actin filaments as well as at ring canals. In both wild-type as well as in ovaries from rescued transallelic females, the appearance of actin bundles, extending inwards from the plasma membrane towards the nucleus, can be seen in stage 10 egg chambers (Fig. R55). In terms of numbers and length of the actin cables, the two egg chambers look indistinguishable. Additionally, in wt as well as in mutant egg chambers, ring canals can be seen with phalloidin-TRITC staining. Ring canals from mutant egg chambers are similar in size and number compared to ring canals from wild-type egg chambers. Taken together, we could not detect any obvious morphological alterations which could explain the dumpless phenotype.



Red: Phalloidin-TRITC

FIGURE R55

Close ups of dissected stage 10 egg chambers. Phalloidin-TRITC staining labels actin filaments and ring canals.

A.&B.) Two sections from *wt* egg chambers. Note the bundled actin and ring canals.

C.&D.) Two sections of egg chambers obtained from transallelic, rescued females.

Actin bundles and ring canals are indistinguishable from *wt*.

8.4.4 Analysis of clone size, cell size and shape of *rack1* mutant tissue in the imaginal disc epithelium

Since *rack1* might be associated with the regulation of the actin cytoskeleton but is also implicated in growth and proliferation, we sought to look at this aspect in a genetically tractable system. *rack1* is widely expressed and also detectable at the RNA level in imaginal tissues (Lydia Michaut, personal communication). Thus, we generated *rack1* loss-of-function mitotic clones in wing and eye imaginal discs and performed a twin-spot analysis. Clones generated with the conventional site-specific mitotic recombination method (FLP/FRT) are negatively labeled, whereas the twin-spot inherits both copies of GFP (Fig. R56. A). Cells which did not undergo mitotic recombination have just one copy of GFP. Thus, all three progenitor cells can be distinguished based on the amount of GFP. Furthermore, the twin-spot clone is an internal control. Since in wing imaginal discs hardly any cell migration has been observed, the cells which undergo site-specific mitotic recombination stay in close proximity and thus the clones abut each other in most cases (Resino et al., 2002). Therefore, we assumed that if *rack1* mutant clones were to display a growth disadvantage, the twin-spot clone should be bigger compared to the mutant clone.

First of all, large *rack1* mutant clones with the alleles *rack1*^{*Ey128*} or *rack1*^{*EMSI-8*} can be generated without discernible morphological anomalies associated with the clonal tissue (Fig. R56, B.). Furthermore, *rack1* mutant clones are comparable in size to the twin-spot clone (Fig. R56, C.) and mutant cells lacking *rack1* show the same morphology than wild-type cells (Fig. R56, D.& E.). Also with respect to cell size, no difference can be seen between the two populations (Fig. R56, D.& E.). The same also applies to the eye imaginal disc (Fig. R56, F-H). Furthermore, clones analyzed in adult eyes suggested that the mutant tissue does not undergo apoptosis (not shown).

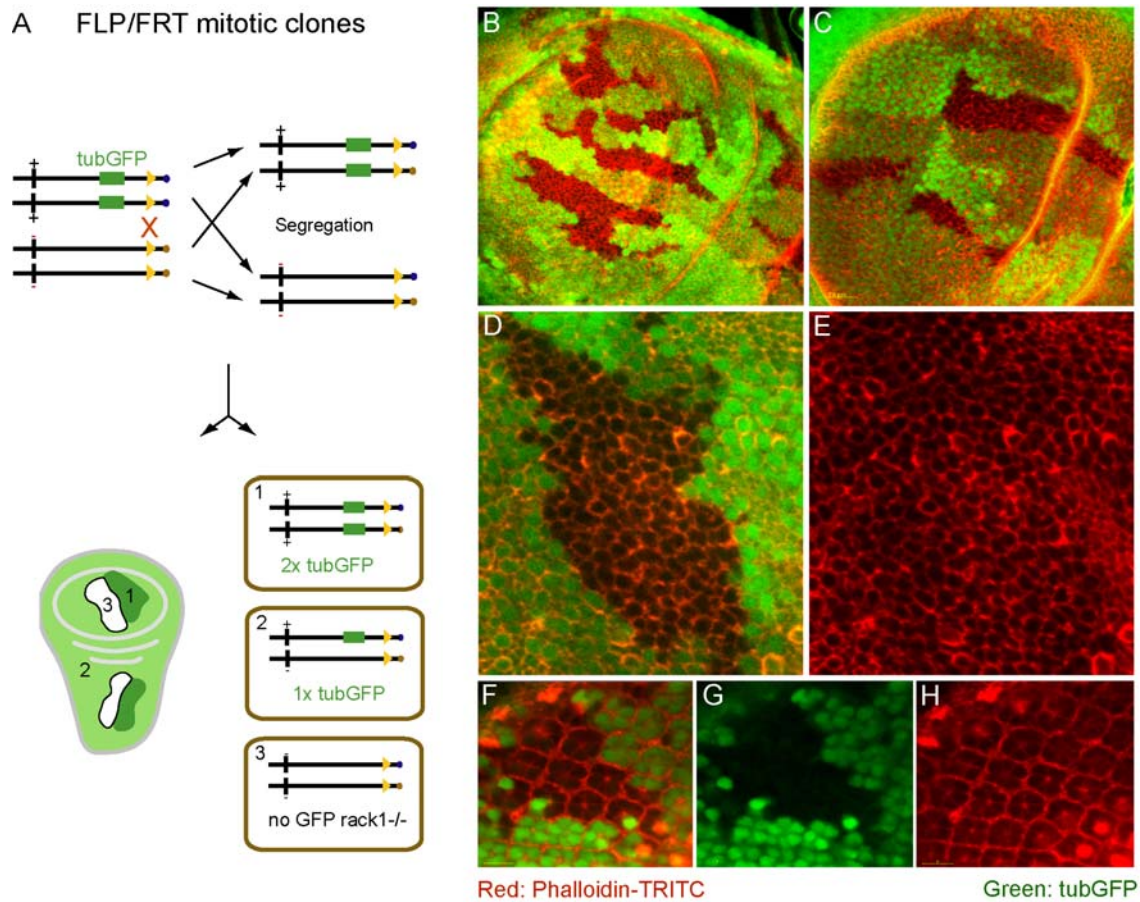


FIGURE R56

Mitotic clones in imaginal tissues

A.) Schematic overview of FLP/FRT site specific mitotic recombination. Note, in contrast to MARCM, the mutant cells do not express GFP and are thus negatively labeled.

B.&C.) Two wing imaginal discs displaying large *rack1* clones. The twin-spot is comparable in size to the *rack1* mutant clone.

D.&E.) Close up of a *rack1* mutant clone. No difference in size or morphology is seen in *rack1* mutant tissue. **F.-H.)** This also applies to the eye imaginal disc.

8.4.5 Analysis of *rack1* mutant clones in the third instar air sac

Since Rack1 has been found to interact with Dof (Battersby et al., 2003; Cabernard, 2000) in yeast two-hybrid screens, we wanted to find out whether *rack1* is required for tracheal cell migration. Due to the high maternal contribution, embryonic phenotypes are not detected and by removing maternal components, only eggs are recovered which do not develop as a consequence of oogenesis defects. Therefore, the embryonic requirements of *rack1* cannot be studied with classical loss-of-function mutants. Thus we used the third instar air sacs as a system to study the function of *rack1* in tracheal cell migration. Although *rack1* mutant third instar larva can be retrieved, we wanted to assay the behavior of *rack1* mutant cells directly in comparison to wild-type cells.

The experiment was performed with the three alleles *rack1*^{*Ey128*}, *rack1*^{*EMSI-8*} and *rack1*^{*PBc04220*}. As described in previous chapters, *rack1* clones were induced early during embryogenesis in order to maximally dilute maternally contributed protein and RNA. Clones were recovered in third instar larva at frequencies comparable to wild-type clones. Terminal cells lacking *rack1* were also found. Moreover, clones in the third instar air sac were predominantly located at the tip. Like in wt, around 70% of the clones populated the leading edge. Only *rack1*^{*Ey128*} clones were found to be 10% less frequent at the leading edge compared to wt. However, since the other alleles are regarded equal in strength, this minor reduction is very likely insignificant (Fig. R57 a4-a12, B., table R15). In terms of clone size, the majority of *rack1* clones falls into the class of medium- to large clones. Thus, also in the third instar air sac, Rack1 is neither required for migration nor for proliferation, growth or survival. However, as seen in Fig. R57, a6, a9, a11, a12, some cells display an unusual shape, not entirely comparable to the morphology of wild-type MARCM clones. Furthermore I noticed that the intensity of the fluorescent signal was weaker compared to wild-type clones albeit in both instances the CD8:GFP marker was used for positive labeling. Currently I do not have an explanation for this result, however, future experiments using other markers should shed light on this issue.

Table R15: Absolute numbers of *rack1*^{Ey128}, *rack1*^{EMS1-8} and *rack1*^{PBc04220} clones with respect to size and distribution

ALLELE	N	ABSOLUTE NUMBER OF CLONES AT TIP	LARGE CLONES	MEDIUM CLONES	SMALL CLONES	LARGE CLONES AT TIP	MEDIUM CLONES AT TIP	SMALL CLONES AT TIP
<i>rack1</i> ^{Ey128}	22	13	4	14	4	4	6	3
<i>rack1</i> ^{EMS1-8}	19	15	8	9	2	8	6	1
<i>rack1</i> ^{PBc04220}	6	4	2	3	1	2	2	0

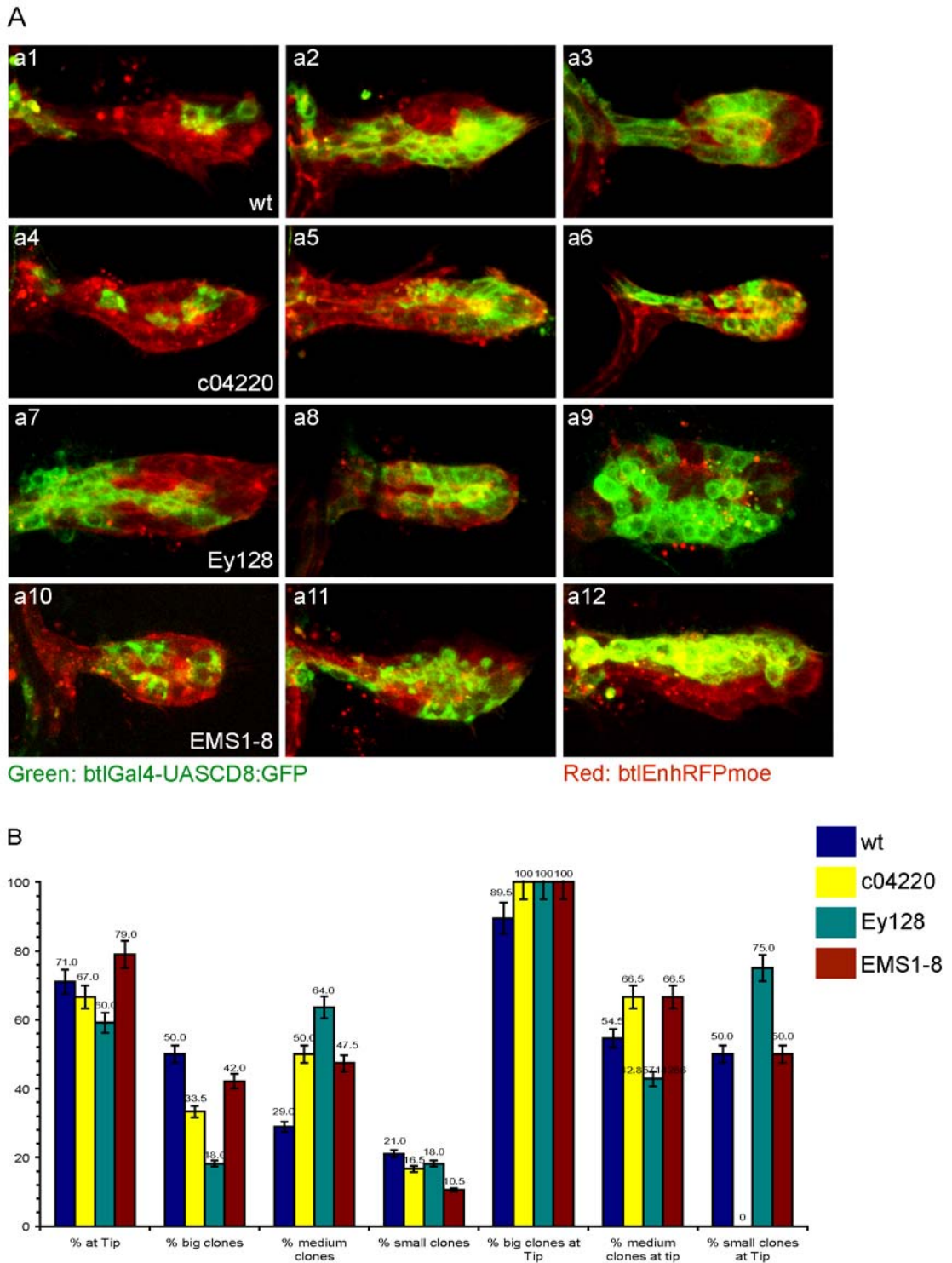


FIGURE R57

rack1 MARCM clones in third instar air sacs.

A.) representative pictures for all three alleles. Clones reach large sizes with all alleles and also often populate the tip. Note the aberrant air sac tracheoblast shape in some air sacs **a6**, **a9**, **a11**, **a12**.

B.) Statistics indicate that neither migration nor growth/proliferation is affected with the tested alleles.

III Discussion

1. FGF signaling and *rack1*; two independent topics?

This thesis aimed at a better understanding of FGF signaling with special emphasis on cell migration. The FGF signaling pathway is used in many developmental processes such as mesoderm formation, limb bud outgrowth, lung development, development of the feather placode, vascular development, wound healing or tissue repair (Affolter et al., 2003; Cardoso, 2000; Chuang and McMahon, 2003; Hogan, 1999; Javerzat et al., 2002; Mandler and Neubuser, 2004; Powers et al., 2000; Xu et al., 1999).

In *Drosophila melanogaster*, FGF has been shown to be required for mesodermal- as well as tracheal cell migration and patterning (Affolter et al., 2003; Cabernard et al., 2004). The fruit fly is an established genetically tractable system, offering a multitude of tools, including a vast number of mutants or strains containing disrupting transposons (Bellen et al., 2004), transgenic lines for the expression of GFP-tagged proteins (Brand, 1995), enhancer trap- (Bellen et al., 2004) or protein trap strains (Clyne et al., 2003; Kelso et al., 2004; Morin et al., 2001) as well as a sequenced and annotated genome (Adams et al., 2000).

We have chosen to study FGF-guided cell migration in the tracheal system of *Drosophila melanogaster*. Tracheal system development starts with the assignment of a number of ectodermal cells to tracheal fates. After two rounds of cell division, the branched network of the trachea is established through cell migration, cell intercalation and cell shape changes. A large number of mutants were isolated, that disrupt specific steps in the development of the tracheal system, including guided cell migration. By disrupting components of the FGF signaling pathway, such as the FGF ligand *branchless (bnl)* (Sutherland et al., 1996), the FGF-receptor *breathless (btl)* (Klamt et al., 1992) or an internal component required for transmitting the signal downstream of the receptor, *downstream of FGFR (dof)* (Imam et al., 1999; Michelson et al., 1998a; Vincent et al., 1998), characteristic cell migration phenotypes were observable. Using Dof as an entry point, we tried to identify additional components required for the interpretation of the extracellular signal provided by Bnl ligand. Biochemical analysis established that Csw, a tyrosine phosphatase homologous to the vertebrate Shp-2 (Perkins et al., 1996; Perkins et al., 1992), is a Dof binding partner and a component of a signaling complex bound to the Btl receptor required for the activation of the Ras/MAPK pathway (Petit et al., 2004). It has also been shown that the Ras/MAPK pathway is not sufficient for activating the migration machinery in tracheal cells (Petit et al., 2004). In order to learn more about the function of Dof, two independent yeast two-hybrid screens were performed with the aim to isolate Dof interaction partners (Battersby et al., 2003; Cabernard, 2000). Both screens identified Receptor of activated protein kinase C (Rack1) (Vani et al.,

1997) as a putative Dof interactor. In order to show an actual requirement of this protein in a developmental context with Dof, we have undertaken a genetic analysis of *rack1*.

rack1 mutants have not been previously described. In order to study the *in vivo* requirements of *rack1*, our aim was to isolate *rack1* loss-of-function alleles. We managed to obtain three independent alleles, two transposon insertions as well as a EMS-induced mutation in the coding region of *rack1*. Molecular analysis of the three alleles shows that all three disrupt the coding region and represent strong loss-of-function alleles. However, probably due to very high maternal contribution, embryos lacking *rack1* develop normally. Removal of the maternal contribution results in eggs which completely fail to develop. In this thesis I provide evidence that this is due to incomplete nurse cell dumping. So far we have not elucidated the exact nature of this phenotype.

Thus, we were faced with a situation that did not allow us to study the *rack1* loss-of-function phenotype during tracheal- or mesodermal development, tissues which rely on Dof function. FGF signaling has also been reported to be required during larval stages either for the recruitment of mesodermal cells into the male genital imaginal disc (Ahmad and Baker, 2002) and for the establishment of the adult tracheal system through the generation of air sacs (Sato and Kornberg, 2002). It has been shown that during air sac formation, FGF signaling is required for the migration and for the proliferation of air sac tracheoblasts. Moreover, *bt1* as well as *dof* were shown to be expressed in this larval tracheal tissue (Sato and Kornberg, 2002). Thus, a reasonable assumption was that this system could be used to elucidate the role of *rack1*. However, since little knowledge was available concerning the development of air sacs, I set out to characterize this system with special emphasis on cell migration and cell proliferation. Furthermore, strains and methods were established, which allow to study the cell-autonomous requirement of candidate genes in genetic mosaics. Subsequently, a genetic analysis was initiated in order to elucidate the requirement of other candidate genes in FGF-mediated cell migration.

Below my findings are summarized and discussed in the context of other relevant literature.

1.1 Air sac development in *Drosophila* third instar larva

Air sac development can be regarded as the *de novo* formation of a structure from an existing tracheal branch. In this regard, air sac formation resembles the formation of the vertebrate lung, which sprouts from the primitive foregut very early in development and through dichotomous branching, culminates in the formation of a huge and heavily branched construction (Warburton et al., 2000).

As reported, known tracheal markers such as *trh*, *btl*, or *dof* are expressed in air sac tracheoblasts (Sato and Kornberg, 2002). Furthermore, the FGF ligand Bnl is secreted from a small number of wing imaginal disc columnar epithelial cells abutting the outgrowing air sac. Air sac outgrowth is initiated at a more or less stereotypical position in the transverse connective (TC), a tracheal branch of embryonic origin that adheres to the wing imaginal disc. During pupal stages, air sacs increase in size, grow bilaterally under the thorax and bifurcate several times to form two major branched structures (Manning and Krasnow, 1993; Sato and Kornberg, 2002). Air sac formation is established through cell proliferation as well as cell migration (Sato and Kornberg, 2002).

Like embryonic tracheal cells, air sac tracheoblasts are polarized cells. This polarization is seen already from very early stages onward and is maintained throughout third instar stages. Furthermore, air sac tracheoblasts become organized into a monolayer epithelium with the apical side facing towards a lumen and the basal side facing outwards. Thus, like embryonic tracheal cells, air sac tracheoblasts extend and migrate with their basal side towards the chemoattractive signal Bnl, whereas the apical side maintains contact with the lumen. However, air sac tracheoblast cells at the tip often disrupt this monolayer since we identified tracheoblasts can be observed in an end to end arrangement with only one cell abutting the lumen. We have not gathered enough data to completely understand the cellular events associated with these cell rearrangements.

Based on the apically secreted marker Pio, we conclude that a lumen is established during air sac development in third instar larva. The lumen, however, does not contain an open connection to the TC in third instar air sacs but it is assumed that such an opening will be generated in later stages. Concerning the physiological role of air sacs, virtually nothing is known. However, since it is a tracheal structure one of its major tasks is most likely gas exchange. Moreover, pupal air sacs are in close association with thoracic flight muscles (Manning and Krasnow, 1993) and it is believed that an interplay between the two tissues generates buoyancy. RNAi expression against *dof* in the tracheal system, does not affect the embryonic tracheal system, but abolishes the formation of air sacs. These larva interestingly

develop until late pupal stages but fail to hatch. Thus, the lack of air sacs could either impede hatching or result in lethality due to decreased gas exchange. Nevertheless, lethality could also be due to defects in other tissues since expression was driven with *btlGal4*, a driver which is also active in certain neuronal lineages.

1.2 Establishment of air sac shape

How is organ shape in general, and air sac shape in particular established and maintained? At the end of third instar development, air sacs usually display a stereotypical shape. The air sac migrated towards the margin of the wing imaginal disc. It usually consist of a thin, branch-like connection between the main air sac body and the TC. It is difficult to interpret this late morphology with the chemoattractive force provided by *Bnl* only. Also, although I did not manage to confirm the *bnl* expression pattern in wing discs, data from M. Sato indicate that the expression is not just located at the very tip of the outgrowing air sac (Sato and Kornberg, 2002). Thus, it is very likely that additional mechanisms play a role which shape the outgrowing air sac. Such mechanisms could include cell division in localized domains of the air sac, cell intercalation as well as cell migration.

Obviously, in order to increase the size of the air sac, cell division has to be taken into account. In contrast to the embryonic tracheal system, which undergoes only two rounds of cell division at the onset of tracheal system formation, continuous cell division has been observed in air sacs. Looking at the expression of the *Drosophila* *cdc25* homologue *string*, a mediator of mitosis (Edgar and O'Farrell, 1989), as well as direct observation of cell division with *tauGFP*, confirms the occurrence of cell division as a mean to increase the size of the air sac. Cell division likely continues throughout pupal stages, since clones generated by mitotic recombination increased tremendously in size. In early to mid stage air sacs, mitotic spindles can be observed in all regions of the air sac, suggesting that cell division is not restricted to specific mitotic domains. In later stages, however, mitotic spindles are excluded from the stalk region indicating that cells ceased to divide in that area of the air sac. This observation is in line with the recovering of small isolated wild-type clones in the stalk region, suggesting that a clone, due to it's distal position did not grow at the same rates as a clone located more distally. However, we also observed the occurrence of small isolated clones at the tip. These could basically originate by two mechanisms. On the one hand, through extensive migration and/or rearrangements of cells in the air sac, a big founder clone could be split up in different smaller islands. If this would be a general mechanism, then most of the retrieved air sacs

containing clones would show a scattered distribution of marked cells. This is not in agreement with our findings since the majority of the clones maintained their integrity. On the other hand, local differences in division rates could explain the occurrence of these small clones. I favor a model which predicts differences in mitotic activity within the air sac.

Furthermore, cell rearrangement is very likely to be required for air sac shaping. Data from C. Ribeiro and M. Neumann (Ribeiro. et al. (2004), in press) show that in order to establish a dorsal branch consisting of end to end arranged cells requires cell intercalation. Studying cell intercalation in the air sac is impeded through the occurrence of cell division. Thus, little data has been provided to show that cell intercalation indeed occurs. Time laps recordings of air sac development shows that the initially broad region at the proximal end of the air sac gradually refines into a thinner stalk. Two factors which might play a role in this process can be evoked . First, most likely, a pulling force is provided through the chemoattractant Bnl. However, just by pulling at the front, one would assume all cells stretch equally. This is not what we observe; The shape of the most proximal cells is altered compared to cells located more distally. Cells in the stalk usually appear elongated and while cells in the main air sac body appear more wedge shaped with a small apical side and a broader basal side. Thus, cells react differently to the pulling force and it is likely that cells in the proximal region rearrange in order to form a stalk. This rearrangement could be facilitated through differences in cell migration velocities. That migration indeed occurs has been observed with live imaging as well as with genetics and will be discussed in the following paragraph.

It is also possible that tissue barriers help in establishing the shape of air sacs to a certain extent as well. Air sacs are, as observed with the expression of *svbGal4*, surrounded by wing disc cells of other origin than tracheal cells. It appears as if this tissue forms grooves in which air sacs migrate. Such grooves were already reported to be important in the *Drosophila* embryo in the establishment of the fine architecture of the tracheal system (Franch-Marro and Casanova, 2000). Thus, physical constraints could be another mechanism in order to establish shape.

1.3 Cell migration during air sac development

It has been reported that one characteristic of air sac development is the migration of air sac tracheoblasts (Sato and Kornberg, 2002). Nevertheless, active migration has not been shown

directly. Based on the expression of the *bnl* and *blt* genes, as well as on the occurrence of filopodia-like structures, cell migration was merely inferred. Other, non-motile wing imaginal disc cells have also been shown to extend filopodia-like structures (De Jossineau et al., 2003). Therefore, the occurrence of filopodia-like extensions in air sacs, which occur not only in the tip, but also in air sac tracheoblasts located elsewhere in the air sac, could also point to a general mechanism for cell-cell interaction and/or cell-cell communication.

However, it is not a trivial matter to directly show the active migration of air sac tracheoblasts. Since cell migration is a dynamic process, the best possible way to document this dynamics is to use live imaging. However, the behavior of air sac tracheoblasts has to be monitored on dissected tissue. Moreover, air sac development takes place over the entire third instar stage, which lasts about 2 days, depending on temperature and culture conditions. For these reasons, live imaging can only be applied for the recording of shorter intervals of maximally several hours. Nevertheless, we established protocols, that allowed to monitor the behavior of air sac tracheoblasts of dissected discs in culture over time. Movies generated in this manner show interesting aspects. First of all, air sac tracheoblast tip cells extend long protrusions, which, after being stabilized, can be used to pull the cell body forward. Secondly, air sac tracheoblasts located in other regions of the air sac also extend actin-based protrusions. Nevertheless, these cells probably move in a sheet-like manner and it is difficult to distinguish to what extent active migration and passive pulling (or pushing) is involved.

Another way to show the occurrence of cell migration is by the use of genetics. Sato and Kornberg tried to show this by removing the chemoattractant *bnl* in the vicinity of air sacs by generating *bnl* clones in the columnar epithelium of wing imaginal disc cells. Indeed, these clones halted air sac formation to a certain extent. In addition, a dominant-negative form of Btl (Btl^{DN}) was expressed in the tracheal system, which lead to a complete absence of air sac formation. However, it is not clear whether this phenotype is due to interfering with cell migration, or cell proliferation or both.

We have chosen another approach to assess by genetic means the involvement of air sac tracheoblast migration, which is by generating mosaic clones in the air sac itself. As reported here, the observation of small labeled wild-type clones can be instructive in terms of mechanism. Clones generated during embryonic development are distributed throughout the larval tracheal system (Samakovlis et al., 1996a). Since air sacs originate from the TC, clones located at positions where the air sac forms become most likely integrated into the air sac. At the beginning of air sac development, clones and wild-type cells should have equal chances of

reaching the tip. Based on the observation that small clones can be recovered at the tip but also at the base of the air sac, differences in migration must occur. Although the distribution of the clones cannot always be sufficiently explained we favor a model suggesting that the size and the position of the founder clone is instructive for the later behavior. The optimal test for this model would be to monitor the fate of clones throughout third instar development.

However, assuming cell migration takes place in air sacs, we reasoned that a cell deficient in migration should, with time, be overtaken or displaced by wild-type air sac tracheoblast in the growing tissue. Following this logic, such a cell should be excluded from the tip of the air sac. Vice versa, individual genetically labeled cells with normal migratory capacity should populate the tip area of the air sac with a certain frequency. We tested this assumption by analyzing the distribution of genetically marked wild-type cells and showed that the majority of these cells (70%) are found at the leading edge. We further predicted that cells mutant for genes required in cell migration, should not be able to migrate at the very tip. In order to test this, clones deficient for *btl* or *dof*, genes of which we know that they are involved in cell migration, were in the embryo generated and the distribution of these clones was analyzed. We found that air sacs formed normally but not a single clone lacking either *dof* or *btl* was found at the tip. Interestingly, in the most extreme cases, when the clones reached considerable sizes, the last third of the air sac was devoid of mutant cells, indicating that these wild-type cells are actively migrating, whereas the majority of air sac tracheoblasts are just passively dragged along. A similar finding was made in the third instar larval tracheal network that is built via cell migration in the embryo. Wild-type clones usually distribute in a random manner and can be recovered in all parts of the tracheal system. Thus, also terminal cells, which lead the outgrowing tracheal branches during tracheal system development and later form long cytoplasmic extensions, are marked. However, no single *btl* or *dof* mutant terminal cell was ever found in the larva, but clones lacking *btl* or *dof* were found in positions just adjacent to the terminal cell, which would correspond to cells just behind the outgrowing tip cell. Several individual terminal cells, adjacent to a *btl* or *dof* mutant cell, were recovered, and these cells also looked properly differentiated based on morphological criteria. This suggests that the leading tip cell requires *btl* to position itself at the tip of the branch, but that cells without *btl* can passively follow them. Adapted to the air sac, it thus indicates that certain air sac tracheoblasts migrate more actively than others.

It would be of major interest to see what happens with a tip cell upon the loss of *btl* or *dof* during migration. Logic would predict that this cell will be replaced by a wild-type cell, as we

infer is the case with early-induced clones. Such an experiment, however is difficult to perform, also due to the fact that MARCM clones cannot be analyzed immediately after clone induction, due to the perdurance of the Gal80 protein. Therefore, 48h after clone induction, the time required to sufficiently dilute Gal80, clones are replaced by wild-type cells.

In summary, based on the distribution of wild-type clones as well as the clones deficient for *dof* or *btl*, we are confident to state that this system can be used for measuring cell migration requirements.

1.4 Genetic dissection of FGF signaling using site-specific mitotic recombination

1.4.1 Clone size versus clone position

Having established a genetic assay to study the cell-autonomous effect of candidate genes on tracheal cell migration, we wanted to identify factors downstream of *btl* required for proper interpretation of the chemotactic signal.

First we wanted to clarify whether FGF indeed acts as a motogen as well as a mitogen, as was reported previously (Sato and Kornberg, 2002). In vertebrates, FGF signaling has been reported to have both effects, depending on cell type and context (reviewed in Boilly et al., 2000). In *Drosophila*, only during air sac development, has it been suggested that FGF signaling is involved in proliferation. Expression of a constitutive active version of Btl (λ Btl) resulted in the increase of air sac tracheoblasts (Sato and Kornberg, 2002). However, overexpression experiments create an artificial situation and may not reflect a physiological situation. Thus, we reasoned that the generation of mitotic clones lacking either *btl* or *dof* should allow us to clarify this question. As we know from wild-type clones, mitotic recombination events results in the generation of a variety of clones, with sizes ranging from small to big. However, the majority of clones is medium- to big sized. A similar finding was obtained with clones lacking either *btl* or *dof*. However, the distribution of these mutant clones in different size categories was not exactly the same as in wild-type. The majority of wild-type clones was big, followed by medium- and then small clones. The majority of *btl* or *dof* clones, however, were clearly medium sized. It could be that the alleles used, do not completely abolish the function of the corresponding gene. Molecular and genetic data indicate that both alleles are at least strong loss-of-function alleles. Testing other *btl* and *dof* alleles should rule out this concern. Furthermore, the grouping of clones into different classes,

especially with respect to medium and big, is arbitrary and not always very easy. Thus, these two groups are often considered together. In this regard *btl* and *dof* clones show the same size distribution than wild-type clones.

In contrast to *btl* and *dof*, the analysis of mutants affecting the Ras/MAPK pathway, such as *sos*, *ras*, *cnk* or *ksr*, demonstrated that they showed much more severe phenotypes in terms of size. Almost all of these clones are of small size and are thus clearly distinct from wild-type (and *btl* or *dof*) clones. Somewhat surprisingly, all of these components also show an equal clone positioning, namely at the back of the air sac and never at the leading tip. We were intrigued by this result since it indicated that clone position seems to be linked to clone size. With wild-type clones, this is clearly not the case. Small wild-type clones are, albeit at a reduced frequency, also recovered and these have a 50% chance to reach the tip. Clearly, and in agreement with intuition, large clones are more likely to extend to the tip. However, the occurrence of small clones at the tip together with the finding that big or medium clones are not necessarily positioned at the tip suggests that clone position is to a certain extent independent of clone size. As already mentioned, this variability could be due to differences in initial founder clone size and position. However, logic would predict that the same should apply for clones lacking *ras*, *ksr*, *cnk* or *sos* unless other cell intrinsic as well as cell extrinsic mechanisms play a role such as clone survival, competition, growth, cell cycle progression and or migration. *In vivo*, Ras has been found to be associated with cell migration in systems such as border cells (Duchek and Rorth, 2001a; Lee et al., 1996a), germ cells (Li et al., 2003) or hemocytes (Cho et al., 2002). Also tracheal cells likely require *ras* for their migration, although Ras activation is not sufficient (Imam et al., 1999; Petit et al., 2004; Vincent et al., 1998). However, in wing imaginal discs *ras* has also been implicated in cellular and clonal growth, cell cycle progression as well as survival (Prober and Edgar, 2000). Old studies in yeast showed that the rates of cellular growth (accumulation of mass) dictates the rates of cell cycle progression (Johnston et al., 1977). Clones lacking *ras* were observed to be small as a consequence of slow growth, reduced proliferation and increased cell death due to cell competition. The model of Prober and Edgar thus predicts that Ras (activated through growth factors) promotes growth via dMyc and probably also other proteins. Furthermore, Ras and dMyc also posttranscriptionally upregulate Cyclin E and thus promote G1/S cell cycle progression. However, the progression of the cell cycle through G2/S is independent of Ras and mediated by String/Cdc25 (in response to growth factors) (Prober and Edgar, 2000). Thus, since *ras* mutant cells grow slower, they are subject to cell competition, a phenomena observed in wing imaginal discs. Slowly growing cells are eliminated when they are next to

cells that grow at a normal rate (Simpson and Morata, 1981). Therefore, the occurrence of small clones in third instar air sacs could also be due to growth defects and thus decreased cell cycle progression, resulting in the elimination of clones by cell competition. However, this model would explain the occurrence of few and small clones as we found in the air sac with *sos*, *ras*, *cnk* and *ksr* clones. Nevertheless, clone position should be independent of competition. Interestingly clones lacking the EGF receptor (DER) are small, show signs of apoptosis but are not strictly located at the back as *sos*, *ras*, *cnk* and *ksr* clones.

We wanted to test directly whether clone position depends on clone size by analyzing genes involved in the cell cycle. We looked at Cdc2 kinase as well as Regulator of cyclin A (Rca1), which both regulate entry into mitosis (Dong et al., 1997; Edgar and O'Farrell, 1989). As expected, clones deficient for either *cdc2* or *rca1* are smaller than their siblings whereas the cells themselves are bigger than normal, which could be due to endoreplication. However, these clones also did not migrate, which was somewhat puzzling. Therefore cell cycle progression seems to be important for clone positioning as well. In the case of *cdc2*, a recent paper provides evidence that this gene is involved in integrin mediated cell migration (Manes et al., 2003). Since cell division requires a lot of the same cytoskeletal components as cell migration, a linkage of these two processes is not entirely unexpected. A screen for egg shell patterning, which also relies on multiple rounds of Ras signaling, identified a number of cytoskeletal loci which interact with ras (Schnorr et al., 2001). Thus, the phenotype of clones lacking *ras* could be explained with reduced growth thus slower cell cycle progression, or in a failure to activate cytoskeletal components required for cell migration/division or both. In order to separate these processes, we try to rescue survival, growth and cell cycle progression in clones mutant for *ras*. A similar phenotype is displayed by clones lacking *PI3K*. This molecule has been shown to be a downstream effector of Ras (Rommel and Hafen, 1998). Furthermore, PI3K has been implicated in regulation of cell size, cell proliferation and/or cell survival (Weinkove et al., 1999). Other reports provide evidence for an involvement of *PI3K* in chemotaxis (Funamoto et al., 2002) as well as Ras-linked cell migration (Sasaki et al., 2004). Thus, the position of *PI3K* clones could be again a consequence of growth or could indicate a lack in cell migration. In the tracheal system, PKB, a PI3K dependent enzyme is required for phosphorylation, nuclear localization and thus functional activation of the transcriptional activator Trachealess (Trh) (Jin et al., 2001). Among Trh target genes are *btl* and *dof* but likely also many others required for tracheal cell migration.

Taken together, reduced rates in growth on the one hand and cell migration on the other hand seem to be equal in likelihood to explain the position of clones affecting the Ras/MAPK pathway as well as PI3K.

1.4.2 Several mutations show clone positioning phenotypes independent of clone size

As already demonstrated with wild-type clones, clone size does not necessarily determine clone position. This is also reflected in the fact that several mutations display much reduced clone positioning at the leading edge despite the fact that clone size is medium to big. This has been observed with the adaptor proteins *shc* or *drk*. In both instances, cells predominantly cluster at the back, while clone size is almost normal. Furthermore, cells mutant for the hypomorphic *sos*^{*XMN1025*} allele are also predominantly found at the back of the air sac. The same is also true for *pten*^{*1*} mutant air sac tracheoblasts. Thus, these data also suggest, that clone size, and thus growth and proliferation do not affect clone positioning in a positive manner. Growth and proliferation alone is not sufficient to push cells (mutant or wild-type) to the very tip, suggesting that wild-type cells, through their more effective migratory response, leave behind their mutant siblings.

It has also been observed that Ras activity levels might play an important role for cellular responses. In the *Drosophila* eye it has been shown, that different thresholds of Ras trigger different cellular outcomes. Low Ras activity is sufficient to increase the size of a *ras* mutant clone (Halfar et al., 2001). A similar correlation also occurs in the case of *sos*^{*XMN1025*} as well as *gap1* clones. Both genes affect the activity of Ras. Whereas Sos controls the exchange of GDP for GTP, the GTPase activity is controlled by Gap1. *sos*^{*XMN1025*} contains a missense mutation in the REM of Sos and thus likely impairs RasGEF function to a certain extent (Silver et al., 2004); in contrast, *gap1* mutants prolong Ras activity. In both instances, however clone size is rescued, indicating that both low as well as high Ras activity levels have no effect on clone size. Clone position could reflect different Ras activity levels, since *sos*^{*XMH1025*} as well as *gap1* clones show reduced air sac tip localization.

Further experiments, which should further clarify whether Ras levels can be brought directly into connection with clone positioning and thus migration, are underway.

1.5 Do border cells and air sac tracheoblast require the same cytoskeletal regulators?

We have also tested components that are well known to regulate the cytoskeleton, such as the Rho family GTPases Rac1, Rac2 and Mtl, the *Drosophila* homologue of Dock180 encoded by *myoblast city* (*mbc*), as well as two effectors, Pak and Chic. Not surprisingly, clones lacking two of the *rac* genes (*rac1*, *rac2*) show a clear reduction in cell migration which is further increased upon removal of one copy of *mtl*. Thus, evidently, these three genes, being regulators of the actin cytoskeleton, are implicated in air sac tracheoblast migration. The requirements for these genes has also been demonstrated in border cell migration (Duchek et al., 2001b; Geisbrecht and Montell, 2004; Murphy and Montell, 1996). An additional component, DIAP1, which is engaged in a complex with Rac as well as with Chic (Profilin), was found to impair border cell migration when mutated. We have not tested the involvement of *diap1* so far in air sac tracheoblast migration but it will be interesting to see whether air sac tracheoblast require *diap1* for their migration. Whereas border cell migration relies on PVR signaling which affects the cytoskeleton via Dock180/*mbc* and Rac (Duchek et al., 2001b), lack of PVR signaling has no effect on clone position in air sacs. Thus, remodeling of the cytoskeleton appears to be cell-type specific with regard to the ligands and receptors, but takes advantage of the same mediators and effectors. Whereas border cells mainly rely on PVR, air sac tracheoblasts use FGF/*bnl* (Sato and Kornberg, 2002). However, we first have to show this on the level of filopodia-like extensions and confirm that PVR does not affect the cytoskeleton of air sac tracheoblasts. We showed here that *btl* loss-of-function clones in air sacs never reach the tip and are thus defective for migration, however, filopodia-like extensions were occasionally seen in some mutant air sac tracheoblasts although this particular allele was used to demonstrate the absence of filopodia in the embryo (Ribeiro et al., 2002). Thus, it is still possible that PVR promotes the formation of filopodia-like structures to a certain extent together with FGF in air sac tracheoblasts.

Assaying the dynamic behavior of filopodia-like extensions in air sac tracheoblasts in other locations than the tip has just begun. I presented data which suggest that also more proximal located cells are capable of forming extension. Although we do not know what functional role they perform, it is of major interest to establish a relation between these structures and the observed filopodia in embryonic tracheal cells. Clearly these structures are actin based and therefore most likely represent filopodia. A better characterization of these structures could help to analyze the phenotype of clones that never manage to reach the tip, such as *ras*. These

experiments could give insight into the question whether mutants, which result in proximal clone locations, do that because of a lack of actin based extensions. Maybe these extensions could provide a direct readout for all mutant classes in terms of cytoskeleton remodeling.

1.6 Air sac development does not require Dpp and/or Hh signaling.

We started to look at other signaling pathways also in search of a pathway, which could explain the strong phenotype of *ras* with respect to clone size. Since *btl* and *dof* clones do not show this proliferation phenotype, we presume that another pathway is required for air sac tracheoblast proliferation (alone or together with FGF). An obvious candidate was the EGFR pathway, since Ras is also downstream of DER (Shilo, 2003). In contrast to other regulators of growth such as Hh or Dpp (Burke and Basler, 1996), which are both not required for air sac tracheoblast proliferation (Basler and Struhl, 1994), *egfr* mutant clones are always small and also show signs of apoptosis. Positioning of *egfr* mutant clones was improved in comparison to *ras* clones, and by rescuing the apoptosis phenotype or by looking at earlier stages, we expect, that more *egfr* mutant clones could be found at the tip. We tentatively suggest that air sac tracheoblasts rely at least on two pathways which might be partially overlapping.

Other signaling pathways, such as Notch, Wingless or the JAK/STAT pathway, have not yet been tested and it will be interesting to see to what extent they contribute to air sac development.

1.7 Rack1 is not required for tracheal cell migration

Finally, this system also allowed us to answer the question whether Rack1, identified as a Dof interacting partner (Battersby et al., 2003; Cabernard, 2000), has any physiological role in FGF signaling. Rack1 seemed to be a prime candidate to connect the FGF signaling pathway via Dof to the cytoskeleton, based on numerous indications. First, Rack1 is expressed in the embryonic tracheal system (Vani et al., 1997). Second, Rack1 has been shown to be induced by FGF in the chicken limb bud (Lu et al., 2001). Third, Rack1 has been reported to be implicated in the regulation of the actin cytoskeleton in the context of cell migration (Buensuceso et al., 2001; Cox et al., 2003; Hermanto et al., 2002). However, despite all this evidence, we showed that in air sac tracheoblast migration, where Dof is involved, Rack1 is

not required. This has been shown with three independent alleles, likely representing strong loss-of-function alleles. Furthermore, we showed evidence that *rack1* is involved in the female germline, namely in the process of rapid nurse cell dumping which explains the female-sterile phenotype of flies carrying *rack1* germ-line clones in the ovary. This finding is also in agreement with the very high maternal contribution provided by the nurse cells of wild-type females. It is not known whether the failure of early embryo development is a consequence of the absence of *rack1* RNA and protein, the impeded nurse cell dumping process or a combination of the two. Several mutants which show nurse cell dumping phenotypes, have been described. Usually, these phenotypes are due to defects in ring canals or the actin network which prevents the nucleus from plugging the ring canals (Cant et al., 1994; Cooley et al., 1992; Dodson et al., 1998). However, nonmuscle myosinII, encoded by *spaghetti squash (sqh)* in *Drosophila*, also shows nurse cell dumping defects as well as a failure in the axial migration of cleavage nuclei in the early embryo. Furthermore, alterations in the actin network or in ring canals were not detected, but myosin II was found to be abnormally distributed (Edwards and Kiehart, 1996; Wheatley et al., 1995). *rack1* mutants do neither show defects in the actin network in nurse cells nor gross alterations in ring canals. However, recent reports provide evidence that Rack1 is a component of the ribosome, involved in its assembly and thus in translational control (Ceci et al., 2003; Sengupta et al., 2004). It is currently not known whether translational control and nurse cell dumping are linked. However, one might speculate on mechanisms, which initiate nurse cell dumping via the control of protein translation. For example, it is possible that nurse cell dumping is only initiated when enough protein has been produced, or, alternatively, when a sensor protein has been translated in sufficient amounts.

1.8 Air sacs as a model to study morphogenesis and cell biological questions

Air sacs, as a structure on its own or in the developmental context in which they form, provide many interesting questions to study. We primarily turned to air sacs because we sought for a system to genetically address very specific questions with respect to cell migration and cell signaling. Other mechanisms, such as cell rearrangements, most likely play important roles during air sac development. Another very interesting question, which arises in the context of air sac development, is how cell division is spatially and temporally controlled: Is the air sac tracheoblast cell cycle synchronous with the cell cycle of the wing

imaginal disc cells? Do air sac tracheoblasts divide symmetrically, asymmetrically or both? How does Bnl protein reach the air sac? By diffusion, or via cellular extensions from Bnl producing cells? Until recently, these questions have not been raised but will eventually have to be taken up and answered. The tools to study most of these questions are now available, including the strains to generate mitotic clones in air sacs as well as in the disc tissue. Furthermore, microscopic methods improved and will further improve.

However, as every system, third instar air sacs have some disadvantages. First, although cell division is a requirement for mitotic recombination, it also makes it more difficult to separate between migration and cell division as seen in the case of clones affecting the Ras/MAPK pathway.

We recently decided to take advantage of this system to perform a genetic screen, aiming at the isolation of novel mutants that affect tracheal cell migration. This work is mainly done by Li Lin, Alain Jung as well as Helène Dechanut in collaboration with the laboratory of Maria Leptin at the University of Cologne. The screen focuses on the left arm of the second chromosome. We were able to find a number of candidates, which show limited air sac migration without affecting cell proliferation. However, since such a screen is very labor intensive, alternative protocols and/or methods should be taken into account to speed up the screening process. One drawback of the current clone induction protocol is the low efficiency. Clones are generated in the entire tracheal system but are not always incorporated into the air sac. Attempts to apply Flipase in a spatially and temporarily more precise manner, such as fusing the flipase coding region directly to the *breathless* enhancer, failed. The reason for this is not known, although we assume that the expression levels are not high enough with this enhancer. Thus, alternative enhancers or combinations of enhancers/promoters might work more efficiently.

Another screening approach would be to screen with established RNAi lines. As experienced in our as well as in other labs, RNAi in the embryo seems not to work very efficiently. However, as the example with RNAi against *dof* shows, larval tracheal structures can be affected very specifically, which very likely also results in lethality. Thus, a RNAi based lethality screen could be taken into account.

1.9 Concluding remarks and working model

This thesis illustrates the use of third instar air sacs as a system to genetically dissect FGF-mediated cell migration. After having established criteria for measuring cell migration and proliferation, we tested a number of genes implicated in signaling, migration, proliferation and other processes, for their involvement in air sac tracheoblast cell migration. The phenotypes we find can be grouped into three classes. The first class represents genes which, when mutated, show cell migration phenotypes inferred from clone positions, but do not affect cell division per se. The second class shows minor migration but major clone size phenotypes. The third class shows phenotypes affecting both, migration and proliferation. Although we have not yet clearly separated these two phenotypes, we think they are not causally linked.

Genes like *btl*, *dof*, *shc*, *drk*, *pten*, *rac*, *mbc* *chic* fall into the first class, *egfr* into the second and *sos*, *ras*, *ksr*, *cnk* and *PI3K* into the third. Based on these data we currently favor a working model which explains the growth and migration of air sac tracheoblasts by using two linked pathways, EGFR as well as FGF (Fig. D1). Whereas EGFR signaling is required for the proliferation as well as the survival of air sac tracheoblasts, migration itself depends on FGF signaling. Both pathways rely on Ras as a central signal transducer which engages effector pathways to control migration and proliferation.

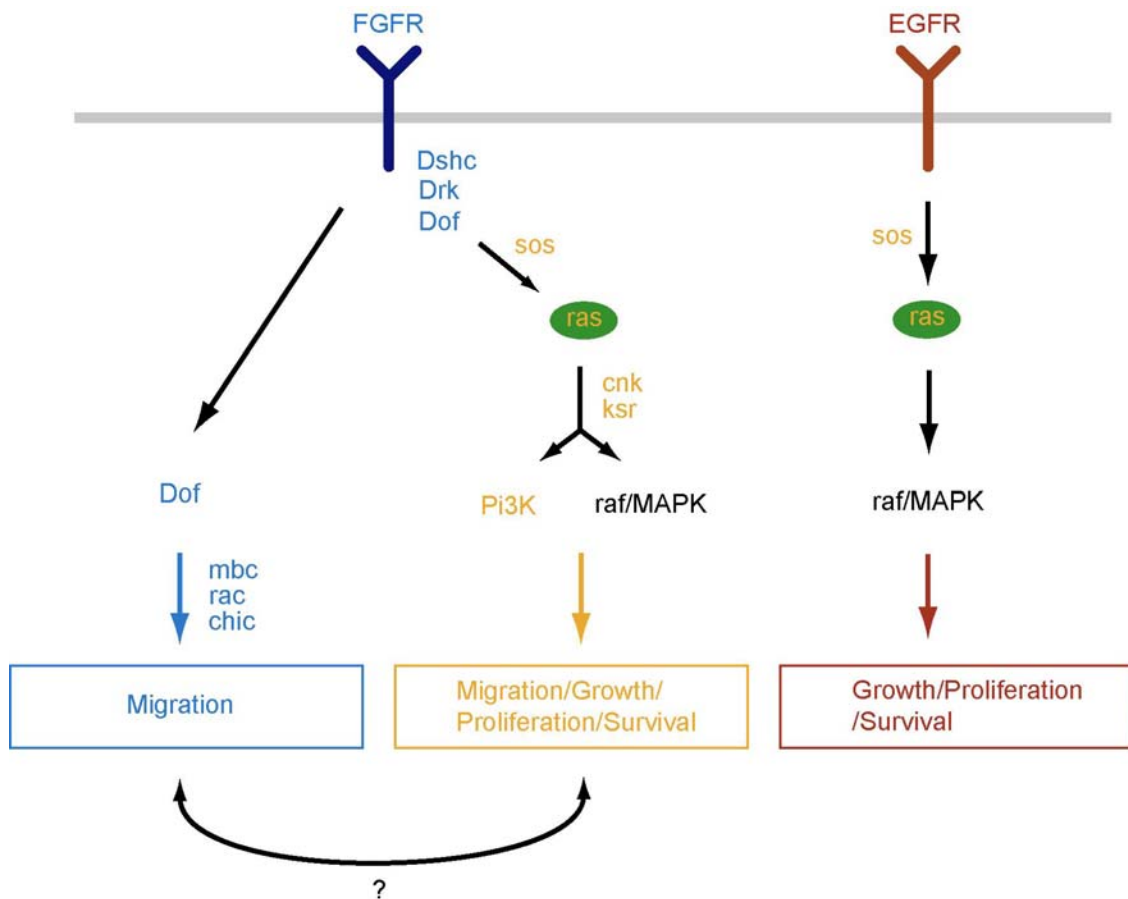


FIGURE D1

Our current working model is based on two signaling inputs, FGF- and EGF signaling. Both elicit downstream responses (colored boxes) via Ras. The genes in color affect a specific readout. We found genes, highlighted in blue, which only affect migration. Yellow and red colored genes affect several processes. A connection between migration and growth/proliferation/survival remains possible.

IV Materials & Methods

1.0 Fly strains and genetics

For targeted gene expression (Brand and Perrimon, 1993) the following lines were used:

btlGal4, *btlGal4-UASactGFP*, *btlGal4-UAStauGFP*, *btlGal4-UAS α CatGFP*, *btlGal4-UASCD8:GFP* and *UASGFPmoe*. All these lines are part of the common lab stock.

Gal4 lines not part of the common lab stock used here are: *svbGAL4* (provided by H. Dechanut), *bnlGal4^{PL00790}* (provided by U. Häcker).

Additionally, the following lines were used: *stringLacZ^{P[w+]STG β 6C}* (generously provided by M. Krasnow), *tub>dsRed2>bnl* (provided by T. Kornberg), *snakeGFP* (GFP protein trap line, trapped gene not known, provided by A. Debec).

1.1 Generation of T-MARCM stocks

The following MARCM stocks were generated. *TubGal80 FRT* chromosomes were obtained from the Bloomington stock center, except for *tubGal80 FRT42B* which was obtained directly from Liqun Luo (Lee and Luo, 1999). T-MARCM stocks were generated as following. First, a fully balanced *hsFLP* stock was generated using the *70FLP* insertion lines as the FLP source (Golic, 1994) with the following genotype: ***hsFLP/hsFLP; Sco/CyO; TM2 Ubx/TM6C Sb***

Also, recombinants were generated containing the *btlEnhRFPmoe* construct, a direct fusion of the *breathless* enhancer with *RFPmoe* (generated by M. Neumann), as well as the GFP markers in the table below. Putative recombinants were balanced using the double balancer stock *yw; Sp/CyO; TM2/TM6B Tb*. Larvae were collected which express GFP and RFP simultaneously in the tracheal system. The males of these larvae were crossed into the fully balanced *hsFLP/hsFLP; Sco/CyO;TM2/TM6C Sb*. Males from the following generation were once more crossed back to the *hsFLP* stock to generate ***hsFLP/hsFLP;btlEnhRFPmoe-btlGal4UASxGFP;TM2/TM6C***.

The same crossings were performed in parallel with the *tubGal80* strains to generate working stocks of the genotype ***hsFLP/hsFLP;tubGal80 FRTx/CyO;TM2/TM6C Sb*** as well as ***hsFLP/hsFLP; Sco/CyO; tubGal80 FRTx/TM6C Sb***. For the first chromosome, the Bloomington stock *w, FRT19A, tubP-GAL80, hsFLP; Pin[Yt]/CyO* was crossed to males of the genotype *yw; btlEnhRFPmoe-btlGal4-UASxGFP/CyO* and the male offspring was

crossed back again to w, FRT19A, tubP-GAL80, hsFLP; Pin[Yt]/CyO. The resulting stocks are listed below.

FRT chromosomes containing neomycin resistance are: FRT19A, FRT40A, FRT80B, FRT82B (Chou and Perrimon, 1996). FRT G13, FRT42B, FRT79A contain a selectable w⁺ marker (Xu and Rubin, 1993).

T-MARCM stocks

1. CHROMOSOME

hsFLP tubGal80 FRT19A/hsFLP tubGal80 FRT19A; btlEnhRFPmoe-btlGal4-UASactGFP

2. CHROMOSOME

2L: hsFLP/hsFLP; tubGal80 FRT40A/tubGal80 FRT40A; btlEnhRFPmoe-btlGal4-UASCD8:GFP/TM6C
 2L: hsFLP/hsFLP; tubGal80 FRT40A/tubGal80 FRT40A; btlEnhRFPmoe-btlGal4- α catGFP/TM6C
 2R: hsFLP/hsFLP; tubGal80 FRTG13/tubGal80 FRTG13; btlEnhRFPmoe-btlGal4-UASCD8:GFP/TM6C
 2R: hsFLP/hsFLP; tubGal80 FRTG13/tubGal80 FRTG13; btlEnhRFPmoe-btlGal4- α catGFP/TM6C
 2R: hsFLP/hsFLP; tubGal80 FRT42B/tubGal80 FRT42B; btlEnhRFPmoe-btlGal4-CD8:GFP/TM6C
 2R: hsFLP/hsFLP; tubGal80 FRT42B/tubGal80 FRT42B; btlEnhRFPmoe-btlGal4- α catGFP/TM6C

3. CHROMOSOME

3L: hsFLP/hsFLP; btlEnhRFPmoe-btlGal4-UAS-actinGFP/CyO; tubGal80 FRT2A/tubGal80 FRT2A
 3L: hsFLP/hsFLP; btlEnhRFPmoe-btlGal4-UAS- α catGFP/CyO; tubGal80 FRT2A/tubGal80 FRT2A
 3L: hsFLP/hsFLP; btlEnhRFPmoe-btlGal4-UAS-tauGFP/CyO; tubGal80 FRT2A/tubGal80 FRT2A
 3L: hsFLP/hsFLP; btlEnhRFPmoe-btlGal4-UAS-actinGFP/CyO; tubGal80 FRT80/tubGal80 FRT80
 3L: hsFLP/hsFLP; btlEnhRFPmoe-btlGal4-UAS- α catGFP/CyO; tubGal80 FRT80/tubGal80 FRT80
 3L: hsFLP/hsFLP; btlEnhRFPmoe-btlGal4-UAS-tauGFP/CyO; tubGal80 FRT80/tubGal80 FRT80
 3R: hsFLP/hsFLP; btlEnhRFPmoe-btlGal4-UAS-actinGFP/CyO; tubGal80 FRT82/tubGal80 FRT82
 3R: hsFLP/hsFLP; btlEnhRFPmoe-btlGal4-UAS- α catGFP/CyO; tubGal80 FRT82/tubGal80 FRT82
 3R: hsFLP/hsFLP; btlEnhRFPmoe-btlGal4-UAS-tauGFP/CyO; tubGal80 FRT82/tubGal80 FRT82

1.2 Experimental crosses

T-MARCM virgins were collected and crossed to males of the mutant of interest. At least 20-30 females were crossed to 10-20 males. After two days of mating, the flies were flipped every 2h for 3 times a day. The tube containing the freshly laid embryos was incubated at 25°C for another 4 hours. These 4-6h AEL embryos were given a heat-shock at 38°C for 1 hour. After the heat-shock the vials were incubated at 25°C until third instar larvae appeared. In order to slow down the development, the tubes were also kept at 18°C for several days. In any case, for at least one day, the embryos could recover after the heat-shock at 25°C before they were put at 18°C.

1.3 Alleles used for MARCM clones

ALLELE	PHENOTYPIC STRENGTH	DONOR	REFERENCE
<i>bt^{H82Δ3-}</i>	Strong loss-of-function/amorph	lab stock	(Reichman-Fried et al., 1994)
<i>dof^{P1749}</i>	Strong loss-of-function/amorph	lab stock	(Imam et al., 1999; Vincent et al., 1998)
<i>drk^{AP24}</i>	Amorph	P. Rorth	(Hou et al., 1995)
<i>dshc^{BG}</i>	Amorph	S. Luschnig	(Luschnig et al., 2000)
<i>ras^{X7B}</i>	Amorph	E. Hafen	(Halfar et al., 2001)
<i>ksr^{S-638}</i>	Loss-of-function	M. Therrien	(Therrien et al., 1995)
<i>sos^{X122}</i>	Amorph	S. Hou	(Diaz-Benjumea and Hafen, 1994)
<i>sos^{M98}</i>	Hypomorph	I. Rebay	(Silver et al., 2004)
<i>sos^{XMN1025}</i>	Hypomorph	I. Rebay	(Silver et al., 2004)
<i>cnk^{I(2)16314}</i>	-	M. Therrien	(Therrien et al., 1998)
<i>rca1²</i>	-	F. Sprenger	(Grosskortenhaus and Sprenger, 2002)
<i>cdc2^{B47}</i>	Amorph	F. Lehner	(Sigris et al., 1995)
<i>gap1^{B2}</i>	amorph	N. Perrimon	(Gaul et al., 1992)
<i>spry^{D5}</i>	Amorph	M. Krasnow	(Hacohen et al., 1998)
<i>PI3K^{Dp110A}</i>	Amorph	J. Montagne	(Weinkove et al., 1999)
<i>pten¹</i>	-	H. McNeill	(Goberdhan et al., 1999)
<i>lgl⁴</i>	Amorph	B. Baum	(Timmons et al., 1993)
<i>rac1^{J11}rac2^Δ</i>	Both Amorphs	Bloomington	(Ng et al., 2002)
<i>rac1^{J10}rac2^ΔmtlΔ</i>	Hypomorph /amorph	Bloomington	(Ng et al., 2002)

<i>mbc</i> ^{D11.2}	Loss-of-function	P. Rorth	(Erickson et al., 1997)
<i>pak1</i>	-	P. Rorth	(Hing et al., 1999)
<i>chic</i> ^{05205a}	amorph	B. Baum	(Wills et al., 1999)
<i>smo</i> ³	amorph	K. Basler	(Chen and Struhl, 1996)
<i>egfr</i> ^{K35}	amorph	M. Freeman	(Schejter and Shilo, 1989)
<i>Df(sal)</i>	amorph		(de Celis et al., 1996)
<i>tkv</i> ^{Q12}	amorph	Lab stock	(Nellen et al., 1994)
<i>slbo</i> ^{E7B}	amorph	D. Montell	(Rorth and Montell, 1992)
<i>pvr</i> ⁵³⁶³	- (strong allele, 61 bp deletion)	H. Sears	(Sears et al., 2003)
<i>tal</i> ^{61G1}	-	D. Montell	(McDonald et al., 2003)
<i>bs</i> ¹⁴	-	Lab stock	(Montagne et al., 1996)
<i>shg</i> ^H	amorph	F. Schweisguth	(Tepass et al., 1996)
<i>bsk</i> ¹	-	Lab stocks	(Riesgo-Escovar et al., 1996)
<i>dock</i> ⁰⁴⁷³²	amorph	P. Rorth	(Garrity et al., 1996)
<i>rack1</i> ^{Ey128}	-	Bloomington	This thesis
<i>rack1</i> ^{EMS1-8}	-	J. Chapin	This thesis and Thesis J. Chapin
<i>rack1</i> ^{c04220}	-	Exelixis via W. Gehring	This thesis

1.4 Gain-of function clones

For tracheal specific gain-of-function clones, the following construct was used generated by M. Neumann.

yw;btlenh>y⁺>Gal4. This construct was crossed to the fully balanced *hsFLP* stock in order to generate ***hsFLP/hsFLP;btlEnh>y⁺>Gal4*** .

1.5. Recombination of mutant alleles on FRT chromosomes.

Mutant alleles were crossed over the appropriate FRT chromosome. Transheterozygous females were collected and crossed to balancer males. Male offspring was single crossed to balancer females and with the resulting offspring of this cross a stock was established. In case, the FRT contains a neomycin marker, flies were cultured on neomycin containing fly

food (25mg/ml geneticin; 300µl/vial). Flies were bred in the neomycin vials for up to three days at 25°C and then flipped into fresh neomycin vials. The 1 batch of vials was incubated another 24-48h at 25°C and subsequently heat-shocked for 1h at 38°C to increase expression of neomycin (which is cloned in a heat-shock vector). For some FRT chromosomes, this procedure is not really necessary, such as FRT40A. With others, the larvae grow very poor. As a test for the culture conditions, always flies from the starter FRT stock as well as from the starter mutant stock are bred under the same conditions. Neomycin resistant offspring is tested by complementation with a deficiency or another independent allele affecting the locus of interest.

1.6 Slide preparation & imaging

Well fed crawling third instar larva, were prescreened for the appearance of clones under the fluorescent binocular. Larvae were dissected in 1x PBS, the discs immediately transferred to the slide containing a drop of S2 Schneider's medium surrounded by Voltalef Oil. The slide also contained two spacers on both sides (two small coverslides on both sides). After the dissection, the discs were flipped in the S2 medium to make sure the air sac faces upwards. The discs were allowed to settle on the slide the chamber was sealed with a cover slide.

Composition of S2 medium:

Schneider's insect medium (Invitrogen) supplemented with 10% Fetal Calf Serum, 2mM L-Glutamine, 50 units/ml Penicillin and 50µg/ml Streptomycin.

Images or time laps recordings were taken on a Leica TCS SP2 confocal system using the Leica Confocal Software. To avoid bleaching, laser power on the laser box was kept on the minimum and at lowest possible levels in the confocal software. Scan speed was performed with the fast mode. 15-40 focal sections were recorded for 3D scans with a spacing of 0.5-0.9 and with 15-25 focal sections for 4D scans. Each recording was averaged 4-6 times. For time lapses, recordings were repeated every 90-300s. Magnification was 20x Z4.0 for overview pictures and 40xZ4.0 for detailed pictures.

Pictures were reconstructed using Imaris (Bitplane) software (newest available version). Colors were adjusted and background reduced using the Imaris filters. Pictures were treated with Photoshop (newest available version).

1.7 Immunostainings and whole-mount *in situ* hybridization

Primary antibodies used were the tracheal lumen specific monoclonal antibody 2A12 (1:10), 22C10 highlighting the PNS, (1:5, kindly provided by B. Egger), α HRP-FITZ for visualizing the CNS (1:20, kindly provided by B. Egger), FasIII for visceral mesoderm and epidermis staining (1:30), α Vasa as a pole cell marker (1:1000, kindly provided by Th. Marty), phalloidin-TRITC, labeling filamentous actin (1:300), α Pio (1:2000, purified batch), α betaGal (1:500) as well as DAPI, (1:4000).

Secondary antibodies included α mouse/rabbit/rat Cy3/Cy5/FITC/TRITC (1:100 for Cy5, else 1:500).

Immunostainings on embryos as well as whole mount *in situs* were performed as previously described (Cabernard, 2000; Dossenbach, 2004).

Ovary immunostainings were performed as following (according to N. Grieder):

Ovaries were dissected in 1x Grace's medium (GIBCO BRL), equilibrated at room temperature (RT). Fixation was performed in a mixture of 400 μ l Grace's and 200 μ l 16 % EM-grade formaldehyde. After two rinses in 2x PBST (1x PBS, 0.1% TritonX-100), ovaries were washed twice for 10 min in PBST. Ovaries were blocked for at least 30 minutes in PBST-NGS/BSA (normal goat serum or Bovine serum). Primary antibody incubation was performed for either 4h at RT or overnight at 4°C. For phalloidin-TRITC stainings, incubation was performed for 30 minutes only. After rinsing and washing with 1x PBST secondary antibody incubation was performed for 2-4 h at RT. DAPI was added at the end for 6 min in 1x PBST (RT). After washing, ovaries were further dissected and mounted in Vectashield.

Immunostainings on imaginal discs were performed as following (according to M. Sato):

Freshly prepared 0.8% as well as 4% formaldehyde (FA) containing also 0.5% NP40 (in PBS) was precooled on ice. Dissected discs were transferred to 0.8% FA/PBS on ice. All discs were then transferred to 4% FA/PBS and fixed for 20 min on slow rotor. For dpERK stainings, 30 minute fixation using 8% FA/PBS is recommended. Discs were then transferred to 0.5%

NP40/PBS and permeabilized for 30 minutes. After several washes in PBST (1x PBS, 0.1% Tween or Triton), blocking was performed in 5-10% BSA/PBST for 30 minutes. Primary antibodies were incubated in 1% BSA/PBST for 1-2 h at RT. After washing in PBST, secondary antibody incubation was performed for 1 hour in 1% BSA/PBST. After washing, discs were removed from the cuticle and mounted on Vectashield.

In situ probes were generated by PCR. cDNA templates were amplified with primers matching the vector sequence 5' and 3' of the inserted cDNA and containing T7/T3/Sp6 sequences (if necessary). For PCR amplification of genomic templates, genomic DNA was isolated as following.

Approximately 5 flies were put into an eppendorf tube and kept on ice. The flies were homogenized using buffer A (100mM Tris/HCl 7.6), 100mM EDTA, 100mM NaCl, 0.5% SDS). 200µl 1.5 M KAc was added, mixed and chilled on ice for 10 minutes. After a 10 minute spin at highest speed (RT), 250µl of the supernatant were transferred to a fresh tube and eventually respinned to remove all debris. 150µl (0.6vol) of isopropanol was added to the supernatant (RT), vortexed, incubated for 5 minutes (RT) and spun for 5 minutes. The DNA pellet was washed with 70% of ethanol and resuspended in 100µl Tris-Cl.

1.8 Cloning of Rack1 rescue construct, transformants and rescue experiment.

The rack1 cDNA (kindly provided by Jym Mohler) was digested with EcoR1 (5' of rack1) and XbaI (3' of rack1) from bluescript and inserted into hsCasper using these enzymes. Clones were screened by PCR, sequenced and injected into yw flies. Transformants were recombined with *rack1^{Ey128}* isogenic flies. Recombinants were screened based on eye color and verified by PCR using primers flanking the hsCasper multiple cloning site.

Several independent recombinant lines were established. For the rescue experiment, hsRack1-*rack1^{Ey128}* recombinants were crossed to the alleles *rack1^{c04220}* and *rack1^{EMS1-8}*. Several heat-shocks were applied during development. Late heat-shocks, after 5-6 days of development also rescued lethality albeit at a lower frequency.

Transheterozygous females were put together with males in fresh vials and fed well. After 1 week, ovaries were dissected and stained as described above.

1.9 Generation of *rack1* clones in the germline, air sacs, imaginal discs and ovaries

Air sac clones were generated using the three *rack1* alleles and the MARCM stock CD8:GFP for FRT40A.

Imaginal disc clones were generated using the line hsFLP/hsFLP; ubiGFP FRT40A/ubiGFP FRT40A (kindly provided by Urs Kloter). Females of this line were crossed to *rack1*-FRT40 males (alleles *rack1*^{*Ey128*} and *rack1*^{*EMS1-8*} were used only). 24-48h old larvae were heat-shocked for 1h at 38°C. Discs were dissected and stained as described.

For ovary clones FLP/FRT, the same stocks were used. Females of the genotype hsFLP/+; *rack1*-FRT40A/ubiGFP FRT40A were fed well, heat-shocked two times within 12 h for 1h at 38°C and dissected one week later.

Clones in the germline using the ovoD/FRT method was performed as following. Males carrying ovoD FRT40A/Cyo were crossed to females of the genotype hsFLP/hsFLP; Sco/CyO. Again, male offspring of the genotype hsFLP/y; ovoD FRT40A/CyO were then crossed to *rack1*-FRT40A females. Clone induction was accomplished as for imaginal disc clones.

Epilogue

One of the most fascinating questions in biology is how to organize a group of cells into a well formed and shaped tissue containing the right number of cells as well as the correct cellular type. Interestingly, biology invented several mechanisms to achieve this task and where it fits best, one, several or all are applied. Thus, a biologist merely studies the individual case and tries to find some underlying principles which can be adapted to other cases as well as understood in a broad, general context. However, often the question starts with the problem, how to address this phenomena? What cellular type, tissue, organ and organism is best suited. Again, also here biologist, depending on their specific question and personal preference, have chosen different systems in order to tackle this and similar problems.

I think that *Drosophila* geneticists have not chosen all too bad. Although we just work with flies, the conservation of numerous genes and pathways justifies often the usage of this model organism. Great achievements have been and will be performed with this model system.

Beyond the choice of the system, biologist are united in the quest to understand the way nature works. Interestingly, nature does not seem to have a detailed plan unlike an architect who supervises the construction of a building.

For my part I tried to contribute to these broad questions by studying a small structure in the fruit fly *Drosophila melanogaster*. I hope thus that these studies, which are far from complete, will be taken up and continued.

And so, this report is at it's end. The story however continues.

V REFERENCES

- Adams, M. D., Celniker, S. E., Holt, R. A., Evans, C. A., Gocayne, J. D., Amanatides, P. G., Scherer, S. E., Li, P. W., Hoskins, R. A., Galle, R. F. et al.** (2000). The genome sequence of *Drosophila melanogaster*. *Science* **287**, 2185-95.
- Affolter, M., Bellusci, S., Itoh, N., Shilo, B., Thiery, J. P. and Werb, Z.** (2003). Tube or not tube: remodeling epithelial tissues by branching morphogenesis. *Dev Cell* **4**, 11-8.
- Affolter, M., Marty, T., Vigano, M. A. and Jazwinska, A.** (2001). Nuclear interpretation of Dpp signaling in *Drosophila*. *Embo J* **20**, 3298-305.
- Affolter, M., Montagne, J., Walldorf, U., Groppe, J., Kloter, U., LaRosa, M. and Gehring, W. J.** (1994). The *Drosophila* SRF homolog is expressed in a subset of tracheal cells and maps within a genomic region required for tracheal development. *Development* **120**, 743-53.
- Ahmad, S. M. and Baker, B. S.** (2002). Sex-specific deployment of FGF signaling in *Drosophila* recruits mesodermal cells into the male genital imaginal disc. *Cell* **109**, 651-61.
- Alcedo, J., Ayzenzon, M., Von Ohlen, T., Noll, M. and Hooper, J. E.** (1996). The *Drosophila* smoothed gene encodes a seven-pass membrane protein, a putative receptor for the hedgehog signal. *Cell* **86**, 221-32.
- Ang, L. H., Kim, J., Stepensky, V. and Hing, H.** (2003). Dock and Pak regulate olfactory axon pathfinding in *Drosophila*. *Development* **130**, 1307-16.
- Anselmo, A. N., Bumeister, R., Thomas, J. M. and White, M. A.** (2002). Critical contribution of linker proteins to Raf kinase activation. *J Biol Chem* **277**, 5940-3.
- Arber, S., Barbayannis, F. A., Hanser, H., Schneider, C., Stanyon, C. A., Bernard, O. and Caroni, P.** (1998). Regulation of actin dynamics through phosphorylation of cofilin by LIM-kinase. *Nature* **393**, 805-9.
- Arman, E., Haffner-Krausz, R., Gorivodsky, M. and Lonai, P.** (1999). Fgfr2 is required for limb outgrowth and lung-branching morphogenesis. *Proc Natl Acad Sci U S A* **96**, 11895-9.
- Bai, J., Uehara, Y. and Montell, D. J.** (2000). Regulation of invasive cell behavior by taiman, a *Drosophila* protein related to AIB1, a steroid receptor coactivator amplified in breast cancer. *Cell* **103**, 1047-58.
- Barrett, K., Leptin, M. and Settleman, J.** (1997). The Rho GTPase and a putative RhoGEF mediate a signaling pathway for the cell shape changes in *Drosophila* gastrulation. *Cell* **91**, 905-15.
- Basler, K. and Struhl, G.** (1994). Compartment boundaries and the control of *Drosophila* limb pattern by hedgehog protein. *Nature* **368**, 208-14.
- Battersby, A., Csiszar, A., Leptin, M. and Wilson, R.** (2003). Isolation of proteins that interact with the signal transduction molecule Dof and identification of a functional domain conserved between Dof and vertebrate BCAP. *J Mol Biol* **329**, 479-93.

- Beccari, S., Teixeira, L. and Rorth, P.** (2002). The JAK/STAT pathway is required for border cell migration during *Drosophila* oogenesis. *Mech Dev* **111**, 115-23.
- Beiman, M., Shilo, B. Z. and Volk, T.** (1996). Heartless, a *Drosophila* FGF receptor homolog, is essential for cell migration and establishment of several mesodermal lineages. *Genes Dev* **10**, 2993-3002.
- Beitel, G. J. and Krasnow, M. A.** (2000). Genetic control of epithelial tube size in the *Drosophila* tracheal system. *Development* **127**, 3271-82.
- Bellen, H. J., Levis, R. W., Liao, G., He, Y., Carlson, J. W., Tsang, G., Evans-Holm, M., Hiesinger, P. R., Schulze, K. L., Rubin, G. M. et al.** (2004). The BDGP gene disruption project: single transposon insertions associated with 40% of *Drosophila* genes. *Genetics* **167**, 761-81.
- Bellusci, S., Grindley, J., Emoto, H., Itoh, N. and Hogan, B. L.** (1997). Fibroblast growth factor 10 (FGF10) and branching morphogenesis in the embryonic mouse lung. *Development* **124**, 4867-78.
- Bellusci, S., Henderson, R., Winnier, G., Oikawa, T. and Hogan, B. L.** (1996). Evidence from normal expression and targeted misexpression that bone morphogenetic protein (Bmp-4) plays a role in mouse embryonic lung morphogenesis. *Development* **122**, 1693-702.
- Bilder, D., Li, M. and Perrimon, N.** (2000). Cooperative regulation of cell polarity and growth by *Drosophila* tumor suppressors. *Science* **289**, 113-6.
- Blair, S. S.** (2003). Genetic mosaic techniques for studying *Drosophila* development. *Development* **130**, 5065-72.
- Boilly, B., Vercoutter-Edouart, A. S., Hondermarck, H., Nurcombe, V. and Le Bourhis, X.** (2000). FGF signals for cell proliferation and migration through different pathways. *Cytokine Growth Factor Rev* **11**, 295-302.
- Botella, J. A., Kretschmar, D., Kiermayer, C., Feldmann, P., Hughes, D. A. and Schneuwly, S.** (2003). Deregulation of the Egfr/Ras signaling pathway induces age-related brain degeneration in the *Drosophila* mutant vap. *Mol Biol Cell* **14**, 241-50.
- Boube, M., Llimargas, M. and Casanova, J.** (2000). Cross-regulatory interactions among tracheal genes support a co-operative model for the induction of tracheal fates in the *Drosophila* embryo. *Mech Dev* **91**, 271-8.
- Bradley, P. L. and Andrew, D. J.** (2001). ribbon encodes a novel BTB/POZ protein required for directed cell migration in *Drosophila melanogaster*. *Development* **128**, 3001-15.
- Brand, A.** (1995). GFP in *Drosophila*. *Trends Genet* **11**, 324-5.
- Brand, A. H. and Perrimon, N.** (1993). Targeted gene expression as a means of altering cell fates and generating dominant phenotypes. *Development* **118**, 401-15.
- Brown, S., Hu, N. and Hombria, J. C.** (2001). Identification of the first invertebrate interleukin JAK/STAT receptor, the *Drosophila* gene domeless. *Curr Biol* **11**, 1700-5.

- Bruckner, K., Kockel, L., Duchek, P., Luque, C. M., Rorth, P. and Perrimon, N.** (2004). The PDGF/VEGF receptor controls blood cell survival in *Drosophila*. *Dev Cell* **7**, 73-84.
- Buensuceso, C. S., Woodside, D., Huff, J. L., Plopper, G. E. and O'Toole, T. E.** (2001). The WD protein Rack1 mediates protein kinase C and integrin-dependent cell migration. *J Cell Sci* **114**, 1691-8.
- Burke, R. and Basler, K.** (1996). Dpp receptors are autonomously required for cell proliferation in the entire developing *Drosophila* wing. *Development* **122**, 2261-9.
- Cabernard, C.** (2000). Yeast two-hybrid screen with Downstream of FGFR, a gene required for cell migration in the mesoderm and trachea of *Drosophila melanogaster*. In *Department of Cell Biology, Biozentrum, University of Basel*, (ed. Basel: University of Basel).
- Cabernard, C., Neumann, M. and Affolter, M.** (2004). Cellular and molecular mechanisms involved in branching morphogenesis of the *Drosophila* tracheal system. *J Appl Physiol* **97**, 2347-53.
- Campbell, R. E., Tour, O., Palmer, A. E., Steinbach, P. A., Baird, G. S., Zacharias, D. A. and Tsien, R. Y.** (2002). A monomeric red fluorescent protein. *Proc Natl Acad Sci U S A* **99**, 7877-82.
- Cant, K., Knowles, B. A., Mooseker, M. S. and Cooley, L.** (1994). *Drosophila* singed, a fascin homolog, is required for actin bundle formation during oogenesis and bristle extension. *J Cell Biol* **125**, 369-80.
- Cantley, L. C.** (2002). The phosphoinositide 3-kinase pathway. *Science* **296**, 1655-7.
- Cardoso, W. V.** (2000). Lung morphogenesis revisited: old facts, current ideas. *Dev Dyn* **219**, 121-30.
- Casci, T., Vinos, J. and Freeman, M.** (1999). Sprouty, an intracellular inhibitor of Ras signaling. *Cell* **96**, 655-65.
- Ceci, M., Gaviraghi, C., Gorrini, C., Sala, L. A., Offenhauser, N., Marchisio, P. C. and Biffo, S.** (2003). Release of eIF6 (p27BBP) from the 60S subunit allows 80S ribosome assembly. *Nature* **426**, 579-84.
- Chen, H. W., Chen, X., Oh, S. W., Marinissen, M. J., Gutkind, J. S. and Hou, S. X.** (2002). mom identifies a receptor for the *Drosophila* JAK/STAT signal transduction pathway and encodes a protein distantly related to the mammalian cytokine receptor family. *Genes Dev* **16**, 388-98.
- Chen, Y. and Struhl, G.** (1996). Dual roles for patched in sequestering and transducing Hedgehog. *Cell* **87**, 553-63.
- Chihara, T., Kato, K., Taniguchi, M., Ng, J. and Hayashi, S.** (2003). Rac promotes epithelial cell rearrangement during tracheal tubulogenesis in *Drosophila*. *Development* **130**, 1419-28.

- Cho, N. K., Keyes, L., Johnson, E., Heller, J., Ryner, L., Karim, F. and Krasnow, M. A.** (2002). Developmental control of blood cell migration by the *Drosophila* VEGF pathway. *Cell* **108**, 865-76.
- Chou, T. B. and Perrimon, N.** (1996). The autosomal FLP-DFS technique for generating germline mosaics in *Drosophila melanogaster*. *Genetics* **144**, 1673-9.
- Chuang, P. T. and McMahon, A. P.** (2003). Branching morphogenesis of the lung: new molecular insights into an old problem. *Trends Cell Biol* **13**, 86-91.
- Clyne, P. J., Brotman, J. S., Sweeney, S. T. and Davis, G.** (2003). Green fluorescent protein tagging *Drosophila* proteins at their native genomic loci with small P elements. *Genetics* **165**, 1433-41.
- Cohen, S. M.** (1993). Imaginal disc development. In *The Development of Drosophila melanogaster*, vol. Vol 2 (ed. A. M.-A. a. M. Bate), pp. 475-517. Cold Spring Harbor, New York: Cold Spring Harbor Laboratory Press.
- Cooley, L., Verheyen, E. and Ayers, K.** (1992). chickadee encodes a profilin required for intercellular cytoplasm transport during *Drosophila* oogenesis. *Cell* **69**, 173-84.
- Cox, E. A., Bennin, D., Doan, A. T., O'Toole, T. and Huttenlocher, A.** (2003). RACK1 regulates integrin-mediated adhesion, protrusion, and chemotactic cell migration via its Src-binding site. *Mol Biol Cell* **14**, 658-69.
- Dahmann, C. and Basler, K.** (2000). Opposing transcriptional outputs of Hedgehog signaling and engrailed control compartmental cell sorting at the *Drosophila* A/P boundary. *Cell* **100**, 411-22.
- Dammai, V., Adryan, B., Lavenburg, K. R. and Hsu, T.** (2003). *Drosophila* awd, the homolog of human nm23, regulates FGF receptor levels and functions synergistically with shi/dynamin during tracheal development. *Genes Dev* **17**, 2812-24.
- de Celis, J. F., Barrio, R. and Kafatos, F. C.** (1996). A gene complex acting downstream of dpp in *Drosophila* wing morphogenesis. *Nature* **381**, 421-4.
- De Jossineau, C., Soule, J., Martin, M., Anguille, C., Montcourrier, P. and Alexandre, D.** (2003). Delta-promoted filopodia mediate long-range lateral inhibition in *Drosophila*. *Nature* **426**, 555-9.
- de Maximy, A. A., Nakatake, Y., Moncada, S., Itoh, N., Thiery, J. P. and Bellusci, S.** (1999). Cloning and expression pattern of a mouse homologue of *drosophila* sprouty in the mouse embryo. *Mech Dev* **81**, 213-6.
- De Moerlooze, L., Spencer-Dene, B., Revest, J., Hajihosseini, M., Rosewell, I. and Dickson, C.** (2000). An important role for the IIIb isoform of fibroblast growth factor receptor 2 (FGFR2) in mesenchymal-epithelial signaling during mouse organogenesis. *Development* **127**, 483-92.

- Delon, I., Chanut-Delalande, H. and Payre, F.** (2003). The Ovo/Shavenbaby transcription factor specifies actin remodelling during epidermal differentiation in *Drosophila*. *Mech Dev* **120**, 747-58.
- Diaz-Benjumea, F. J. and Hafen, E.** (1994). The sevenless signaling cassette mediates *Drosophila* EGF receptor function during epidermal development. *Development* **120**, 569-78.
- Dodson, G. S., Guarnieri, D. J. and Simon, M. A.** (1998). Src64 is required for ovarian ring canal morphogenesis during *Drosophila* oogenesis. *Development* **125**, 2883-92.
- Dong, X., Zavitz, K. H., Thomas, B. J., Lin, M., Campbell, S. and Zipursky, S. L.** (1997). Control of G1 in the developing *Drosophila* eye: rca1 regulates Cyclin A. *Genes Dev* **11**, 94-105.
- Dossenbach, C.** (2004). Functional dissection of the *Drosophila melanogaster* Fibroblast Growth Factor signaling pathway in branching morphogenesis of the developing tracheal system. In *Biozentrum, dept. of cell biology*, (ed., pp. 151. Basel: University of Basel.
- Dossenbach, C., Rock, S. and Affolter, M.** (2001). Specificity of FGF signaling in cell migration in *Drosophila*. *Development* **128**, 4563-72.
- Douziech, M., Roy, F., Laberge, G., Lefrancois, M., Armengod, A. V. and Therrien, M.** (2003). Bimodal regulation of RAF by CNK in *Drosophila*. *Embo J* **22**, 5068-78.
- Duchek, P. and Rorth, P.** (2001a). Guidance of cell migration by EGF receptor signaling during *Drosophila* oogenesis. *Science* **291**, 131-3.
- Duchek, P., Somogyi, K., Jekely, G., Beccari, S. and Rorth, P.** (2001b). Guidance of cell migration by the *Drosophila* PDGF/VEGF receptor. *Cell* **107**, 17-26.
- Edgar, B. A., Lehman, D. A. and O'Farrell, P. H.** (1994). Transcriptional regulation of string (*cdc25*): a link between developmental programming and the cell cycle. *Development* **120**, 3131-43.
- Edgar, B. A. and O'Farrell, P. H.** (1989). Genetic control of cell division patterns in the *Drosophila* embryo. *Cell* **57**, 177-87.
- Edwards, K. A. and Kiehart, D. P.** (1996). *Drosophila* nonmuscle myosin II has multiple essential roles in imaginal disc and egg chamber morphogenesis. *Development* **122**, 1499-511.
- Erickson, M. R., Galletta, B. J. and Abmayr, S. M.** (1997). *Drosophila* myoblast city encodes a conserved protein that is essential for myoblast fusion, dorsal closure, and cytoskeletal organization. *J Cell Biol* **138**, 589-603.
- Eulenberg, K. G. and Schuh, R.** (1997). The tracheae defective gene encodes a bZIP protein that controls tracheal cell movement during *Drosophila* embryogenesis. *Embo J* **16**, 7156-65.
- Franch-Marro, X. and Casanova, J.** (2000). The alternative migratory pathways of the *Drosophila* tracheal cells are associated with distinct subsets of mesodermal cells. *Dev Biol* **227**, 80-90.

- Friedl, P.** (2004). Prespecification and plasticity: shifting mechanisms of cell migration. *Curr Opin Cell Biol* **16**, 14-23.
- Fulga, T. A. and Rorth, P.** (2002). Invasive cell migration is initiated by guided growth of long cellular extensions. *Nat Cell Biol* **4**, 715-9.
- Funamoto, S., Meili, R., Lee, S., Parry, L. and Firtel, R. A.** (2002). Spatial and temporal regulation of 3-phosphoinositides by PI 3-kinase and PTEN mediates chemotaxis. *Cell* **109**, 611-23.
- Furthauer, M., Lin, W., Ang, S. L., Thisse, B. and Thisse, C.** (2002). Sef is a feedback-induced antagonist of Ras/MAPK-mediated FGF signaling. *Nat Cell Biol* **4**, 170-4.
- Gabay, L., Seger, R. and Shilo, B. Z.** (1997). MAP kinase in situ activation atlas during Drosophila embryogenesis. *Development* **124**, 3535-41.
- Garcia-Higuera, I., Fenoglio, J., Li, Y., Lewis, C., Panchenko, M. P., Reiner, O., Smith, T. F. and Neer, E. J.** (1996). Folding of proteins with WD-repeats: comparison of six members of the WD-repeat superfamily to the G protein beta subunit. *Biochemistry* **35**, 13985-94.
- Garcia-Higuera, I., Gaitatzes, C., Smith, T. F. and Neer, E. J.** (1998). Folding a WD repeat propeller. Role of highly conserved aspartic acid residues in the G protein beta subunit and Sec13. *J Biol Chem* **273**, 9041-9.
- Garrity, P. A., Rao, Y., Salecker, I., McGlade, J., Pawson, T. and Zipursky, S. L.** (1996). Drosophila photoreceptor axon guidance and targeting requires the dreadlocks SH2/SH3 adapter protein. *Cell* **85**, 639-50.
- Gaul, U., Mardon, G. and Rubin, G. M.** (1992). A putative Ras GTPase activating protein acts as a negative regulator of signaling by the Sevenless receptor tyrosine kinase. *Cell* **68**, 1007-19.
- Geisbrecht, E. R. and Montell, D. J.** (2002). Myosin VI is required for E-cadherin-mediated border cell migration. *Nat Cell Biol* **4**, 616-20.
- Geisbrecht, E. R. and Montell, D. J.** (2004). A role for Drosophila IAP1-mediated caspase inhibition in Rac-dependent cell migration. *Cell* **118**, 111-25.
- Genova, J. L., Jong, S., Camp, J. T. and Fehon, R. G.** (2000). Functional analysis of Cdc42 in actin filament assembly, epithelial morphogenesis, and cell signaling during Drosophila development. *Dev Biol* **221**, 181-94.
- Ghabrial, A., Luschnig, S., Metzstein, M. M. and Krasnow, M. A.** (2003). Branching morphogenesis of the Drosophila tracheal system. *Annu Rev Cell Dev Biol* **19**, 623-47.
- Gibson, M. C. and Schubiger, G.** (2000). Peripodial cells regulate proliferation and patterning of Drosophila imaginal discs. *Cell* **103**, 343-50.

- Gisselbrecht, S., Skeath, J. B., Doe, C. Q. and Michelson, A. M.** (1996). heartless encodes a fibroblast growth factor receptor (DFR1/DFGF-R2) involved in the directional migration of early mesodermal cells in the *Drosophila* embryo. *Genes Dev* **10**, 3003-17.
- Goberdhan, D. C., Paricio, N., Goodman, E. C., Mlodzik, M. and Wilson, C.** (1999). *Drosophila* tumor suppressor PTEN controls cell size and number by antagonizing the Chico/PI3-kinase signaling pathway. *Genes Dev* **13**, 3244-58.
- Golic, K. G.** (1991). Site-specific recombination between homologous chromosomes in *Drosophila*. *Science* **252**, 958-61.
- Golic, K. G.** (1994). Local transposition of P elements in *Drosophila melanogaster* and recombination between duplicated elements using a site-specific recombinase. *Genetics* **137**, 551-63.
- Golic, K. G. and Golic, M. M.** (1996). Engineering the *Drosophila* genome: chromosome rearrangements by design. *Genetics* **144**, 1693-711.
- Golic, K. G. and Lindquist, S.** (1989). The FLP recombinase of yeast catalyzes site-specific recombination in the *Drosophila* genome. *Cell* **59**, 499-509.
- Grosskortenhaus, R. and Sprenger, F.** (2002). Rca1 inhibits APC-Cdh1(Fzr) and is required to prevent cyclin degradation in G2. *Dev Cell* **2**, 29-40.
- Gryzik, T. and Muller, H. A.** (2004). FGF8-like1 and FGF8-like2 encode putative ligands of the FGF receptor Htl and are required for mesoderm migration in the *Drosophila* gastrula. *Curr Biol* **14**, 659-67.
- Guild, G. M., Connelly, P. S., Shaw, M. K. and Tilney, L. G.** (1997). Actin filament cables in *Drosophila* nurse cells are composed of modules that slide passively past one another during dumping. *J Cell Biol* **138**, 783-97.
- Guillemin, K., Groppe, J., Ducker, K., Treisman, R., Hafen, E., Affolter, M. and Krasnow, M. A.** (1996). The pruned gene encodes the *Drosophila* serum response factor and regulates cytoplasmic outgrowth during terminal branching of the tracheal system. *Development* **122**, 1353-62.
- Hacker, U. and Perrimon, N.** (1998). DRhoGEF2 encodes a member of the Dbl family of oncogenes and controls cell shape changes during gastrulation in *Drosophila*. *Genes Dev* **12**, 274-84.
- Hacohen, N., Kramer, S., Sutherland, D., Hiromi, Y. and Krasnow, M. A.** (1998). sprouty encodes a novel antagonist of FGF signaling that patterns apical branching of the *Drosophila* airways. *Cell* **92**, 253-63.
- Hadari, Y. R., Gotoh, N., Kouhara, H., Lax, I. and Schlessinger, J.** (2001). Critical role for the docking-protein FRS2 alpha in FGF receptor-mediated signal transduction pathways. *Proc Natl Acad Sci U S A* **98**, 8578-83.

- Haddad, E., Zugaza, J. L., Louache, F., Debili, N., Crouin, C., Schwarz, K., Fischer, A., Vainchenker, W. and Bertoglio, J.** (2001). The interaction between Cdc42 and WASP is required for SDF-1-induced T-lymphocyte chemotaxis. *Blood* **97**, 33-8.
- Hakeda-Suzuki, S., Ng, J., Tzu, J., Dietzl, G., Sun, Y., Harms, M., Nardine, T., Luo, L. and Dickson, B. J.** (2002). Rac function and regulation during Drosophila development. *Nature* **416**, 438-42.
- Halfar, K., Rommel, C., Stocker, H. and Hafen, E.** (2001). Ras controls growth, survival and differentiation in the Drosophila eye by different thresholds of MAP kinase activity. *Development* **128**, 1687-96.
- Han, D. D., Stein, D. and Stevens, L. M.** (2000). Investigating the function of follicular subpopulations during Drosophila oogenesis through hormone-dependent enhancer-targeted cell ablation. *Development* **127**, 573-83.
- Heino, T. I., Karpanen, T., Wahlstrom, G., Pulkkinen, M., Eriksson, U., Alitalo, K. and Roos, C.** (2001). The Drosophila VEGF receptor homolog is expressed in hemocytes. *Mech Dev* **109**, 69-77.
- Hermanto, U., Zong, C. S., Li, W. and Wang, L. H.** (2002). RACK1, an insulin-like growth factor I (IGF-I) receptor-interacting protein, modulates IGF-I-dependent integrin signaling and promotes cell spreading and contact with extracellular matrix. *Mol Cell Biol* **22**, 2345-65.
- Hing, H., Xiao, J., Harden, N., Lim, L. and Zipursky, S. L.** (1999). Pak functions downstream of Dock to regulate photoreceptor axon guidance in Drosophila. *Cell* **97**, 853-63.
- Hogan, B. L.** (1999). Morphogenesis. *Cell* **96**, 225-33.
- Horwitz, R. and Webb, D.** (2003). Cell migration. *Curr Biol* **13**, R756-9.
- Hou, X. S., Chou, T. B., Melnick, M. B. and Perrimon, N.** (1995). The torso receptor tyrosine kinase can activate Raf in a Ras-independent pathway. *Cell* **81**, 63-71.
- Hudson, A. M. and Cooley, L.** (2002a). A subset of dynamic actin rearrangements in Drosophila requires the Arp2/3 complex. *J Cell Biol* **156**, 677-87.
- Hudson, A. M. and Cooley, L.** (2002b). Understanding the function of actin-binding proteins through genetic analysis of Drosophila oogenesis. *Annu Rev Genet* **36**, 455-88.
- Humbert, P., Russell, S. and Richardson, H.** (2003). Dlg, Scribble and Lgl in cell polarity, cell proliferation and cancer. *Bioessays* **25**, 542-53.
- Hutterer, A., Betschinger, J., Petronczki, M. and Knoblich, J. A.** (2004). Sequential roles of Cdc42, Par-6, aPKC, and Lgl in the establishment of epithelial polarity during Drosophila embryogenesis. *Dev Cell* **6**, 845-54.
- Imam, F., Sutherland, D., Huang, W. and Krasnow, M. A.** (1999). stumps, a Drosophila gene required for fibroblast growth factor (FGF)-directed migrations of tracheal and mesodermal cells. *Genetics* **152**, 307-18.

- Ip, Y. T. and Gridley, T.** (2002). Cell movements during gastrulation: snail dependent and independent pathways. *Curr Opin Genet Dev* **12**, 423-9.
- Isaac, D. D. and Andrew, D. J.** (1996). Tubulogenesis in Drosophila: a requirement for the tracheless gene product. *Genes Dev* **10**, 103-17.
- Itoh, N. and Ornitz, D. M.** (2004). Evolution of the Fgf and Fgfr gene families. *Trends Genet* **20**, 563-9.
- Jacinto, A. and Wolpert, L.** (2001). Filopodia. *Curr Biol* **11**, R634.
- Jacinto, A., Wood, W., Woolner, S., Hiley, C., Turner, L., Wilson, C., Martinez-Arias, A. and Martin, P.** (2002a). Dynamic analysis of actin cable function during Drosophila dorsal closure. *Curr Biol* **12**, 1245-50.
- Jacinto, A., Woolner, S. and Martin, P.** (2002b). Dynamic analysis of dorsal closure in Drosophila: from genetics to cell biology. *Dev Cell* **3**, 9-19.
- Jaglarz, M. K. and Howard, K. R.** (1994). Primordial germ cell migration in Drosophila melanogaster is controlled by somatic tissue. *Development* **120**, 83-9.
- Jaglarz, M. K. and Howard, K. R.** (1995). The active migration of Drosophila primordial germ cells. *Development* **121**, 3495-503.
- Jarecki, J., Johnson, E. and Krasnow, M. A.** (1999). Oxygen regulation of airway branching in Drosophila is mediated by branchless FGF. *Cell* **99**, 211-20.
- Javerzat, S., Auguste, P. and Bikfalvi, A.** (2002). The role of fibroblast growth factors in vascular development. *Trends Mol Med* **8**, 483-9.
- Jazwinska, A., Ribeiro, C. and Affolter, M.** (2003). Epithelial tube morphogenesis during Drosophila tracheal development requires Piopio, a luminal ZP protein. *Nat Cell Biol* **5**, 895-901.
- Jin, J., Anthopoulos, N., Wetsch, B., Binari, R. C., Isaac, D. D., Andrew, D. J., Woodgett, J. R. and Manoukian, A. S.** (2001). Regulation of Drosophila tracheal system development by protein kinase B. *Dev Cell* **1**, 817-27.
- Johnson Hamlet, M. R. and Perkins, L. A.** (2001). Analysis of corkscrew signaling in the Drosophila epidermal growth factor receptor pathway during myogenesis. *Genetics* **159**, 1073-87.
- Johnston, G. C., Pringle, J. R. and Hartwell, L. H.** (1977). Coordination of growth with cell division in the yeast *Saccharomyces cerevisiae*. *Exp Cell Res* **105**, 79-98.
- Kamimura, K., Fujise, M., Villa, F., Izumi, S., Habuchi, H., Kimata, K. and Nakato, H.** (2001). Drosophila heparan sulfate 6-O-sulfotransferase (dHS6ST) gene. Structure, expression, and function in the formation of the tracheal system. *J Biol Chem* **276**, 17014-21.
- Keenan, C. and Kelleher, D.** (1998). Protein kinase C and the cytoskeleton. *Cell Signal* **10**, 225-32.

- Kelso, R. J., Buszczak, M., Quinones, A. T., Castiblanco, C., Mazzalupo, S. and Cooley, L.** (2004). Flytrap, a database documenting a GFP protein-trap insertion screen in *Drosophila melanogaster*. *Nucleic Acids Res* **32 Database issue**, D418-20.
- Kim, H. J. and Bar-Sagi, D.** (2004). Modulation of signaling by Sprouty: a developing story. *Nat Rev Mol Cell Biol* **5**, 441-50.
- Klamt, C., Glazer, L. and Shilo, B. Z.** (1992). *breathless*, a *Drosophila* FGF receptor homolog, is essential for migration of tracheal and specific midline glial cells. *Genes Dev* **6**, 1668-78.
- Klein, T.** (2001). Wing disc development in the fly: the early stages. *Curr Opin Genet Dev* **11**, 470-5.
- Knust, E. and Muller, H. J.** (1998). *Drosophila* morphogenesis: orchestrating cell rearrangements. *Curr Biol* **8**, R853-5.
- Kobielak, A. and Fuchs, E.** (2004). Alpha-catenin: at the junction of intercellular adhesion and actin dynamics. *Nat Rev Mol Cell Biol* **5**, 614-25.
- Kouhara, H., Hadari, Y. R., Spivak-Kroizman, T., Schilling, J., Bar-Sagi, D., Lax, I. and Schlessinger, J.** (1997). A lipid-anchored Grb2-binding protein that links FGF-receptor activation to the Ras/MAPK signaling pathway. *Cell* **89**, 693-702.
- Kramer, S., Okabe, M., Hacohen, N., Krasnow, M. A. and Hiromi, Y.** (1999). Sprouty: a common antagonist of FGF and EGF signaling pathways in *Drosophila*. *Development* **126**, 2515-25.
- Krishnan, K. S., Rikhy, R., Rao, S., Shivalkar, M., Mosko, M., Narayanan, R., Etter, P., Estes, P. S. and Ramaswami, M.** (2001). Nucleoside diphosphate kinase, a source of GTP, is required for dynamin-dependent synaptic vesicle recycling. *Neuron* **30**, 197-210.
- Kunwar, P. S., Starz-Gaiano, M., Bainton, R. J., Heberlein, U. and Lehmann, R.** (2003). Tre1, a G protein-coupled receptor, directs transepithelial migration of *Drosophila* germ cells. *PLoS Biol* **1**, E80.
- Lai, K. M., Olivier, J. P., Gish, G. D., Henkemeyer, M., McGlade, J. and Pawson, T.** (1995). A *Drosophila* *shc* gene product is implicated in signaling by the DER receptor tyrosine kinase. *Mol Cell Biol* **15**, 4810-8.
- Lebeche, D., Malpel, S. and Cardoso, W. V.** (1999). Fibroblast growth factor interactions in the developing lung. *Mech Dev* **86**, 125-36.
- Lee, T., Feig, L. and Montell, D. J.** (1996a). Two distinct roles for Ras in a developmentally regulated cell migration. *Development* **122**, 409-18.
- Lee, T., Hacohen, N., Krasnow, M. and Montell, D. J.** (1996b). Regulated *Breathless* receptor tyrosine kinase activity required to pattern cell migration and branching in the *Drosophila* tracheal system. *Genes Dev* **10**, 2912-21.

- Lee, T. and Luo, L.** (1999). Mosaic analysis with a repressible cell marker for studies of gene function in neuronal morphogenesis. *Neuron* **22**, 451-61.
- Lee, T. and Luo, L.** (2001). Mosaic analysis with a repressible cell marker (MARCM) for *Drosophila* neural development. *Trends Neurosci* **24**, 251-4.
- Leptin, M.** (1999). Gastrulation in *Drosophila*: the logic and the cellular mechanisms. *Embo J* **18**, 3187-92.
- Li, J., Xia, F. and Li, W. X.** (2003). Coactivation of STAT and Ras is required for germ cell proliferation and invasive migration in *Drosophila*. *Dev Cell* **5**, 787-98.
- Li, W. X.** (2004). Receptor Tyrosine Kinase Signaling and Primordial Germ Cell Development. *Cell Cycle* **3**, 249-251.
- Lin, X., Buff, E. M., Perrimon, N. and Michelson, A. M.** (1999). Heparan sulfate proteoglycans are essential for FGF receptor signaling during *Drosophila* embryonic development. *Development* **126**, 3715-23.
- Liu, W. S. and Heckman, C. A.** (1998). The sevenfold way of PKC regulation. *Cell Signal* **10**, 529-42.
- Liu, Y. and Montell, D. J.** (1999). Identification of mutations that cause cell migration defects in mosaic clones. *Development* **126**, 1869-78.
- Liu, Y. and Montell, D. J.** (2001). Jing: a downstream target of slbo required for developmental control of border cell migration. *Development* **128**, 321-30.
- Locascio, A. and Nieto, M. A.** (2001). Cell movements during vertebrate development: integrated tissue behaviour versus individual cell migration. *Curr Opin Genet Dev* **11**, 464-9.
- Lu, H. C., Swindell, E. C., Sierralta, W. D., Eichele, G. and Thaller, C.** (2001). Evidence for a role of protein kinase C in FGF signal transduction in the developing chick limb bud. *Development* **128**, 2451-60.
- Luo, L.** (2000). Rho GTPases in neuronal morphogenesis. *Nat Rev Neurosci* **1**, 173-80.
- Luschnig, S., Krauss, J., Bohmann, K., Desjeux, I. and Nusslein-Volhard, C.** (2000). The *Drosophila* SHC adaptor protein is required for signaling by a subset of receptor tyrosine kinases. *Mol Cell* **5**, 231-41.
- Macara, I. G.** (2004). Parsing the polarity code. *Nat Rev Mol Cell Biol* **5**, 220-31.
- Mailleux, A. A., Tefft, D., Ndiaye, D., Itoh, N., Thiery, J. P., Warburton, D. and Bellusci, S.** (2001). Evidence that SPROUTY2 functions as an inhibitor of mouse embryonic lung growth and morphogenesis. *Mech Dev* **102**, 81-94.
- Mandler, M. and Neubuser, A.** (2004). FGF signaling is required for initiation of feather placode development. *Development* **131**, 3333-43.

- Manes, T., Zheng, D. Q., Tognin, S., Woodard, A. S., Marchisio, P. C. and Languino, L. R.** (2003). Alpha(v)beta3 integrin expression up-regulates cdc2, which modulates cell migration. *J Cell Biol* **161**, 817-26.
- Manning, G. and Krasnow, M. A.** (1993). Development of the *Drosophila* tracheal system. In *The development of Drosophila melanogaster*, vol. Volume I (ed. M. Bate and A. Martinez Arias), pp. 609-685: Cold Spring Harbor Laboratory press.
- McCahill, A., Warwicker, J., Bolger, G. B., Houslay, M. D. and Yarwood, S. J.** (2002). The RACK1 scaffold protein: a dynamic cog in cell response mechanisms. *Mol Pharmacol* **62**, 1261-73.
- McDonald, J. A., Pinheiro, E. M. and Montell, D. J.** (2003). PVF1, a PDGF/VEGF homolog, is sufficient to guide border cells and interacts genetically with Taiman. *Development* **130**, 3469-78.
- McLeod, M., Shor, B., Caporaso, A., Wang, W., Chen, H. and Hu, L.** (2000). Cpc2, a fission yeast homologue of mammalian RACK1 protein, interacts with Ran1 (Pat1) kinase To regulate cell cycle progression and meiotic development. *Mol Cell Biol* **20**, 4016-27.
- Michelson, A. M., Gisselbrecht, S., Buff, E. and Skeath, J. B.** (1998a). Heartbroken is a specific downstream mediator of FGF receptor signaling in *Drosophila*. *Development* **125**, 4379-89.
- Michelson, A. M., Gisselbrecht, S., Zhou, Y., Baek, K. H. and Buff, E. M.** (1998b). Dual functions of the heartless fibroblast growth factor receptor in development of the *Drosophila* embryonic mesoderm. *Dev Genet* **22**, 212-29.
- Min, H., Danilenko, D. M., Scully, S. A., Bolon, B., Ring, B. D., Tarpley, J. E., DeRose, M. and Simonet, W. S.** (1998). Fgf-10 is required for both limb and lung development and exhibits striking functional similarity to *Drosophila* branchless. *Genes Dev* **12**, 3156-61.
- Minowada, G., Jarvis, L. A., Chi, C. L., Neubuser, A., Sun, X., Hacoheh, N., Krasnow, M. A. and Martin, G. R.** (1999). Vertebrate Sprouty genes are induced by FGF signaling and can cause chondrodysplasia when overexpressed. *Development* **126**, 4465-75.
- Miralles, F., Posern, G., Zaromytidou, A. I. and Treisman, R.** (2003). Actin dynamics control SRF activity by regulation of its coactivator MAL. *Cell* **113**, 329-42.
- Montagne, J., Groppe, J., Guillemin, K., Krasnow, M. A., Gehring, W. J. and Affolter, M.** (1996). The *Drosophila* Serum Response Factor gene is required for the formation of intervein tissue of the wing and is allelic to blistered. *Development* **122**, 2589-97.
- Montell, D. J.** (2003). Border-cell migration: the race is on. *Nat Rev Mol Cell Biol* **4**, 13-24.
- Montell, D. J., Rorth, P. and Spradling, A. C.** (1992). slow border cells, a locus required for a developmentally regulated cell migration during oogenesis, encodes *Drosophila* C/EBP. *Cell* **71**, 51-62.

- Moore, L. A., Broihier, H. T., Van Doren, M., Lunsford, L. B. and Lehmann, R.** (1998). Identification of genes controlling germ cell migration and embryonic gonad formation in *Drosophila*. *Development* **125**, 667-78.
- Morin, X., Daneman, R., Zavortink, M. and Chia, W.** (2001). A protein trap strategy to detect GFP-tagged proteins expressed from their endogenous loci in *Drosophila*. *Proc Natl Acad Sci U S A* **98**, 15050-5.
- Murphy, A. M., Lee, T., Andrews, C. M., Shilo, B. Z. and Montell, D. J.** (1995). The breathless FGF receptor homolog, a downstream target of *Drosophila* C/EBP in the developmental control of cell migration. *Development* **121**, 2255-63.
- Murphy, A. M. and Montell, D. J.** (1996). Cell type-specific roles for Cdc42, Rac, and RhoL in *Drosophila* oogenesis. *J Cell Biol* **133**, 617-30.
- Nellen, D., Affolter, M. and Basler, K.** (1994). Receptor serine/threonine kinases implicated in the control of *Drosophila* body pattern by decapentaplegic. *Cell* **78**, 225-37.
- Ng, J., Nardine, T., Harms, M., Tzu, J., Goldstein, A., Sun, Y., Dietzl, G., Dickson, B. J. and Luo, L.** (2002). Rac GTPases control axon growth, guidance and branching. *Nature* **416**, 442-7.
- Niewiadomska, P., Godt, D. and Tepass, U.** (1999). DE-Cadherin is required for intercellular motility during *Drosophila* oogenesis. *J Cell Biol* **144**, 533-47.
- Nolan, K. M., Barrett, K., Lu, Y., Hu, K. Q., Vincent, S. and Settleman, J.** (1998). Myoblast city, the *Drosophila* homolog of DOCK180/CED-5, is required in a Rac signaling pathway utilized for multiple developmental processes. *Genes Dev* **12**, 3337-42.
- Nusslein-Volhard, C. and Wieschaus, E.** (1980). Mutations affecting segment number and polarity in *Drosophila*. *Nature* **287**, 795-801.
- Oda, H. and Tsukita, S.** (1999). Dynamic features of adherens junctions during *Drosophila* embryonic epithelial morphogenesis revealed by a α -catenin-GFP fusion protein. *Dev Genes Evol* **209**, 218-25.
- Ohshiro, T. and Saigo, K.** (1997). Transcriptional regulation of breathless FGF receptor gene by binding of TRACHEALESS/dARNT heterodimers to three central midline elements in *Drosophila* developing trachea. *Development* **124**, 3975-86.
- Okada, T., Maeda, A., Iwamatsu, A., Gotoh, K. and Kurosaki, T.** (2000). BCAP: the tyrosine kinase substrate that connects B cell receptor to phosphoinositide 3-kinase activation. *Immunity* **13**, 817-27.
- Olivier, J. P., Raabe, T., Henkemeyer, M., Dickson, B., Mbamalu, G., Margolis, B., Schlessinger, J., Hafen, E. and Pawson, T.** (1993). A *Drosophila* SH2-SH3 adaptor protein implicated in coupling the sevenless tyrosine kinase to an activator of Ras guanine nucleotide exchange, Sos. *Cell* **73**, 179-91.
- Ong, S. H., Hadari, Y. R., Gotoh, N., Guy, G. R., Schlessinger, J. and Lax, I.** (2001). Stimulation of phosphatidylinositol 3-kinase by fibroblast growth factor receptors is mediated

by coordinated recruitment of multiple docking proteins. *Proc Natl Acad Sci U S A* **98**, 6074-9.

Ornitz, D. M. (2000). FGFs, heparan sulfate and FGFRs: complex interactions essential for development. *Bioessays* **22**, 108-12.

Ornitz, D. M. and Itoh, N. (2001). Fibroblast growth factors. *Genome Biol* **2**, REVIEWS3005.

Payre, F., Vincent, A. and Carreno, S. (1999). *ovo/svb* integrates Wingless and DER pathways to control epidermis differentiation. *Nature* **400**, 271-5.

Pepicelli, C. V., Lewis, P. M. and McMahon, A. P. (1998). Sonic hedgehog regulates branching morphogenesis in the mammalian lung. *Curr Biol* **8**, 1083-6.

Perkins, L. A., Johnson, M. R., Melnick, M. B. and Perrimon, N. (1996). The nonreceptor protein tyrosine phosphatase corkscrew functions in multiple receptor tyrosine kinase pathways in *Drosophila*. *Dev Biol* **180**, 63-81.

Perkins, L. A., Larsen, I. and Perrimon, N. (1992). corkscrew encodes a putative protein tyrosine phosphatase that functions to transduce the terminal signal from the receptor tyrosine kinase torso. *Cell* **70**, 225-36.

Peters, K., Werner, S., Liao, X., Wert, S., Whitsett, J. and Williams, L. (1994). Targeted expression of a dominant negative FGF receptor blocks branching morphogenesis and epithelial differentiation of the mouse lung. *Embo J* **13**, 3296-301.

Petit, V., Nussbaumer, U., Dossenbach, C. and Affolter, M. (2004). Downstream-of-FGFR is a fibroblast growth factor-specific scaffolding protein and recruits Corkscrew upon receptor activation. *Mol Cell Biol* **24**, 3769-81.

Petit, V., Ribeiro, C., Ebner, A. and Affolter, M. (2002). Regulation of cell migration during tracheal development in *Drosophila melanogaster*. *Int J Dev Biol* **46**, 125-32.

Pinheiro, E. M. and Montell, D. J. (2004). Requirement for Par-6 and Bazooka in *Drosophila* border cell migration. *Development* **131**, 5243-51.

Pollard, T. D. and Borisy, G. G. (2003). Cellular motility driven by assembly and disassembly of actin filaments. *Cell* **112**, 453-65.

Powers, C. J., McLeskey, S. W. and Wellstein, A. (2000). Fibroblast growth factors, their receptors and signaling. *Endocr Relat Cancer* **7**, 165-97.

Prober, D. A. and Edgar, B. A. (2000). Ras1 promotes cellular growth in the *Drosophila* wing. *Cell* **100**, 435-46.

Prokopenko, S. N., Brumby, A., O'Keefe, L., Prior, L., He, Y., Saint, R. and Bellen, H. J. (1999). A putative exchange factor for Rho1 GTPase is required for initiation of cytokinesis in *Drosophila*. *Genes Dev* **13**, 2301-14.

- Raabe, T., Olivier, J. P., Dickson, B., Liu, X., Gish, G. D., Pawson, T. and Hafen, E.** (1995). Biochemical and genetic analysis of the Drk SH2/SH3 adaptor protein of *Drosophila*. *Embo J* **14**, 2509-18.
- Raffioni, S., Thomas, D., Foehr, E. D., Thompson, L. M. and Bradshaw, R. A.** (1999). Comparison of the intracellular signaling responses by three chimeric fibroblast growth factor receptors in PC12 cells. *Proc Natl Acad Sci U S A* **96**, 7178-83.
- Raftopoulou, M. and Hall, A.** (2004). Cell migration: Rho GTPases lead the way. *Dev Biol* **265**, 23-32.
- Raz, E.** (2004). Guidance of primordial germ cell migration. *Curr Opin Cell Biol* **16**, 169-73.
- Reich, A., Sapir, A. and Shilo, B.** (1999). Sprouty is a general inhibitor of receptor tyrosine kinase signaling. *Development* **126**, 4139-47.
- Reichman-Fried, M., Dickson, B., Hafen, E. and Shilo, B. Z.** (1994). Elucidation of the role of breathless, a *Drosophila* FGF receptor homolog, in tracheal cell migration. *Genes Dev* **8**, 428-39.
- Reichman-Fried, M. and Shilo, B. Z.** (1995). Breathless, a *Drosophila* FGF receptor homolog, is required for the onset of tracheal cell migration and tracheole formation. *Mech Dev* **52**, 265-73.
- Renault, A. D., Sigal, Y. J., Morris, A. J. and Lehmann, R.** (2004). Soma-Germline Competition for Lipid Phosphate Uptake Regulates Germ Cell Migration and Survival. *Science*.
- Resino, J., Salama-Cohen, P. and Garcia-Bellido, A.** (2002). Determining the role of patterned cell proliferation in the shape and size of the *Drosophila* wing. *Proc Natl Acad Sci U S A* **99**, 7502-7.
- Ribeiro, C., Ebner, A. and Affolter, M.** (2002). In vivo imaging reveals different cellular functions for FGF and Dpp signaling in tracheal branching morphogenesis. *Dev Cell* **2**, 677-83.
- Ribeiro, C., Petit, V. and Affolter, M.** (2003). Signaling systems, guided cell migration, and organogenesis: insights from genetic studies in *Drosophila*. *Dev Biol* **260**, 1-8.
- Ridley, A. J.** (2001). Rho family proteins: coordinating cell responses. *Trends Cell Biol* **11**, 471-7.
- Ridley, A. J., Schwartz, M. A., Burridge, K., Firtel, R. A., Ginsberg, M. H., Borisy, G., Parsons, J. T. and Horwitz, A. R.** (2003). Cell migration: integrating signals from front to back. *Science* **302**, 1704-9.
- Riento, K. and Ridley, A. J.** (2003). Rocks: multifunctional kinases in cell behaviour. *Nat Rev Mol Cell Biol* **4**, 446-56.

- Riesgo-Escovar, J. R., Jenni, M., Fritz, A. and Hafen, E.** (1996). The Drosophila Jun-N-terminal kinase is required for cell morphogenesis but not for DJun-dependent cell fate specification in the eye. *Genes Dev* **10**, 2759-68.
- Robinson, D. N., Cant, K. and Cooley, L.** (1994). Morphogenesis of Drosophila ovarian ring canals. *Development* **120**, 2015-25.
- Rommel, C. and Hafen, E.** (1998). Ras--a versatile cellular switch. *Curr Opin Genet Dev* **8**, 412-8.
- Rorth, P.** (1996). A modular misexpression screen in Drosophila detecting tissue-specific phenotypes. *Proc Natl Acad Sci U S A* **93**, 12418-22.
- Rorth, P.** (2002). Initiating and guiding migration: lessons from border cells. *Trends Cell Biol* **12**, 325-31.
- Rorth, P. and Montell, D. J.** (1992). Drosophila C/EBP: a tissue-specific DNA-binding protein required for embryonic development. *Genes Dev* **6**, 2299-311.
- Rorth, P., Szabo, K. and Texido, G.** (2000). The level of C/EBP protein is critical for cell migration during Drosophila oogenesis and is tightly controlled by regulated degradation. *Mol Cell* **6**, 23-30.
- Rosin, D., Schejter, E., Volk, T. and Shilo, B. Z.** (2004). Apical accumulation of the Drosophila PDGF/VEGF receptor ligands provides a mechanism for triggering localized actin polymerization. *Development* **131**, 1939-48.
- Roy, F., Laberge, G., Douziech, M., Ferland-McCollough, D. and Therrien, M.** (2002). KSR is a scaffold required for activation of the ERK/MAPK module. *Genes Dev* **16**, 427-38.
- Samakovlis, C., Hacohen, N., Manning, G., Sutherland, D. C., Guillemin, K. and Krasnow, M. A.** (1996a). Development of the Drosophila tracheal system occurs by a series of morphologically distinct but genetically coupled branching events. *Development* **122**, 1395-407.
- Samakovlis, C., Manning, G., Steneberg, P., Hacohen, N., Cantera, R. and Krasnow, M. A.** (1996b). Genetic control of epithelial tube fusion during Drosophila tracheal development. *Development* **122**, 3531-6.
- Santos, A. C. and Lehmann, R.** (2004a). Germ cell specification and migration in Drosophila and beyond. *Curr Biol* **14**, R578-89.
- Santos, A. C. and Lehmann, R.** (2004b). Isoprenoids control germ cell migration downstream of HMGCoA reductase. *Dev Cell* **6**, 283-93.
- Sasaki, A. T., Chun, C., Takeda, K. and Firtel, R. A.** (2004). Localized Ras signaling at the leading edge regulates PI3K, cell polarity, and directional cell movement. *J Cell Biol* **167**, 505-18.
- Sato, M. and Kornberg, T. B.** (2002). FGF is an essential mitogen and chemoattractant for the air sacs of the drosophila tracheal system. *Dev Cell* **3**, 195-207.

- Schechtman, D. and Mochly-Rosen, D.** (2001). Adaptor proteins in protein kinase C-mediated signal transduction. *Oncogene* **20**, 6339-47.
- Schejter, E. D. and Shilo, B. Z.** (1989). The Drosophila EGF receptor homolog (DER) gene is allelic to faint little ball, a locus essential for embryonic development. *Cell* **56**, 1093-104.
- Schnorr, J. D., Holdcraft, R., Chevalier, B. and Berg, C. A.** (2001). Ras1 interacts with multiple new signaling and cytoskeletal loci in Drosophila eggshell patterning and morphogenesis. *Genetics* **159**, 609-22.
- Schumacher, S., Gryzik, T., Tannebaum, S. and Muller, H. A.** (2004). The RhoGEF Pebble is required for cell shape changes during cell migration triggered by the Drosophila FGF receptor Heartless. *Development* **131**, 2631-40.
- Sears, H. C., Kennedy, C. J. and Garrity, P. A.** (2003). Macrophage-mediated corpse engulfment is required for normal Drosophila CNS morphogenesis. *Development* **130**, 3557-65.
- Sekine, K., Ohuchi, H., Fujiwara, M., Yamasaki, M., Yoshizawa, T., Sato, T., Yagishita, N., Matsui, D., Koga, Y., Itoh, N. et al.** (1999). Fgf10 is essential for limb and lung formation. *Nat Genet* **21**, 138-41.
- Sengupta, J., Nilsson, J., Gursky, R., Spahn, C. M., Nissen, P. and Frank, J.** (2004). Identification of the versatile scaffold protein RACK1 on the eukaryotic ribosome by cryo-EM. *Nat Struct Mol Biol* **11**, 957-62.
- Sepp, K. J. and Auld, V. J.** (2003). RhoA and Rac1 GTPases mediate the dynamic rearrangement of actin in peripheral glia. *Development* **130**, 1825-35.
- Shilo, B. Z.** (2003). Signaling by the Drosophila epidermal growth factor receptor pathway during development. *Exp Cell Res* **284**, 140-9.
- Shim, K., Blake, K. J., Jack, J. and Krasnow, M. A.** (2001). The Drosophila ribbon gene encodes a nuclear BTB domain protein that promotes epithelial migration and morphogenesis. *Development* **128**, 4923-33.
- Shishido, E., Higashijima, S., Emori, Y. and Saigo, K.** (1993). Two FGF-receptor homologues of Drosophila: one is expressed in mesodermal primordium in early embryos. *Development* **117**, 751-61.
- Sigrist, S., Ried, G. and Lehner, C. F.** (1995). Dmcdc2 kinase is required for both meiotic divisions during Drosophila spermatogenesis and is activated by the Twine/cdc25 phosphatase. *Mech Dev* **53**, 247-60.
- Silver, D. L. and Montell, D. J.** (2001). Paracrine signaling through the JAK/STAT pathway activates invasive behavior of ovarian epithelial cells in Drosophila. *Cell* **107**, 831-41.
- Silver, S. J., Chen, F., Doyon, L., Zink, A. W. and Rebay, I.** (2004). New class of Son-of-sevenless (Sos) alleles highlights the complexities of Sos function. *Genesis* **39**, 263-72.

- Simon, M. A., Dodson, G. S. and Rubin, G. M.** (1993). An SH3-SH2-SH3 protein is required for p21Ras1 activation and binds to sevenless and Sos proteins in vitro. *Cell* **73**, 169-77.
- Simpson, P. and Morata, G.** (1981). Differential mitotic rates and patterns of growth in compartments in the Drosophila wing. *Dev Biol* **85**, 299-308.
- Smallhorn, M., Murray, M. J. and Saint, R.** (2004). The epithelial-mesenchymal transition of the Drosophila mesoderm requires the Rho GTP exchange factor Pebble. *Development* **131**, 2641-51.
- Smith, T. F., Gaitatzes, C., Saxena, K. and Neer, E. J.** (1999). The WD repeat: a common architecture for diverse functions. *Trends Biochem Sci* **24**, 181-5.
- Somers, W. G. and Saint, R.** (2003). A RhoGEF and Rho family GTPase-activating protein complex links the contractile ring to cortical microtubules at the onset of cytokinesis. *Dev Cell* **4**, 29-39.
- Somogyi, K. and Rorth, P.** (2004). Evidence for tension-based regulation of Drosophila MAL and SRF during invasive cell migration. *Dev Cell* **7**, 85-93.
- Starz-Gaiano, M., Cho, N. K., Forbes, A. and Lehmann, R.** (2001). Spatially restricted activity of a Drosophila lipid phosphatase guides migrating germ cells. *Development* **128**, 983-91.
- Starz-Gaiano, M. and Lehmann, R.** (2001). Moving towards the next generation. *Mech Dev* **105**, 5-18.
- Stathopoulos, A., Tam, B., Ronshaugen, M., Frasch, M. and Levine, M.** (2004). pyramus and thisbe: FGF genes that pattern the mesoderm of Drosophila embryos. *Genes Dev* **18**, 687-99.
- Steeg, P. S., Bevilacqua, G., Kopper, L., Thorgeirsson, U. P., Talmadge, J. E., Liotta, L. A. and Sobel, M. E.** (1988). Evidence for a novel gene associated with low tumor metastatic potential. *J Natl Cancer Inst* **80**, 200-4.
- Stein, J. A., Broihier, H. T., Moore, L. A. and Lehmann, R.** (2002). Slow as molasses is required for polarized membrane growth and germ cell migration in Drosophila. *Development* **129**, 3925-34.
- Stocker, H., Andjelkovic, M., Oldham, S., Laffargue, M., Wymann, M. P., Hemmings, B. A. and Hafen, E.** (2002). Living with lethal PIP3 levels: viability of flies lacking PTEN restored by a PH domain mutation in Akt/PKB. *Science* **295**, 2088-91.
- Stocker, H. and Hafen, E.** (2000). Genetic control of cell size. *Curr Opin Genet Dev* **10**, 529-35.
- Stone, D. M., Hynes, M., Armanini, M., Swanson, T. A., Gu, Q., Johnson, R. L., Scott, M. P., Pennica, D., Goddard, A., Phillips, H. et al.** (1996). The tumour-suppressor gene patched encodes a candidate receptor for Sonic hedgehog. *Nature* **384**, 129-34.

- Sutherland, D., Samakovlis, C. and Krasnow, M. A.** (1996). branchless encodes a Drosophila FGF homolog that controls tracheal cell migration and the pattern of branching. *Cell* **87**, 1091-101.
- Tepass, U., Fessler, L. I., Aziz, A. and Hartenstein, V.** (1994). Embryonic origin of hemocytes and their relationship to cell death in Drosophila. *Development* **120**, 1829-37.
- Tepass, U., Gruszynski-DeFeo, E., Haag, T. A., Omatyar, L., Torok, T. and Hartenstein, V.** (1996). shotgun encodes Drosophila E-cadherin and is preferentially required during cell rearrangement in the neurectoderm and other morphogenetically active epithelia. *Genes Dev* **10**, 672-85.
- Tepass, U., Tanentzapf, G., Ward, R. and Fehon, R.** (2001). Epithelial cell polarity and cell junctions in Drosophila. *Annu Rev Genet* **35**, 747-84.
- Therrien, M., Chang, H. C., Solomon, N. M., Karim, F. D., Wassarman, D. A. and Rubin, G. M.** (1995). KSR, a novel protein kinase required for RAS signal transduction. *Cell* **83**, 879-88.
- Therrien, M., Wong, A. M. and Rubin, G. M.** (1998). CNK, a RAF-binding multidomain protein required for RAS signaling. *Cell* **95**, 343-53.
- Thorpe, J. L., Doitsidou, M., Ho, S. Y., Raz, E. and Farber, S. A.** (2004). Germ cell migration in zebrafish is dependent on HMGC_oA reductase activity and prenylation. *Dev Cell* **6**, 295-302.
- Timmons, L., Hersperger, E., Woodhouse, E., Xu, J., Liu, L. Z. and Shearn, A.** (1993). The expression of the Drosophila awd gene during normal development and in neoplastic brain tumors caused by lgl mutations. *Dev Biol* **158**, 364-79.
- Tsang, M., Friesel, R., Kudoh, T. and Dawid, I. B.** (2002). Identification of Sef, a novel modulator of FGF signaling. *Nat Cell Biol* **4**, 165-9.
- van der Geer, P., Wiley, S., Lai, V. K., Olivier, J. P., Gish, G. D., Stephens, R., Kaplan, D., Shoelson, S. and Pawson, T.** (1995). A conserved amino-terminal Shc domain binds to phosphotyrosine motifs in activated receptors and phosphopeptides. *Curr Biol* **5**, 404-12.
- Van Doren, M., Broihier, H. T., Moore, L. A. and Lehmann, R.** (1998). HMG-CoA reductase guides migrating primordial germ cells. *Nature* **396**, 466-9.
- Vani, K., Yang, G. and Mohler, J.** (1997). Isolation and cloning of a Drosophila homolog to the mammalian RACK1 gene, implicated in PKC-mediated signaling. *Biochim Biophys Acta* **1358**, 67-71.
- Verheyen, E. M. and Cooley, L.** (1994). Profilin mutations disrupt multiple actin-dependent processes during Drosophila development. *Development* **120**, 717-28.
- Vincent, S., Wilson, R., Coelho, C., Affolter, M. and Leptin, M.** (1998). The Drosophila protein Dof is specifically required for FGF signaling. *Mol Cell* **2**, 515-25.

- Wang, S. L., Hawkins, C. J., Yoo, S. J., Muller, H. A. and Hay, B. A.** (1999). The Drosophila caspase inhibitor DIAP1 is essential for cell survival and is negatively regulated by HID. *Cell* **98**, 453-63.
- Warburton, D., Schwarz, M., Tefft, D., Flores-Delgado, G., Anderson, K. D. and Cardoso, W. V.** (2000). The molecular basis of lung morphogenesis. *Mech Dev* **92**, 55-81.
- Warn, R. M., Gutzeit, H. O., Smith, L. and Warn, A.** (1985). F-actin rings are associated with the ring canals of the Drosophila egg chamber. *Exp Cell Res* **157**, 355-63.
- Weaver, M., Dunn, N. R. and Hogan, B. L.** (2000). Bmp4 and Fgf10 play opposing roles during lung bud morphogenesis. *Development* **127**, 2695-704.
- Weaver, M., Yingling, J. M., Dunn, N. R., Bellusci, S. and Hogan, B. L.** (1999). Bmp signaling regulates proximal-distal differentiation of endoderm in mouse lung development. *Development* **126**, 4005-15.
- Weaver, T. A. and White, R. A.** (1995). headcase, an imaginal specific gene required for adult morphogenesis in Drosophila melanogaster. *Development* **121**, 4149-60.
- Webb, D. J., Parsons, J. T. and Horwitz, A. F.** (2002). Adhesion assembly, disassembly and turnover in migrating cells -- over and over and over again. *Nat Cell Biol* **4**, E97-100.
- Weinkove, D., Neufeld, T. P., Twardzik, T., Waterfield, M. D. and Leever, S. J.** (1999). Regulation of imaginal disc cell size, cell number and organ size by Drosophila class I(A) phosphoinositide 3-kinase and its adaptor. *Curr Biol* **9**, 1019-29.
- Wheatley, S., Kulkarni, S. and Karess, R.** (1995). Drosophila nonmuscle myosin II is required for rapid cytoplasmic transport during oogenesis and for axial nuclear migration in early embryos. *Development* **121**, 1937-46.
- Wilk, R., Weizman, I. and Shilo, B. Z.** (1996). tracheless encodes a bHLH-PAS protein that is an inducer of tracheal cell fates in Drosophila. *Genes Dev* **10**, 93-102.
- Wills, Z., Marr, L., Zinn, K., Goodman, C. S. and Van Vactor, D.** (1999). Profilin and the Abl tyrosine kinase are required for motor axon outgrowth in the Drosophila embryo. *Neuron* **22**, 291-9.
- Wilson, R., Battersby, A., Csiszar, A., Vogelsang, E. and Leptin, M.** (2004). A functional domain of Dof that is required for fibroblast growth factor signaling. *Mol Cell Biol* **24**, 2263-76.
- Wilson, R. and Leptin, M.** (2000). Fibroblast growth factor receptor-dependent morphogenesis of the Drosophila mesoderm. *Philos Trans R Soc Lond B Biol Sci* **355**, 891-5.
- Wolf, C., Gerlach, N. and Schuh, R.** (2002). Drosophila tracheal system formation involves FGF-dependent cell extensions contacting bridge-cells. *EMBO Rep* **3**, 563-8.
- Won, M., Park, S. K., Hoe, K. L., Jang, Y. J., Chung, K. S., Kim, D. U., Kim, H. B. and Yoo, H. S.** (2001). Rkp1/Cpc2, a fission yeast RACK1 homolog, is involved in actin

cytoskeleton organization through protein kinase C, Pck2, signaling. *Biochem Biophys Res Commun* **282**, 10-5.

Wong, A., Lamothe, B., Lee, A., Schlessinger, J., Lax, I. and Li, A. (2002). FRS2 alpha attenuates FGF receptor signaling by Grb2-mediated recruitment of the ubiquitin ligase Cbl. *Proc Natl Acad Sci U S A* **99**, 6684-9.

Woodcock, S. A. and Hughes, D. A. (2004). p120 Ras GTPase-activating protein associates with fibroblast growth factor receptors in *Drosophila*. *Biochem J* **380**, 767-74.

Xu, T. and Rubin, G. M. (1993). Analysis of genetic mosaics in developing and adult *Drosophila* tissues. *Development* **117**, 1223-37.

Xu, X., Weinstein, M., Li, C. and Deng, C. (1999). Fibroblast growth factor receptors (FGFRs) and their roles in limb development. *Cell Tissue Res* **296**, 33-43.

Yokoyama, K., Su Ih, I. H., Tezuka, T., Yasuda, T., Mikoshiba, K., Tarakhovsky, A. and Yamamoto, T. (2002). BANK regulates BCR-induced calcium mobilization by promoting tyrosine phosphorylation of IP(3) receptor. *Embo J* **21**, 83-92.

Zhang, N., Zhang, J., Purcell, K. J., Cheng, Y. and Howard, K. (1997). The *Drosophila* protein Wunen repels migrating germ cells. *Nature* **385**, 64-7.

Zhang, S., Lin, Y., Itaranta, P., Yagi, A. and Vainio, S. (2001). Expression of Sprouty genes 1, 2 and 4 during mouse organogenesis. *Mech Dev* **109**, 367-70.

VI PUBLICATIONS

Cabernard, C., Neumann, M. and Affolter, M. (2004). Cellular and molecular mechanisms involved in branching morphogenesis of the *Drosophila* tracheal system. *J Appl Physiol* 97, 2347-53.

In this review, we describe the advantage of *Drosophila melanogaster* as a model system to study branching morphogenesis. We discuss FGF signaling, but also cell rearrangements, ZP proteins as well as tracheal system physiology. Furthermore, we summarize air sac development and put it into the context of FGF signaling and possible applications.

Ebner, A., Cabernard, C., Affolter, M. and Merabet, S. Recognition of distinct target sites by a unique Labial/Extradenticle/Homothorax complex. *Development*. 2005 Apr;132(7):1591-600.

This paper resulted from a collaboration with A. Ebner, M. Affolter and S. Merabet. Initially, Andi Ebner performed an *in silico* approach to screen for Lab target genes based on the consensus Lab/Exd/Hth sites. My contribution to this project was the screening for expressed sequence tags (ESTs) both up and downstream of the found target sites. In addition, we performed *in situ* hybridisation experiments, to test the expression of these putative target genes.

VII CURRICULUM VITAE

Name: Cabernard
First name: Clemens
Date of birth: December 1st, 1975
Place of birth: Burgdorf, Switzerland
Citizenship: Swiss
Marital status: unmarried

Private address: Lehenmattstrasse 91 Phone: ++41 61/ 311 44 28
 CH-4052 Basel, Switzerland

Institute address: Biozentrum, University of Basel Phone: ++41 61/ 267 20 77
 Dept. of Cell Biology
 Klingelbergstrasse 70
 CH-4056 Basel, Switzerland

Email address: clemens.cabernard@unibas.ch

Education and Research Experience:

1982-1990 Primary & secondary school, Oberburg, Switzerland

1990-1996 Gymnasium Sarnen, Switzerland

1995 Participation in the “Schweizer Jugend Forscht” molecular biology study week at the Biozentrum, University of Basel, workshop and contest.

1996 Matur, Typus B (Graduation)

1996-2000 Diploma studies in biology II
 Biozentrum, University of Basel, Switzerland

1999-2000 Diploma work under Prof. Dr. M. Affolter
 Department of cell biology, Biozentrum, University of Basel

Topic: Yeast two-hybrid screen with *Downstream of FGFR*, a gene required for cell migration in the mesoderm and trachea of *Drosophila melanogaster*

2000 Graduation as “dipl. phil. II” (Master of Science)

2001- 2004 PhD studies in Prof. M. Affolter's group
 Department of cell biology, Biozentrum, University of Basel

Topic: Studying Fibroblast growth factor (FGF) mediated cell migration in *Drosophila* air sacs

Courses

2002 Cold Spring Harbor Summer Advanced Course in "Advanced *Drosophila* Genetics" at the Cold Spring Harbor Laboratories, Cold Spring Harbor, NY, USA

Meetings

2003 44th Annual *Drosophila* Research Conference, Chicago, USA
 Poster presentation: *In vivo* characterization of *Receptor of activated protein Kinase C (rack1)*

2004 45th Annual *Drosophila* Research Conference, Washington DC, USA
 Poster presentation: Mosaic analysis of air sac tracheoblasts to study cell proliferation and cell migration in the larval tracheal system.

Publications

Cabernard, C., Neumann, M. and Affolter, M. (2004). Cellular and molecular mechanisms involved in branching morphogenesis of the *Drosophila* tracheal system. *J Appl Physiol* 97, 2347-53.

Ebner, A., Cabernard, C., Affolter, M. and Merabet, S. Recognition of distinct target sites by a unique Labial/Extradenticle/Homothorax complex. *Development*. 2005 Apr;132(7):1591-600.

Cabernard, C. and Affolter, M. Genetic dissection of the FGF signaling pathway in *Drosophila melanogaster*. In preparation.

Cabernard, C. and Affolter, M. *In vivo* characterization of *Receptor of activated protein kinase C (Rack1)*. In preparation.

Lectures/courses

During my studies, I attended lectures of the following instructors:

M. Affolter, W. J. Gehring, S. Arber, T. Bickle, A. Eberle, K. Ballmer-Hofer, P. Caroni, M. Hall, H. Riezmann, M. Spiess, C. Thompson, M. Rüegg, M. Dürrenberger, D. Monard, K. Kirschner, J. Seelig, A. Seelig, J. Engel, T. Schirmer, P. Philippsen, U. A. Meyer, H.-P. Hauri, U. Jenal, D. Monard, P. Jenö, W. Keller, Y.-A. Barde, A. Engel, C.-A. Schönenberger, M. Ashburner, S. Hawley, K. Golic, R. Lehmann, K. Burtis, P. Rorth, S. Henikoff, U. Gaul.

VIII Eid

Ich erkläre, dass ich die Dissertation, „Studying Fibroblast growth factor (FGF) mediated cell migration in *Drosophila* larval air sacs“, nur mit der darin angegebenen Hilfe verfasst und bei keiner anderen Fakultät eingereicht habe.

Basel, im Dezember 2004-11-26

Clemens Cabernard